A comparison between able-bodied and wheelchair dependent individuals during manual wheelchair propulsion using a dynamometer

by

Scott Alan Draper

A Thesis Submitted to the

Graduate Faculty in Partial Fulfillment of the

Requirements for the degree of

MASTER OF SCIENCE

Interdepartmental Program: Biomedical Engineering
Major: Biomedical Engineering

Iowa State University
Ames, Iowa

1995

TABLE OF CONTENTS

LIST OF FIGURES

LIST OF TABLES

INTRODUCTION

There are an estimated 1.2 million people in the United States who use wheelchairs as their primary source of mobility. Nearly 300,000 of these people have spinal cord injuries, with the rest being nursing home residents and those with congenital defects such as cerebral palsy, osteogenesis imperfecta, muscular dystrophy, and multiple sclerosis (Phillips and Nicosia, 1990). Therapists and physicians who prescribe wheelchairs often have little more than a one hour lecture on the subject in college. Ignorance of wheelchair selections available on the part of the prescriber as well as the patient often results in the prescription of a non-optimal wheelchair configuration for the user. Furthermore, wheelchair prescription is largely trial and error, with few established criteria used for positioning the patient and very little work done in minimizing cardiorespiratory and electromyographic responses during propulsion testing. Due to the inefficient nature of manual wheelchair propulsion, it is unfortunate that propulsion limitations exist that are foreseeable and correctable by the prescriber as well as by wheelchair designers who must rely on current wheelchair research results as design criteria.

The study of manual wheelchair propulsion has been ongoing for several years. Wheelchair mechanics, propulsion physiology, electromyography, kinematics, propulsion modeling, and muscle and joint modeling are some of the

main areas which have been studied. Furthermore, several methods have been used to study wheelchair propulsion, ranging from free-wheeling techniques to specially designed wheelchair ergometers and treadmills. In reviewing the literature, it was noted that a variety of subject pools were used in these studies. Some investigators employ wheelchair dependent individuals in their studies, which would seem to be the ideal situation. However, variations between the subjects, even within a group with a given lesion level, as well as availability of these subjects often prevents this approach from being taken. In contrast, some investigators have chosen to not use any wheelchair dependent subjects at all, employing only able-bodied subjects in their research. Although they are easier to find and they navigate better through a study, several obvious problems arise when using able-bodied subjects, especially when extrapolations are made to the wheelchair dependent population. In addition, the results of many of these studies involving physiological parameters such as heartrate and oxygen uptake have been extrapolated to the wheelchair dependent population as a whole. This can result in serious errors, since it is known that there are significant physiological differences between the able-bodied and wheelchair dependent populations which may or may not prevent valid inferences to be made on the wheelchair dependent group based on data obtained from studies involving only able-bodied individuals (Hoffman, 1986; Hjeltnes, 1993).

In order to identify errors arising from the use of able-bodied individuals while studying manual wheelchair propulsion, the present study was initiated. Various physiological and kinematic parameters were compared between wheelchair dependent and able-bodied groups while they were propelling a manually powered wheelchair on a specially designed wheelchair dynamometer, instrumented to measure the power output or work done per unit time by the subject.

The purpose of this study was to determine whether the use of able-bodied subjects is justifiable when conducting research involving manual wheelchair propulsion in the various types of parameters normally evaluated by researchers. This information may provide new insights for future investigators to consider when choosing the subject pools for their studies. Furthermore, these results may provide information to manual wheelchair designers and prescribers who currently base their design information on the available research which includes a variety of subject pools. Finally, this study will attempt to verify some of the previous findings regarding the differences in physiological makeup between able-bodied and wheelchair dependent individuals, as well as potentially providing some new insights in this area.

LITERATURE REVIEW

This chapter is divided into five main sections. The first section discusses the neural anatomy and physiology relevant to the spinal cord injured population as well as spinal injury classification and functional significance of spinal cord injuries. Cardiovascular effects of spinal cord injury are presented next since it is the cardiovascular system in conjunction with neural dysfunction which produces differences between the able-bodied and wheelchair dependent populations. Metabolic and physical work concepts are then discussed as well as their relation to propulsion efficiency. Previous research conducted pertaining to propulsion efficiency is also reviewed. Kinematic parameters frequently studied as well as previous kinematic research is then presented, followed by electromyographic concepts and past research.

Neural Anatomy and Physiology Related to Spinal Injury

Before discussing manual wheelchair propulsion research, it is imperative that some knowledge of the anatomical and physiological makeup of the spinal column as well as neural innervation of the muscles be understood. This knowledge is especially important when considering the wheelchair dependent population, since it is largely due to anatomical and physiological differences that differences in wheelchair propulsion parameters may be found. The anatomy and physiology of able-bodied individuals will be considered first,

followed by a brief overview of the most common types of spinal cord injuries. Finally, a discussion of the functional significance of spinal cord injuries will be presented.

Vertebral column

The vertebral column is an elastic and flexible bony structure which supports and protects the spinal cord. The column is divided into five main sections; cervical, thoracic, lumbar, sacral, and coccygeal, with 7 cervical, 12 thoracic, 5 lumbar, 5 fused sacral, and 3 to 5 fused coccygeal vertebrae (Burke and Murray, 1975). The vertebrae are separated by cartilage disks, which permit a small amount of movement between each adjacent vertebrae. However, when taken as a whole, the vertebral column is capable of fairly large movements in both the anteroposterior and lateral planes as well as rotational movements (Sutton, 1973). The vertebral column contains several curves in order to transmit the weight of the body through the spinal column most efficiently (Martini, 1992). Each vertebra contains a central canal, the vertebral foramen, which contains the spinal cord. Surrounding the vertebral foramen are bony structures which protect the spinal cord. Ventrally, the spinal cord is protected by the vertebral body, dorsally, by the laminae, and laterally by the pedicles (Burke and Murray, 1975).

Spinal cord

The spinal cord, or medulla spinalis, is about 45 cm long in males and 42 cm in females. It extends from the upper border of the atlas (first cervical vertebra) to the lower border of the first lumbar vertebra (Guttmann, 1973). The spinal cord is enlarged in the cervical (C4 to T1) and lumbosacral (L2 to S3) regions, with spinal nerves branching from these enlargements which innervate the upper and lower limbs via the brachial plexus and the lumbo-sacral plexus. The brachial plexus innervates the shoulder girdle and arm, while the lumbo-sacral plexus innervates the pelvic girdle and leg. The brachial plexus and lumbo-sacral plexus consist of bundles of nerves interwoven together to innervate the upper and lower extremities (Martini, 1992). Altogether, there are 31 pairs of spinal nerves branching from the spinal cord (8 cervical, 12 thoracic, 5 lumbar, 5 sacral, and 1 coccygeal).

Figure 1 shows the relationships between the spinal cord, vertebrae, and spinal nerves. A cross section of the spinal cord reveals a butterfly-shaped central gray region, surrounded by a white region. The neurons have their cell bodies in the gray region, with their axons traveling up and down the spinal cord to conduct afferent (sensory) and efferent (motor) impulses via the spinal nerves to and from peripheral receptors and effectors. In the anterior gray region, somatic or efferent impulses are initiated, innervating the skeletal muscles. The lateral gray region sends impulses to the autonomic (visceral)

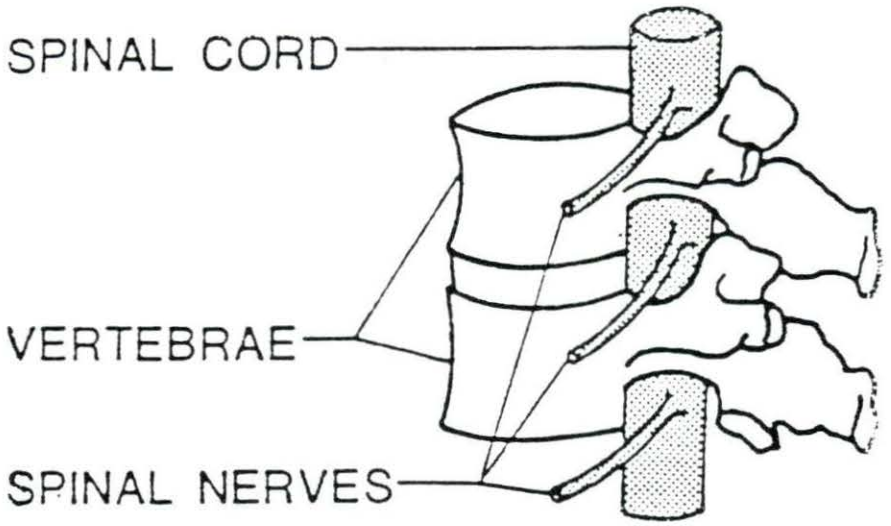

Figure 1 **Spinal cord, nerves, and vertebrae (from Heartquist, 1985)**

nervous system. The posterior gray region conducts the afferent impulses to the spinal cord from the skeletal muscles, cutaneous structures, and visceral structures, which then travel to the brain via tracts in the white region. The white region conducts efferent and afferent impulses via ascending (sensory) and descending (motor) pathways (Guttmann, 1973). There are also various reflex mechanisms in which a sensory impulse synapses directly onto a motor neuron in the gray region and a peripheral effector is activated. An example of this is the stretch reflex, in which muscle spindles containing intrafusal muscle fibers are stimulated due to stretching of the muscle. This stimulus travels to the posterior gray region, passing through the dorsal root ganglion in which the

sensory neuron cell bodies are contained. This stimulates a motor neuron, also in the gray region, which results in contraction of the muscle. The stretch reflex is important in maintaining muscle tone and posture (Martini, 1992).

Ascending and descending tracts in the white region

The white region is divided into regions or columns which contain tracts, or fasciculi, which convey either sensory or motor information, with all of the axons within a tract carrying information in the same direction. Ascending tracts carry sensory information to the brain, while descending tracts carry motor commands down the spinal cord (Martini, 1992). Although sensory information is extremely important in determining the level of spinal injury, as well as in the daily life of a spinal injury patient, the descending motor pathways are of much more significance in determining the limitations of a person with a spinal injury since it is these pathways which, if injured, prevent the relaying of efferent information to the skeletal muscles. The motor (somatic) pathways can be classified into upper and lower motor neurons. The upper motor neurons are located in the higher motor centers and relay information to the lower motor neurons, which serve as the final common pathway between the central nervous system and skeletal muscles. The lower motor neurons are located in the cranial and spinal nerves and terminate at the motor end plate on the skeletal muscles which they innervate. The upper motor neurons regulate the activity of the

lower motor neurons by issuing commands from the cerebral cortex and the brainstem and provide muscle tone, reflexes, and maintenance of posture (Carola et al., 1992). The upper and lower motor neurons play an important role in terms of spinal cord injuries. For instance, if the lower motor neuron is damaged or destroyed, paralysis of the skeletal muscles which it innervates will occur. However, if the damage is to an upper motor neuron, uncoordinated contractions or muscle rigidity/flaccidity may occur but the skeletal muscle is still capable of contracting via reflex action due to the intact lower motor neuron contacting its motor end plate (Martini, 1992). However, voluntary contraction of the muscle will not be possible, and any activity which may occur in the muscle is due to reflex action only.

Types of spinal column injuries

There are virtually an infinite number of ways in which the spinal column may be injured. Furthermore, there appears to be no consistent method of injury classification, with each author using a different classification scheme. Also, not all vertebral column injuries result in injury to the spinal cord. Inversely, particularly in children, spinal cord injury may be present even when no apparent vertebral injuries exist, as can occur in hyperextension or hyperflexion injuries due to the elasticity of their vertebral column. Therefore, the most common spinal column injuries will be discussed as classified by Burke

and Murray (1975) for the thoracic and lumbar regions of the spine, corresponding to the injury levels of the subjects participating in this study.

The most common type of injury to the spinal column in the thoracic and lumbar regions involves a flexion-rotation dislocation or fracture dislocation injury. This consists of the upper vertebra moving forward with respect to a lower, usually resulting in a complete disruption of spinal function, either due to complete transection of the spinal cord or due to massive trauma from pinching of the cord between the two vertebrae. This injury is the most common at the T12-L1 vertebral level. Compression fractures occur when a downward force causes compression of the spinal column, resulting in a decrease in height. This is a common injury and usually results in no neurological damage. Hyperextension injuries are unusual in the thoracic-lumbar region although when they do occur they usually result in complete neurological disruption of the spinal cord. Open injuries that occur as the result of gunshot or stab wounds may result in complete neurological damage depending upon the severity of the wound.

Most injuries to the spinal column result in damage to the upper motor neurons, resulting in loss of voluntary control over skeletal muscles as well as an increase in muscle tone. However, in injuries below the level of the spinal cord (L1), lower motor neuron damage is much more likely, also resulting in a

loss of voluntary function and a decrease in muscle tone (Burke and Murray, 1975).

Functional significance of spinal injury level

There are three general classifications which are used to describe a person with spinal cord damage due to injury or disease. Paraplegia involves the motor and/or sensory loss in both lower extremities. The spinal cord is usually transected between the upper thoracic and lower lumbar regions, which results in immediate paralysis below the lesion. In addition to the loss of sensory and motor control in the legs, excretory and sexual functions are also affected as well as bowel and bladder control since the pelvic nerve originates in the sacral region of the nervous system (Sutton, 1973).

Quadriplegia involves the paralysis of all four extremities in addition to all of the body parts below the level of injury. It usually consists of injury to the C8 through T1 levels of the body, although injury at the C4-8 levels is not uncommon. In addition to the loss of the functions due to paraplegia, the cardiovascular and respiratory systems are often affected. The diaphragm, intercostal, and abdominal muscles are all important to respiratory function, although the diaphragm is the major muscle involved. If the injury level is at C4 or above, diaphragm function will also be lost, resulting in the need for a respirator. Although persons with paraplegia have losses of both abdominal

muscles as well as some intercostal muscles, respiratory function is usually not severely impaired, particularly at the T5 level where inspiratory function of the lungs is very strong (Guttmann, 1973). Peripheral blood vessels are also affected due to loss of sympathetic nervous system control below the injury level, preventing the constriction of blood vessels and resulting in a loss of thermal regulation and blood pressure control. This also occurs below the level of injury in a person with paraplegia.

Hemiplegia involves the paralysis of the upper and lower extremities on only one side of the body, usually resulting from a stroke. Paralysis occurs on the opposite side of the lesion since the corticospinal tract switches sides prior to reaching the spinal cord. (Carola et al., 1992).

Figure 2 shows the major areas of control of the spinal nerves. In diagnosing the extent of a spinal cord injury, both the sensory and the motor functions of the individual need to be ascertained. Sensory function is determined with the use of a dermatome, which is defined as that segment of skin which is supplied by the sensory fibers of a peripheral nerve from a single posterior nerve root (Sutton, 1973). Thus, there are 30 dermatomes, one for each spinal nerve except C1, which does not innervate the skin (Carola et al., 1992). The dermatomes have been mapped but there is overlap of adjacent segmental nerves, making the mapping of dermatomes a rather inexact science. However, even with significant variation between individuals, dermatomes are useful in obtaining a

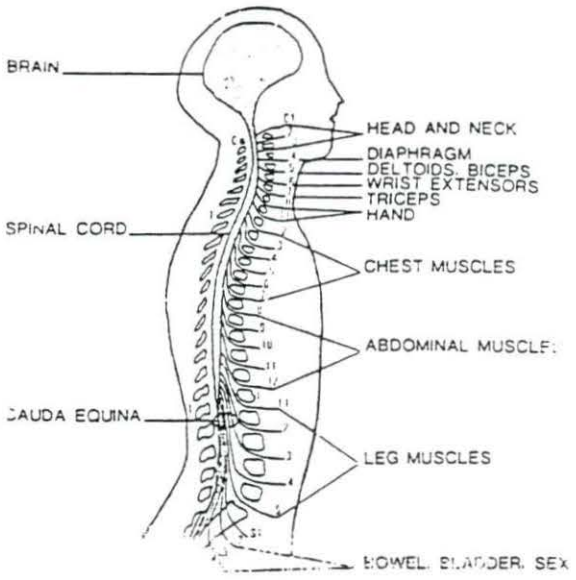

Figure 2 Spinal nerves and their major areas of control (from Heartquist, 1985)

general sense of the level of damage to the dorsal regions of the spinal cord.

Perhaps of greater significance than sensory loss is the extent of motor loss. Myotomes, or groups of muscles supplied by each spinal segment, have been charted so that a general determination of an individual's muscle loss can be gained with knowledge of the injury level. Many muscles are innervated by more than one spinal segment so it is often necessary to determine the extent of motor loss by asking the individual to voluntary contract specific muscles. Charts of myotomes can be found in Sutton (1973) and Guttmann (1973).

Long and Lawton (1955) describes the expected performance of individuals with spinal injuries at several critical levels. A person who has a spinal injury below T1 is classified as a paraplegic and has full innervation of the upper

extremities, including full use of the hand. However, a loss of all intercostal and abdominal muscles impairs respiratory function and likely reduces activity duration before tiring. Trunk stability is also lacking, although the person can transfer to and from a wheelchair without aid. Some loss of the pectoralis muscles may also occur, although most pectoral innervation comes from the C5-C8 regions of the spinal cord (Guttmann, 1973).

A person with a spinal injury below T6 gains the use of most of the intercostal muscles as well as some abdominal control, giving additional respiratory reserve and increasing endurance. Trunk stability is also increased over that with a T1 injury, resulting in the ability to drive a hand-controlled car as well as transfer to and from a wheelchair with greater ease.

Cardiovascular Effects due to Spinal Cord Injury

The loss of neurological function associated with spinal cord injury is not limited to merely a loss of sensation and motor function. In fact, cardiovascular disorders are the major cause of death in those with spinal cord injuries (Hoffman, 1986). Therefore, it is necessary to understand the effects that spinal cord injury may have on the cardiorespiratory system. These effects will influence oxygen uptake, thus affecting propulsion efficiency. Furthermore, these effects may constrain the wheelchair user to a specific pattern of wheelchair propulsion and may also influence EMG activity in the muscles used.

Manual wheelchair propulsion has been shown to be highly stressful on the cardiovascular system. Although it has been shown that the energy requirement of wheelchair propulsion on level ground is the same or less than that of walking at the same velocity, studies have shown increased heart rates during wheelchair usage as compared with normal walking (Hoffman, 1986).

The sympathetic division of the autonomic nervous system is largely responsible for cardiovascular regulation. If the spinal injury level is between T1 and L3, the sympathetic preganglionic neurons in the spinal cord are likely to be non-functional, thus preventing synapse onto the postganglionic neurons in the sympathetic chain. The sympathetic nervous system is responsible for, among other things, constriction and dilation of blood vessels in order to regulate blood pressure and venous return to the heart. The regulatory mechanisms in the medulla responsible for this will not be discussed. However, the absence of venoconstrictor function results in a pooling of blood in the veins below the injury level, resulting in a reduction in diastolic return to the heart, thus causing a decrease in end-diastolic volume. This phenomenon has been substantiated by research in which persons with paraplegia were exercised and the stroke volumes were found to be lower than those for able-bodied individuals (Hopman et al., 1993; Hjeltnes, 1993). The muscular atrophy that occurs as a result of spinal cord injury also results in reduced total blood volume, thus reducing venous return (Hjeltnes 1993). In order to compensate for this

decreased stroke volume and maintain an adequate cardiac output, the heart rate is higher in persons with paraplegia than in able-bodied subjects during arm exercise. However, during maximal exercise, the heart rate reaches a maximum and a reduced cardiac output results since the stroke volume is still lower due to a lack of sympathetic venoconstriction. Since the cardiac output is lower, it follows that the oxygen consumption will also be lower as compared with able-bodied individuals. Furthermore, since the muscle mass of the spinal cord injured person is lower than that of an able-bodied person, a lower maximum oxygen consumption will occur. This has been found in previous research comparing spinal cord injured and able-bodied individuals (Hopman et al., 1993). The effects of sympathetic damage are not limited to the blood vessels. The sympathetic division also is responsible for increasing the heart rate during exercise. However, if the spinal injury is above T6, this sympathetic innervation may be disturbed and parasympathetic innervation will overrule, resulting in difficulty to increase the heart rate. This will result in the person reaching the maximum heart rate, cardiac output, and oxygen consumption at lower exercise levels than able-bodied individuals or persons with spinal injuries below T6 (Hopman et al., 1993). The problems described above can be reduced through exercise and training (Hjeltnes, 1993), although normal daily wheelchair use is not sufficient to produce cardiorespiratory improvement (van der Woude, 1993). However, a common problem which exists in the spinal cord

injured population is that of leading a sedentary lifestyle. A reduction in physical activity results in the person becoming deconditioned and a lower capacity for doing work results, resulting in more physical restrictions (Hoffman, 1986).

Manual Wheelchair Propulsion Parameters and Research

Several investigators have conducted wheelchair propulsion research in recent years, most with different objectives in mind. Some focus primarily on the physiological comparisons between wheelchair propulsion and other, more common forms of locomotion, such as bicycle riding (Glaser et al., 1979). Others tend to concentrate primarily on the mechanical and ergonomic aspects of propulsion (Brubaker and McLaurin, 1982; van der Woude et al., 1989a; Stoboy et al., 1971). Still others focus primarily on the kinematics of various body segments during a propulsion cycle (Sanderson and Sommer, 1985; Veeger et al., 1989). While each area is of importance, the results published in the literature appear to be rather fragmented, with few common standards employed between studies. This section will explain some of the most common parameters of interest in studying wheelchair propulsion, as well as some results from previous studies pertaining to each parameter.

Determination of metabolic work

There are at least three main reasons for studying the physiological events which accompany wheelchair propulsion. The first involves the calculation of energy cost or metabolic power output so that the propulsion efficiency can be calculated. The propulsion efficiency can be used to optimize a wheelchair configuration or design, as well as to determine the best configuration for a particular patient. The second reason is to evaluate a particular individual based on physiological measurements in order to attain an "ideal" wheelchair prescription. Finally, the third reason is simply to obtain information. As in many research areas, it is often unknown whether any information gathered will prove useful at a later date. Often, the physiological parameters are compared with the corresponding parameters for more well understood forms of exercise, such as stationary bicycling or rowing, under similar power levels and environmental conditions.

Although the metabolic work done is dependent to a large extent upon physiological factors such as conditioning level, skeletal muscle makeup and distribution, size of muscles used, etc., the amount of work done does not depend upon the physiological makeup of the person but rather depends upon external factors. To a physicist, work is simply force times distance. In other words, if a force is applied to an object, causing that object to move, work is being done. However, if no motion takes place, no mechanical work is being done although

the individual may tire very quickly, such as when holding a weight. Work can further be divided into two categories; positive and negative work. Positive work occurs when an object moves in the same direction as the force application, such as when going up stairs or lifting a weight. This type of work is also known as concentric work, which results from the shortening of muscles. Negative work occurs when the motion of an object is opposite the direction of the application of force, such as when going down stairs or lowering a weight. This type of work is known as eccentric work and results in the lengthening of muscles (Rodgers and Cavanagh, 1984). The pure definition of work, W=Fd, is rarely representative of the amount of work done as seen from a physiological standpoint. For instance, if a runner runs 100 feet vertically and then descends 100 feet, the net work done by the runner is zero since the net vertical distance is zero. However, the runner's body will show signs of exercise and energy expenditure. Thus, physiologists frequently look at the amount of energy used in performing an activity rather than the physical definition W=Fd (Karpovich and Sinning, 1971).

Oxygen uptake, steady state, and oxygen deficit

One of the most common physiological parameters of interest in wheelchair propulsion is oxygen uptake (VO_2). The oxygen uptake during exercise depends upon the level of work and the size of the muscle groups involved, larger muscles

requiring more oxygen. It is also a function of the level of training of the individual, with well-trained athletes having higher maximum oxygen uptakes. The oxygen uptake provides an indirect measurement of the amount of energy used in performing an activity.

During exercise, the oxygen uptake does not immediately rise to steady state conditions but rather increases over a period of time of two to three minutes before reaching a plateau, at which oxygen consumption does not increase further as long as the workload remains constant. The oxygen uptake does not rise to a steady state level immediately because the initial energy used for muscular work is provided by the breakdown of ATP (adenosine triphosphate) in the muscle. This is a non-oxygen consuming process. However, once the initial stored energy in the muscle has been depleted, oxygen is used to provide energy for the muscle to contract and a steady state oxygen consumption is reached. The period of time in which stored energy is used to perform muscular work is called the "oxygen deficit" and is normally between two and five minutes following the start of exercise for most individuals (McArdle et al., 1991). During this time, the amount of oxygen used by the body is less than that predicted under steady state conditions. It has been shown that, for manual wheelchair propulsion, three minutes is a sufficient amount of time for the steady state to be reached, regardless of previous workloads experienced (van

der Woude et al., 1988a). Figure 3 shows a typical oxygen uptake curve obtained during submaximal exercise at a constant workload.

Open or closed circuit indirect calorimetry is most often used to measure oxygen uptake. The closed circuit method involves the subject inhaling oxygen from a spirometer. The subject then exhales, passing the exhaled gases through a carbon dioxide absorbent and then back to the spirometer. The oxygen

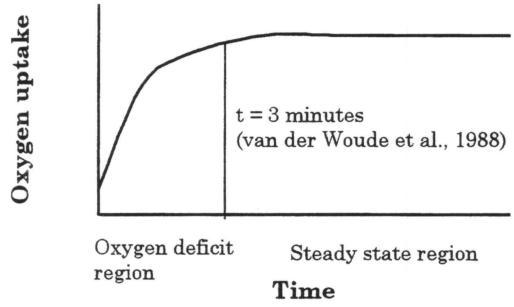

Figure 3 Oxygen uptake curve showing oxygen deficit and steady state regions

consumption is then the amount of oxygen in the inhaled air minus the amount in the exhaled air. One-way valves allow the movement of gases in one direction only. A graphical recording is obtained plotting liters of oxygen consumed against time. The slope of this line is then found to be the oxygen consumption. The open circuit method involves the subject breathing atmospheric air. The subject exhales air, which is collected in an airtight bag, called a Douglas bag, or

the exhaled air may pass into a mixing chamber with a sampling tube attached. Samples of this expired air are analyzed for the oxygen and carbon dioxide contents. The amount of oxygen consumed and carbon dioxide given off can then be calculated since the composition of atmospheric air is known and is essentially unchanging. The quantity of a gas (by weight) in a unit volume is dependent upon the pressure and temperature. Therefore, the data is often converted to standard conditions of 0° C, 760 mm Hg, and dry conditions. This condition is denoted as STPD (Standard Temperature and Pressure Dry).

Once the oxygen consumption in liters per minute is known, the metabolic energy expenditure can be found. The average value for energy equivalent is 5 kcal of energy for each liter of oxygen used. The exact value is dependent on the types of substrates metabolized (fat, carbohydrate, protein, etc.) and varies between 4.686 and 5.047 kcal/l (Karpovich and Sinning, 1971). The value used for the energy equivalent is obtained from knowledge of the respiratory exchange ratio (RER) which is the ratio of CO_2 produced to O_2 used at the lung level and is an estimator of the respiratory quotient (RQ) which is the ratio of CO_2 to O_2 at the tissue level. The RQ is an indicator of the substance that is being consumed during muscular work, whether it be fats or carbohydrates. At an RQ of 0.83, approximately 50% carbohydrates are being used and 50% fats. At an RQ of 1.0, 100% carbohydrates are being used and at an RQ of 0.7, 100% fats are being metabolized by the body (Karpovich and Sinning, 1971). It is

apparent that each individual is likely to be using a different percentage of carbohydrates and fats in doing muscular work. Some investigators use the average value of 5.00 kcal/liter in determining energy expenditure (Brubaker and McLaurin, 1982). However, if the RER is known, tables can be used to determine a more precise energy equivalent in order to eliminate as a variable the subject's physical makeup in terms of the substances metabolized in doing muscular work. It is also known that 1 kcal/min = 69.755 Watts of power. Therefore, oxygen consumption in l/min can be converted to Watts by the use of Equation 1 (Brubaker and McLaurin, 1982).

VO_2 (l/min) x (4.686 to 5.047) kcal/l x 69.755 Watts/kcal/min = Energy Expenditure (Watts)

Equation 1 Determination of metabolic power output

Several studies have been conducted to determine the energy expenditure of wheelchair propulsion under various conditions. In reviewing these studies, care must be taken to note the environmental conditions before attempting to compare values. For example, wheelchair ergometers, dynamometers, treadmills, and free-wheeling techniques are all used by various researchers. Each setup has its own benefits and limitations as well as effects on the energy expenditure produced to overcome a specified work load. In addition, the type of chair, as well as the physical conditioning, sex, level of disability, if any of the

subject, and the time spent in the wheelchair all play significant roles in influencing the energy expenditure. Therefore, great care must be taken when making comparisons between individuals and drawing conclusions between groups of subjects, particularly when using small group sizes.

Determination of work and power output

The amount of work done, or work output, is measured with a device called an ergometer. This device produces a resistance which the muscles must overcome to accomplish work. For example, a bicycle ergometer may consist of a braking belt wrapped around a flywheel. The tension in this belt can be adjusted to provide more or less frictional resistance to motion. This frictional force can be monitored by the use of spring scales to indicate the amount of resistance to motion that is present. Thus, in the equation W=Fd, the force F is known, and the total work done can be found by simply recording the distance traveled and multiplying this distance by the resistance to motion.

In terms of wheelchair propulsion efficiency, the rate of doing work, or power, is generally of more interest than the total amount of work done. Power is defined as "the time rate at which work is performed" (Gettys et al., 1989) and has the unit of watt in the SI system, which is also equal to 1 Joule per second, with one Joule being the amount of work (W) accomplished in moving an object with a force of one Newton a distance (d) of one meter. It can be shown that

$P = \frac{\Delta W}{\Delta T} = \frac{F\Delta d}{\Delta T} = Fv$, where F is the amount of force resulting in a given velocity, v. Since , for circular motion, $v = r\omega$, with ω being angular velocity and r being the distance from the force application to the axis of rotation, $P = Fr\omega = M\omega$. Therefore, in manual wheelchair propulsion, the power output can be found by knowing the moment or torque applied to the handrim of the wheelchair multiplied by the angular velocity of the wheelchair wheels. In addition, the power output can also be found by multiplying the linear velocity of the wheelchair handrims by the applied force acting tangential to them. Further information concerning the wheelchair dynamometer power calculations used in this study is presented in the materials and methods section.

Determination of propulsion efficiency

The energy expenditure or metabolic work found from oxygen uptake measurements is always higher than the physical or actual work performed due to inefficiencies within the system. In fact, wheelchair propulsion efficiencies have been reported to be in the range of 5% for an untrained person propelling a standard wheelchair on carpet to 20% for a trained wheelchair athlete in a specially designed wheelchair (Brubaker and McLaurin, 1982). This implies that the metabolic work is 5 to 20 times the actual work done. One must take care to note whether the gross or net efficiency is being reported in the literature. The net efficiency deducts the energy required for maintenance of

the bodily functions at rest from the total energy expenditure and, therefore, represents the energy used to perform the task. Therefore, net efficiencies will generally be higher than gross efficiencies at a given work load. In order to calculate the gross propulsion efficiency, the power output obtained from the wheelchair ergometer is simply divided by the metabolic power output obtained from open or closed calorimetry and is usually expressed as a percentage.

Wheelchair propulsion efficiency research

Six nondisabled subjects were tested at the University of Virginia while propelling a wheelchair at power outputs of 0.2, 0.25, and 0.4 W/kg body weight at speeds of 2 and 3 km/h on a wheelchair dynamometer. It was determined that efficiency (gross and net) increases with increased power output and decreases with increased speed at equivalent power outputs (Brubaker and McLaurin, 1982). Other investigations have shown similar results. Veeger et al. (1992), conducted a study in which nine able-bodied subjects propelled a wheelchair ergometer against power outputs of 0.25 and 0.50 W/kg of body weight and speeds of 0.83, 1.11, 1.39, and 1.67 m/s. Although the power output remained constant, the mechanical efficiency decreased 2% over the velocity range, while the efficiency increased with higher power output. It has been speculated that this decrease in efficiency with increasing speed is due to internal factors such as an increase in muscular friction (Powers et al., 1980)

and/or a change-over from slow-twitch to fast-twitch muscle fibers (Gaesser Brooks, 1975) as well as external factors such as excessive limb movements (Glaser et al., 1980) and/or a less accurate force application to the handrim (Sanderson and Sommer, 1985).

Van der Woude et al. (1988a) conducted an experiment in which eight wheelchair athletes propelled their own wheelchairs on a motor-driven treadmill. Two workload strategies were employed. In the first, the slope was kept constant while the speed increased in regular intervals. In the second, the speed was kept constant while the slope increased. It was found that the gross mechanical efficiency was significantly higher for the "low speed and high slope" condition than for the "high speed, low slope" condition under equal power output levels. This shows that efficiencies cannot be calculated based on only the power level, but they must take into account the speed and slope (resistance) characteristics. Therefore, each combination of velocity and resistance must be treated as a separate testing condition even if two or more power outputs are equal.

In addition to speed and resistance effects, the efficiency of propulsion is also influenced by physical factors such as the wheelchair configuration and the type of device used to study the propulsion. In a study by van der Woude et al. (1988b), the effect of handrim diameter was studied using eight male wheelchair athletes as subjects. The subjects propelled a racing wheelchair on which five

different rim diameters were mounted (0.3, 0.35, 0.38, 0.47, 0.56 m). The tests were conducted on a treadmill at a constant inclination, with the belt velocity increasing every 3 minutes. The study found that the smallest handrim produced 20-30% less cardiorespiratory effect than the largest hand rim at a given speed. This corresponds to a lower mechanical advantage, which is equal to the ratio between the effect of an input force on the handrims and its effect on the wheels and is also equal to the handrim radius divided by the wheel radius (Veeger et al., 1992). In other words, a lower mechanical advantage generates a lower heart rate, oxygen cost, and ventilation response.

The positioning of the seat with respect to the handrims also has an effect on the propulsion efficiency. The conventional position is for the backrest to be directly above the axle. This configuration is not consistent with the position for maximum efficiency. Studies were done at the University of Virginia Rehabilitation Engineering Center (Brubaker and McLaurin, 1982) in which the seat position was varied vertically in 5 centimeter increments with the lowest position 13 cm above the axle. The seat was also varied horizontally in three positions 20 cm apart with the back edge of the seat directly above the axle in the forward position. The subjects propelled the wheelchair on a dynamometer at an average speed of 2.5 km/h at a power output of 0.25 W/kg of body mass. The highest efficiencies were found with the seat in the two lowest positions vertically and the forward and middle positions horizontally. It is evident that

the most rearward seat position is the most inefficient of those tested, along with the high-rear position, which, ironically, is the convention on standard wheelchairs. The fact that the lowest efficiencies were found with the most rearward seat position contradicts the idea of minimizing rolling resistance by keeping the center of gravity as far rearward as possible since the coefficient of rolling resistance is inversely proportional to wheel radius (Kauzlarich and Thacker, 1985). Therefore, rolling resistance can be minimized by keeping the center of gravity as much over the rear wheels as possible. However, it is apparent from the literature that the most rearward seat position is the poorest in terms of propulsion efficiency, suggesting that the positive effect of the increased stroke arc due to a lower and forward seating position outweighs the negative effects of applying too much weight on the front wheels. This indicates an optimal position horizontally for the seat. If the seat is too far forward, the negative effect of rolling resistance is sure to outweigh the positive kinematic effects. If the seat is positioned too far rearward, the stability of the wheelchair is sacrificed, resulting in possible injury to the person.

The position of the shoulder joint with respect to the axle and the dimensions of the arm segments affect the range of motion possible at various seat positions and are the primary reasons why the efficiency varies. When the seat position is high, the hand cannot travel as far down the rim during the power stroke, resulting in a shorter stroke arc than for a lower seat position. For the high seat

position, the stroke arc is shorter and, therefore, the stroke frequency must increase in order to maintain a given power output. This not only results in a greater force being applied to the handrim per unit time, but more recovery strokes are necessary per unit time as well, each requiring metabolic energy and decreasing the efficiency (McLaurin and Brubaker, 1991). Previous research has shown that the optimal positioning in terms of cardiorespiratory responses for daily use and basketball wheelchairs is 120 degree elbow flexion with the hands placed on the handrims at top-dead center (Veeger et al., 1992).

Efficiency comparisons have also been made between manual wheelchair propulsion and other activities, such as stationary bicycling and arm cranking exercises. It has been shown that exercise performed on a wheelchair ergometer produces significantly higher physiological responses (VO_2, heartrate, RER) than exercise on a bicycle ergometer at equivalent power levels (Glaser et al., 1979). In comparing wheelchair locomotion to walking, it was found that wheelchair propulsion produces a lower energy expenditure. However, the heartrate is higher during wheelchair propulsion than during walking at equivalent velocities, thus indicating a higher load on the circulatory system. Furthermore, an increase in power level produces a much greater heartrate increase during wheelchair propulsion than during walking, indicating a lower energy reserve for wheelchair propulsion (Dreissinger and Londeree, 1982).

Energy consumption is also greater for manual wheelchair propulsion than for arm-cranking at equivalent power levels (Hildebrandt et al., 1968).

Kinematics of Manual Wheelchair Propulsion

Kinematics is the study of how objects move (Riley and Sturges, 1993) and has been previously investigated with regard to manual wheelchair propulsion. However, no known studies have been undertaken in which attempts have been made to ascertain differences and/or trends in kinematic parameters between able-bodied and wheelchair dependent individuals, although van der Woude, et al. (1989) conducted a kinematic study in which two of the subjects were experienced wheelchair users while four subjects were non-users. However, the subjects were treated as a group with no comparisons made between the wheelchair users and non-users. This section will focus on the kinematic parameters most often studied with regard to manual wheelchair propulsion as well as some of the findings from previous kinematic research.

Kinematic parameters

There are two phases associated with the wheelchair propulsion stroke: the propulsive phase (PT) and the recovery phase (RT). The propulsive phase is the period in which the person's hands are in contact with the wheelchair handrim and the person is applying force. The recovery phase is the period in which the person's hands leave the handrim following the propulsive phase and return to

the handrim to begin a new propulsion cycle. However, these phases are subject to interpretation. For instance, during the propulsive phase, the subject's hands may be in contact with the wheelchair handrim but may not be applying any force, as in the beginning of the propulsive phase in which the hands may be in contact with the handrims but may be accelerating to the current handrim velocity. In fact, the hands may even exert a braking force to the handrims while accelerating (Sanderson and Sommer, 1985). It is therefore important to note in defining the propulsive phase whether it is based upon cinematographic techniques in which the propulsive phase is generally defined from first handrim contact to handrim release (Sanderson and Sommer, 1985; Veeger et al., 1989) or torque/velocity characteristics (van der Woude, et al., 1989) in which the propulsive phase is defined in terms of force application to the handrims or wheelchair handrim velocity. The total cycle time (CT) is merely the sum of the propulsive and recovery phase times. Figure 4 illustrates the propulsion time, recovery time, and total cycle time parameters for manual wheelchair propulsion.

Other commonly studied kinematic parameters include stroke frequency (1/CT), % propulsion time (PT/CT*100), % recovery time (RT/CT*100), start angle (SA), end angle (EA), and push angle (PA). High-speed cinematographic techniques allow the digitization of various body segments, the most common being the shoulder, elbow, wrist, neck, and trunk movements. Displacement

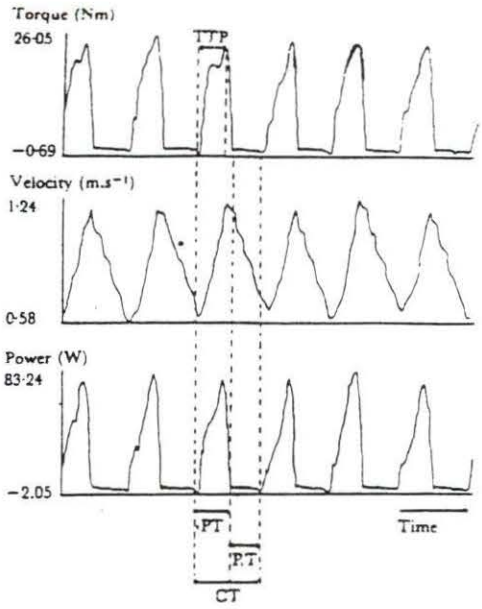

Figure 4 **Example of push time, recovery time, and total cycle time during manual wheelchair propulsion (from Veeger et al., 1989)**

information as well as angular velocity and acceleration information can be obtained and plotted, showing each subject's individual stroke characteristics and patterns of movement.

Previous kinematic research

Sanderson and Sommer (1985) used high-speed cinematography to analyze the movement patterns of the trunk, shoulder joint, elbow joint, and hand of three male paraplegics while they pushed their own wheelchairs on a motor driven treadmill. The subjects propelled their wheelchairs for 80 minutes at 60-65% of their previously established VO_2 maximum. Filming was conducted every 20 minutes and included at least three complete stroke cycles per filming

session. Small black ink marks were placed at the acromial process, lateral condyle of the elbow, and styloid process at the distal end of the ulna to enable digitization. An important finding was that there were very small differences in propulsion technique by each subject over the 80 minute trial period, particularly during the propulsive phase, indicating the reliability of assigning a specific stroke pattern to a subject based on only a small sample of stroke data. It was suggested that, due to the constraint imposed upon the subject when the hands are in contact with the handrims, the propulsive phase movement pattern is largely dictated by the handrim movements. During the recovery phase, the arms are free to return to the handrims in an infinite number of paths. However, the recovery patterns of each subject also changed very little over the trial period. There were large differences between the subjects, with two of the three subjects employing a circular stroke action with the other subject using a pump arm action. Steadward (1979) suggested that the circular pattern is more efficient than the pump action because of the abrupt changes in hand direction necessary at the end of the propulsive and recovery phases, resulting in greater neuromuscular activity in order to brake and accelerate the limbs (Sanderson and Sommer, 1985). A circular motion results in a better matching of the hand and handrim velocities upon handrim contact, thus reducing braking forces as the hand accelerates to the handrim velocity.

Veeger et al. (1989) conducted a similar study in which five male wheelchair athletes propelled a wheelchair on a motor driven treadmill with increasing velocity every three minutes. Propulsion efficiency was also calculated as well as the typical kinematic parameters of propulsion time, recovery time, cycle time, start angle, end angle, and push angle. It was found that the recovery phase was longer than the propulsion phase, with the propulsion phase decreasing greatly with increasing velocity and the recovery phase only slightly decreasing. Thus, percent propulsion time decreased with increasing velocity. As was found in the study by Sanderson and Sommer (1985), there was very little within-subject variation in stroke technique. Furthermore, one of the subjects who used a circular propulsion technique was found to have a significantly higher efficiency. However, a causal relationship between propulsion style and efficiency could not be made because the subjects had significantly different power outputs ($p < 0.05$).

In a study by van der Woude et al. (1989), six male subjects (two experienced wheelchair users, four non-users) propelled a wheelchair on a specially designed ergometer at increasing velocities of 0.55, 0.83, 1.11, and 1.29 m/s with an increase in velocity every three minutes. Instead of using cinematographic techniques, the timing parameters were found from a plot of the handrim torque, which could be found from a force transducer at the wheel center. Metabolic parameters such as oxygen uptake, heartrate, pulmonary ventilation,

respiratory exchange ratio, and gross mechanical efficiency were also evaluated. Each of these parameters increased with increasing velocity. However, the increase in gross mechanical efficiency with increasing velocity is contradictory to the results obtained by Veeger et al. (1992) in which it was found that mechanical efficiency varies inversely with propulsion velocity. An explanation as to this discrepancy was not given in the literature. However, it should be noted that in the latter study, nine male non-users were used as subjects rather than the mixed pool used in the former. As stated earlier, it is the intent of this study to determine if the use of able-bodied subjects may account for this and other differences in measured propulsion parameters. The cycle time and propulsion time also decreased with increasing velocity with the recovery time remaining relatively constant, as was also found in the study by Veeger et al. (1989) mentioned above.

Electromyography

Although not widely employed as a technique for investigating wheelchair propulsion performance, electromyography has the potential to be quite useful in studying wheelchair propulsion, as well as in the diagnosis of neuromuscular pathologies. The EMG signal is a direct reflection of the activity in the muscle and therefore coincides with the propulsion efficiency, which has been shown above to be influenced by external factors such as seat position, handrim

diameter, etc. Furthermore, electromyography may be useful in comparing able-bodied vs. wheelchair dependent individuals to study the effects of muscular atrophy or, inversely, increased conditioning due to increased specialization and recruitment.

Before discussing the theory of electromyography, a brief overview of the pertinent muscular physiology will be given. A skeletal muscle consists of muscle fibers, each of which is a single cell resembling a very fine thread. Each fiber can be up to 30 cm long but is less than 100 μm wide. The muscle fiber can shorten to about 57% of its original length upon contraction (Basmajian et al, 1975). Each muscle fiber is surrounded by a cell membrane, called the sarcolemma. At a point on the sarcolemma, the terminal ending of a nerve fiber forms the myoneural junction. It is at this junction that a chemical transmission takes place (acetylcholine) which initiates the process of depolarization and muscle contraction. Details of the contractile mechanism will not be presented here since they are not necessary to understand the EMG signal. It is sufficient to know that, when a neural impulse reaches the myoneural junction, or motor end-plate, a wave of depolarization spreads throughout the fiber which causes a brief twitch, varying from a few milliseconds to 1/4 second, followed by relaxation. The electrical potential that causes the twitch also spreads in the surrounding tissue and can be picked up by electrodes, amplified, and recorded as the electromyographic, or EMG, signal.

Motor units

Not all of the skeletal muscle fibers contract at the same time. However, all of the muscle fibers which are supplied by the terminal branches of one nerve fiber do contract within a few ms of one another. The nerve fiber, its terminal branches, and all of the muscle fibers supplied by these branches is called a motor unit and is the basic functional unit of skeletal muscle (Basmajian et al, 1975). The number of muscle fibers in a motor unit varies depending upon the function of the muscle, with fine controlling muscles (eyes) having fewer muscle fibers per motor unit than muscles generating mainly large movements (thigh). During a muscle contraction, it appears as though all of the muscle fibers are contracting together. However, the motor units are actually contracting and relaxing at various frequencies, which are generally below 50 Hz. (Basmajian, 1978). The contraction is then the summation of all of the motor units contracting at various frequencies. The electrical signal generated from a skeletal motor unit is triphasic in form and has a duration of 3-15 ms. The amplitude is between 20 and 2000 μV, depending upon the size of the motor unit. As stated earlier, the frequency of discharge is between 6 and 50 Hz (Webster, 1992).

The number and types of motor units activated depends upon the level of contraction needed. Smaller motor units are the first to be activated, or recruited. As the contraction is increased, larger motor units are then recruited.

Also, all of the motor units increase their frequency of twitching. The summation of all of these asynchronous twitches results in a smooth contraction. In the past, skeletal muscles have been classified into three fiber types ; slow twitch, fatigue resistant (S), fast twitch, fatigue resistant (FR), and fast twitch, fatigable (FF). Previous studies have shown that motor units are recruited in the reverse order of their ability to fatigue (S, FR, FF), with FR and FF motor units activated at higher force levels or during rapid movements (Matsui and Kobayashi, 1983). Therefore, the degree of contraction influences both the size and type of the motor units involved. Furthermore, skeletal muscle is also broken down into "fast" fibers and "slow" fibers. Most of the skeletal muscle fibers in the human body are "fast" fibers. They are called "fast" because they can contract in 0.01 seconds or less after stimulation. However, they fatigue rapidly so are only useful for a short period of time. A common example of "fast" fibers are the muscles in the wings of a chicken. They provide short bursts of energy for quick movements but fatigue too rapidly to allow the chicken to fly. "Slow" fibers are about half the diameter of "fast" fibers and take about three times as long to contract following stimulation. These muscles are highly vascularized to increase oxygen supply to the muscle and allow long periods of contraction without fatigue. Thus, the muscle has a more "reddish" appearance than "fast" muscle, which is whiter in color. Muscles in chicken legs are an

example of "slow" fibers since chickens use their legs for long periods of time and therefore the muscle cannot fatigue easily (Martini, 1992).

Surface electrodes

Probably the most important component of an electromyography procedure is the type of electrode used to detect the summed electrical activity produced by the contracting motor units. There are two main classifications of electrodes used: surface and inserted. As their names imply, surface electrodes are noninvasive while inserted electrodes use a wire or needle to penetrate into the muscle under study. Each type has its own advantages as well as limitations. Since surface electrodes are being used in the present study, a discussion of inserted electrodes will not be presented.

Surface silver-silver chloride electrodes consist of small silver discs, originally adapted from those used for electroencephalography, and are the most convenient type of electrode to use. They are easy to obtain, easy to apply, and give little discomfort to the subject. A very important consideration when using surface electrodes is to make sure that the electrical insulation between the electrode and the muscle is kept to a minimum. There are several ways to accomplish this. Before applying the electrode, the layers of dead skin and protective oils are removed by light abrasion of the skin. A conductive electrode jelly is applied between the electrode and the skin to further reduce the

impedance to practical levels of 2000 to 3000 ohms. Most surface electrodes are of a concave shape. This allows the electrode jelly to be "sandwiched" between the electrode and the skin more effectively. After the electrode is applied, pressure is maintained on the electrode to ensure a good electrical contact between the electrode and muscle (Basmajian, 1978).

The advantages of using surface electrodes are that they are non-invasive, cause little discomfort to the subject, and require little training to learn to apply and use properly. However, their use is limited to superficial muscles since their area of electrical pickup is far too widespread to isolate the activity of a deeper muscle. Since they have a large area of electrical pickup, they are often used for exploring the activity of muscle groups without isolating specific muscles within the group. Another disadvantage of the surface electrode is that a loss of high frequency components occurs due to low-pass filtering of the electrical signal. This varies depending upon the separation between the electrodes and the distance to the muscle fibers (Basmajian, 1978). This results in a rounding of the spikes of the waveform, as well as less resolution. However, as long as precision is not needed, surface electrodes can be used satisfactorily if their limitations are observed.

EMG signal processing

In order for the EMG signal to be analyzed, it must first be processed. Signal processing involves the process of manipulating the raw signal to remove undesirable components, such as 60 Hz noise, low frequency movement artifacts, other bio-electric signals, such as the ECG or respiratory phenomena, and interference from the measuring equipment itself. Also, unless visual analysis of the signal is desired, the signal must be manipulated to facilitate analysis and quantification of the signal. This can include amplification, integration, spike counting, zero crossing, RMS, signal averaging, and power spectral analysis. This section will discuss some of the various methods of processing the raw EMG signal.

Although not commonly thought of as a stage of signal processing, the type and position of the electrodes change the characteristics of the signal. As mentioned earlier, surface electrodes act as low pass filters. In other words, the high frequencies are removed and a smoothing of the curve takes place. The peaks of the spikes are more rounded, as well as being at a decreased amplitude when they are compared with the signals obtained with needle electrodes. However, this phenomenon does not necessarily cause great concern, particularly if the limitations of surface electrodes are observed. The positioning of the electrodes also plays a role in pre-processing the signal. Two electrodes are generally used to obtain the EMG signal (bipolar) with the voltage difference

between them being amplified and further processed. This method has the advantage of removing the undesirable "noise" picked up equally by both electrodes, such as 60 Hz interference, movement artifacts, or ECG artifacts.

One common technique employed in processing the raw EMG signal is that of first rectifying and then integrating the signal. Since integration represents the area between the signal and the time axis and is a continually increasing function of time, the signal must first be rectified since the area between the raw EMG signal and the time axis is essentially zero. A single number representative of the entire EMG waveform may be obtained by integrating for a specific time period rather than integrating the entire waveform continuously. The mean of the rectified and integrated EMG can also be found. This has been shown to be an approximate linear relationship to muscle tension for isometric (Lippold, 1952) and isotonic (Bigland et al., 1953) contractions. Equation 2 is the mathematical formula used in deriving the integrated rectified EMG signal in which the raw EMG is designated as $s(\tau)$ and the integrated rectified EMG is designated as $i(\tau)$ (Basmajian et al., 1975).

$$i(\tau) = \int_0^t |s(\tau)| d\tau$$

Equation 2 Mathematical integrated rectified EMG

Another commonly used EMG processing technique is that of obtaining the true RMS (root mean square) of the signal. In this technique, the signal is first squared, integrated, and then multiplied by 1/t, where t represents the time along the x-axis in which the EMG signal is of interest. The square root is then taken to yield $s_{rms}(t)$. Equation 3 shows the mathematical formula used in deriving the true rms EMG signal (Basmajian et al., 1975).

$$S_{rms}(t) = \sqrt{1/t \int_0^t S^2(\tau) d\tau}$$

Equation 3 Mathematical true rms EMG

Finally, a technique which seems to be quite popular due to its ease of application in processing the raw EMG signals obtained during manual wheelchair propulsion as well as arm cranking exercises (Harburn and Spaulding, 1986; Newall et al., 1981) is that of rectifying and then smoothing the EMG waveform. This technique is sometimes referred to as the "rectified linear envelope" and has been shown to closely resemble the muscle tension curve (Harburn and Spaulding, 1986). Smoothing can consist of a number of techniques from signal averaging to low pass filtering, either digitally or using analog filtering equipment. Unfortunately, the exact smoothing schemes used

are often not reported in the literature, and it is, therefore, up to the individual researcher to determine when adequate smoothing of the signal has taken place.

Normalization

It is not prudent to compare the absolute values obtained from the raw EMG signals between subjects due to many variable subject characteristics such as muscle size, skin impedance, force generation within the muscle, cellular structure, etc. All of these have an effect on the EMG voltage. It is necessary to scale the raw EMG data for each subject to a normalized value for that subject. The maximum voluntary contraction (MVC) or other contraction condition known to produce the same signal strength each time it is performed can be used. The maximum voluntary contraction is the most frequently used signal for this determination. EMG signals obtained at less than the maximum may also be used as long as each subject experiences the same testing conditions as the other subjects and the normalization signal is reproducible (Basmajian et al., 1975). Once the normalization signal is obtained, the experimental signal is then divided by the normalization signal to yield values which represent the normalized signal. This allows comparisons to be made between subjects based on each subject's normalized EMG values.

Basmajian and DeLuca (1985) warned against the use of isometrically determined maximum voluntary contractions in conjunction with an EMG

obtained when the length of the muscle is changing. When a muscle is allowed to change in length (anisometric), several factors come into play which are not relevant during an isometric contraction. The skin may change its position relative to the contracting muscle fibers, thus moving the surface electrodes relative to the motor end plate of the muscle, changing the EMG signal amplitude. It is also known that the force output of a muscle is dependent upon its length, with maximal force generated when the muscle is 1.2-1.3 times its resting length. An isometrically determined MVC may not be taken with the muscle at an optimum length, thus resulting in the anisometric EMG amplitude being larger than the MVC. This may not be a problem, as long as the isometric MVC is repeatable and is conducted in a manner that is representative of the dynamic situation. In manual wheelchair propulsion, great care must be taken in recording an isometric maximum voluntary contraction. With the subject pushing on the handrims isometrically, agonist-antagonistic muscle activity may come into play due to stabilization of the joints and, thus not reflect actual wheelchair propulsion characteristics. Furthermore, there may be a neural mechanism that inhibits the recruitment of all available motor units under isometric conditions (Newall et al., 1981). For these reasons, normalization will not be used to attempt to quantify EMG signal amplitudes in this study.

Temporal analysis

Sometimes it is not desirable to process the raw EMG signal. For example when determining the muscle activation and deactivation points correlated with a known movement pattern, it is usually sufficient to determine when the muscle is active by merely plotting the raw EMG signal against a tracing of the known movement pattern. However, if the signal contains excess noise or if it is not easily apparent when the muscle is activating or deactivating, it may be necessary to process the raw EMG signal using one of the techniques discussed earlier.

EMG studies involving wheelchair propulsion and arm ergometry

Relatively little work has been done pertaining to electromyography during manual wheelchair propulsion. Temporal studies, in which the raw or rectified smoothed signal is used to correlate muscle activity with specific portions of the propulsion cycle, have been conducted (Ross and Brubaker, 1984). Other investigators have attempted to use electromyography to compare relative amplitudes of the EMG signal, usually expressed as a percent of MVC, between groups of subjects (Harburn and Spaulding, 1986). However, as discussed above, comparisons in this way are questionable, particularly when using a maximum voluntary contraction obtained statically (isometrically) in conjunction with dynamic movements. Several EMG studies have been conducted in which muscle activity during arm cranking and bilateral sanding

exercises (Spaulding and Robinson, 1984) as well as diagonal exercise movements resisted by weight-and-pulley circuits (Ekholm et al., 1978; Antti, 1977) have been investigated. Finally, the role of the diaphragm in trunk flexion and extension has been investigated by electromyographic techniques (Sinderby et al., 1992a; Sinderby et al., 1992b) No studies have been conducted in which frequency analysis has been used to determine the extent of muscular fatigue during manual wheelchair propulsion. This would be indicated by a decrease in the EMG frequency with increasing fatigue (Petrofsky, 1979). A recent study has shown muscular activity over a greater portion of the propulsion phase when the subjects were fatigued (Rodgers et al., 1994). Fatigue analysis may be useful in optimizing wheelchair designs for wheelchair racers or in assessing the functionality of a wheelchair for individuals with low level quadriplegia or high level paraplegia. In these cases only a few muscles may be functional for propelling the wheelchair, therefore there would be a higher strain on them which would possibly induce fatigue.

Temporal analysis used in manual wheelchair propulsion research

Ross and Brubaker (1984) used electromyography to determine the temporal sequences of EMG activity of several muscles at power outputs of 20 and 40 watts. The muscles monitored were thought to be involved in wheelchair propulsion and included the brachioradialis, biceps brachii (long head), triceps

brachii (lateral head), pectoralis major (clavicular head), anterior deltoid, posterior deltoid, seratus anterior, and the trapezius (upper fibers). The subjects were three paraplegics (T8-9 to L1) and three physically normal subjects. Plots of the raw EMG data with respect to the handrim torque were used to determine the muscle activity associated with each part of the stroke cycle. The total muscular activity was found to be greater for the 40 watt condition for most of the muscles in most of the subjects. The EMG patterns also suggested that a pull-push type of propulsion stroke pattern was being used by the subjects. However this finding has not been substantiated consistently (Veeger et al., 1991). The pectoralis major and the anterior deltoid were found to be the most active muscles during the propulsion phase of the stroke, consistent with the findings of Veeger et al. (1991). The other muscles show varying degrees of activity throughout the propulsion and recovery phases of the stroke. There were no apparent differences in the EMG patterns between the wheelchair dependent and able-bodied subjects. However, these wheelchair dependent subjects could use most of their abdominal muscles to help support their trunks and thus required very little upper body musculature to accomplish this. Wheelchair dependent subjects whose lesion levels are higher (T4-6) have little abdominal support, and it may be found that the muscles of the arms, chest, and upper back are used for trunk support and may, thus, exhibit slightly different EMG patterns during the propulsion stroke.

Harburn and Spaulding (1986) used electromyography to monitor muscle activity in the pectoralis major, biceps brachii, anterior, middle, and posterior deltoids, medial triceps brachii, and lateral triceps brachii. Three able-bodied persons, three persons with paraplegia, and three persons with quadriplegia (C5 and C6) were studied. The raw EMG signals were rectified and smoothed and were plotted as a percentage of an isometric maximum voluntary contraction obtained earlier. No attempts were made to associate muscle activity to phases of the propulsion stroke. Muscle activity over the entire stroke was considered. It was found that the most active muscles were the middle and posterior deltoids and the triceps brachii. It was also found that the persons with quadriplegia used the highest percentage of their MVC in performing the propulsion stroke, with the paraplegic and normal subjects following. It was suggested that the persons with quadriplegia need to use more of their available motor units in their available muscles in order to compensate for lost muscle function, thus taxing them to complete the stroke. This theory also applies to the paraplegic group, although to a lesser extent. However, as discussed earlier, normalization of EMG signals during dynamic movements in which the MVC was taken statically may be in error, thus invalidating these results.

MATERIALS AND METHODS

The design and calibration of the dynamometer used in this study is presented in this section. Materials and methods pertinent to the subject testing conducted are also presented here. Recommended dynamometer improvements are presented prior to discussing the subject testing.

Wheelchair Dynamometer

In order to provide a stationary platform to study manual wheelchair propulsion, as well as to provide a means for determining power output, a wheelchair dynamometer was constructed. The design of the dynamometer was based upon a previous design by O'Reagan (1978) at the University of Virginia. Several modifications were made to accommodate the present study.

Rollers

The dynamometer consists of two 4" diameter aluminum rollers in which the rear wheels of the wheelchair rest. These rollers are supported by self-aligning bearings so that, as the wheelchair wheel rotates, the rollers turn and allow the wheelchair to remain stationary. Thus, the tangential velocities of the wheelchair and rollers are equal, assuming no slippage at the interface between the wheelchair wheel and the roller. Experimentation found this to be a good assumption, with only a modest amount of weight in the wheelchair, even under conditions of high acceleration. The bearings were originally grease-packed.

However, this introduced a large resistance to the propulsion effort so the grease was removed and replaced with a lighter weight sewing machine oil. This reduced the bearing frictional losses dramatically, resulting in a much more realistic simulation of wheelchair propulsion under normal conditions.

Loading platform

A loading platform was constructed to support the front wheelchair castors and to enable loading and unloading of the wheelchair from the dynamometer. It was initially found that the wheelchair tended to drift sideways and ultimately off the edge of the rollers while being propelled. To remedy this, the castor bearings were tightened to prevent rotation. Loading ramps were also constructed to provide access for the wheelchair dependent subjects.

Alternator

Since the main purpose of the dynamometer was to determine power output, it was necessary to measure the amount of force or torque applied to the handrim of the wheelchair. Since extensive wheelchair modification would be necessary to monitor the force on the handrims directly, a strain-gaged alternator assembly and power supply were used in order to apply a resistance to the front roller and to monitor the amount of force produced at the wheelchair handrim. The alternator consisted of an automobile alternator with the alternator shaft (rotor) supported by the self-aligning bearings as described

above. The rotor was coupled to the front roller of the dynamometer via a timing belt and two sprockets, one on the roller shaft and one on the rotor. Several gearing combinations were tried. However, the combinations producing the best strain gage signal also produced the greatest resistance to propulsion. It was therefore concluded that an 11.4 cm. diameter sprocket on the alternator rotor, combined with a 5.7 cm. sprocket on the front roller shaft would provide both a realistic resistance to wheelchair propulsion as well as an adequate strain gage signal.

A power supply was used to provide an electric current to the field coils of the alternator to provide the resistance to propulsion. As the wheelchair was propelled the rotor turned and, because of the magnetic coupling between the windings and the alternator housing, the housing tried to turn with the rotor. However, the movement of the alternator housing was prevented by a strain-gaged steel arm, rigidly attached to the alternator housing and pinned at the opposite end. Thus, as the alternator housing attempted to rotate, the steel arm bent, yielding a strain gage response which was linearly related to the amount of force applied to the handrim of the wheelchair. Therefore, knowing the strain gage output voltage allowed calculation of the force applied to the wheelchair handrim for the calculation of power output.

Strain gages

In order to monitor the torque applied to the handrims, a strain-gaged steel arm was constructed. The steel arm was rigidly attached to the alternator housing on one end and pinned at the other, allowing rotation of the beam to follow the motion of the housing, as explained above. In other words, the steel arm could be modeled as a cantilever beam on one end and a pinned connection at the other. Two strain gages (MicroMeasurements EA-06-125PC-120, Raleigh, NC) were mounted on each side of the beam, each being a component of a full bridge circuit. These gages were chosen based upon availability and size, with four gages implemented to increase the output signal and reduce the nonlinearity which exists with only one gage (Starr, 1992). As the steel arm bends due to rotation of the alternator housing, the strain gages resistances change, causing small changes in voltage from the resting state. This signal was then fed into a strain gage signal-conditioning component (Analog Devices 1B31, Norwood, MA) which was wired to provide the desired gain, bridge balancing, and filtering functions needed before sending the signal into the computer for data acquisition and analysis. This component was chosen to allow the strain gage circuitry to become a permanent part of the dynamometer system without having to acquire strain gage amplifiers and filters each time the dynamometer was to be used. The circuit was permanently soldered to a breadboard and mounted inside an instrumentation box for exclusive use with the dynamometer.

Velocity Measurement

In order for the subject to obtain velocity feedback, as well as to provide velocity information for computer analysis and power calculations, a velocity measurement circuit was constructed for use with the wheelchair dynamometer. The circuit consisted of three main components: a slotted disk, an optointerrupter module, and a display panel.

Slotted disk

The disk was the only mechanical component in the system and was the component which generated the pulses needed for velocity calculations. It consisted of a 3" diameter aluminum disk with 6 slots cut around the outside edge. The disk was rigidly mounted to the rear roller axle of the dynamometer and thus had an angular velocity equal to that of the rear roller. The number of holes drilled was chosen carefully to avoid the counter incrementing past 99, but to still allow the use of the entire range (0-99) during normal wheelchair operating speeds of 0.56 to 1.11 m/s (Lemaire et al., 1991). The use of aluminum resulted in a lightweight yet rigid disk which did not significantly increase system friction. Other velocity measuring devices, such as tach-generators, which were used in the O'Reagan (1978) design, increase system friction.

Optointerrupter module

The conversion of rotational motion into electrical pulses was accomplished through the use of an optointerrupter module and Schmidt trigger. The optointerrupter consists of an infrared emitter and detector pair. As the holes in the disk rotated through the infrared signal, pulses were generated at the detector. The Schmidt trigger was then used to square and invert the pulses for use by the counting and display circuitry. Figure 5 shows the relationship between the velocity disk and the optocoupling device circuit.

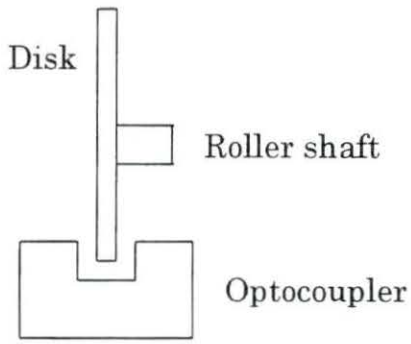

Figure 5 Velocity optocoupler and disk relationship

Display panel

A display panel was constructed and mounted directly in front of the subject for continuous monitoring of velocity. The panel consisted of a dual 7-segment LED module, an on/off switch, an on/off LED indicator, and an update LED indicator. Digital circuitry accomplished the counting, updating, and displaying

functions. The pulse outputs from a Schmidt trigger were input to an AND gate, along with a timer generated pulse of duration 3.5 seconds with a duty cycle of 3.5 seconds. The output of the AND gate went high as long as both inputs were high. This occurred during the 3.5 second timer interval in conjunction with each Schmidt trigger pulse. Thus, counting took place for 3.5 seconds and was then updated each 3.5 seconds. This was found to be an appropriate update time to allow the subject to make adequate velocity compensations to velocity changes. The output of the AND gate was then fed into a counter/latch/driver chip which incremented during each high output from the AND gate, stored the results of the count in a latch, and dumped the latch contents to the driver upon a clock input each 3.5 seconds. Thus, the result of the previous count was displayed while the next counting sequence occurred.

Although the use of a digital bicycle speedometer was initially considered, it became apparent that the velocity characteristics of a wheelchair are significantly different from that of a bicycle. A bicyclist typically holds a relatively constant velocity, thus obtaining instantaneous velocity feedback. However, the velocity characteristics of a wheelchair are cyclical in nature. An instantaneous velocity reading such as that obtained from a commercially available bicycle speedometer would be inadequate; therefore, a relatively long update period of 3.5 seconds was used in the design of the velocity counting circuitry.

Velocity calculation

Using the number of holes on the disk, the roller and wheelchair wheel and handrim diameters, and the counting interval (3.5 sec), the average velocity over the counting interval was computed. For example, for an LED readout showing the number "68", the wheelchair handrim velocity is found by dividing the velocity display by the time interval (3.5 sec) and then by the number of pulses per revolution (6), giving 3.24 rev/sec of the rear roller. Since the wheelchair wheel diameter is 0.62 m and the roller diameter is 0.10 m, the angular velocity of the wheelchair is 3.24 rev/sec ÷ 6.2 = 0.52 rev/sec. This is also equivalent to the angular velocity of the wheelchair handrim. Since handrim circumference is πd = 1.70 m, the linear velocity of the wheelchair handrim was 0.52 rev/sec x 1.70 m/rev = 0.88 m/sec.

Thus, it can be seen that by taking into account the various constants used in the above calculation, the velocity V (m/s) = 0.0129 x LED readout. It should be noted that since it was assumed that the propulsion force was applied at the wheelchair handrim, the handrim velocity must also be used in the computation of power output.

Power Measurement

In order to compute the propulsion efficiency, both the metabolic power input and the power output (work done per unit time) must be known. As explained

in the literature review, the metabolic power input can be obtained from oxygen uptake readings. However, the power output is the product of the linear velocity and the applied force to the wheelchair handrim. In other words, the power output is the product of a known resistance to propulsion and the rate at which that resistance is overcome. The velocity can be held relatively constant at the desired setting by the use of the digital display circuit discussed above. Although instantaneous handrim force values cannot be controlled by the subject, the average force applied to the handrims over the data sampling period could be calculated from knowledge of the strain gage mean voltage obtained. Therefore, it was possible to compute the average power output over the time interval sampled.

It was found that the strain gage output was linearly dependent upon both the velocity of the wheelchair and the force applied to the rim of the wheelchair. (See calibration section which follows.) The average force applied to the handrim of the wheelchair at a given mean velocity will be the same from individual to individual, regardless of the stroke frequency or technique. This is an important consideration since power = force x velocity. Since the force applied to the handrim can be determined from a knowledge of velocity only, force = kv, where k is a constant. Thus, power = kv^2. This indicates that once the strain gages on the dynamometer have been initially calibrated, the power output can be determined from a knowledge of the velocity only. However, the

strain gage output was sampled independently of velocity in order to verify that the propulsion resistance remained unchanged from subject to subject. In calibrating the system the relationship between applied force and strain gage output was determined, rather than the relationship between velocity and strain gage output.

System Calibration and Analysis

Strain gage linearity

In order to verify that the strain gage system was wired correctly and that all components were operational, a linearity check was made by applying known moments at the gages and observing the output voltage responses. A linear strain gage response was expected because one of the characteristics of a strain gage is that the change in resistance of the gage varies linearly with strain for most materials on which the gage is mounted (Starr, 1992). However, this assumption is valid only as long as the material to which the strain gage is mounted remains within the elastic range of strain. If the material is strained above the elastic limit, permanent deformation takes place, and the gage response will no longer be linear.

In order to verify the strain gage linearity, a wooden arm was constructed and mounted on the opposite side of the alternator housing from the gaged steel arm. Known weights were then hung from this arm, causing the housing to

rotate, and, because the steel arm was pinned, a moment was generated at the strain gages on the steel arm. A moment at the gages caused them to change their resistance, unbalancing the wheatstone bridge and resulting in a voltage difference across the bridge. This was amplified and displayed on a digital multimeter. This voltage response was then monitored for various weights on the wooden arm and a plot was constructed. Figure 6 shows the linear characteristics of the strain gage system with increasing moment at the gages.

Since known weights large enough to generate the desired voltage output of 3.5 volts were not available, pennies were used in increments of 27.5 grams (0.2698 N). This is equivalent to 10 pennies. This allowed moments at the gages to vary between 0.022 N-m (+0.07 volts) and 0.904 N-m (+3.51 volts). It

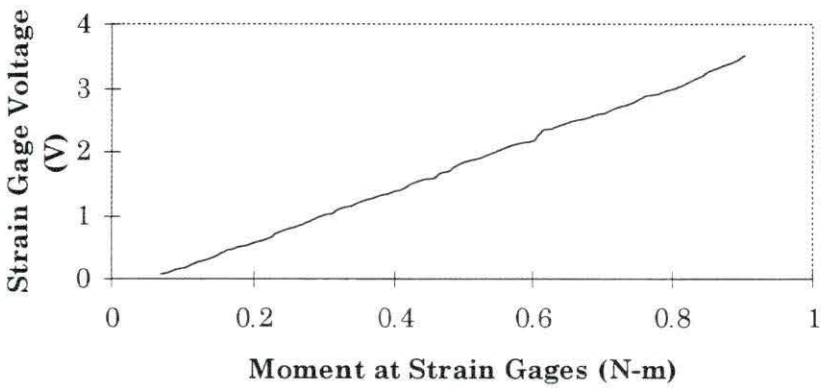

Figure 6 Strain gage voltage response to increasing moment at gages verifying strain gage linearity

was previously determined that a voltage output of 3.5 volts was well above that generated during a maximal propulsion effort (approximately 2.5-3.0 volts based upon pre-test experimentation). Furthermore, it can be shown that, at a voltage output of 3.51 volts, the steel arm was still being stressed within the region of elastic deformation. As previously stated, the moment at the centerline of the gages was maximized at 0.904 N-m. Since $\sigma = Mc/I$, where σ is the stress occurring at the beam surface, M is the moment at the strain gages, c is the distance from the neutral axis of the beam to the surface (1/2 h), and I is the second moment of area of the beam about the neutral axis (1/12 bh^3). Solving for σ yields $\sigma = 0.9038(0.0012)/7.3728E^{-12} = 147.1$ MPa. Since the elastic strength of 1018 steel is approximately 430 MPa, the surface of the beam remained within the elastic region. Knowing the stress at the gages, as well as the modulus of elasticity, E, of the material (210×10^9 Pa), the strain was calculated as $\varepsilon = \sigma/E = 147.1 \times 10^6/210 \times 10^9 = 700$ $\mu\varepsilon$ (microstrain) per gage.

Figure 7 shows the testing arrangement and the pertinent dimensions needed to calculate the moment at the strain gages given a known weight suspended from the wooden arm.

The moment at the strain gages was given by $W(L_1/L_2)L_3$ where W is the weight in Newtons, L_1 is the distance from the end of the wooden beam to the alternator bearing center (0.13 m), L_2 is the distance from the alternator bearing center to the pin on the steel arm (0.15 m), and L_3 is the distance from the steel

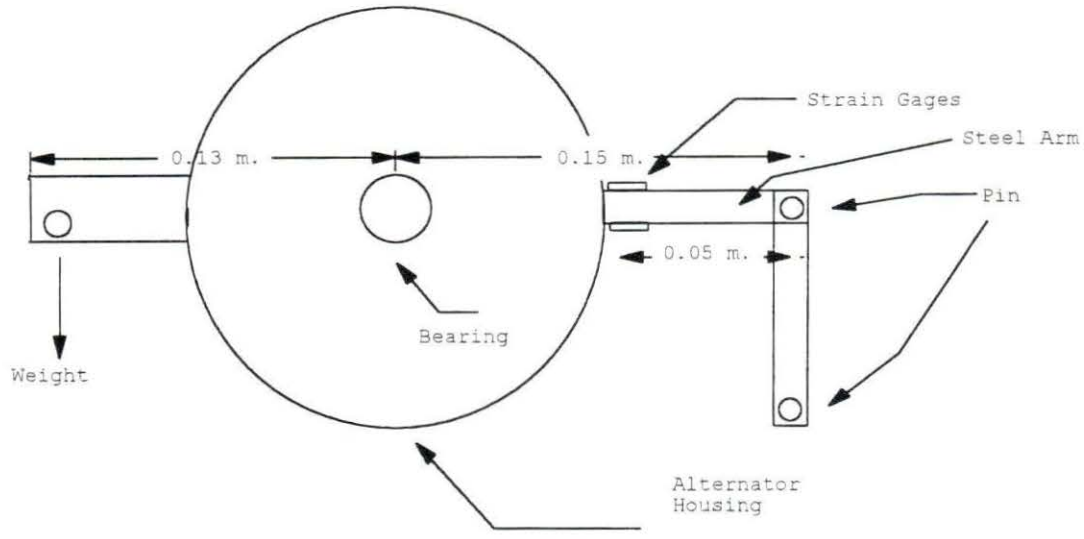

Figure 7 Alternator assembly and dimensions used in verifying linear strain gage response to increasing moment at the gages

arm pin to the strain gage centerline (0.05 m). This gave M_{gages} = W(0.13/0.15)0.05 = .04W.

Voltage response to velocity

It was observed from studying the voltage output curves during several practice trials that the voltage output was cyclic in nature and was highly correlated with the propulsion cycle. The voltage output rose during the propulsion phase and fell again during the recovery phase. This indicates that, given a constant current source going into the alternator, the resistant magnetic field fluctuates according to the angular velocity of the rotor resulting in

increased magnetic coupling and an increased bending moment at the strain gages. Thus, the resistant torque is related to the velocity of propulsion.

The relationship between velocity and strain gage voltage output and body weight needed to be determined at a given velocity. In order to make this determination, three individuals of different body weights were asked to maintain velocities of 40-100 in increments of 10 on the velocity display and the mean voltage output was noted as calculated by the LabWindows® software. Three trials at each velocity level were conducted, and the results averaged at each velocity level to produce seven velocity-voltage output data points for each subject. These points were plotted and a linear regression was performed on the data, resulting in linear relationships for all three subjects. Table 1 depicts the averaged values for each velocity level used in determining the velocity-voltage relationship.

One of the objectives in conducting these tests was to determine if body weight had a significant effect on the voltage output at a given velocity. The Tukey test for multiple comparisons (Neter et al., 1990), using an alpha level of 0.05, or significance at the 95% level, was used. The results of these tests showed that, while significant differences in the mean strain gage voltage output between the subjects existed in two cases (see Table 2), the mean strain gage output was predictable knowing the velocity of propulsion. This was expected since voltage output is only a function of the angular velocity of the

Table 1 Strain gage voltage response to dynamometer velocity display

	Subject C1		Subject C2		Subject C3	
Goal Vel.	Ave. Vel.	Ave. Volt.	Ave. Vel.	Ave. Volt.	Ave. Vel.	Ave. Volt.
40	39.9	0.85	43	0.86	41.6	0.83
50	49.7	1.04	50.5	1.07	51.7	1.05
60	59.3	1.30	61.8	1.22	61.1	1.19
70	68.7	1.42	71	1.45	70.2	1.28
80	77.4	1.63	78.6	1.53	77.9	1.39
90	90.9	1.88	89.9	1.71	91	1.63
100	99.3	1.96	98.4	1.81	101.8	1.74

Table 2 Significant differences found between subjects according to the Tukey test of multiple comparisons, $\alpha = 0.05$

	Subject C1	Subject C2
Subject C1	N/A	
Subject C2	Vel. 40	N/A
Subject C3	Volt. 80, Volt. 90	Vel. 100

alternator rotor which has no dependence upon the weight of the individual in the wheelchair. The Tukey test revealed significant differences between subjects at the 80 and 90 velocity levels. However, the velocity tests showed that the subjects maintained the same velocities at both levels. Therefore, it is most likely that the differences can be attributed to errors in reading the velocity display or in velocity display readings inconsistent with the time period over which the data was collected, which was possible since the velocity display update time (3.5 sec) and the period of data collection (5 sec) were not the same. Thus, it is possible that velocity fluctuations which occurred outside of the data collection period may have resulted in velocity display readings not actually reflecting the velocities maintained during the data sampling period. Even with these differences, the system was highly reliable as the measurement error was only 2/21 or 9.5%. In addition, the Tukey test of multiple comparisons yielded no significant differences in any of the mean strain gage voltage responses at the $\alpha = 0.01$ level.

The Tukey test of multiple comparisons was also conducted on the velocity display data to ensure that each subject maintained the same average velocities as compared with the other two subjects. Again, no significant differences were found between velocity levels except at the 40 and 100 levels (see Table 2). This was an interesting finding in that these represent the lowest and highest velocity levels tested. These velocity levels were particularly difficult for the

subjects to maintain. The 40 level seemed abnormally slow while the 100 level was rather fast. Therefore, the ability for the subject to reliably maintain these velocity levels was diminished. Again, these differences were not significant at the $\alpha = .01$ level. These findings are significant in that the mean voltage output can be predicted by knowing only the mean velocity during the period of time under study.

As previously stated, the mean voltage output was found to be linearly dependent upon the mean velocity level for each of the three subjects. Figure 8 shows the results obtained after averaging the velocities and mean strain gage outputs for all three subjects. Plots of the results of individual subjects can be found in Appendix B.

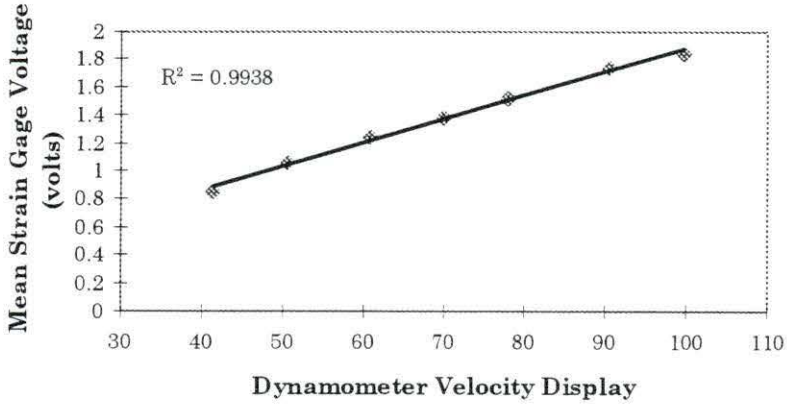

Figure 8 Mean strain gage voltage response to wheelchair velocity, subjects pooled and averaged

Voltage response to handrim force

The relationship of handrim force to strain gage voltage output was found in calibrating the dynamometer. However, prior to calibration, it was necessary to determine whether subject characteristics such as body weight and mass distribution were influential in determining the strain gage voltage output arising from a known force to the handrim. In order to determine this, four subjects of varying body weights were seated in the wheelchair. A string was wrapped around the spacers separating the handrim from the wheelchair wheel and a spring scale attached. With the subject seated in the chair, the wheelchair was set into motion by attempting to maintain a constant force on the spring scale while walking away from the dynamometer. The subject was seated in the wheelchair merely to provide a known weight to the system. A five second sample of data was collected, and the mean strain gage voltage output calculated and plotted with respect to the force applied. Since it quickly became apparent that it was difficult to maintain a constant force on the spring scale while walking, ten trials were done at each force level and the results averaged at each force level. Four force levels were attempted (4 lb - 8 lb) for each person. The tests were also repeated with no weight in the wheelchair. However, the 8 lb condition could not be completed in this case since the wheelchair tires began slipping on the rollers due to a small normal force acting on the rollers to

maintain a sufficient amount of friction between the tire and roller to prevent slipping.

Linear regression analysis showed that the mean strain gage voltage output was linearly related to the applied force on the wheelchair handrim for all cases tested. Figure 9 shows the results obtained from subject CA4. The large amount of variability between the responses at each force level was most likely the result of errors in maintaining constant forces on the spring scale while propelling the wheelchair. The plots for the other cases tested can be found in Appendix B.

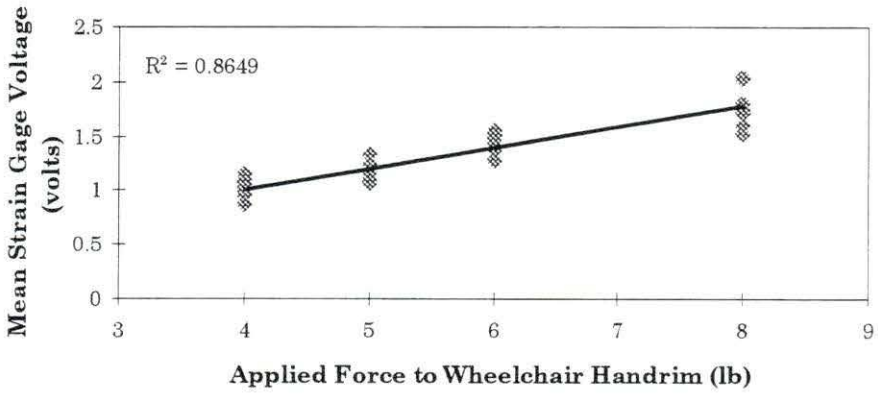

Figure 9 Mean strain gage voltage response to applied force at the wheelchair handrim, subject CA4, all points plotted

Figure 10 shows an improved linear relationship when the strain gage voltage outputs are averaged at each force level.

While Figure 9 and Figure 10 demonstrate the highly linear relationship between handrim force and mean strain gage response, it was also necessary to test whether the same calibration curve could be used for all subjects, regardless of body weight. In order to verify this, a statistical analysis was undertaken

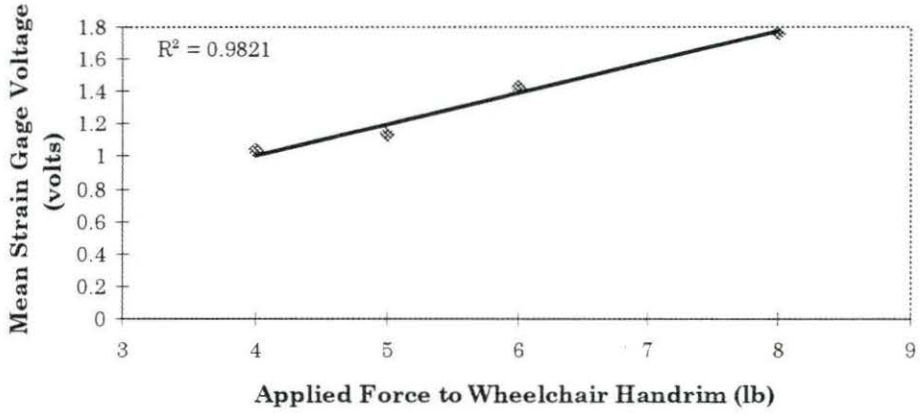

Figure 10 Mean strain gage voltage response to applied force at the wheelchair handrim, subject CA4, averaged responses

using the Tukey method of multiple comparisons at each force level tested. Significance was set at the 95% confidence level for these tests, with the mean strain gage voltage being the factor studied. The results showed no significant differences in mean strain gage response between the subjects at any of the force levels. Thus, it was decided that the same calibration curve would be used for

all of the subjects in determining the amount of force applied to the wheelchair handrim based on the strain gage output observed. Figure 11 verifies the statistical findings visually. Each of the mean strain gage outputs at each force level is very close to the others for all of the subjects tested.

Since the mean force applied to the wheelchair handrim can be calculated with only a knowledge of the mean strain gage voltage, regardless of subject

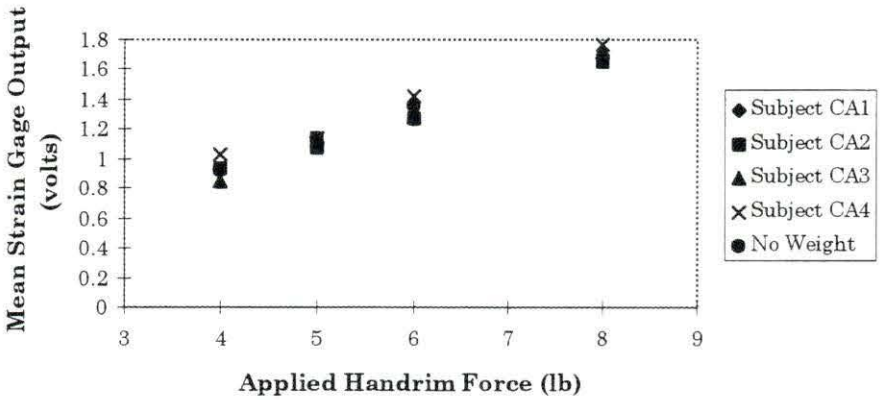

Figure 11 Mean strain gage voltage response to applied force at the wheelchair handrim, all subjects, averaged responses

differences, all of the trials at each force level could be pooled to find the appropriate constants to relate the strain gage voltage to the handrim force. Averaging all of the trials at each force level results in the plot shown in Figure 12. The value of $R^2 = 0.9995$ indicated a highly linear relationship between handrim force and mean strain gage output. However, this curve was not used

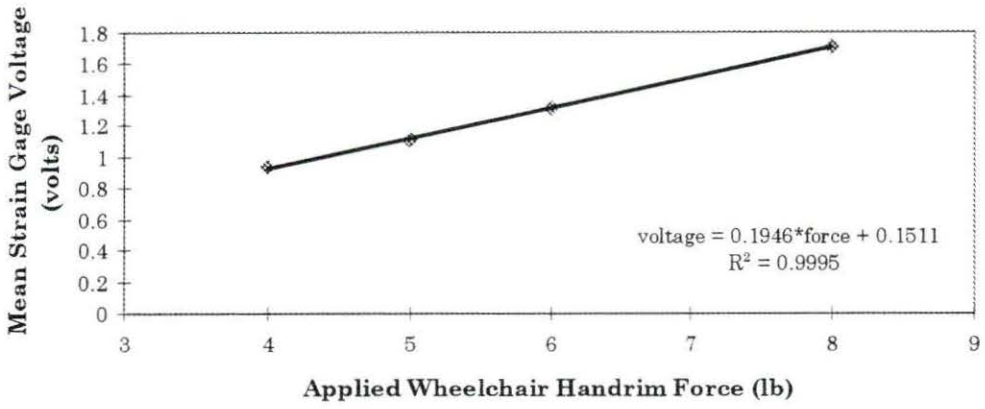

Figure 12 Mean strain gage voltage response to applied force at the wheelchair handrim, pooled subjects, averaged responses

in the final calibration of the dynamometer since the tests were run prior to moving the dynamometer to the location of the study.

Final strain gage calibration

The wheelchair dynamometer was calibrated again after moving it to the location of the study. This recalibration was necessary to account for changes in the alternator orientation, belt tension, or strain gage gain or balance that may have occurred in transport. In addition, recalibration was necessary since the strain gage amplifier gain was adjusted slightly while testing the operation of the strain gage amplification circuit.

The final calibration of the dynamometer was conducted in the same manner as explained earlier, using a spring scale and string wrapped around the

wheelchair handrim spacers. However, since the mean strain gage voltages obtained at a given spring scale force were statistically identical regardless of the subject used, only two subjects were used in this final calibration. Four force levels were used (5, 6, 8, 10 lb). The 10 lb. level was added in this calibration because it was not previously possible to conduct tests at this force level due to space limitations. Five tests were done at each force level. The results are shown in Figure 13. As can be seen from Figure 13, the mean strain gage voltage is highly linearly dependent ($R^2 = 0.995$) upon the applied force to the wheelchair handrim. The equation relating the mean strain gage output to the applied force is: mean s.g. voltage = 0.2663 x applied handrim force - 0.1201. Since 1 lb = 4.448 N, the above equation can be expressed in terms of S.I. units as: mean s.g. voltage = 0.0599 x applied handrim force - 0.1201. Because the

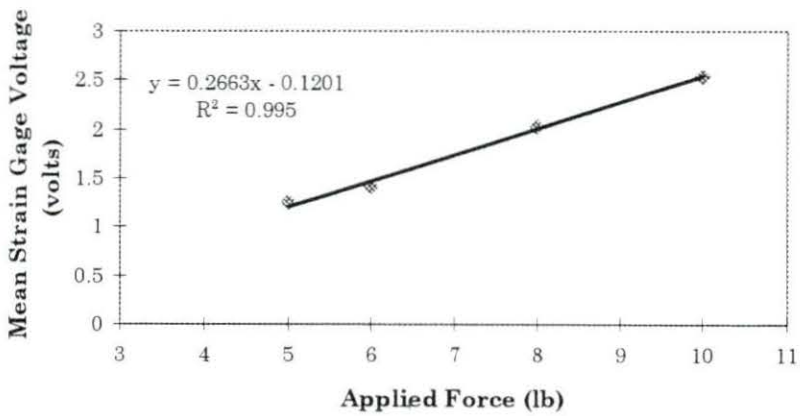

Figure 13 Mean strain gage voltage response to applied force at the wheelchair handrim, final calibration, pooled and averaged subjects

objective of the dynamometer calibration was to determine the amount of force applied to the wheelchair handrim from knowledge of the mean strain gage voltage output, the equation was rearranged to give: mean handrim force (N) = mean s.g. voltage (volts) ÷ .0599 + 2.005.

Further dynamometer modification would be beneficial, particularly equipping it to maintain a constant resistance regardless of alternator rotor velocity. This would entail monitoring the strain gage output voltage and using this voltage to vary the electric current to the alternator accordingly. This would enable studies to be conducted in which velocity and resistance could be varied independently of one another. Inertial study of the dynamometer would also be valuable to enable acceleration and deceleration characteristics to be simulated by adding or removing inertial disks in order to achieve equivalent inertia levels normally experienced during wheelchair propulsion.

Subjects, Equipment, and Testing Protocol

Subjects

The subject pool consisted of ten male volunteers ranging in age from 24 to 36. Five of the subjects were able-bodied while the other five were wheelchair dependent individuals residing in the Ames, Iowa area. Since the purpose of this study was to compare able-bodied individuals with wheelchair dependent individuals, males were used to eliminate any variability due to gender.

Research has shown that VO_{2max} and stroke volume are higher in males than in females at equivalent work loads, even when corrected for differences in body weight (Hjeltnes, 1993). Each subject was informed of the purpose of the study and the risks involved and their rights to terminate participation. Each subject read and signed a statement of informed consent prior to testing. The study was approved by the University Human Subjects Review Committee (Appendix E). Table 3 shows the pertinent subject data. No significant differences in body weight, shoulder to elbow distance, elbow to wrist distance, trochanter distance, or elbow angle were found between the two subject groups.

Wheelchair

The wheelchair used in this study was an Everest & Jennings 18" standard hospital grade chair. It was obtained from the Woodward State Hospital Adaptive Equipment Center (Woodward, Iowa). The seat and back were removed and replaced with custom-built solid replacements to provide greater support for the subjects. Additional handrim spacers were added providing a framework for the calibration string to be wrapped around the wheel.

Strain gage and EMG data collection

The collection and processing of the strain gage voltages and EMG signals used a data acquisition card (National Instruments AT-MIO-16) in conjunction with a graphical user interface package (National Instruments Lab Windows®).

Table 3 Subject data

Subject	AB-1	AB-2	AB-3	AB-4	AB-5	Average	Std. Dev.
Age	28	26	25	25	24	25.60	1.52
Weight (lb)	210	185	145	165	185	178.00	24.39
Shoulder to Elbow (cm)	38	36	32	38	37	36.20	2.49
Elbow to Wrist (cm)	28	25	24	25	26	25.60	1.52
Trochanter Distance (cm)	10	10	8	8	9	9.00	1.00
Elbow Angle	115	120	120	110	110	115.00	5.00
Exercise	No	Yes	Yes	No	No		

Subject	WD-1	WD-2	WD-3	WD-4	WD-5	Average	Std. Dev.
Age	33	33	30	31	36	32.60	2.30
Weight (lb)	170	205	165	210	140	178.00	29.28
Disorder*	T4	T5	T5	T5	OP		
Time in Chair (years)	14.5	7	7	15	33	15.30	10.63
Shoulder to Elbow (cm)	38	36	30	36	33	34.60	3.13
Elbow to Wrist (cm)	28	28	27	24	27	26.80	1.64
Trochanter Distance (cm)	9	10	11	10	8	9.60	1.14
Elbow Angle	100	110	110	115	105	108.00	5.70
Exercise**	Yes	No	No	No	No		

* T-thoracic vertebra, OP-Osteogenesis Imperfecta (brittle bone disease)

** Three or more days per week, at least 20 minutes per day

A computer program (Appendix F) was written for Lab Windows® to perform all of the data collection, filtering, plotting, and data saving and retrieving functions. The data was sampled at a rate of 1000 samples per second for a period of five seconds. This yielded two to six complete propulsion cycles per sampling period. A low pass Butterworth digital filter was used at 3 Hz on the raw strain gage data to eliminate the noise caused by the alternator windings. This same filter was used during the force calibration prior to determining the mean strain gage voltage. Therefore, identical data processing techniques were used for the calibration and the experimental data. Following data collection, the raw data was saved in ASCII form to disk for later analysis. A light emitting diode (LED) was wired to the digital out port of the data acquisition card and was programmed to remain on during the data acquisition period. This LED was in view of the videocamera to allow the time interval in which the data acquisition occurred to be found on the videotape.

EMG equipment

Miniature silver-silver chloride bipolar surface electrodes (Beckman 11 mm, Anaheim, CA) were used for both muscles and the ground electrodes. Electrode gel (Sensor Medics, Yorba Linda, CA) was used in conjunction with the electrodes to lower the electrical resistance. The electrodes were held in place with adhesive disks. The ground electrode was also held in place with a piece of

elastic tape because it tended to come loose during testing. The electrode signals were sent via a connection box to an amplifier (Lafayette Instrument Co. Mini-Graph, Lafayette, IN) with a gain of approximately 4800. The amplifier was calibrated prior to the testing of each subject to ensure that the gain did not change between tests. The unfiltered, amplified signals were then sent to a homemade data collection box which was interfaced to the data acquisition card.

Computer

An IBM compatible PC (Apex 386) running at 25 megahertz with four megabytes of RAM was used to collect, process, and save the strain gage and EMG data. All data was first saved on the hard drive and then copied to high density (1.44 Mbyte) 3.5" floppy disks.

Videotape equipment

To analyze joint movement patterns and to provide data synchronization for the EMG and strain gage signals, videotaping was conducted using a videocamera (Panasonic Digital 5100, Secaucus, NJ) with a shutter speed of 1/250 second. This high shutter speed was chosen to minimize blurring on the videotape, due to high hand velocities during propulsion, while maintaining adequate lighting. The image was recorded on a standard VHS format videotape at 30 frames per second. A timer (Horita TRG-50, Mission Viejo, CA) was used to provide a running clock on the video frames. The camera was set at

a distance of 8.25 meters from the wheelchair handrim and positioned orthogonal to the subject's sagittal plane. A Panasonic television monitor was used to allow visualization of the camera's field of view. Prior to each test, the camera's zoom was adjusted so that the video frame was bordered on the bottom by the wheelchair wheel axis and on the left side by a division in the wall behind the dynamometer. Prior to each test, a brief recording of a known length of wood (58 cm) held in the plane of the wheelchair handrim was made to provide calibration information for the digitizing software.

Physiological measuring equipment

Room air was inspired and passed through an air flow meter which was connected to a computer interface box (Vista, Ventura, CA) for monitoring the volume of air inspired. Exhaled air was then sent to a mixing chamber through an attached air sampling tube. Valves in the mouthpiece allowed air to flow in one direction only. All of the inspired air passed through the air flow meter and all expired air passed into the mixing chamber for sampling. The sampled air was then passed through an anhydrous $CaSO_4$ desiccant (Drierite) to remove moisture prior to reaching the O_2 (Applied Electrochemistry Inc., S-3A, Sunnyvale, CA) and CO_2 (Beckman Medical Gas Analyzer, LB-2) analyzers. The analyzers were also connected to the computer interface box. Computer software (Vista TurboFit) performed all data collection, calculation, and display functions.

The system was calibrated prior to running each subject. The calibration procedures used can be found in Appendix A.

Experimental Procedure

Initial preparation

After reading and signing the informed consent form and having questions answered, the subject was seated in the wheelchair (transferred in the case of the wheelchair dependent subjects). Body measurements were then taken as well as the subject information displayed in Table 3. The subject was then positioned on the wheelchair dynamometer and instructed to propel the wheelchair for a few cycles in order to get a feel for the equipment. The armrests were removed to provide a clear view of the subject's left arm for the videocamera and to help prevent the EMG electrodes from becoming snagged during the testing.

EMG electrode attachment

The EMG electrodes were placed according to the methods described by Zipp (1982), assuming bilateral symmetry. A permanent black marker was used to mark the acromion, lateral epicondyle, and olecranon of the subject. A flexible tape measure was then used to determine the proper electrode locations for the recording of the middle deltoid and lateral triceps with an interelectrode distance of two centimeters. The electrode positions were marked and emory

cloth used to abrade the electrode area. Care was taken to abrade only the electrode site without abrading the span between the electrodes. Electrically conductive gel was applied to the electrode, and a small amount of the gel was worked into the skin at the electrode site prior to the electrode being placed. An electrical resistance measurement was then taken between each pair of electrodes at each muscle location to ensure an adequately low impedance. The electrodes were reapplied if a measurement of 10,000 ohms or greater was obtained. A ground electrode was attached on the wrist of the subject, with resistance measurements being taken between it and each of the other electrodes to ensure an impedance of 10,000 ohms or less. The electrodes were then plugged into the electrode interface box. The electrodes were then taped to the wheelchair to ensure an adequate range of motion and to minimize the chance of becoming tangled during the testing. The subject was asked to briefly propel the chair at a comfortable pace while data was collected and viewed to ensure a proper EMG signal prior to the start of the test.

Wheelchair propulsion test protocol

Following the EMG setup, reflective markers were placed on the acromion, lateral epicondyle, and styloid process for motion analysis. The subject was instructed to breathe into the mouthpiece for two minutes prior to testing to allow the oxygen and carbon dioxide analyzers to stabilize and to allow the

subject to become acclimated. The subject's nose was pinched shut to ensure that all inspired air passed through the air flow meter.

The subject was instructed to propel the wheelchair at a velocity of 50 on the display unit (0.64 m/s linear handrim velocity). After one minute, a five second sample of strain gage, middle deltoid EMG, and lateral triceps EMG data was taken at a sampling rate of 1000 samples per second, viewed, and saved to the hard drive. The velocity display corresponding to the period of time that the data was sampled was saved also. After two minutes, the subject was instructed to maintain a velocity of 70 on the display unit (0.92 m/s linear handrim velocity). Data was again taken and saved at the three minute mark. Velocity was increased to 90 on the display unit (1.17 m/s) after four minutes. Data was again taken after five minutes and testing was stopped at six minutes. The subject was then allowed to rest for fifteen minutes and the test repeated, beginning with 1.17 m/s and ending with 0.64 m/s. The order of the velocities was reversed in the second test to ensure that data was obtained with the muscles fairly well rested at each velocity level in case muscle fatigue became a problem. In addition, more propulsion cycles were obtained by completing the test a second time, providing additional data for analysis if necessary. However, the data from the second testing period was not used in the final analysis since it was found that a sufficient amount of data was obtained during the first half of testing.

During the testing periods, the subject's oxygen consumption (VO_2) and respiratory exchange ratio (RER) were automatically updated every thirty seconds and displayed. Videotaping took place during both tests and at all velocity levels.

Although previous research has shown three minutes sufficient to reach steady state for manual wheelchair propulsion (van der Woude et al., 1988a), each velocity level was maintained for two minutes based upon pre-test experimentation. It was found that two minutes at each velocity level produced a cardiorespiratory response great enough to warrant concern over the safety of the subjects. The wheelchair dependent subjects were of particular concern because they are more susceptible to cardiorespiratory problems. Furthermore, accurate stroke patterns as well as EMG signals were desired at all three velocity levels. This was not likely to occur if the subject was excessively tired by the time the high velocity condition was reached. Analysis of a typical oxygen uptake curve revealed that most of the increase in oxygen uptake that occurs with exercise occurs within the first couple of minutes (85-95%) with little gain in VO_2 from the second to third minute (McArdle et al., 1991). Therefore, to assure reliable data in all areas of study, it was decided that two minutes at each velocity level was the best solution. The results of this study are presented in the next chapter and show that steady state or near steady state conditions were achieved.

Wheelchair dependent subject feedback

Each of the wheelchair dependent subjects was asked to give a subjective evaluation of the wheelchair dynamometer arrangement, particularly as to the degree in which actual wheelchair propulsion was simulated and the amount of resistance encountered (slight, moderate, steep downhill/uphill or level surface). Suggestions were solicited as to improvements that could be made to the arrangement to more accurately reflect manual wheelchair propulsion. All of the wheelchair dependent subjects felt that the setup accurately reflected manual wheelchair propulsion on a very slight uphill grade. The velocities maintained in the present study ranged from 0.64 m/s to 1.22 m/s with power outputs ranging from 17.6 W to 53.6 W. Typical wheelchair operating speeds are in the range of 0.56 to 1.11 m/s (Lemaire et al., 1991) with power output levels ranging from 5 to 34 W (Sawka et al., 1993). Therefore, since the velocity levels maintained in the present study were only slightly higher than those commonly encountered in day-to-day manual wheelchair propulsion, the higher than typical power output levels encountered in the present study are due to an uphill simulation of resistance. This agrees with the observations of the wheelchair dependent subjects. Suggestions included removing the wheelchair brakes to keep the hands from hitting them during the propulsion stroke and propping the front casters up to more accurately reflect a slight uphill grade.

Data Reduction

Oxygen uptake, respiratory exchange ratio, and energy input

At each velocity level, the oxygen uptake and RER values for the final minute were averaged and the result used to represent the value for that level. Thus, the values obtained at 1:30 and 2:00 were averaged for the low velocity condition, 3:30 and 4:00 for the medium velocity, and 5:30 and 6:00 for the high velocity condition. The kilocalorie equivalent for each RER was obtained from a table (McArdle et al., 1991) to provide a more exact representation of nutrient metabolism at the cellular level rather than using the standard of 5.00 KCal per liter of O_2 commonly used in research of this kind (Brubaker and McLaurin, 1982). The kilocalorie equivalent was then multiplied by the oxygen uptake to yield the energy input in KCal/min. This value was converted to units of watts by multiplying by 69.755 W·min/KCal. Table 4 shows an example of the computer generated oxygen uptake and respiratory exchange ratio values along with the kilocalorie equivalent and energy input values used in determining propulsion efficiency.

Mean velocity, mean handrim force, and mean energy output

An analysis program (Appendix F) was written for use by Lab Windows to read the raw data and process it for further analysis. The velocity display

Table 4 Example of oxygen uptake, RER, kilocalorie equivalent, and energy input values used in determining propulsion efficiency, Subject WD-2

Time	VO_2 L/min	RER	Avg. VO_2 L/min	Avg. RER	KCal. Eq.	Energy Input W
:30	0.49	0.91				
1:00	0.66	0.82				
1:30	0.72	0.79				
2:00	0.83	0.82	0.775	0.805	4.813	260.2
2:30	0.76	0.87				
3:00	0.8	0.83				
3:30	0.88	0.84				
4:00	0.94	0.83	0.91	0.835	4.85	307.9
4:30	0.94	0.81				
5:00	1.16	0.85				
5:30	1.19	0.86				
6:00	1.13	0.9	1.16	0.88	4.899	396.4

values were converted to units of meters per second by multiplying the display value by 0.0129. To determine the mean force exerted on the handrims, a routine was written to isolate two, three, or four complete propulsion strokes, depending upon how many strokes the subject was able to complete in the five second time period. The mean strain gage voltage was then found and converted to units of force (N) by the calibration equation mean handrim force (N) = mean s.g. voltage (volts) ÷ .0599 + 2.005. This was written into the software to automate the calculation. The mean velocity and mean force were then multiplied together to yield the mean power output at that velocity level for use

in calculating the propulsion efficiency. The same filters were used in processing the strain gage data as were used during calibration to avoid signal attenuation differences in the mean signal levels as a result of filtering.

EMG and kinematic data reduction

The Lab Windows analysis program was also written to allow processing of the EMG data. The raw data was read and rectified since negative voltages also reflect muscle activity but cancel out the positive voltages when computing the mean voltage or when using a smoothing filter. A moving average routine was written to smooth the raw data and obtain the rectified linear envelope. The raw and smoothed data, along with the smoothed strain gage data, were then saved to file in ASCII form. The EMG data was plotted along with the strain gage data for one complete propulsion cycle to determine the points along the cycle in which the muscle was active. In order to accomplish this, the digital filters supplied with Lab Windows® were not used since they shift the output array along the time axis. Since both the EMG and strain gage data had to be held to the same point in time at which the signal was generated, moving average smoothing filters were written so that each i^{th} array value would remain in the same location in the array after smoothing. Microsoft Excel was used to read in the EMG and strain gage data. The "max" and "min" functions were used to identify the starting and stopping array indices of each propulsion cycle

as well as the start of the recovery phase within each cycle. Three complete consecutive propulsion cycles were read into Excel when possible. However, at the low velocity level, some subjects only completed two complete cycles during the five second period. For EMG analysis, the second complete cycle was used with the rectified and smoothed EMG data plotted along with the strain gage cycle so that muscle activity could be analyzed qualitatively with respect to the propulsion cycle (propulsion or recovery phase).

Kinematic parameters of propulsion time (PT), recovery time (RT), cycle time (CT), percent propulsion time (%PT = PT/CT x 100), and percent recovery time (%RT = RT/CT x 100) were computed based upon the Excel "min" and "max" function results for two or three consecutive cycles. Some of the subjects did not complete three full cycles during the low velocity test. Averages were computed for each parameter over the number of complete cycles obtained. It was found that three consecutive cycles were sufficient to assure that the results would be representative of that subject. This confirmed the findings of other investigators (Sanderson and Sommer, 1985). Figure 14 shows typical results obtained for three consecutive propulsion cycles. The propulsion time was taken from the beginning (low voltage) to the peak voltage in the cycle, with the recovery time being from the peak voltage to the beginning of the next cycle. This method of determining propulsion stroke times has been used by other investigators (Ronchi et al., 1993) and is a better reflection of torque application than

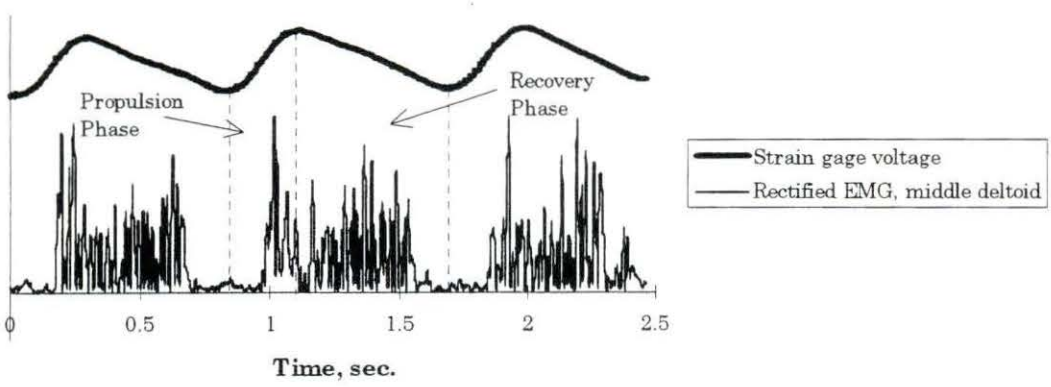

Figure 14 **Example of three consecutive propulsion cycles showing propulsion and recovery phases as well as middle deltoid EMG activity correlated with each phase, subject AB-1, medium velocity**

videotape handrim contact determination since it is often difficult to determine the points of handrim contact and release. In addition, the hand may be in contact with the handrim but may be enacting a braking force to the rim or may be coasting with the rim prior to handrim release, thus not reflecting actual torque application to the handrims. The rectified middle deltoid activity is also shown. It is active mostly during the recovery phase of the propulsion cycle in this case.

The work done per stroke (WS) was found by multiplying the mean power output by the total cycle time at each velocity level. The videotape was analyzed qualitatively to determine the approximate start angle (SA), end angle (EA), and push angle (PA = EA - SA) for each subject at each velocity level. These angles

were defined relative to a horizontal through the wheel axle, with 0° being toward the rear of the wheelchair. It was difficult to determine the precise moment when the hands were in contact with the handrim due to the camera being perpendicular to the plane of motion. Therefore, hand position was estimated to the nearest one-quarter of a wheelchair spoke span (13°).

RESULTS AND DISCUSSION

The results of this study are presented in three parts; (1) propulsion efficiency and oxygen uptake, (2) kinematics, and (3) electromyography. The results of the present study were similar to those of other researchers in each of the studied areas (efficiency, kinematics, electromyography). It was the intent to focus on subject group differences throughout the discussion rather than absolute values, as has been the case in most of the literature to date. Where appropriate, velocity and power output level trends have been noted. T-tests were used to identify significant differences between the subject groups ($p < 0.05$) with the Tukey test of multiple comparisons used to identify velocity dependent differences within each group. Several plots showed trends which were not determined to be significant; these should be flagged for additional study, possibly incorporating additional subjects and/or test conditions. The intent was not to imply that the differences found can be extrapolated to predict differences found between any group of wheelchair dependent subjects compared with any group of able-bodied subjects. The differences found in this study should only be viewed in light of the subjects who participated in this study. A different group of wheelchair dependent subjects may show lesser or greater differences. However, the differences identified are likely to occur to some extent regardless of the population sample studied, particularly for propulsion efficiency and oxygen uptake, since the differences found can be explained by

physiological principles. The kinematic trends seen may be more dependent upon the subject groups used, especially where trends were seen but significant differences were not shown.

Steady State, Propulsion Efficiency, and VO_2

Verification of steady state conditions

Since the amount of time spent at each velocity level (two minutes) was less than the three minutes previously established in the literature to achieve steady state conditions (van der Woude et al., 1988a), it was necessary to verify the existence of a steady state before meaningful propulsion efficiency results could be presented. In order to accomplish this, the oxygen uptake was plotted against time for each subject. Figure 15 shows a plateauing of the oxygen uptake curve at, or prior to, the end of the low and medium velocity time periods, indicating probable steady state or near steady state conditions. This trend was seen in the plots of all subjects (Appendix A). It is also interesting to note that, at the high velocity condition (1.17 m/s), all of the wheelchair dependent subjects exhibited this trend, with none of the able-bodied subjects showing a decrease in slope of the oxygen uptake curve. Therefore, it appears that the wheelchair dependent subjects in this study were sufficiently close to steady state to allow the reporting of efficiencies.

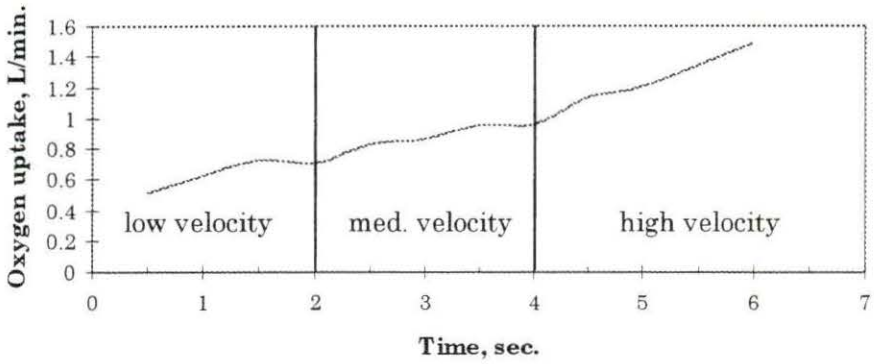

Figure 15 Oxygen uptake as a function of time depicting steady state conditions at the low and medium velocities indicated by a "plateauing" of the oxygen uptake curve at or prior to times 2 and 4 minutes, subject AB-1

Efficiencies reported here for the able bodied subjects will be overestimated. However, this is not a problem because it will be shown that the wheelchair dependent subjects exhibited higher efficiencies at all three velocity levels. In addition, three of the subjects were asked to propel the wheelchair at the medium velocity (0.92 m/s) for five minutes. This is a sufficient amount of time for steady state to be reached. The VO_2 values during the final minute were averaged and compared with the VO_2 values obtained during the actual test for the fourth minute. The difference between the steady state and test conditions was expressed as a percentage of the steady state condition.

The results shown in Table 5 verify the results plotted in Figure 15 for the medium velocity condition. At least 80 to 90 percent of steady state conditions

Table 5 Results of steady state vs actual test conditions for the medium velocity (0.92 m/s) case

Subject	1	2	3
Weight, lb	145	205	210
VO_2, actual test, L/min	0.98	0.91	0.82
VO_2, steady state, L/min	0.96	0.99	0.94
% of steady state	102.6	92.4	87.2

were likely achieved during the actual testing. Subject 1 weighed the least and Subject 3 the most; thus the body weights spanned the entire range of the subjects participating in the study. It is known that, even for non-weight bearing activities such as manual wheelchair propulsion, energy cost can be as much as 5% higher due to body mass alone (McArdle et al., 1991). Therefore, it seems reasonable that a person with greater body mass will take a longer period of time to reach steady state conditions than a person with less body mass. This is probably the reason for the increasing deviation from steady state conditions with increasing body mass shown in Table 5.

In light of the above discussion, propulsion efficiency will be considered for all three power levels in this study with the understanding that the efficiencies may be overestimated slightly, particularly for the able bodied subjects at the

high power output level. Appendix A contains the oxygen uptake and respiratory exchange ratio data for all of the subjects and oxygen uptake plots for each.

Propulsion efficiency between subject groups

Table 6, Table 7, and Table 8 show the values obtained for the parameters necessary to calculate the wheelchair propulsion efficiency for the low (0.64 m/s), medium (0.92 m/s), and high (1.17 m/s) velocity levels, respectively. The gross propulsion efficiencies ranged from 7.3 (WD-2, low velocity) to 15.5 (WD-3, medium velocity). These values are comparable to those found in the literature for manual wheelchair propulsion (Brubaker and McLaurin, 1982; Veeger et al., 1992; Brubaker et al., 1984).

Figure 16 shows the propulsion efficiency results obtained for all of the subjects at all three velocity levels. Although there is considerable variation between the subjects, both in gross propulsion efficiency and in velocity effects, a common finding is that the propulsion efficiency increased for all subjects from the low to medium velocity conditions. Previous research has shown that efficiency increases with increased power output and decreases with increasing velocity at equivalent power output levels (Brubaker and McLaurin, 1982; Veeger et al., 1992; van der Woude et al., 1988a). This decrease with increasing velocity has been suggested to be caused by an increase in muscular friction

Table 6 Propulsion efficiency data for the low velocity condition (0.64 m/s)

Subj.	VO2 l/min	RER	KCal. Eq.	KCal/min	Energy Input, W	Vel. m/s	H.R. Force, N	Energy Output, W	% Gross Eff.
AB-1	0.72	0.98	5.02	3.62	252.22	0.68	28.88	19.64	7.79
AB-2	0.61	0.77	4.76	2.88	201.05	0.70	27.21	19.05	9.47
AB-3	0.64	0.98	5.02	3.21	224.20	0.68	27.00	18.36	8.19
AB-4	0.52	0.92	4.95	2.55	177.75	0.68	27.75	18.87	10.62
AB-5	0.73	0.72	4.70	3.43	239.43	0.65	27.02	17.56	7.34
Avg.	0.64	0.87	4.89	3.14	218.93	0.68	27.57	18.70	8.68
S.D.	0.09	0.12	0.15	0.43	29.88	0.02	0.79	0.78	1.34
WD-1	0.52	0.89	4.91	2.53	176.42	0.69	28.53	19.69	11.16
WD-2	0.78	0.81	4.81	3.73	260.19	0.64	29.73	19.03	7.31
WD-3	0.64	0.79	4.79	3.04	212.08	0.71	31.42	22.31	10.52
WD-4	0.76	0.77	4.76	3.60	250.90	0.68	30.25	20.57	8.20
WD-5	0.69	0.74	4.73	3.24	225.87	0.73	28.99	21.16	9.37
Avg.	0.67	0.80	4.80	3.23	225.09	0.69	29.78	20.55	9.31
S.D.	0.10	0.06	0.07	0.48	33.30	0.03	1.13	1.28	1.59

Table 7 Propulsion efficiency data for the medium velocity condition (0.92 m/s)

Subj.	VO2 l/min	RER	KCal. Eq.	KCal/min	Energy Input, W	Vel. m/s	H.R. Force, N	Energy Output, W	% Gross Eff.
AB-1	0.96	1.10	5.05	4.85	337.97	0.93	37.15	34.55	10.22
AB-2	0.79	0.84	4.85	3.81	265.57	0.93	36.08	33.55	12.63
AB-3	0.98	1.21	5.05	4.95	345.01	1.05	36.67	38.50	11.16
AB-4	0.88	0.99	5.04	4.41	307.31	0.94	35.71	33.57	10.92
AB-5	0.99	0.86	4.88	4.80	334.95	0.82	33.67	27.61	8.24
Avg.	0.92	1.00	4.97	4.56	318.17	0.93	35.86	33.56	10.64
S.D.	0.09	0.16	0.10	0.47	32.70	0.08	1.34	3.90	1.60
WD-1	0.65	0.93	4.96	3.22	224.94	0.87	36.17	31.47	13.99
WD-2	0.91	0.84	4.85	4.41	307.86	0.93	36.71	34.14	11.09
WD-3	0.82	0.88	4.90	3.99	278.51	1.09	39.62	43.19	15.51
WD-4	0.96	0.86	4.88	4.66	324.75	0.94	37.43	35.18	10.83
WD-5	0.80	0.80	4.80	3.82	266.24	0.91	35.50	32.31	12.13
Avg.	0.83	0.86	4.88	4.02	280.46	0.95	37.09	35.26	12.71
S.D.	0.12	0.05	0.06	0.56	38.74	0.08	1.58	4.67	2.00

Table 8 Propulsion efficiency data for the high velocity condition (1.17 m/s)

Subj.	VO2 l/min	RER	KCal. Eq.	KCal/min	Energy Input, W	Vel. m/s	H.R. Force, N	Energy Output, W	% Gross Eff.
AB-1	1.49	1.20	5.05	7.52	524.56	1.09	43.39	47.30	9.02
AB-2	1.23	1.12	5.05	6.21	433.03	1.11	44.02	48.86	11.28
AB-3	1.51	1.06	5.05	7.62	531.60	1.19	43.51	51.78	9.74
AB-4	1.42	1.15	5.05	7.17	499.92	1.17	41.46	48.51	9.70
AB-5	1.57	1.01	5.05	7.92	552.61	1.14	39.66	45.21	8.18
Avg.	1.44	1.11	5.05	7.29	508.34	1.14	42.41	48.33	9.58
S.D.	0.13	0.08	0.00	0.66	46.12	0.04	1.82	2.40	1.14
WD-1	0.91	0.97	5.01	4.56	318.02	1.05	42.66	44.79	14.08
WD-2	1.16	0.88	4.90	5.68	396.41	1.22	43.90	53.56	13.51
WD-3	1.12	1.07	5.05	5.63	392.54	1.22	43.71	53.33	13.58
WD-4	1.35	1.01	5.05	6.79	473.51	1.10	43.68	48.05	10.15
WD-5	1.09	0.86	4.88	5.29	368.96	1.22	42.65	52.03	14.10
Avg.	1.12	0.96	4.98	5.59	389.89	1.16	43.32	50.35	13.09
S.D.	0.16	0.09	0.08	0.81	56.23	0.08	0.61	3.81	1.67

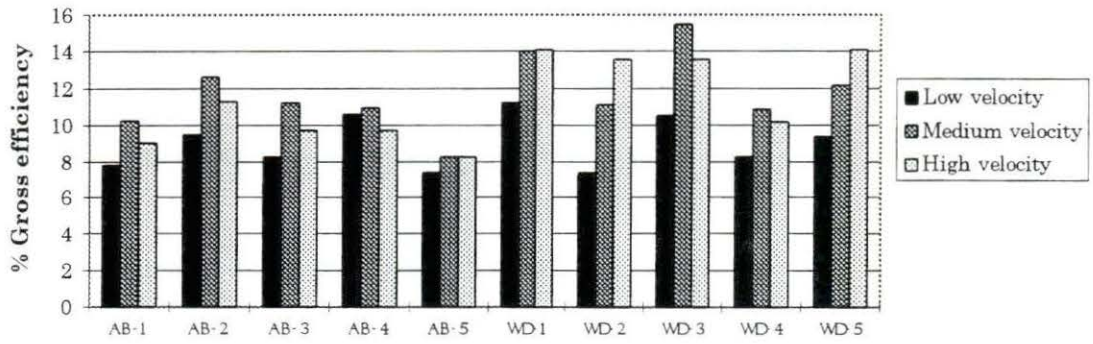

Figure 16 Propulsion efficiency results for all subjects at all velocity levels

(Powers et al., 1980), a change over from slow twitch to fast twitch muscle fibers (Gaesser and Brooks, 1975), excessive limb movements (Glaser et al., 1980) and/or a less accurate force application to the handrim (Sanderson and Sommer, 1985). A limitation of the wheelchair dynamometer used in this study is that power output is velocity dependent. Therefore, it is not possible to separate the two to observe the effects of increasing velocity at a constant power output. Propulsion efficiency did not increase from the medium to high velocity conditions for any of the able-bodied subjects. However, three of the five wheelchair dependent subjects showed an increase in efficiency from the medium to high velocity levels. It is possible that velocity increase effects outweigh the positive efficiency effects due to increasing power output, resulting in a decrease in efficiency with increasing velocity. However, in subjects WD1, WD2, and WD5, improved stroke techniques and training may result in

efficiency increases sufficient to overcome the negative effects of an increase in velocity.

Figure 17 shows the averaged propulsion efficiencies obtained for both the able-bodied and wheelchair dependent groups at all three velocity levels. It is readily apparent that the wheelchair dependent group attained higher propulsion efficiencies than the able-bodied group at all three velocity levels.

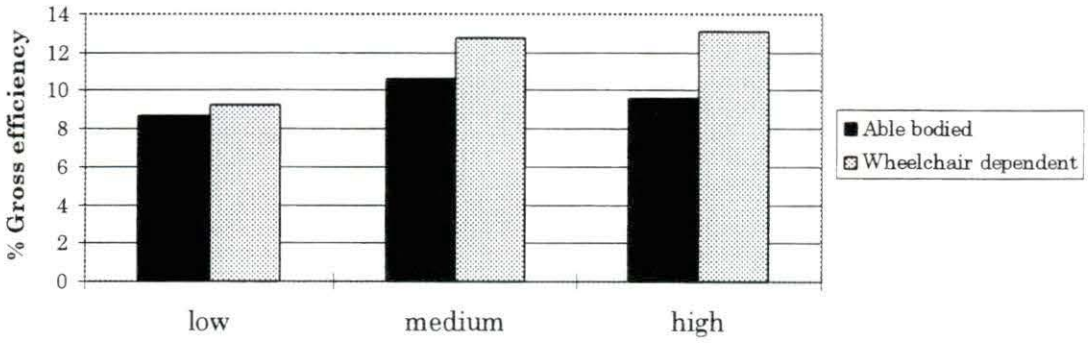

Figure 17 Averaged gross propulsion efficiencies for the low, medium and high velocity conditions

However, statistical analysis (Appendix A) revealed that only the high velocity difference was significant ($\alpha = 0.05$). Significant differences are difficult to show for such small sample sizes so it may be that with greater sample sizes significant differences could also be shown at the low and medium velocity levels. Also, since the able-bodied subjects did not achieve steady state conditions during the high velocity trials, the difference between the wheelchair

dependent and the able-bodied groups would likely be even more pronounced if steady state were achieved.

It is important to verify when comparing efficiencies that each group of subjects experienced statistically the same mean power output level during the event and that differences found in propulsion efficiency are caused by differences due to metabolic power output rather than differences in power output level experienced. Therefore, t-tests were conducted comparing the means of both the metabolic power output and the actual power output between the two groups of subjects at all three velocity levels.

Table 9 indicates that significant differences were obtained ($p < 0.05$) for the low velocity energy output and high velocity energy input conditions only, indicating that, for the low velocity condition, the difference in mean efficiencies is not accounted for by metabolic or physiological differences. Table 6 shows that the wheelchair dependent subjects maintained a slightly higher mean velocity during the low velocity condition, thus experiencing a slightly higher power output level than the able-bodied subjects. However, in the case of the high velocity, the significant efficiency difference found was due to power input differences, with both groups experiencing the same power output level.

Table 9 Energy input and output means, tested for significant differences between the subject groups

	Low Velocity		Medium Velocity		High Velocity	
	Energy Input (W)	Energy Output (W)	Energy Input (W)	Energy Output (W)	Energy Input (W)	Energy Output (W)
AB	218.9	18.7	318.2	33.6	508.3	48.3
WD	225.1	20.6	280.5	35.3	389.9	50.4
	$p > 0.05$	$p < 0.05$	$p > 0.05$	$p > 0.05$	$p < 0.05$	$p > 0.05$

Oxygen uptake between groups

Unlike efficiency, oxygen uptake comparisons are generally made with respect to body mass because it is known that body mass plays a significant role in the amount of oxygen required to perform a task, particularly in weight-bearing forms of exercise such as walking or jogging (McArdle et al., 1991). However, in activities in which body weight is supported, such as stationary cycling and manual wheelchair propulsion, the effect of body mass upon oxygen uptake is small, with differences mainly due to differences in the weight of the particular body limbs used in performing the work. Nevertheless, oxygen uptake was expressed in terms of body mass in order to eliminate effects due to body mass differences. Table 10 presents the values obtained for oxygen uptake for all ten subjects, at all three velocity levels, expressed both in absolute form and per kilogram of body mass.

Table 10 Comparison of oxygen uptake between able-bodied and wheelchair dependent subjects

		Low Velocity		Medium Velocity		High Velocity	
Subject	Mass (kg)	VO_2 L/min	VO_2 $L \cdot min^{-1} \cdot kg^{-1}$	VO_2 L/min	VO_2 $L \cdot min^{-1} \cdot kg^{-1}$	VO_2 L/min	VO_2 $L \cdot min^{-1} \cdot kg^{-1}$
AB-1	95.20	0.72	0.0076	0.96	0.0101	1.49	0.0157
AB-2	83.90	0.61	0.0072	0.79	0.0094	1.23	0.0147
AB-3	65.80	0.64	0.0097	0.98	0.0149	1.51	0.0229
AB-4	74.80	0.52	0.0069	0.88	0.0117	1.42	0.0190
AB-5	83.90	0.73	0.0087	0.99	0.0117	1.57	0.0187
Mean	80.72	0.64	0.0080	0.92	0.0116	1.44	0.0182
S.D.	11.04	0.09	0.0012	0.09	0.0021	0.13	0.0033
WD-1	77.10	0.52	0.0067	0.65	0.0084	0.91	0.0118
WD-2	93.00	0.78	0.0083	0.91	0.0098	1.16	0.0125
WD-3	74.80	0.64	0.0085	0.82	0.0109	1.12	0.0149
WD-4	95.20	0.76	0.0079	0.96	0.0100	1.35	0.0141
WD-5	63.50	0.69	0.0108	0.80	0.0125	1.09	0.0171
Mean	80.72	0.67	0.0084	0.83	0.0103	1.12	0.0141
S.D.	13.28	0.10	0.0015	0.12	0.0015	0.16	0.0021

Figure 18 visually presents the data found in Table 10. As expected, oxygen uptake increased with increasing velocity (power output) for all subjects. It is interesting to note that subject WD-5 exhibited the highest oxygen uptake within the wheelchair dependent group at all three velocity levels. This subject did not have a spinal injury as the other wheelchair dependent subjects but rather a brittle bone disease (osteogenesis imperfecta). Thus, although the subject had muscular atrophy in the leg muscles, upper body muscle function is normal including abdominal and intercostal muscle innervation as well as other

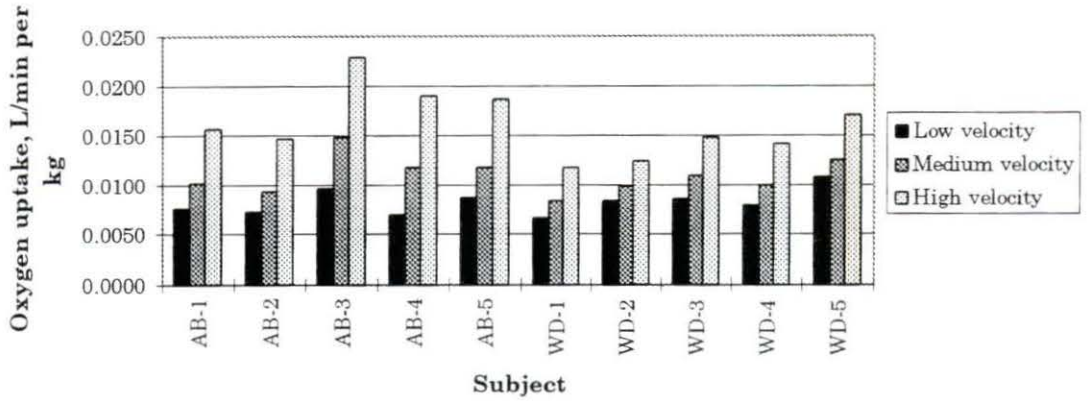

Figure 18 Oxygen uptake per kilogram body mass

muscles supporting the trunk. The subject also has sympathetic innervation of the blood vessels in the legs and heart, allowing cardiac output to remain relatively normal and allowing greater oxygen exchange in the lungs. This results in a higher oxygen uptake.

Figure 19 shows the mean oxygen uptake per kilogram of body mass at all three velocity levels for the two subject groups. Statistical analysis (t-test) showed a significant difference only at the high velocity condition, as was shown for propulsion efficiency (Appendix A). At low submaximal work loads, the heart rate of paraplegics has been found to be higher than that of able-bodied subjects at the same workload (Hopman et al., 1993). Also, due to the absence of the musculoskeletal pump in the legs and a lack of sympathetic regulation in the legs and abdomen resulting in decreased preload to the heart, stroke volume is

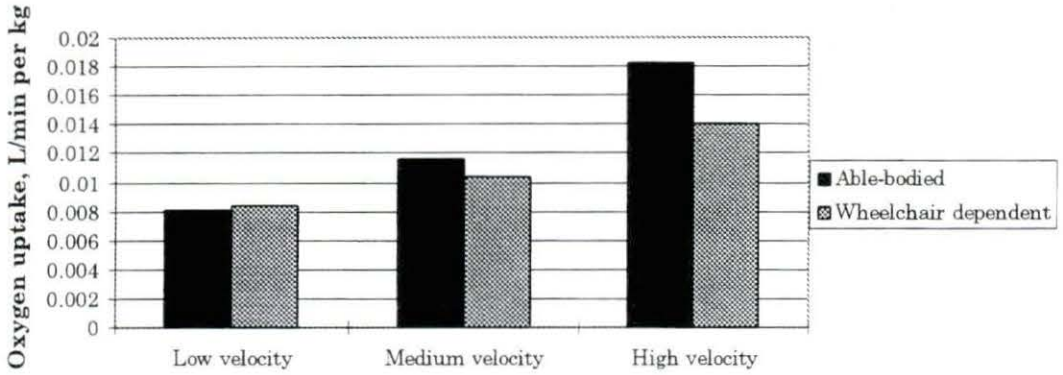

Figure 19 Averaged oxygen uptakes for the low, medium and high velocity conditions

lower in paraplegics than in able-bodied individuals at the same submaximal work load. Therefore, in paraplegics the heartrate is higher to attempt to maintain a sufficient cardiac output (heartrate x stroke volume) to support the metabolic needs of the individual during exercise. However, at high submaximal work loads, such as existed during the high velocity portion of this test, heartrate reaches a maximum due to lack of cardiac sympathetic innervation, particularly in persons with a spinal cord lesion above T6. Since stroke volume is also reduced, cardiac output drops as compared with able-bodied individuals. With this drop in cardiac output, oxygen consumption also drops because there is not enough blood passing through the pulmonary circulation to carry all of the oxygen that has been inspired. The smaller active muscle mass in the wheelchair dependent group also contributes to a lower

oxygen consumption. Normally, when a muscle is contracted during exercise, the blood vessels within the muscle dilate due to vasodilator metabolites as well as an accumulation of potassium which has vasodilatory effects. The partial pressure of oxygen in the tissues decreases (PO_2) resulting in a higher pressure gradient between the oxygen in the vessels and that in the tissues. Also, the temperature rises in the muscle, further dilating the vessels. Along with this dilation, there is increased blood flow through the muscle. Furthermore, there is a decrease in affinity for oxygen by the hemoglobin and more oxygen is also given up by the blood due to the temperature increase, shifting the oxygen-hemoglobin dissociation curve to the right. In other words, the hemoglobin gives off oxygen since a higher oxygen partial pressure is required to maintain the same hemoglobin oxygen saturation percentage. These changes may result in a 100-fold increase in oxygen consumption of the skeletal muscle during exercise (Ganong, 1991). Since persons with paraplegia do not have the use of several of the stabilization muscles of the lower trunk, back, and legs as do the able-bodied individuals, less oxygen is used by the body in performing work.

Oxygen consumption also decreases with increasing age, with maximal oxygen consumption decreasing about 1% per year after age 25 (McArdle et al., 1991). Since the mean age of the wheelchair dependent group was seven years greater than that of the able-bodied group, it can be expected that some of the reduction in oxygen consumption (about 7% maximum) was related to age.

However, there still exists a 15.5% decrease in the oxygen uptake of the wheelchair dependent subjects after 7% has been subtracted due to age differences at the high velocity condition, with a 4% decrease at the medium velocity. It must be kept in mind that the steady state oxygen consumption of the able-bodied group is most likely higher than the figures in Table 10 show since they did not reach steady state at the high velocity level, thus expanding the difference in oxygen consumption between the two groups. Also, at submaximal work loads, aging effects are not likely to be as great as is found at maximal oxygen uptake levels so 7% is a conservative estimate of the reduction in oxygen consumption due to aging since the tests were run submaximally. In fact, Adams (1966) found no significant differences due to age in oxygen uptake while subjects were riding a bicycle ergometer at a submaximal workload. It was suggested that the effect of age on oxygen consumption is not significant during moderate work until a more advanced age is reached.

Kinematic Analysis

Between groups

Analysis of the timing and movement patterns showed considerable variation in technique, particularly between the wheelchair dependent subjects. It is probable that the able-bodied subjects, having no prior manual wheelchair propulsion experience, did not have an opportunity to adapt their propulsion

technique to maximize efficiency, but the wheelchair dependent subjects, due to individual adaptation, had maximized their efficiency. The wheelchair dependent subjects used a propulsion style developed specifically to be of greatest benefit to them. Since no practice on the test wheelchair was given prior to the testing, it was anticipated that the wheelchair dependent subjects would show little adaptation to the test chair and would use a propulsion technique similar to that used in their own wheelchairs. Due to the extreme variability within each subject group, as well as the small sample sizes studied, it is difficult to show significant differences between the parameters studied. However, some differences between the two groups were found, with some being statistically significant.

Table 11 shows significant parameter differences due to increasing velocity (Tukey test of multiple comparisons, $\alpha = 0.05$). However, other trends were observed in the parameters due to increasing velocity, as well as differences between the two subject groups that may not have been statistically significant, particularly due to the large variances found within the wheelchair dependent subjects. Furthermore, statistical analysis was used to determine whether the samples studied can be assumed to be taken from the same population based on the sample means. Since generalizations should not be made, particularly concerning the wheelchair dependent subjects, it is sometimes desirable to consider only the subjects under study without assuming that the same results

Table 11 Differences due to increasing velocity, Tukey test, $\alpha = 0.05$

	AB	WD
PT	l-h, m-h	N.S.
RT	l-h	N.S.
CT	l-h	N.S.
%PT	N.S.	l-h
%RT	N.S.	l-h
WS	l-h, l-m	l-h
PA	N.S.	N.S.
SA	N.S.	N.S.

l - low
m - medium
h - high
N.S. - not significant

can be applied to the general population. Therefore, both statistical significance as well as observational analysis will be discussed, with statistical significance being used primarily to underscore the most dominant differences found between the subject groups and the increasing velocity effects.

Propulsion time, recovery time, cycle time, % propulsion time, % recovery time, and work per stroke were compared between the able-bodied and wheelchair dependent groups using a t-test ($p < 0.05$). The F-test for analysis of variance was used prior to performing the t-test since, in several cases, the wheelchair dependent group showed significantly greater variance within a parameter than did the able-bodied group. Table 12 shows the results obtained

Table 12 Results of temporal parameter T and F tests with significance at $p < 0.05$

	Comparison of means, T-test					
	Propulsion Time	Recovery Time	Cycle Time	% Prop. Time	% Rec. Time	Work per Stroke
Low velocity	$p > 0.05$	$p > 0.05$	$p > 0.05$	$p < 0.05$	$p < 0.05$	$p > 0.05$
Medium velocity	$p > 0.05$	$p > 0.05$	$p > 0.05$	$p < 0.05$	$p < 0.05$	$p > 0.05$
High velocity	$p > 0.05$	$p > 0.05$	$p > 0.05$	$p < 0.05$	$p < 0.05$	$p > 0.05$
	Comparison of variance, F-test					
	Propulsion Time	Recovery Time	Cycle Time	% Prop. Time	% Rec. Time	Work per Stroke
Low velocity	$p < 0.05$	$p > 0.05$	$p > 0.05$	$p > 0.05$	$p > 0.05$	$p > 0.05$
Medium velocity	$p > 0.05$	$p > 0.05$	$p > 0.05$	$p > 0.05$	$p > 0.05$	$p > 0.05$
High velocity	$p < 0.05$	$p < 0.05$	$p < 0.05$	$p > 0.05$	$p > 0.05$	$p < 0.05$

from the T and F tests for PT, RT, CT, %PT, %RT, and WS for each of the velocity levels. It can be seen that a significant difference in variance was found in five cases; PT-low velocity, PT-high velocity, RT-high velocity, CT-high velocity, and WS-high velocity. It is interesting to note that four of the five variance differences occurred during the high velocity test. Furthermore, the wheelchair dependent subjects showed higher variances than the able-bodied subjects in each of these cases. Therefore, the wheelchair dependent subjects were adjusting their individual techniques to obtain maximum efficiency at the high velocity level more than were the able-bodied subjects. This is supported by the efficiency results shown earlier in which the wheelchair dependent

subjects showed a significantly higher propulsion efficiency at the high velocity level. This also suggests that individual subject propulsion styles may best be ascertained from tests conducted at high power output levels. Table 12 also shows that significant differences were not found in PT, RT, CT, or WS between the two groups at any of the velocity levels. Unfortunately, the high variances of the wheelchair dependent subjects in each of these parameters makes significant differences difficult to show, although there may appear to be differences by visual analysis of the data plots.

Figure 20 shows a decrease in propulsion time with increasing velocity for both the able-bodied and wheelchair dependent subject groups. However, significant differences were found only between the high-medium and high-low

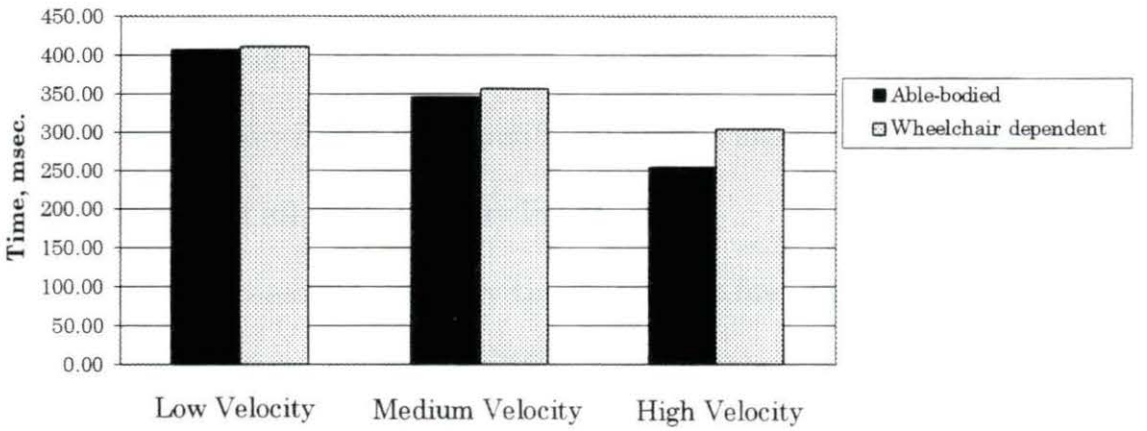

Figure 20 Averaged propulsion time for the low, medium, and high velocity conditions

propulsion times for the able-bodied subjects according to the Tukey test for multiple comparisons ($p < 0.05$). No significant differences in propulsion times due to increasing velocity were found for the wheelchair dependent subjects. A decrease in propulsion time with increasing velocity has been reported by various researchers (Veeger et al., 1989; van der Woude et al., 1988a; van der Woude et al., 1989). However, Veeger et al. (1991) found a strong increase in both propulsion time and cycle time with increasing resistance to propulsion. Therefore, since velocity and resistance were inseparable in the present study, it appears that the effects of increased velocity are more dominant than those of increased propulsion resistance, resulting in trends similar to those seen by the former research groups. Although not statistically significant, the wheelchair dependent subjects also showed a slight decrease in propulsion time with increasing velocity. No significant differences in propulsion time were found between the able-bodied and wheelchair dependent subjects at any velocity level. However, the wheelchair dependent subjects showed slightly greater propulsion times at all three velocity levels.

Significant decreases in recovery time were also found between the low and high velocity conditions for the able-bodied group. No significant differences were found for the wheelchair dependent group, but the wheelchair dependent subjects again showed a slight decrease in recovery time with increasing velocity (Figure 21). Therefore, it appears that the wheelchair dependent subjects

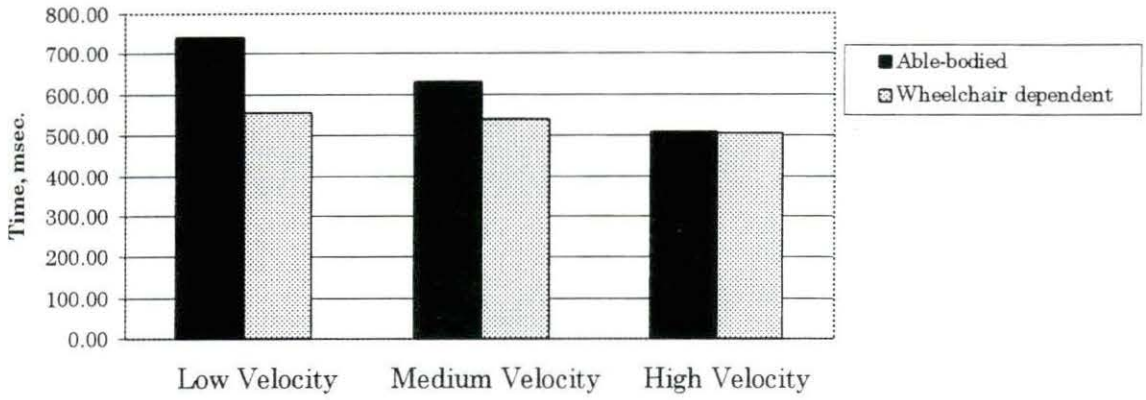

Figure 21 Averaged recovery time for the low, medium, and high velocity conditions

decreased their propulsion times more than their recovery times to compensate for increased velocity and power output. Veeger et al. (1989) found that propulsion time decreased strongly with increasing velocity while recovery time showed only a slight decrease. This implies that the decrease in cycle time is caused mainly by a reduction in propulsion time. Therefore, it is expected that a decrease in %PT should be seen with increasing velocity as was found in the present study. Although not statistically significant, the wheelchair dependent subjects were found to have lower recovery times at all three velocity levels than the able-bodied subjects.

Figure 22 shows a decrease in total cycle time for increasing velocity levels for both groups. Only the low to high velocity condition change for the able-

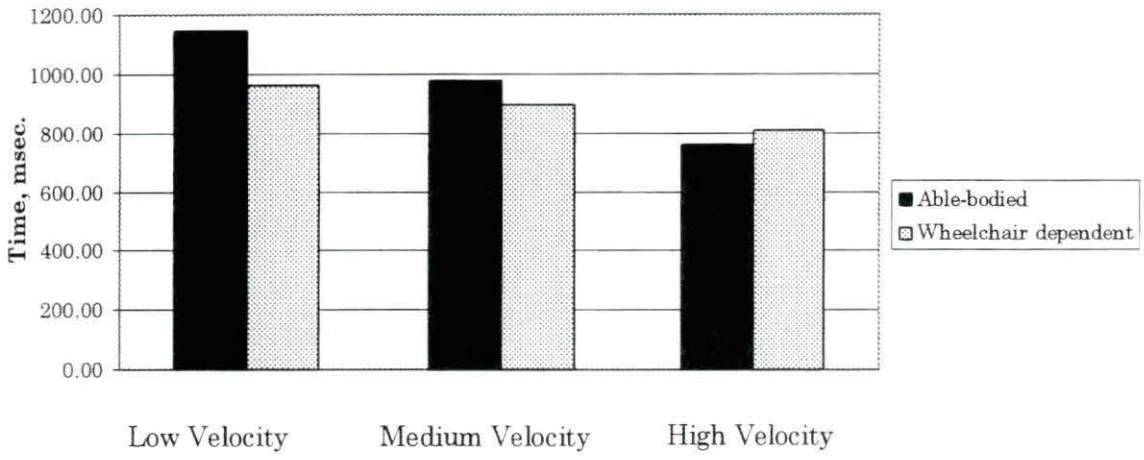

Figure 22 Averaged total cycle time for the low, medium, and high velocity conditions

bodied subjects was found to be significant. Total cycle times appear to be less for the wheelchair dependent subjects at the low and medium velocity conditions and slightly greater for the high velocity condition. Since the recovery time at the high velocity condition appears to be slightly lower for the wheelchair dependent than for the able-bodied subjects, the increase in cycle time found was due mainly to an increase in propulsion time at the high velocity level.

The % propulsion time was found to significantly decrease with the % recovery time increasing from the low to high velocity conditions for the wheelchair dependent subjects only. However, Figure 23 shows that %PT decreased with increasing velocity for both subject groups and Figure 24 shows that %RT increased, although not statistically significantly. Similar results

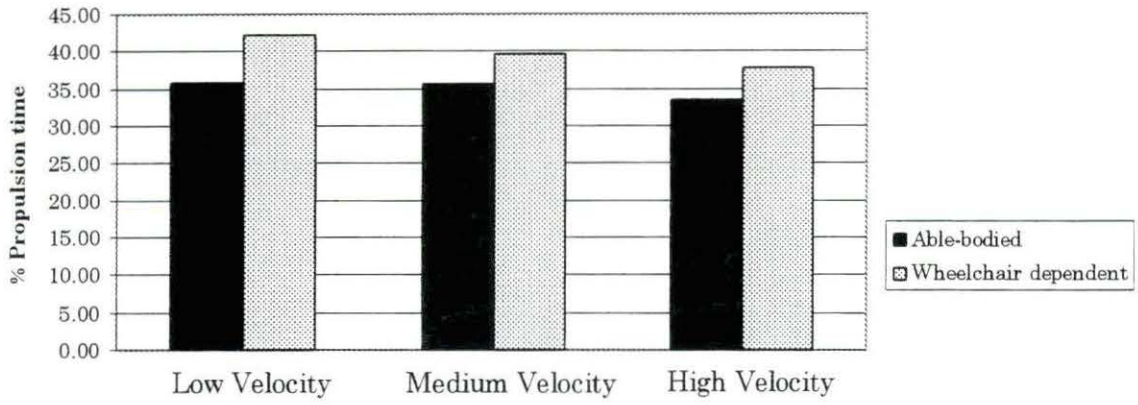

Figure 23 Averaged % propulsion time for the low, medium, and high velocity conditions

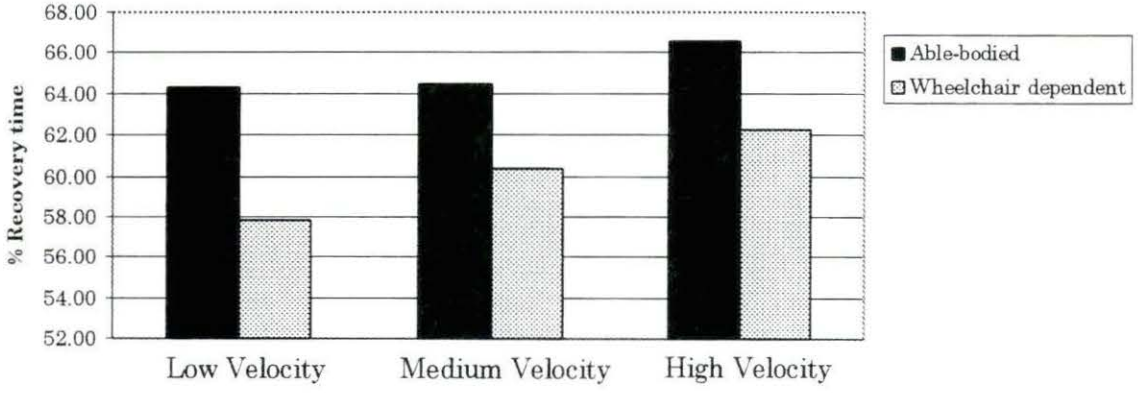

Figure 24 Averaged % recovery time for the low, medium, and high velocity conditions

were obtained by van der Woude et al. (1988b). They found a decrease in % propulsion time (55 to 30%) and an increase in % recovery time (45 to 70%) with increasing velocity while using eight male wheelchair sportsmen as subjects and a velocity range from 0.83 m/s to 4.17 m/s. This indicates that, although no significant differences were found in propulsion, recovery, or cycle times for the wheelchair dependent subjects, differences arise when the ratios of propulsion and recovery times to cycle times are taken. The reduction in variance which occurred for %PT and %RT is likely the reason for the ability to show significance, as compared with PT, RT, and CT. Therefore, it appears that %PT and %RT may be better parameters to use in making generalizations about the stroke timing patterns of wheelchair dependent subjects than the absolute values of PT, RT, and CT.

Perhaps of greatest importance is that %PT was found to be significantly higher for the wheelchair dependent subjects at all three velocity levels with %RT being significantly lower at all levels. Because energy is required to move the arms back to the handrim during the recovery phase, with no work being produced, it seems reasonable that propulsion efficiency can be maximized by minimizing the recovery phase and maximizing the propulsion phase of the stroke cycle. This idea has been mentioned (McLaurin and Brubaker, 1991) in relation to seat height. Lower elbow flexion and, therefore, less energy is required during the recovery stroke with a higher seating position. The

wheelchair dependent subjects have likely developed a stroke technique which allows a greater percentage of propulsion time than recovery time. This idea is particularly important in considering wheelchair design, since designs based upon data collected from able-bodied subjects may be directed at obtaining relative subject/wheelchair positions which do not utilize the full range of motion which the wheelchair dependent person might desire to increase the percentage of propulsion time during the stroke.

Since the total cycle time did not decrease as rapidly as the increase in power output due to increased velocity, the work per stroke (P.O. x CT) must also increase with increasing velocity. This trend can be seen in Figure 25 in which WS increased with increasing velocity for both groups. Significant differences

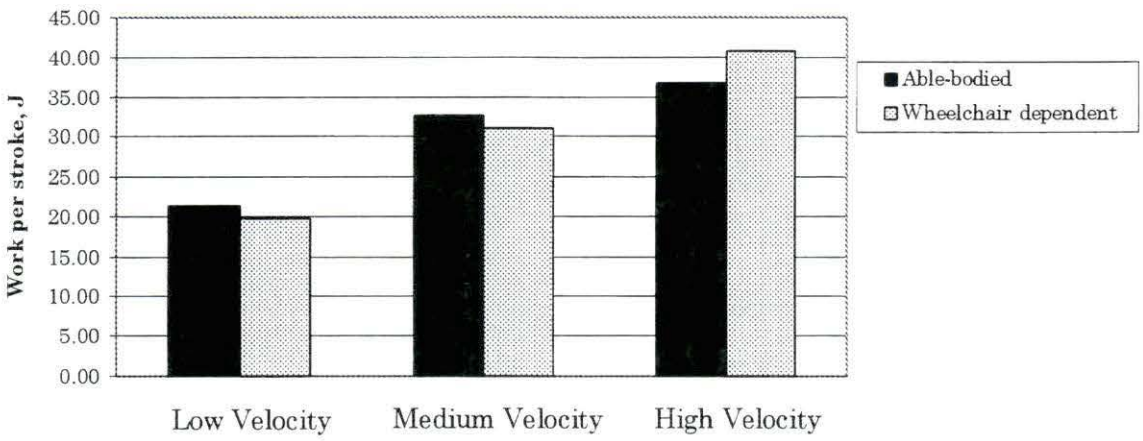

Figure 25 Averaged work per stroke for the low, medium, and high velocity conditions

were found for the low to medium and low to high conditions for the able-bodied subjects and from the low to high velocities for the wheelchair dependent subjects. No significant differences were found between the groups at any of the velocity levels, although the wheelchair dependent subjects showed a higher WS at the high velocity level, probably due to the greater CT at this level as shown in Figure 22.

Figure 26 shows that the effective push angle increased with increasing velocity, with the wheelchair dependent subjects exhibiting higher push angles during the medium and high velocity conditions. The difference in push angle was found to be significant at the high velocity condition, while the increases in push angle with increasing velocity seen in Figure 26 were not found to be significant according to the Tukey test of multiple comparisons. The higher

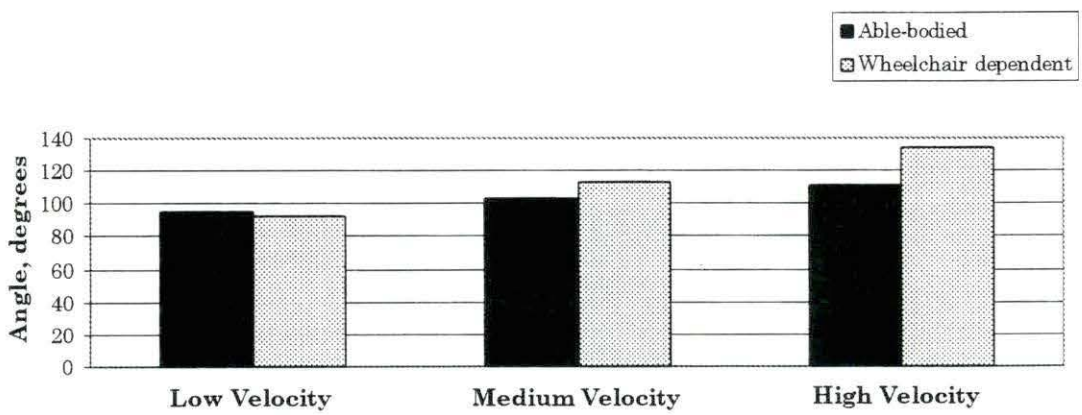

Figure 26 Averaged push angle for the low, medium, and high velocity conditions

push angle used by the wheelchair dependent subjects at the high velocity condition indicates that these subjects were using a greater portion of the wheelchair handrim in accomplishing their force application. This also corresponds with a greater propulsion time at the high velocity condition as shown in Figure 20. Since the hands must be in contact with the handrim during the propulsion phase, a longer propulsion time at a given velocity requires a larger push angle.

Figure 27 indicates that the start angle decreased (further rearward) with increasing velocity, although not significantly, with a significantly lower start angle seen at the high velocity condition for the wheelchair dependent group. In order for the wheelchair dependent subjects to achieve a larger push angle, it

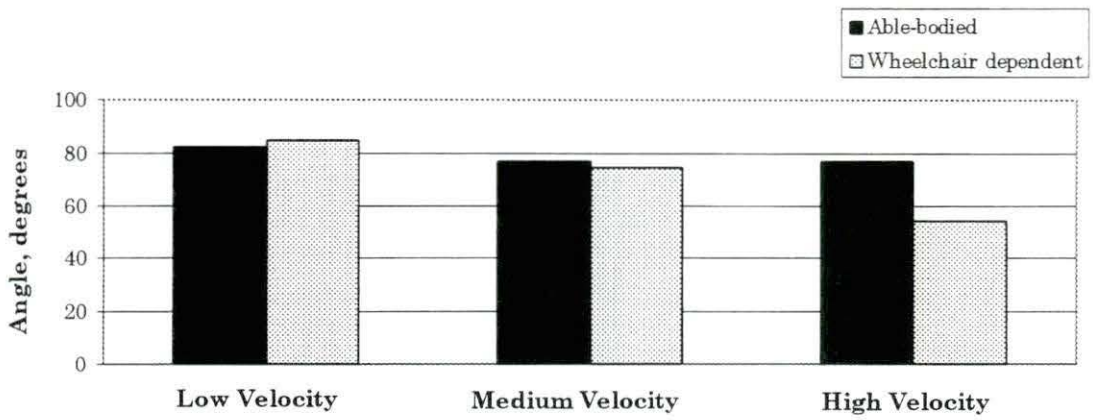

Figure 27 Averaged start angle for the low, medium, and high velocity conditions

was necessary for them to grasp the handrim further back since it was not possible for these subjects to gain much motion in the forward direction because they were already nearly fully extending their elbow joints. Furthermore, the wheelchair dependent subjects could not lean forward in order to gain additional range of motion as could the able-bodied subjects. Their lack of trunk support to prevent their falling forward prevented this. One must bear in mind that the angular data was obtained qualitatively and is merely a rough estimate of the wheelchair handrim contact positions. Further investigation should be done, preferably using three-dimensional videotaping techniques, to better determine the points in which wheelchair handrim contact occurs.

Within groups

Figures 28 through 34 show the individual results obtained for propulsion time, recovery time, cycle time, % propulsion time, % recovery time, work per stroke, and push angle from all of the subjects. All of the able-bodied subjects exhibited a decrease in propulsion time with increasing velocity. However, two of the wheelchair dependent subjects did not conform to this pattern (WD-1 and WD-3). WD-1 showed an increase in propulsion time with increasing velocity while WD-3 showed an increase from the medium to high velocity levels. Analysis of the videotape revealed that subject WD-1 took very short, fast strokes at the low velocity level, resulting in decreased cycle time and push

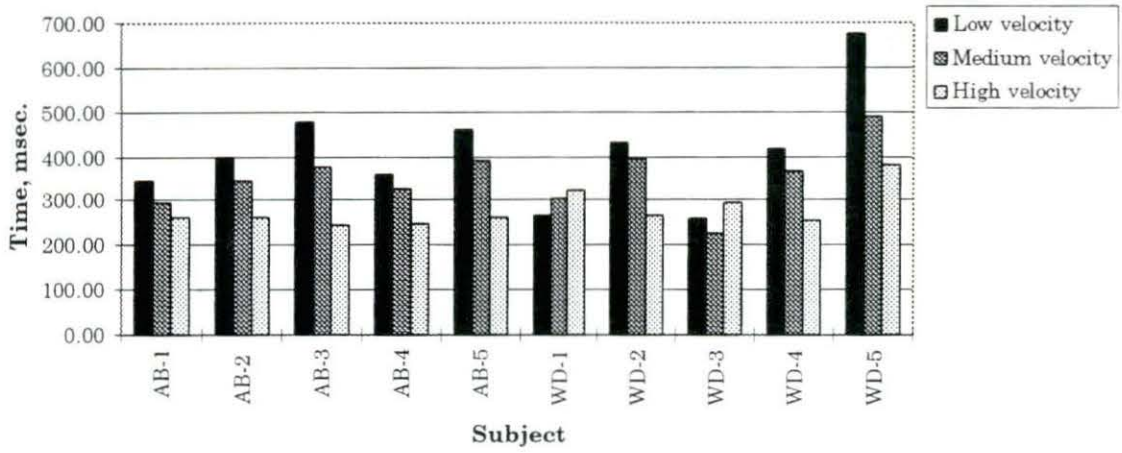

Figure 28 Propulsion time

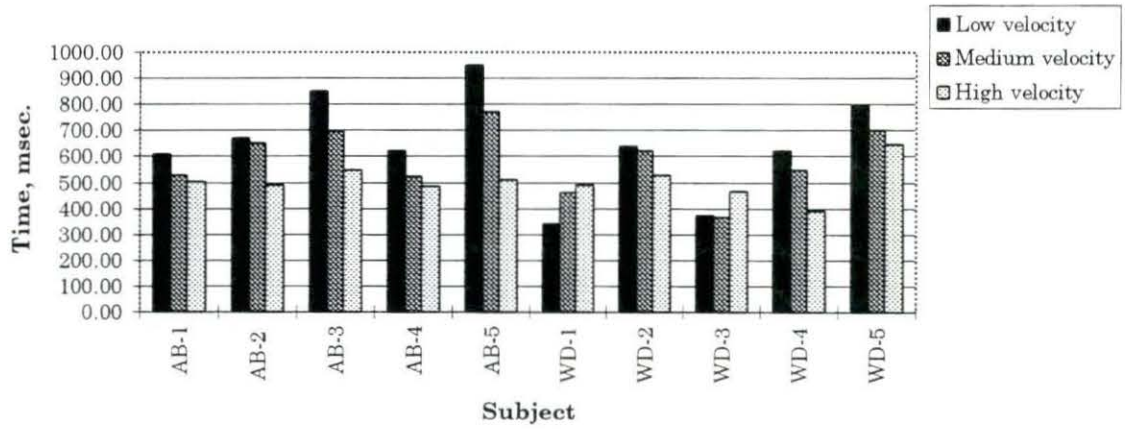

Figure 29 Recovery time

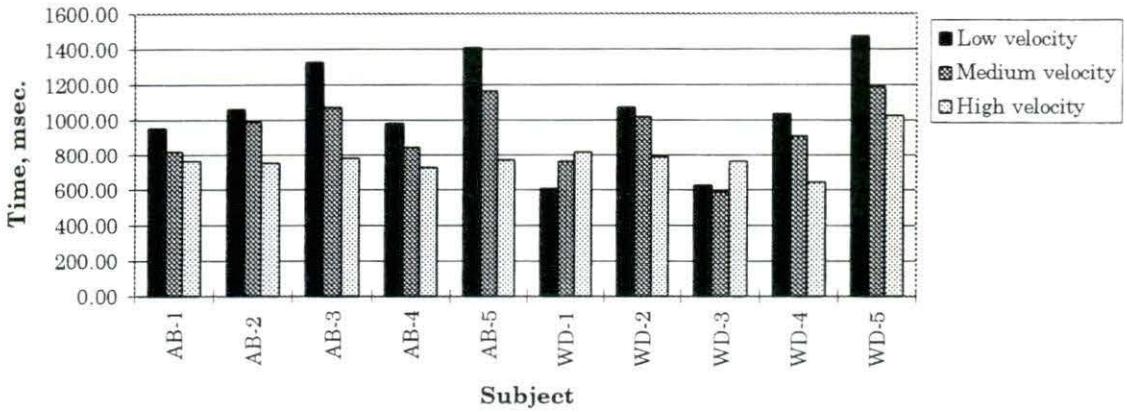

Figure 30 Cycle time

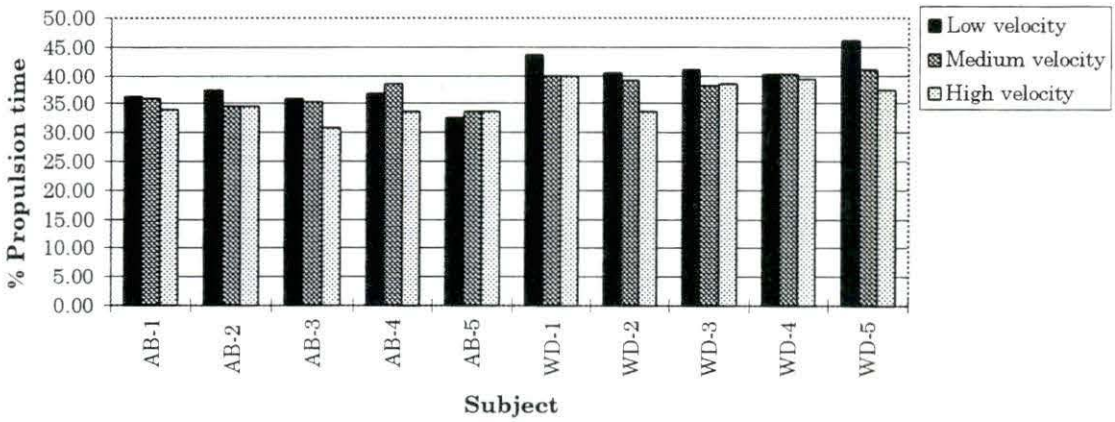

Figure 31 % Propulsion time

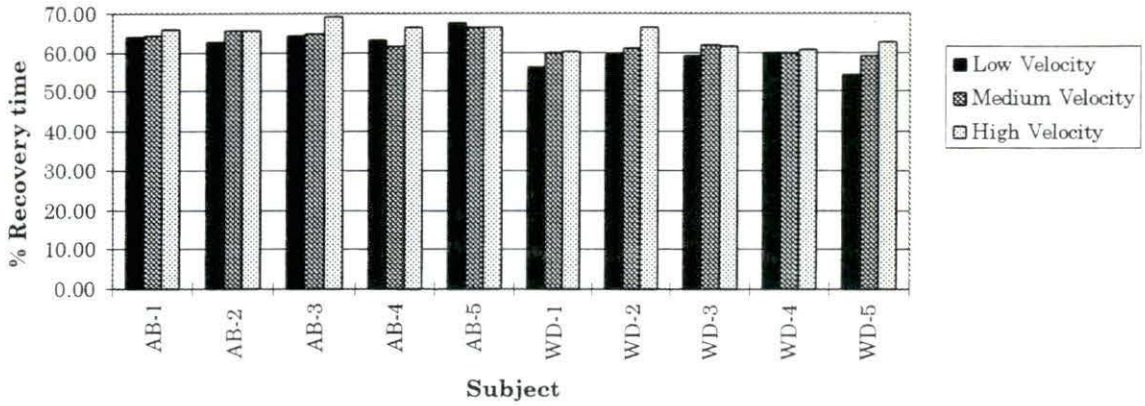

Figure 32 % Recovery time

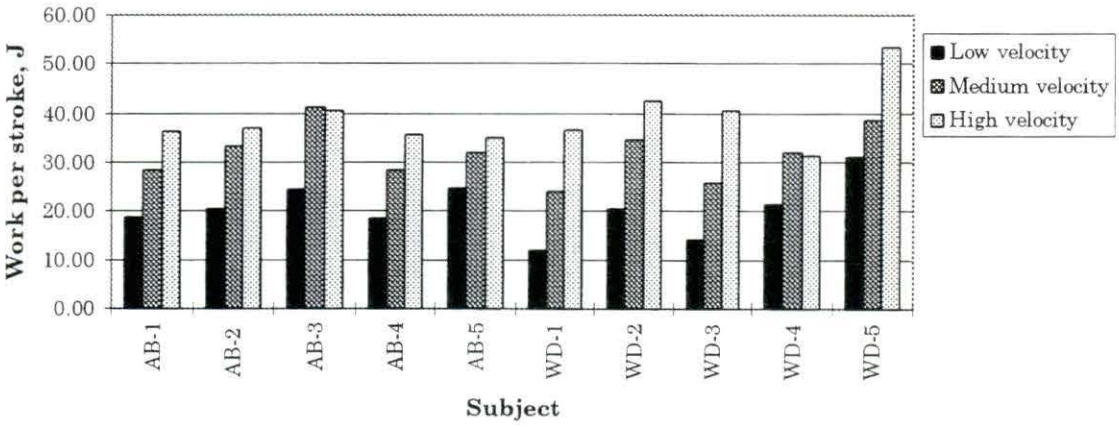

Figure 33 Work per stroke

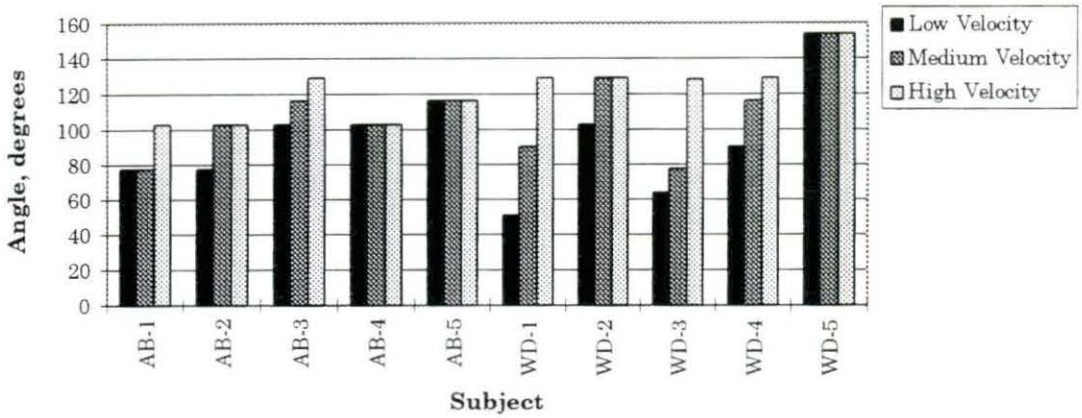

Figure 34 Push angle

angle. As velocity increased, the subject decreased the start angle, thus increasing the push angle and resulting in an increase in propulsion, recovery, and cycle times. Therefore, rather than increasing stroke frequency with increasing velocity, subject WD-1 showed responses more typical of an increase in resistance at a constant velocity as found by Veeger et al. (1991). They found that propulsion time and cycle time increased with increasing resistance. This suggests that velocity differences may not affect the stroke technique of this subject as greatly as the effects of increased resistance. Subject WD-3 appeared to take long, more forceful strokes at the high velocity, thus increasing cycle time, push angle, and recovery time.

Subject WD-5 had a much higher propulsion time than any of the other subjects, particularly at the low and medium velocity levels. Videotape analysis

revealed that this subject, and subject WD-2, employed a circular motion during the recovery phase, rather than the pumping or linear motion of the hand seen by the other subjects. This circular motion allowed the subject to grasp the handrim further back, yielding a much greater push angle. The subject took long, powerful strokes, yielding larger %PT and lower %RT than the other wheelchair dependent subjects. This was particularly true at the low and medium velocity conditions. This subject showed the highest work per stroke at all three velocity levels. This subject had a large upper body, was a former weightlifter, and had been in the wheelchair the longest of all of the wheelchair dependent subjects (33 years). The subject's weightlifting background may explain the use of lower frequency, more powerful strokes as well as a circular recovery stroke motion. This has been suggested (Steadward, 1979) to be more efficient since the pump motion requires abrupt changes in hand direction, requiring greater neuromuscular activity to brake and accelerate the limbs. The circular motion makes it easier to match the handrim velocity upon contact, thus preventing hand braking forces from hampering propulsion efforts. Subject WD-2 also used a circular recovery stroke motion, also resulting in high propulsion, recovery, and cycle times as well as larger push angles for the low and medium velocity conditions. In fact, subjects WD-2 and WD-5 had the highest propulsion, recovery, and cycle times as well as push angles for the low and medium velocities of any of the wheelchair dependent subjects. However, these

subjects did not display the highest gross propulsion efficiencies; therefore a circular recovery technique does not necessarily provide greater efficiency.

Subjects AB-3 and AB-5 showed greater values than the other able-bodied subjects at the low and medium velocity levels in propulsion time, recovery time, cycle time, work per stroke, and push angle. Videotape analysis revealed that these subjects, although not employing a circular stroke technique, utilized a greater portion of the handrim than the other able-bodied subjects, thus resulting in an increased push angle, PT, RT, CT, and WS.

Electromyography

Middle deltoid

Qualitative analysis of the rectified and smoothed EMG plots showed middle deltoid activity during the latter portion of the propulsion phase and throughout the recovery phase. This pattern of activity, reported by other investigators (Ross and Brubaker, 1984), was seen in all of the subjects and at all velocity levels. All of the subjects showed a lapse in activity during the early portion of the recovery phase, thus separating the deltoid EMG activity into two separate regions: one confined to the latter part of the propulsion phase and one during the mid to latter portion of the recovery phase. This trend was not specific to any particular velocity, although it was more pronounced during the medium and high velocity trials for some subjects (AB-4, AB-5, WD-3, and WD-4).

However, there was too much intersubject variation to associate this pattern with any particular velocity or group of subjects. This bimodal trend was also found by Veeger et al. (1991) for the biceps brachii and tricep brachii muscle groups. It has been suggested to be caused by the transition from pulling to pushing on the wheelchair handrim. However, the bimodal pattern seen in this study did not support this conclusion since the break in muscle activity occurred during the recovery phase of the propulsion stroke. Therefore, it is much more likely that joint movement patterns account for the EMG activity patterns seen. The principle function of the middle deltoid muscle is to abduct the arm, with the anterior deltoid flexing and medially rotating the arm and the posterior deltoid extending and laterally rotating the arm (Carola et al., 1992). The activity seen during the latter portion of the propulsion phase is due to arm flexion occurring as the hands followed the handrim motion. Flexion was maximal during the latter part of the propulsion phase, thus producing a greater degree of deltoid involvement. Medial rotation of the arm during the propulsion phase may have also contributed to deltoid activity. It is probable that anterior deltoid activity was picked up by the electrodes, resulting in the propulsion phase activity seen. The activity seen during the recovery phase was due to arm abduction. As the hands were brought back to the handrim for the start of another stroke, the arms were abducted so that the hands remained clear of the handrim, with more abduction occurring as the hands were moved further up

and back. Spaulding and Robinson (1984) found extensive deltoid activity during bilateral inclined sanding exercises, which consist of arm extension during the up phase of the sanding. It was also found that less deltoid activity occurred when the shoulder was maintained in an adducted position. Therefore, it would seem that wheelchair designs which minimize abduction of the shoulder should produce minimum deltoid activity, although possibly at the expense of increased activity in other muscles. Lateral motion of the arms was difficult to identify on the videotape since the camera was perpendicular to the plane of motion. Videotaping from the front or rear of the subject would allow better visualization of arm abduction and thus, correlation between degree of abduction and middle deltoid activity. There were no apparent differences seen between the subjects using a circular recovery motion (WD-2 and WD-5) and the rest of the subjects. Rodgers et al. (1994) found that fatigued muscles were active for a slightly larger portion of the propulsion cycle than non-fatigued muscles. This trend was not found, thus verifying the unlikelihood of muscle fatigue. However, a frequency analysis has not been conducted for manual wheelchair propulsion, and it might yield useful information regarding wheelchair prescription criteria, particularly for persons with quadriplegia who must rely on a relatively small percentage of upper body muscles to achieve propulsion. There were no apparent differences in middle deltoid EMG patterns

at any of the velocity levels between the able-bodied and wheelchair dependent subject groups.

Total EMG activity increased for all subjects from the low to medium and medium to high velocity conditions. Table 13 shows the EMG amplitudes

Table 13 Rectified smoothed amplitudes of middle deltoid EMG

	Low Velocity	Medium Velocity	High Velocity
AB-1	47.33	69.51	119.90
AB-2	43.52	62.11	109.10
AB-3	28.03	36.15	69.47
AB-4	50.01	108.09	148.73
AB-5	48.63	63.22	105.87
WD-1	211.79	223.21	282.70
WD-2	40.48	60.85	65.74
WD-3	101.40	147.68	179.44
WD-4	19.38	30.20	58.40
WD-5	27.93	30.69	33.08

obtained from the rectified and smoothed EMG arrays for the deltoid muscle studied. Since normalization was not used in this study, amplitudes between subjects or groups cannot be compared. However, it is evident that, for the deltoid muscle, activity increased with increasing velocity (increasing handrim force). Bigland-Ritchie and Woods (1974) found that, for forces less than about

75% MVC, the relationship between EMG and force is linear. Furthermore, at low force levels (25% to 75% MVC), little change in firing frequency of individual motor units occurs. Therefore, it appears that recruitment of additional motor units is largely responsible for increasing the force of a voluntary contraction (Bigland-Ritchie and Woods, 1974). Fast-twitch muscle fibers are generally larger in diameter than slow-twitch fibers and therefore produce a higher amplitude action potential. The fast-twitch muscle fibers are recruited as force increases so that, with increasing force, there is a greater percentage of fast-twitch to slow-twitch muscle fibers. Therefore, the amplitude of the EMG signal increases with increasing force (Basmajian and DeLuca, 1985). It therefore appears as though additional recruitment of motor units as well as recruitment of fast-twitch muscle fibers may both have acted to increase the mean deltoid activity with increasing velocity. Ross and Brubaker (1984) also found total activity to be greater for higher power output conditions than for lower.

Lateral triceps

Triceps activity was found to be much more varied between the subjects than deltoid activity. Movement artifact also resulted in a shifting baseline so that it was difficult to tell whether motor unit activity or an increased baseline was occurring. This shifting baseline required careful comparison of the rectified smoothed plots with the rectified plots since the smoothed plots did not

discriminate between motor unit activity and movement artifact. Digital filtering of the movement artifact was not possible since the EMG signal and artifact were of the same general frequency. Nevertheless, conclusions could still be made as to EMG activity patterns. However, relative amplitudes could not be compared between velocity levels since the movement artifact contribution to the amplitude did not reflect actual EMG activity and was not constant across velocity levels or subjects. Thus, the movement artifact would add to the actual EMG signal in computing the mean amplitude but would not reflect muscle activity reliably.

Lateral tricep activity was found to vary greatly, ranging from the propulsion phase to various portions of the recovery phase. However, it appears that, for most subjects, EMG activity could be associated with the propulsion phase of the stroke cycle. Ross and Brubaker (1984) found lateral tricep activity during the latter portion of the propulsion phase and throughout the recovery phase while Masse et al. (1992) identified triceps activity with the latter part of the propulsion phase. It is likely that the lateral tricep functioned primarily as a forearm extensor during the propulsion phase of the stroke. It is interesting to note that subject WD-5, who used a circular stroke technique during the recovery phase, showed lateral tricep activity throughout the recovery phase. This occurred primarily during the low velocity condition in which he appeared to exhibit the greatest circular stroke pattern. Analysis of the videotape

revealed that this subject maintained an extended elbow throughout the recovery phase, thus resulting in tricep activity since the main function of the tricep is to extend the elbow joint (Carola et al., 1992). Subject WD-2, who also used a circular stroke technique, primarily showed tricep activity during the recovery phase for the medium velocity condition. Small amounts of tricep activity during the recovery phase were also seen in the low and high velocity conditions. However, this subject did not employ a recovery stroke pattern nearly as circular as subject WD-5. Further study should be conducted in this regard since two subjects are not sufficient to draw conclusions concerning EMG pattern based on recovery stroke technique.

SUMMARY AND CONCLUSIONS

Propulsion Efficiency and Oxygen Uptake

The wheelchair dependent subject group exhibited higher propulsion efficiencies than the able-bodied subject group at all three velocity levels, with the efficiency differences at the high velocity level being significant. Also, the wheelchair dependent subjects showed a significantly lower oxygen uptake than the able-bodied group at the high velocity level. Significant power output effects were found for both propulsion efficiency and oxygen uptake, with both parameters increasing with increasing power output. However, the able-bodied group did not show a propulsion efficiency that was significantly dependent upon power output level. These results suggest that propulsion efficiency and oxygen uptake differences between able-bodied and wheelchair dependent subject groups may best be found under conditions of relatively high power output. This is due to the inability of the wheelchair dependent subjects to properly maintain cardiorespiratory functions at these levels. Normal wheelchair operating speeds are from 0.56 to 1.11 m/s on level surfaces (Lemaire et al., 1991), consistent with the velocity conditions in the present study. Since significant differences were not shown for propulsion efficiency and oxygen uptake at the low and medium velocity levels, able-bodied subjects may appear to be appropriate for use in studies conducted at relatively low manual

wheelchair operating conditions. However, this conclusion could lead to serious errors in assumptions concerning the ability of a recently injured person to operate a manual wheelchair, particularly if the level of spinal cord injury is higher than the level of the subjects who participated in this study. For instance, a new wheelchair design may yield higher propulsion efficiencies and lower oxygen uptakes for both able-bodied and wheelchair dependent individuals. However, higher efficiencies found for wheelchair dependent individuals are not likely due to improved propulsion techniques, particularly in recently injured individuals who have no established technique, but are more likely to be the result of cardiorespiratory deficiencies which actually reduce the likelihood that the wheelchair will be satisfactory for the individual. Therefore, propulsion efficiency and absolute oxygen uptake measurements are not good indicators of the ability for a spinal cord injured subject to operate a manual wheelchair. Efficiency is a misleading term in that it implies a positive benefit. In fact, the higher the efficiency (lower oxygen uptake), the greater are the chances that the individual will tire too quickly during day to day activities for a manual wheelchair to be considered an option. If oxygen uptake measurements are to be used in determining one's ability to operate a manually powered wheelchair, normalization should be used in which the oxygen uptake during a submaximal test situation is evaluated based on a percentage of maximum oxygen uptake for that individual. This would give a better indication of how

strenuous manual wheelchair operation is based upon the physiological characteristics of that individual. Since cardiorespiratory function is a major limitation for wheelchair dependent individuals, wheelchair designs which minimize the load on the cardiorespiratory system should be pursued. Wheelchair studies should always consider cardiorespiratory effects prior to drawing conclusions. For instance, a seating position which maximizes handrim contact or minimizes EMG signals but produces a greater cardiorespiratory response will not be beneficial to the wheelchair dependent individual.

Kinematic Parameters

Probably the most significant finding in the present study was that the wheelchair dependent subjects showed a significantly higher percentage of propulsion time as well as a significantly lower percentage of recovery time than the able-bodied subjects at all three velocity levels. This indicates that, through training and adaptation, the wheelchair dependent subjects have learned to use a greater portion of the handrim, as evidenced from the significantly higher push angle found during the high velocity condition, during the propulsion stroke. Thus, they minimize the wasted energy of the recovery phase. This idea has great potential in manual wheelchair design. Designs which maximize handrim contact and encourage a circular recovery motion should be pursued. Subject position relative to the handrims is crucial, requiring careful positioning

analysis during wheelchair prescription. Anthropometric criteria could be established to help the wheelchair prescriber obtain correct positioning based on body measurements. However, any established criteria concerning manual wheelchair prescription should be recognized as being the general case, with fine tuning done based on the individual requirements of the patient. It seems reasonable that the lower, forward positions of the wheelchair user relative to the handrims should provide maximum handrim contact since this positioning allows the individual to maintain handrim contact further down the rim at the end of the propulsion phase of the stroke. This position was found to yield the highest propulsion efficiencies by Brubaker and McLaurin (1982), although it seems that a forward seating position should increase rolling resistance by placing the center of gravity more over the front casters. Further research in this area is necessary to determine whether increased rolling resistance is significant as compared with efficiency benefits when seating the individual further forward. Three dimensional videotaping should be conducted to better identify individual subject recovery stroke patterns as well as to identify the causes of EMG signals, such as arm abduction, which are difficult to distinguish using two-dimensional techniques. Further studies should also be conducted in order to determine whether a correlation exists between subject seating position and percent propulsion and recovery times.

Electromyography

Although differences were not found in the present study between the able-bodied and wheelchair dependent subject groups, the middle deltoid and lateral tricep activity seen was similar to that found by Ross and Brubaker (1984). Deltoid activity occurred during the latter part of the propulsion phase and throughout the recovery phase and appeared to be due primarily to flexion and medial rotation of the arm during the propulsion phase and abduction during the recovery phase. Tricep activity occurred mainly during the propulsion phase and was probably due to extension of the elbow joint. Electromyography has perhaps the greatest potential in terms of manual wheelchair prescription. Few studies have been conducted utilizing electromyography to investigate manual wheelchair propulsion. None of these studies have addressed the potential benefits of electromyography in terms of wheelchair prescription or design. The muscles responsible for achieving wheelchair propulsion have been established in the literature (Harburn and Spaulding, 1986; Ross and Brubaker, 1984). However, more studies need to be conducted concerning recruitment and firing frequency differences as well as signal amplitude differences between able-bodied and wheelchair dependent individuals. Although normalization has been used to attempt to quantify and compare signal amplitudes, there appears to be some question of the validity of using a statically determined baseline signal in conjunction with dynamic movements. Amplitude analysis could be useful in

wheelchair design, with design criteria being the minimization of EMG activity. Frequency analysis has not been used to date to study muscle fatigue during manual wheelchair propulsion. This could be particularly valuable in wheelchair prescription. The patient could be monitored electromyographically throughout a series of tests and muscle fatigue could be identified. Early fatigue problems or fatigue in key propulsion muscles could be used to rule out the manual wheelchair option for the patient. It appears from this and former studies that qualitative temporal analysis alone is insufficient to identify differences between able-bodied and wheelchair dependent subjects, particularly due to the excessive subject variability found.

Summary

The present study has shown the need for careful subject pool consideration when investigating manual wheelchair propulsion. Several differences were found between the two subject groups:

1. Wheelchair dependent individuals showed lower oxygen uptakes and higher propulsion efficiencies than the able-bodied individuals, with differences being more apparent with increasing workload.
2. Wheelchair dependent individuals showed higher percent propulsion and lower percent recovery times than the able-bodied individuals, regardless of workload level.

3. Wheelchair dependent individuals exhibited more individualized stroke techniques than the able-bodied individuals, particularly at high workloads.
4. Wheelchair dependent individuals showed a greater ability to overcome negative handrim velocity effects than the able-bodied individuals. This is most likely due to a more accurate force application to the handrim by the wheelchair dependent individuals.

The present study has also confirmed the results of other investigators:

1. Gross manual wheelchair propulsion efficiencies were low, ranging from 7.3 to 15.5 and being in general agreement with the findings of other investigators (Brubaker and McLaurin, 1982; Veeger et al., 1992; Brubaker et al., 1984).
2. At high velocities, propulsion efficiency decreased (Brubaker and McLaurin, 1982; Veeger et al., 1992; van der Woude et al., 1988a) although some wheelchair dependent individuals may overcome velocity effects due to manual wheelchair propulsion experience.
3. Propulsion time, recovery time, total cycle time, and percent propulsion time decreased while percent recovery time increased with increasing velocity (Veeger et al., 1989; van der Woude et al., 1988a; van der Woude et al., 1989)

4. Middle deltoid EMG is associated with the end of the propulsion phase (arm flexion, medial rotation) and throughout the recovery phase (arm abduction) while lateral tricep EMG is associated with the propulsion phase (elbow extension) (Ross and Brubaker, 1984).

Future Research

Immediate research ideas include muscle fatigue analysis using frequency domain techniques on the EMG signal, three dimensional videotaping and digitization for stroke technique analysis, and verification of the results of the present study by incorporating subjects with different spinal injury levels as well as comparisons between wheelchair dependent males and females. Acceleration and deceleration characteristics could be studied following dynamometer modification to account to the linear inertia normally experienced by a manual wheelchair user, as well as equipping the dynamometer to maintain a constant resistance regardless of wheelchair velocity. Comparisons between subject groups could also be conducted using different types of wheelchairs and components.

Future research should focus on establishing standards for the wheelchair prescriber to follow when prescribing a manual wheelchair for a patient. Electromyography, oxygen uptake/propulsion efficiency monitoring, and kinematic stroke training all have tremendous potential benefits in helping to

achieve the most ideal manual wheelchair prescription possible. However, standards must first be developed which are applicable to all manual wheelchair users with the flexibility to adjust the standards to the individual under consideration. Additional training will be required for the wheelchair prescriber to correctly use the physiological and kinematic tools to the advantage of the patient. Lastly, researchers, designers, and prescribers need to work together so that data gathered in the laboratory can be used to benefit the manual wheelchair user. Hopefully, in the near future, the principle limitation to the wheelchair dependent individual will not be the wheelchair itself.

REFERENCES

Adams, W.C. 1966. Influence of age, sex, and body weight on the energy expenditure of bicycle riding. Journal of Applied Physiology 22(3): 539-545.

Antti, C.J. 1977. Relationship between time means of external load and EMG amplitude in long term myoelectric studies. Electromyography and Clinical Neurophysiology 17: 45-53.

Basmajian, J.V. 1978. Muscles Alive: Their Functions Revealed by Electromyography. Williams and Wilkins Co., Baltimore, Maryland. 495 pp.

Basmajian, J.V. and DeLuca, C.J. 1985. Muscles Alive: Their Functions Revealed by Electromyography. Williams and Wilkins Co., Baltimore, Maryland. 561 pp.

Basmajian, J.V., Clifford, H.C., McLeod, W.D. and Nunnally, H.N. 1975. Computers in Electromyography. Butterworths, Reading, Massachusetts. 138 pp.

Bigland, B., Lippold, O.C.J. and Wrench, A. 1953. Electrical activity in isotonic contractions of human calf muscles. Journal of Physiology 120: 40-41.

Bigland-Ritchie, B., and Woods, J. 1974. Integrated EMG and oxygen uptake during dynamic contractions of human muscles. Journal of Applied Physiology 36(4): 475-479.

Brubaker, C.E., McClay, I.S. and McLaurin, C.A. 1984. Effect of seat position on wheelchair propulsion efficiency. Proceedings of the 2nd International Conference on Rehabilitation Engineering - Ottawa. 12-14.

Brubaker, C.E., and McLaurin, C.A. 1982. Ergonomics of wheelchair propulsion. Pages 22-42 in F.L. Golbranson and R.W. Wirta (eds.). Wheelchair, Vol. III. RESNA, Washington D.C.

Burke, D.C. and Murray, D.D. 1975. Handbook of Spinal Cord Medicine. The Macmillan Press Limited, London. 90 pp.

Carola, R., Harley, J.P. and Noback, C.R. 1992. Human Anatomy and Physiology. McGraw-Hill, Inc., New York, New York. 978 pp.

Dreissinger, T.E. and Londeree, B.R. 1982. Wheelchair exercise: a review. Paraplegia 20: 20-34.

Ekholm, J., Arborelius, U.P., Hillered, L. and Ortqvist, A. 1978. Shoulder muscle EMG and resisting moment during diagonal exercise movements resisted by weight-and-pulley-circuit. Scandinavian Journal of Rehabilitation Medicine 10: 179-185.

Gaesser, G.A. and Brooks, G.A. 1975. Muscular efficiency during steady-rate exercise: effects of speed and work rate. Journal of Applied Physiology 38(6): 1132-1139.

Ganong, W.F. 1991. Review of Medical Physiology. Appleton and Lange, Norwalk, Connecticut 754 pp.

Gettys, W.E., Keller, F.J. and Skove, M.J. 1989. Physics. McGraw-Hill, Inc., New York, New York. 984 pp.

Glaser, R.M., Sawka, M.N., Young, R.E. and Suryaprasad, A.G. 1980. Applied physiology for wheelchair design. Journal of Applied Physiology 48(1): 41-44.

Glaser, R.M., Sawka, M.N., Laubach, L.L. and Suryaprasad, A.G. 1979. Metabolic and cardiopulmonary responses to wheelchair and bicycle ergometry. Journal of Applied Physiology 46(6): 1066-1070.

Guttmann, L. 1973. Spinal Cord Injuries: Comprehensive Management and Research. Blackwell Scientific Publications, London. 694 pp.

Harburn, K.L. and Spaulding, S.J. 1986. Muscle activity in the spinal cord-injured during wheelchair ambulation. The American Journal of Occupational Therapy 40(9): 629-637.

Heartquist, P.E. 1985. Physiological requirements for full-time employment of physically handicapped. Ph.D. Dissertation, University of Southern California. 162 pp.

Hildebrandt, G., Voigt, E., Bahn, D., Berendes, B. and Kroger, J. 1968. Energy costs of propelling wheelchair at various speeds: cardiac response and effect on steering accuracy. Archives of Physical Medicine and Rehabilitation, March: 131-136.

Hjeltnes, N. 1993. Changes in cardiovascular responses to graded arm ergometry in tetra- and paraplegic patients during primary rehabilitation. Pages 79-91 in Ergonomics of Manual Wheelchair Propulsion: State of the art. IOS Press, Washington D.C.

Hoffman, M.D. 1986. Cardiorespiratory fitness and training in quadriplegics and paraplegics. Sports Medicine 3:312-330.

Hopman, M.T.E., Oeseburg B. and Binkhorst, R.A. 1993. Cardiovascular aspects in spinal cord injured subjects. Pages 103-108 in Ergonomics of Manual Wheelchair Propulsion: State of the art. IOS Press, Washington D.C.

Karpovich, P.V. and Sinning, W.E. 1971. Physiology of Muscular Activity (7th ed.). W.B. Saunders Co., Philadelphia, Pennsylvania. 374 pp.

Kauzlarich, J.J. and Thacker, J.G. 1985. Wheelchair tire rolling resistance and fatigue. Journal of Rehabilitation Research and Development 22(3):25-41.

Lemaire, E.D., Lamontagne, M., Barclay, H.W., John, T. and Martel, G. 1991. A technique for the determination of center of gravity and rolling resistance for tilt-seat wheelchairs. Journal of Rehabilitation Research and Development 28(3):51-58.

Lippold, O.C.J. 1952. The relation between integrated action potentials in human muscle and its isometric tension. Journal of Physiology 117: 492-499.

Long, C. and Lawton, E.B. 1955. Functional significance of spinal cord lesion level. Archives of Physical Medicine and Rehabilitation, April: 249-255.

Martini, F.H. 1992. Fundamentals of Anatomy and Physiology (2nd ed.). Prentice Hall, Englewood Cliffs, New Jersey. 985 pp.

Masse, L.C., Lamontagne, M. and O'Riain, M.D. 1992. Biomechanical analysis of wheelchair propulsion for various seating positions. Journal of Rehabilitation Research and Development 29(3):12-28.

Matsui, H. and Kobayashi, K. 1983. Biomechanics VIII: Proceedings of the Eighth International Congress of Biomechanics. Human Kinetics Publishers, Champaign, Illinois.

McArdle, W.D., Katch, F.I. and Katch, V.L. 1991. Exercise Physiology: Energy, Nutrition, and Human Performance (3rd ed.). Lea and Febiger, Philadelphia, Pennsylvania. 853 pp.

McLaurin, C.A. and Brubaker, C.E. 1991. Biomechanics and the wheelchair. Prosthetics and Orthotics International 15: 24-37.

Neter, J., Wasserman, W. and Kutner, M.H. 1990. Applied Linear Statistical Models (3rd ed.). Irwin, Inc., Homewood, Illinois. 1181 pp.

Newall, A.R., Robinson, K.L. and Spaulding, S.J. 1981. An electromyographic study of shoulder muscles during bilateral sanding: a pilot study. Canadian Journal of Occupational Therapy 48: 163-168.

O'Reagan, J.R. 1978. The Design of a Wheelchair Dynamometer. M.S. Thesis, University of Virginia.

Petrofsky, J.S. 1979. Frequency and amplitude analysis of the EMG during exercise on the bicycle ergometer. European Journal of Applied Physiology 41: 1-15.

Phillips, L. and Nicosia, A. 1990. Clinical perspectives on wheelchair selection. Journal of Rehabilitation Research and Development - Clinical Supplement No. 2 March: 1-7.

Powers, S.K., Beadle, R.E. and Mangum, M. 1980. Exercise efficiency during arm ergometry. Journal of Applied Physiology 49: 784-788.

Riley, W.F. and Sturges, L.D. 1993. Engineering Mechanics: Dynamics. John Wiley and Sons, Inc., New York, New York. 567 pp.

Rodgers, M.M. and Cavanagh, P.R. 1984. Glossary of biomechanical terms, concepts, and units. Physical Therapy 64(12): 1886-1902.

Rodgers, M.M., Gayle, W.G., Figoni, S.F., Kobayashi, M., Lieh, J. and Glaser, R.M. 1994. Biomechanics of wheelchair propulsion during fatigue. Archives of Physical Medicine and Rehabilitation 75: 85-93.

Ronchi, R., Ferrarin, M., Palmieri, R., Rabuffetti, M. and Spagnolin, A. 1993. Method for biomechanical analysis of wheelchair locomotion. Pages 241-253 in Ergonomics of Manual Wheelchair Propulsion: State of the art. IOS Press, Washington D.C.

Ross, S.A. and Brubaker, C.E. 1984. Electromyographic analysis of selected upper extremity muscles during wheelchair propulsion. Proceedings of the 2nd International Conference on Rehabilitation Engineering. Ottawa: 7-9.

Sanderson, D.J. and Sommer, H.J. III. 1985. Kinematic features of wheelchair propulsion. Journal of Biomechanics 18(6): 423-429.

Sawka, M.N., Latzka, W.A. and Pandolf, K.B. 1993. Upper body exercise: application for wheelchair propulsion and spinal cord injured populations. Pages 151-161 in Ergonomics of Manual Wheelchair Propulsion: State of the art. IOS Press, Washington D.C.

Sinderby, C., Ingvarsson, P., Sullivan, L., Wickstrom, I. and Lindstrom, L. 1992a. Electromyographic registration of diaphragmatic fatigue during sustained Trunk flexion in cervical cord injured patients. Paraplegia 30: 669-677.

Sinderby, C., Ingvarsson, P., Sullivan, L., Wickstrom, I. and Lindstrom, L. 1992b. The role of the diaphragm in trunk extension in tetraplegia. Paraplegia 30: 389-395.

Spaulding, S.J. and Robinson, K.L. 1984. Electromyographic study of the upper extremity during bilateral sanding: unresisted and resisted conditions. The American Journal of Occupational Therapy 38(4): 258-262.

Starr, J.E. 1992. Basic strain gage characteristics. Pages 1-77 in Strain Gage Users' Handbook. Elsevier Applied Science, Bethel, Connecticut.

Steadward, R.D. 1979. Technique analysis - wheelchair racing. R.D. Steadward and C. Walsh (eds.). Proceedings of the First International Conference on Sport and Training of the Physically Disabled Athlete. Department of Physical Education, University of Alberta.

Stoboy, H., Rich, B.W. and Lee, M. 1971. Workload and energy expenditure during wheelchair propelling. Paraplegia 8: 223-230.

Sutton, N.G. 1973. Injuries of the Spinal Cord: The Management of Paraplegia and Tetraplegia. Butterworth and Co., London. 185 pp.

Veeger, H.E.J., Woude, L.H.V. van der and Rozendal, R.H. 1992. Effect of handrim velocity on mechanical efficiency in wheelchair propulsion. Medicine and Science in Sports and Exercise 24(1): 100-107.

Veeger, H.E.J., Woude, L.H.V. van der and Rozendal, R.H. 1989. Wheelchair propulsion technique at different speeds. Scandinavian Journal of Rehabilitation Medicine 21: 197-203.

Veeger, H.E.J., Woude, L.H.V. van der and Rozendal, R.H. 1991. Within-cycle characteristics of the wheelchair push in sprinting. Medicine and Science in Sports and Exercise 23(2): 264-271.

Webster, J.G. 1992. Medical Instrumentation: Application and Design (2nd ed.). Houghton Mifflin Co., Boston, Massachusetts. 814 pp.

Woude, L.H.V. van der. 1993. The wheelchair-user interface: the core of ergonomics?. Pages 271-292 in Ergonomics of Manual Wheelchair Propulsion: State of the art. IOS Press, Washington D.C.

Woude, L.H.V. van der, Hendrich, K.M.M., Veeger, H.E.J., Schenau, G.J. van ingen, Rozendal, R.H., DeGroot, G. and Hollander, A.P. 1988a. Manual wheelchair propulsion: effects of power output on physiology and technique. Medicine and Science in Sports and Exercise 20(1): 70-78.

Woude, L.H.V. van der, Veeger, H.E.J. and Rozendal, R.H. 1989. Propulsion technique in hand rim wheelchair ambulation. Journal of Medical Engineering and Technology 13(1/2): 136-141.

Woude, L.H.V. van der, Veeger, H.E.J., Rozendal, R.H., Schenau, G.J. van ingen, Rooth, F. and Nierop, P. van 1988b. Wheelchair racing: effects of rim diameter and speed on physiology and technique. Medicine and Science in Sports and Exercise 20(5): 492-500.

Zipp, P. 1982. Recommendations for the standardization of lead positions in surface electromyography. European Journal of Applied Physiology 50: 41-54.

ACKNOWLEDGEMENTS

I would like to thank my major professor, Dr. Patrick Patterson, for his advice and guidance throughout this project. I also wish to thank Dr. Mary Helen Greer for serving on my program of study committee and for graciously providing the resources and funding needed to complete this project as well as my graduate studies. Thanks also to Dr. Jeffrey Huston for serving on my committee and providing insights on the dynamometer mechanics.

I wish to express my gratitude to the faculty and staff in the department of Health and Human Performance at Iowa State University for allowing me to use their equipment and facilities to conduct this research. I would also like to thank the Woodward State Hospital Adaptive Equipment Center for providing the wheelchair used in this study.

I wish to express my appreciation to my parents for their love and support throughout my undergraduate and graduate careers.

Finally, I thank my wife, Diane, for the love and encouragement that made this project possible.

APPENDIX A:

VO_2 TABLES AND PLOTS
EFFICIENCY AND VO_2 STATISTICAL ANALYSIS TABLES
O_2 AND CO_2 ANALYZER CALIBRATION PROCEDURES
KILOCALORIE EQUIVALENT TABLE

Subject AB-1 - Oxygen uptake and respiratory exchange ratio

Time	VO_2 (l/m)	RER
:30	0.51	0.97
1:00	0.62	0.95
1:30	0.73	0.97
2:00	0.71	0.99
2:30	0.83	1.01
3:00	0.86	1.05
3:30	0.96	1.08
4:00	0.96	1.11
4:30	1.13	1.16
5:00	1.21	1.18
5:30	1.49	1.17
6:00	1.49	1.23

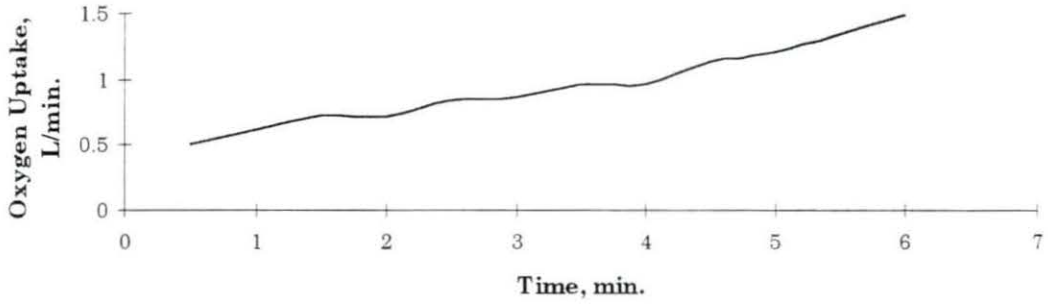

Subject AB-2 - Oxygen uptake and respiratory exchange ratio

Time	VO_2 (l/m)	RER
:30	0.63	0.68
1:00	0.52	0.73
1:30	0.59	0.76
2:00	0.62	0.77
2:30	0.62	0.72
3:00	0.77	0.83
3:30	0.8	0.89
4:00	0.77	0.79
4:30	0.97	0.77
5:00	1.07	1
5:30	1.15	1.15
6:00	1.31	1.08

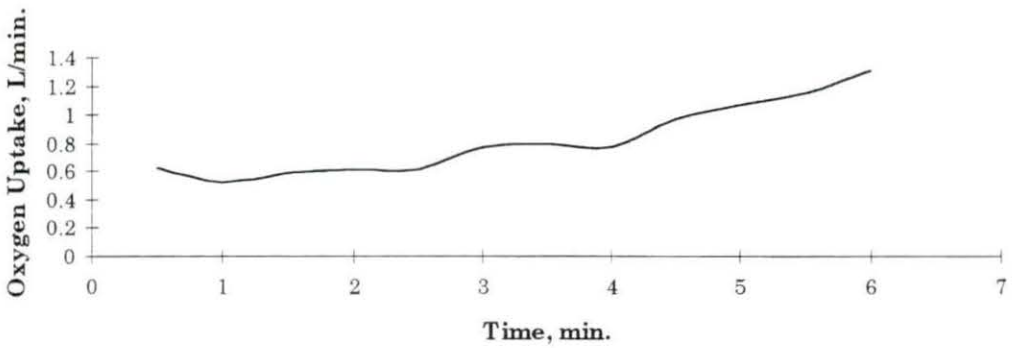

Subject AB-3 - Oxygen uptake and respiratory exchange ratio

Time	VO_2 (l/m)	RER
:30	0.52	1.13
1:00	0.52	1.02
1:30	0.55	0.94
2:00	0.73	1.02
2:30	0.65	0.97
3:00	0.88	1.04
3:30	0.99	1.21
4:00	0.97	1.2
4:30	1.18	1.16
5:00	1.27	1.11
5:30	1.44	1.07
6:00	1.58	1.05

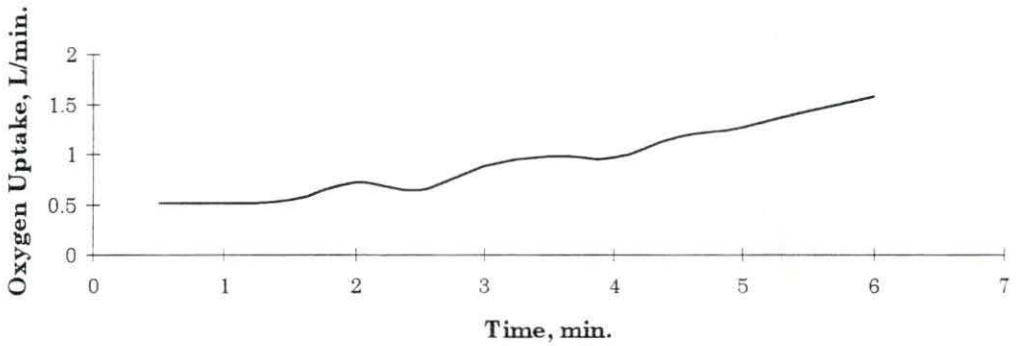

Subject AB-4 - Oxygen uptake and respiratory exchange ratio

Time	VO_2 (l/m)	RER
:30	0.44	0.92
1:00	0.56	0.91
1:30	0.41	0.92
2:00	0.62	0.92
2:30	0.69	0.97
3:00	0.76	0.97
3:30	0.85	0.98
4:00	0.9	0.99
4:30	1.14	1.03
5:00	1.14	1.05
5:30	1.31	1.11
6:00	1.53	1.18

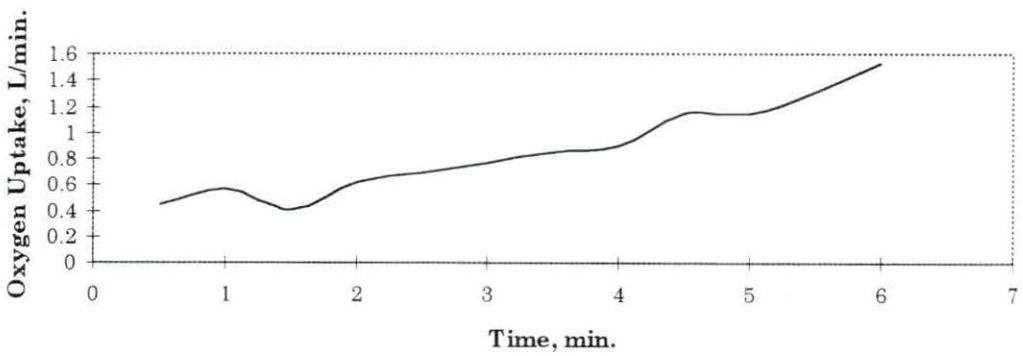

Subject AB-5 - Oxygen uptake and respiratory exchange ratio

Time	VO_2 (l/m)	RER
:30	0.6	0.7
1:00	0.51	0.71
1:30	0.78	0.7
2:00	0.68	0.74
2:30	0.86	0.78
3:00	0.9	0.81
3:30	0.96	0.84
4:00	1.01	0.87
4:30	1.09	0.85
5:00	1.33	0.91
5:30	1.47	1
6:00	1.67	1.01

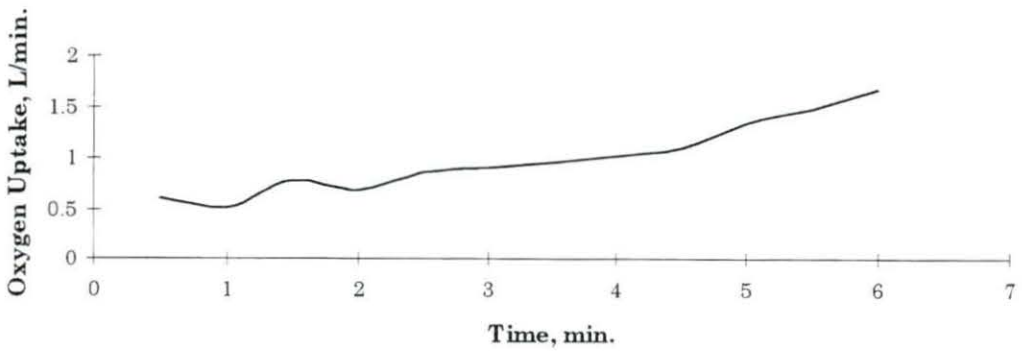

Subject WD-1 - Oxygen uptake and respiratory exchange ratio

Time	VO_2 (l/m)	RER
:30	0.4	0.91
1:00	0.5	0.88
1:30	0.61	0.88
2:00	0.42	0.9
2:30	0.61	0.86
3:00	0.69	0.91
3:30	0.62	0.93
4:00	0.68	0.92
4:30	0.8	0.92
5:00	0.86	0.95
5:30	0.88	0.96
6:00	0.94	0.97

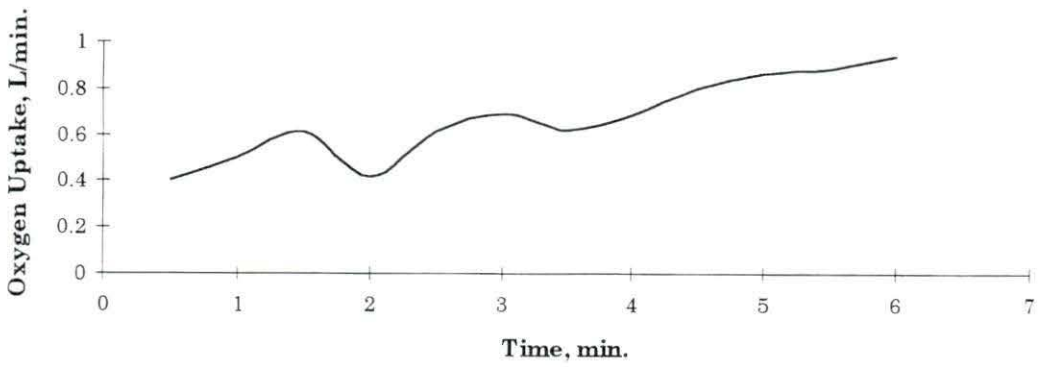

Subject WD-2 - Oxygen uptake and respiratory exchange ratio

Time	VO_2 (l/m)	RER
:30	0.49	0.91
1:00	0.66	0.82
1:30	0.72	0.79
2:00	0.83	0.82
2:30	0.76	0.87
3:00	0.8	0.83
3:30	0.88	0.84
4:00	0.94	0.83
4:30	0.94	0.81
5:00	1.16	0.85
5:30	1.19	0.86
6:00	1.13	0.9

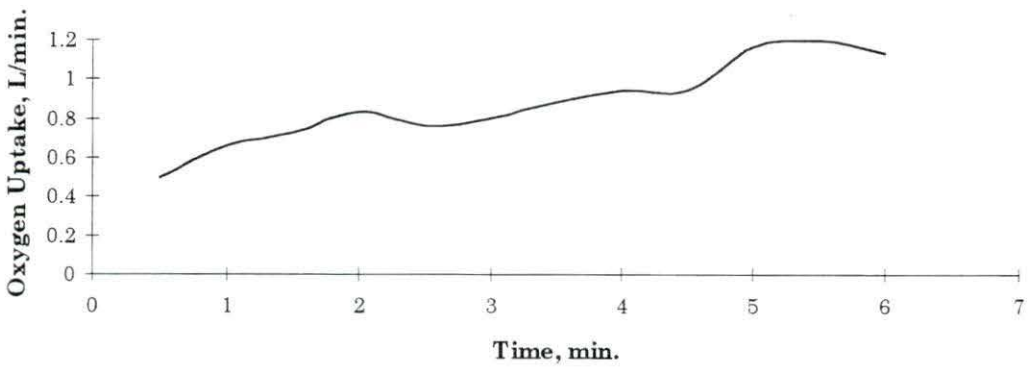

Subject WD-3 - Oxygen uptake and respiratory exchange ratio

Time	VO_2 (l/m)	RER
:30	0.51	0.65
1:00	0.64	0.7
1:30	0.59	0.76
2:00	0.68	0.82
2:30	0.71	0.87
3:00	0.7	0.84
3:30	0.78	0.86
4:00	0.85	0.9
4:30	0.86	0.86
5:00	1.04	0.9
5:30	1.05	1.04
6:00	1.18	1.1

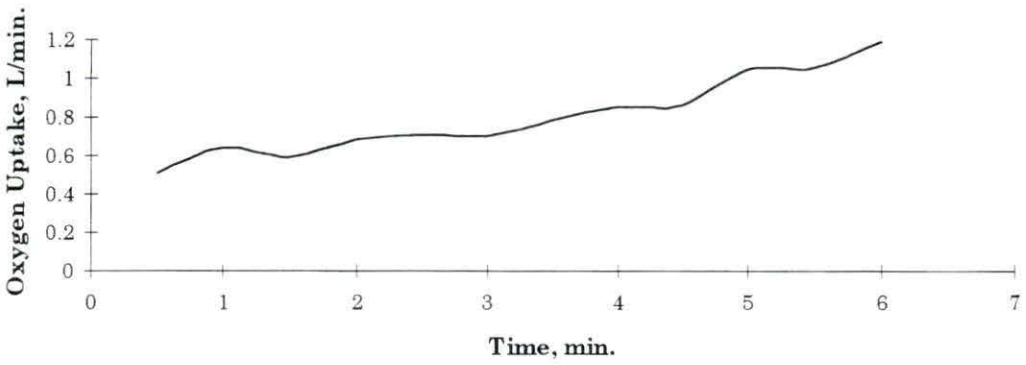

Subject WD-4 - Oxygen uptake and respiratory exchange ratio

Time	VO_2 (l/m)	RER
:30	0.49	0.8
1:00	0.68	0.73
1:30	0.73	0.75
2:00	0.78	0.78
2:30	0.78	0.85
3:00	0.83	0.82
3:30	0.89	0.86
4:00	1.02	0.86
4:30	1.03	0.9
5:00	1.2	0.9
5:30	1.32	1
6:00	1.37	1.01

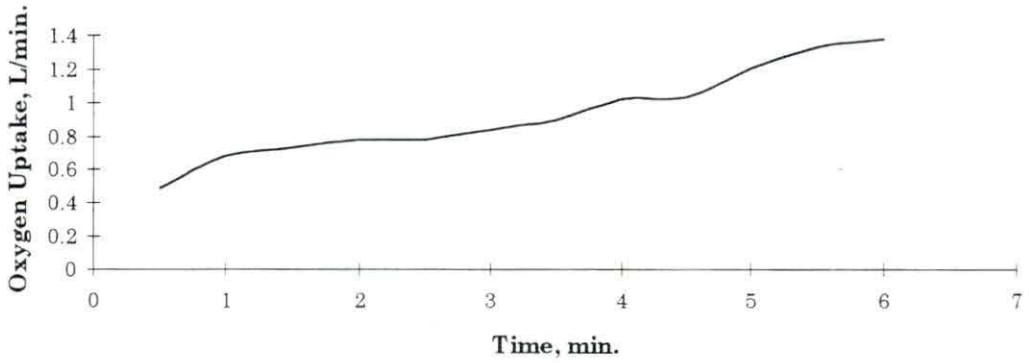

Subject WD-5 - Oxygen uptake and respiratory exchange ratio

Time	VO_2 (l/m)	RER
:30	0.61	0.66
1:00	0.68	0.7
1:30	0.71	0.74
2:00	0.66	0.74
2:30	0.69	0.76
3:00	0.8	0.76
3:30	0.79	0.8
4:00	0.8	0.79
4:30	0.88	0.81
5:00	1.02	0.83
5:30	1.04	0.85
6:00	1.13	0.86

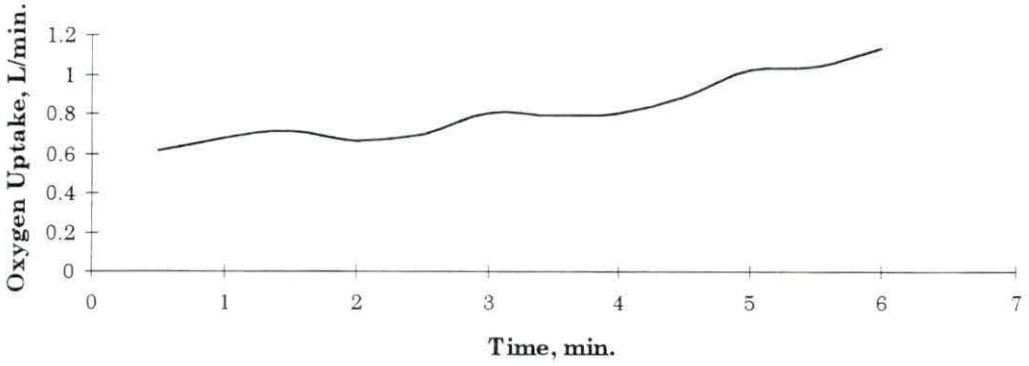

Gross propulsion efficiency F-test for variance Low velocity		
	AB	*WD*
Mean	8.6801	9.3116
Variance	1.8066	2.5262
Observations	5.0000	5.0000
df	4.0000	4.0000
F	1.3984	
P(F<=f) one-tail	0.3766	
F Critical one-tail	0.1565	

Gross propulsion efficiency - Low velocity T-test		
	AB	*WD*
Mean	8.6801	9.3116
Variance	1.8066	2.5262
Observations	5.0000	5.0000
Pooled Variance	2.1664	
Hypothesized Mean Difference	0.0000	
df	8.0000	
t Stat	-0.6784	
P(T<=t) one-tail	0.2583	
t Critical one-tail	1.8595	
P(T<=t) two-tail	0.5167	
t Critical two-tail	2.3060	

Gross propulsion efficiency F-test for variance Medium velocity		
	AB	*WD*
Mean	10.6366	12.7106
Variance	2.5625	3.9832
Observations	5.0000	5.0000
df	4.0000	4.0000
F	1.5544	
P(F<=f) one-tail	0.3398	
F Critical one-tail	0.1565	

Gross propulsion efficiency - Med. velocity T-test		
	AB	*WD*
Mean	10.6366	12.7106
Variance	2.5625	3.9832
Observations	5.0000	5.0000
Pooled Variance	3.2728	
Hypothesized Mean Difference	0.0000	
df	8.0000	
t Stat	-1.8127	
P(T<=t) one-tail	0.0537	
t Critical one-tail	1.8595	
P(T<=t) two-tail	0.1074	
t Critical two-tail	2.3060	

Gross propulsion efficiency F-test for variance High velocity		
	AB	*WD*
Mean	9.5849	13.0861
Variance	1.3044	2.7744
Observations	5.0000	5.0000
df	4.0000	4.0000
F	2.1270	
P(F<=f) one-tail	0.2414	
F Critical one-tail	0.1565	

Gross propulsion efficiency - High velocity T-test		
	AB	*WD*
Mean	9.5849	13.0861
Variance	1.3044	2.7744
Observations	5.0000	5.0000
Pooled Variance	2.0394	
Hypothesized Mean Difference	0.0000	
df	8.0000	
t Stat	-3.8764	
P(T<=t) one-tail	0.0023	
t Critical one-tail	1.8595	
P(T<=t) two-tail	0.0047	
t Critical two-tail	2.3060	

Oxygen uptake F-test for variance Low velocity		
	AB	***WD***
Mean	0.008017259	0.00844407
Variance	1.38174E-06	2.22058E-06
Observations	5	5
df	4	4
F	1.607083936	
P(F<=f) one-tail	0.328512081	
F Critical one-tail	0.156537894	

Oxygen uptake - Low velocity T-test		
	AB	***WD***
Mean	0.008017259	0.00844407
Variance	1.38174E-06	2.22058E-06
Observations	5	5
Pooled Variance	1.80116E-06	
Hypothesized Mean Difference	0	
df	8	
t Stat	-0.502839047	
P(T<=t) one-tail	0.314312889	
t Critical one-tail	1.85954832	
P(T<=t) two-tail	0.628625778	
t Critical two-tail	2.306005626	

Oxygen uptake F-test for variance Medium velocity		
	AB	*WD*
Mean	0.011554411	0.010332495
Variance	4.54969E-06	2.27715E-06
Observations	5	5
df	4	4
F	1.997975401	
P(F<=f) one-tail	0.259559453	
F Critical one-tail	6.388233942	

Oxygen uptake - Med. velocity T-test		
	AB	*WD*
Mean	0.011554411	0.010332495
Variance	4.54969E-06	2.27715E-06
Observations	5	5
Pooled Variance	3.41342E-06	
Hypothesized Mean Difference	0	
df	8	
t Stat	1.04572297	
P(T<=t) one-tail	0.163126893	
t Critical one-tail	1.85954832	
P(T<=t) two-tail	0.326253786	
t Critical two-tail	2.306005626	

Oxygen uptake F-test for variance High velocity		
	AB	*WD*
Mean	0.018191322	0.014079431
Variance	1.06123E-05	4.37312E-06
Observations	5	5
df	4	4
F	2.42671352	
P(F<=f) one-tail	0.205780546	
F Critical one-tail	6.388233942	

Oxygen uptake - High velocity T-test		
	AB	*WD*
Mean	0.018191322	0.014079431
Variance	1.06123E-05	4.37312E-06
Observations	5	5
Pooled Variance	7.49271E-06	
Hypothesized Mean Difference	0	
df	8	
t Stat	2.375155475	
P(T<=t) one-tail	0.022441891	
t Critical one-tail	1.85954832	
P(T<=t) two-tail	0.044883781	
t Critical two-tail	2.306005626	

Power input - Low velocity T-test		
	AB	*WD*
Mean	218.9305318	225.0915027
Variance	892.9742423	1109.116942
Observations	5	5
Pooled Variance	1001.045592	
Hypothesized Mean Difference	0	
df	8	
t Stat	-0.307887623	
P(T<=t) one-tail	0.383015702	
t Critical one-tail	1.85954832	
P(T<=t) two-tail	0.766031403	
t Critical two-tail	2.306005626	

Power input - Med. velocity T-test		
	AB	*WD*
Mean	318.1655294	280.4605105
Variance	1069.611347	1500.453537
Observations	5	5
Pooled Variance	1285.032442	
Hypothesized Mean Difference	0	
df	8	
t Stat	1.663076096	
P(T<=t) one-tail	0.067434357	
t Critical one-tail	1.85954832	
P(T<=t) two-tail	0.134868714	
t Critical two-tail	2.306005626	

Power input - High velocity T-test		
	AB	*WD*
Mean	508.3433293	389.8876902
Variance	2126.891073	3161.364461
Observations	5	5
Pooled Variance	2644.127767	
Hypothesized Mean Difference	0	
df	8	
t Stat	3.642373906	
P(T<=t) one-tail	0.003283188	
t Critical one-tail	1.85954832	
P(T<=t) two-tail	0.006566375	
t Critical two-tail	2.306005626	

Power output - Low velocity T-test		
	AB	*WD*
Mean	18.69568	20.55076
Variance	0.609544812	1.633249993
Observations	5	5
Pooled Variance	1.121397402	
Hypothesized Mean Difference	0	
df	8	
t Stat	-2.769828468	
P(T<=t) one-tail	0.012151559	
t Critical one-tail	1.85954832	
P(T<=t) two-tail	0.024303119	
t Critical two-tail	2.306005626	

Power output - Med. velocity T-test		
	AB	*WD*
Mean	33.55684	35.25664
Variance	15.20674476	21.79744258
Observations	5	5
Pooled Variance	18.50209367	
Hypothesized Mean Difference	0	
df	8	
t Stat	-0.624823552	
P(T<=t) one-tail	0.274744275	
t Critical one-tail	1.85954832	
P(T<=t) two-tail	0.54948855	
t Critical two-tail	2.306005626	

Power output - High velocity T-test		
	AB	*WD*
Mean	48.33096	50.35164
Variance	5.746638713	14.54023975
Observations	5	5
Pooled Variance	10.14343923	
Hypothesized Mean Difference	0	
df	8	
t Stat	-1.003170913	
P(T<=t) one-tail	0.172576174	
t Critical one-tail	1.85954832	
P(T<=t) two-tail	0.345152347	
t Critical two-tail	2.306005626	

MEASUREMENT OF OXYGEN CONSUMPTION AND ENERGY EXPENDITURE DURING EXERCISE

Calibration of gas analyzers and computer.

A. Turn on flow control switch.
B. Allow 20 min warmup.
C. Check Drierite and replace if pink.
D. Attach electrical cables from O2 analyzer, CO2 analyzer, and gas meter to the interface box on the computer. (If not already attached).
E. Turn on computer power. Also make sure monitor and printer are turned on.
F. Start Vista program (see details below).
G. With the calibration screen showing on the computer, begin calibrating the gas analyzers:
    1. Take reading on room air first with sample hose exposed to room and away from your breathing. Make sure selector switch of O2 analyzer is on REFERENCE and range dial is on %O2.
    2. Reading on O2 analyzer should be 20.93. If not, adjust reading using the REFERENCE ADJUST knob.
    3. Reading on CO2 analyzer should be 0.03. If not, adjust reading using ZERO knob.
    4. Open main valve of gas tank (large valve on top of tank).
    5. Place sampling tube into syringe barrel taped on or near tank.
    6. Open regulator valve on tank (small knob) so that a quiet whisper of air is flowing from tank into syringe barrel (make sure tip of sampling tube is not resting against bottom of syringe barrel).
    7. Flip selector switch on O2 analyzer to UNKNOWN. Once air flows into syringe barrel, the analyzers should begin to register a change in gas composition. Allow 1-2 min for readings to stabilize. Compare readings on O2 and CO2 analyzers to those printed on the tape attached to the compressed gas tank.
    8. If value on O2 analyzer does not agree with gas tank, then adjust reading using the CELL ZERO knob.
    9. If value on CO2 analyzer does not agree with gas tank, then adjust its reading using the GAIN knob.
    10. Turn off air flow from tank and expose sample tube to room air. Allow analyzers to stabilize.
    11. Change selector switch on O2 analyzer back to REFERENCE ADJUST and repeat calibration on room air.
    12. Repeat procedure for tank air calibration.
    13. Continue going back and forth between room air and tank several times to make sure both the analyzers and the computer are reading properly.

Setting up for VO2 Measurement with Vista TurboFit Computer System

A. Calibrate analyzers and setup breathing circuit according to prior procedure.
B. Make sure inputs from analyzers are plugged into Vista interface box.
C. Start Windows by typing WIN at DOS prompt.
D. Start Vista program by double clicking on Vista icon.
E. Double click on FORM1 icon if it appears in lower left of screen.
F. Click on CALIBRATION.

AirFlow Meter Calibration

1. Click on VOLUME CALIBRATION then select "AirFlow meter".
2. Enter "10" for LITERS/REVOLUTION and click CONTINUE.
3. Using inspired hose, inspire enough air to move indicator needle on meter exactly 2 revolutions (make sure needle is in contact with potentiometer arm at beginning of inspiration).
4. Click on CONTINUE.

Gas Calibration

1. Analyzers should be reading room air.
   a. Click on small tank under CO2. This checks calibration of CO2 analyzer to low span gas (0.03%).
   b. Once the green light comes on, you should receive the message "Good Calibration". If not, contact your local software wizard (Sharp or King).
   c. Click on large tank icon under O2. This checks high span gas (20.93%) for the O2 analyzer. Wait for the "Good Calibration" message.
   d. Move gas sample tube to the tank syringe and turn on tank gas. Make sure analyzers are displaying correct % readings.
   e. Click on large tank under CO2. Wait for "Good Calibration" message.
   f. Click on small tank under O2. Wait for "Good Calibration" message.
   g. When all four frames around the tank icons have changed color, you know that gas calibration is complete.

G. Enter correct temperature, barometric pressure, and relative humidity by clicking in the appropriate field and typing the data.
H. Confirm that software is set for "Inspired Gas". If not, click on this button to toggle between EXPIRED and INSPIRED.
I. Exit Calibration screen by clicking on SAVE and QUIT.

From Main Menu click on STRESS to enter subject data.

1. Click on NEW to clear the fields.
2. Enter requested subject data.
3. Select the data reporting interval by clicking on TEST REPORT AT (usually 30 sec for max tests; longer for steady state tests).
4. Enter maximum test time (at end of this period, test will NOT terminate but graph will automatically rescale for continued readings).
5. Click NO for "HR by ECG".
6. Click NO for "save raw data".
7. Click on PROTOCOL button to select a protocol. After screen changes, select the protocol, then click the OK button to return to the Patient Data Screen. OR, you may skip step "7" completely.
8. Click on CONTINUE to start test (subject should be breathing through the system before starting test).
9. Check to see if data are reasonable (no negative numbers, etc.).
10. Click on RESET TEST and the test will start in earnest and data will be saved.
11. Terminate test by clicking on the STOP TEST button.

Table 1. Expected VO2 on Cycle Ergometer

At 50 watts VO2 should be about 0.9 L/min
At 100 watts VO2 should be about 1.5 L/min
At 150 watts VO2 should be about 2.1 L/min
At 200 watts VO2 should be about 2.7 L/min

$$VO_2(L/min) = \frac{watts * 6.12 * 2 + 300}{1000}$$

Caloric Equivalents of Oxygen Uptake at Various Respiratory Quotients

Nonprotein RQ	Kcal per liter O2 uptake	Percentage Kcal Derived from		Grams per liter O2 Uptake	
		Carbohydrate	Fat	Carbohydrate	Fat
0.70	4.686	0.0	100.0	0.000	0.521
0.71	4.690	1.1	98.9	0.013	0.515
0.72	4.702	4.8	95.2	0.056	0.497
0.73	4.714	8.4	91.6	0.099	0.480
0.74	4.727	12.0	88.0	0.142	0.462
0.75	4.739	15.6	84.4	0.185	0.444
0.76	4.750	19.2	80.8	0.228	0.426
0.77	4.764	22.8	77.2	0.272	0.409
0.78	4.776	26.3	73.7	0.314	0.391
0.79	4.788	29.9	70.1	0.358	0.373
0.80	4.801	33.4	66.6	0.401	0.355
0.81	4.813	36.9	63.1	0.444	0.337
0.82	4.825	40.3	59.7	0.486	0.320
0.83	4.838	43.8	56.2	0.530	0.302
0.84	4.850	47.2	52.8	0.572	0.285
0.85	4.862	50.7	49.3	0.616	0.266
0.86	4.875	54.1	45.9	0.659	0.249
0.87	4.887	57.5	42.5	0.703	0.231
0.88	4.899	60.8	39.2	0.745	0.213
0.89	4.911	64.2	35.8	0.788	0.195
0.90	4.924	67.5	32.5	0.831	0.178
0.91	4.936	70.8	29.2	0.874	0.160
0.92	4.948	74.1	25.9	0.917	0.142
0.93	4.961	77.4	22.6	0.960	0.125
0.94	4.973	80.7	19.3	1.003	0.107
0.95	4.985	84.0	16.0	1.047	0.089
0.96	4.998	87.2	12.8	1.090	0.071
0.97	5.010	90.4	9.6	1.132	0.053
0.98	5.022	93.6	6.4	1.175	0.036
0.99	5.035	96.8	3.2	1.218	0.018
1.00	5.047	100.0	0.0	1.262	0.000

APPENDIX B:

DYNAMOMETER CALIBRATION DATA
VELOCITY DISPLAY AND STRAIN GAGE CIRCUIT SCHEMATICS
DYNAMOMETER PHOTOGRAPHS

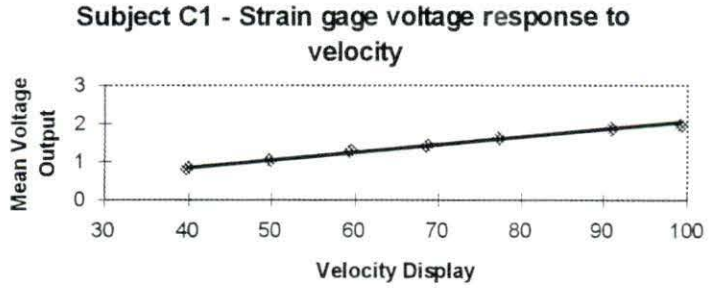
Subject C1 - Strain gage voltage response to velocity
Mean Voltage Output
3
2
1
0
30
40
50
60
70
80
90
100
Velocity Display

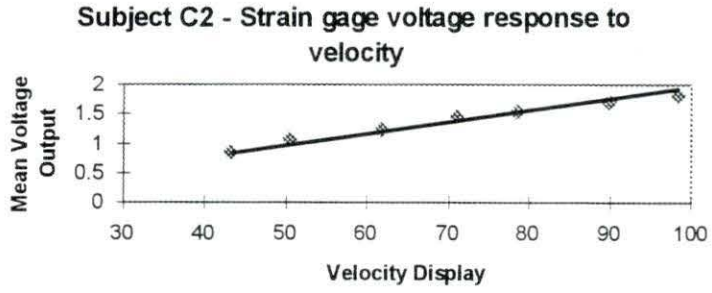
Subject C2 - Strain gage voltage response to velocity
Mean Voltage Output
2
1.5
1
0.5
0
30
40
50
60
70
80
90
100
Velocity Display

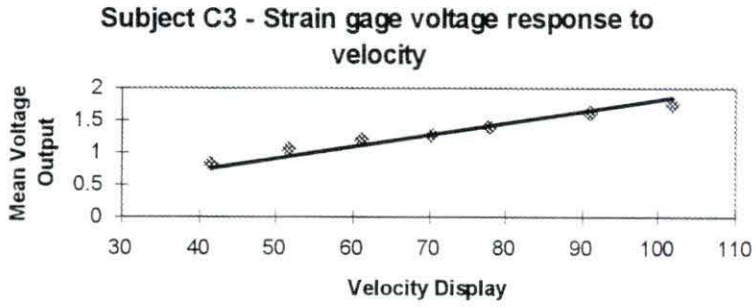
Subject C3 - Strain gage voltage response to velocity
Mean Voltage Output
2
1.5
1
0.5
0
30
40
50
60
70
80
90
100
110
Velocity Display

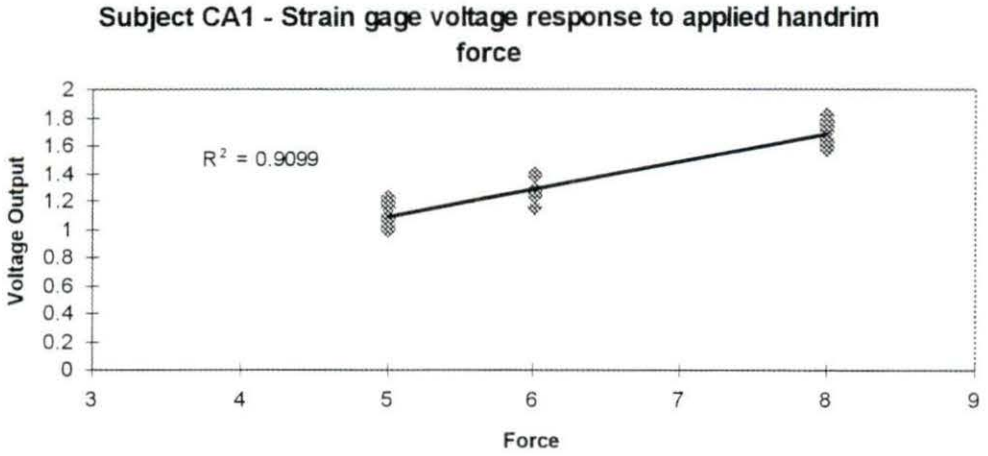

Initial calibration, subject weight - 210 lb

Trial #	5 lb	6 lb	8 lb
1	1.02	1.24	1.59
2	1.18	1.27	1.82
3	1.22	1.28	1.7
4	1.09	1.25	1.57
5	1.1	1.39	1.64
6	1	1.28	1.62
7	1.15	1.38	1.74
8	1.06	1.16	1.65
9	1.19	1.26	1.76
10	1.03	1.16	1.78
Mean	**1.104**	**1.267**	**1.687**
S.D.	0.07763	0.07616	0.08551

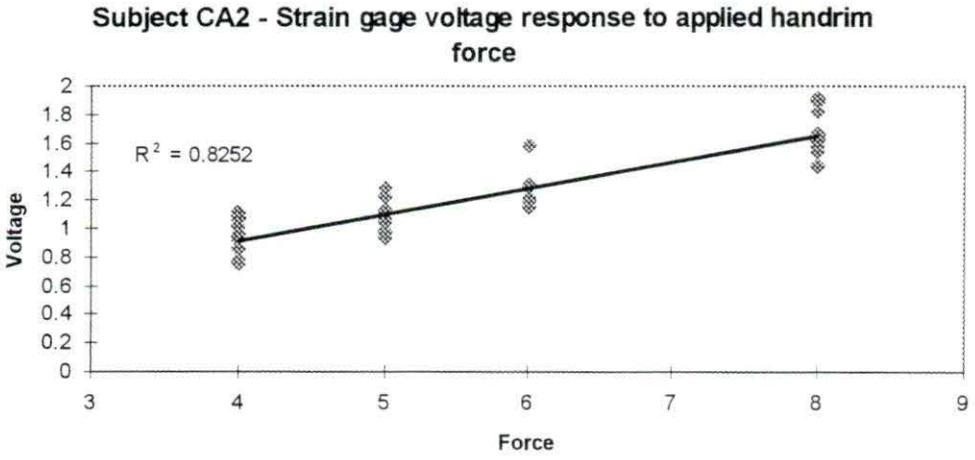

Initial calibration, subject weight - 185 lb

Trial #	4 lb	5 lb	6 lb	8 lb
1	0.78	1.23	1.2	1.62
2	0.93	1.05	1.15	1.57
3	0.92	1.28	1.3	1.82
4	1.07	1.05	1.58	1.65
5	1.01	0.93	1.29	1.91
6	1.11	0.97	1.3	1.44
7	0.85	0.98	1.29	1.66
8	0.95	0.98	1.21	1.63
9	0.75	1.12	1.15	1.54
10	1.08	1.07	1.19	1.89
Mean	**0.945**	**1.066**	**1.266**	**1.673**
S.D.	0.12492	0.11481	0.12571	0.15377

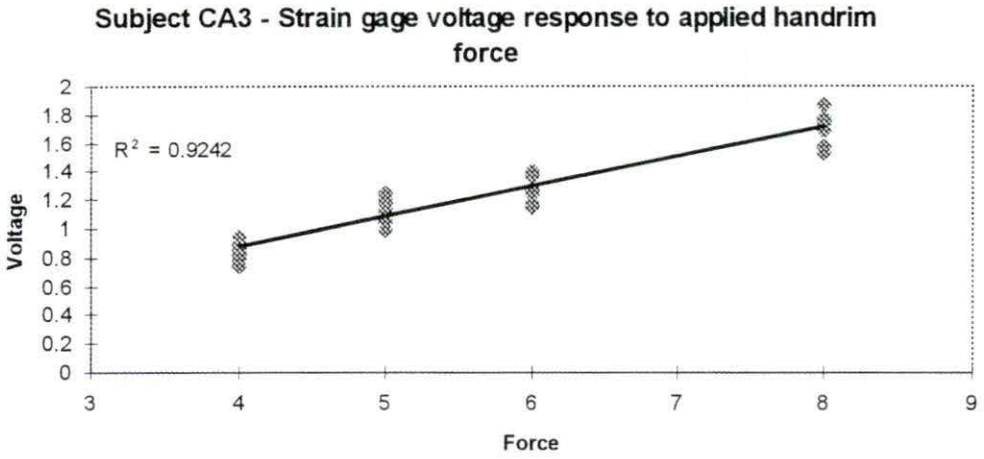

Initial calibration, subject weight - 145 lb

Trial #	4 lb	5 lb	6 lb	8 lb
1	0.94	0.99	1.18	1.53
2	0.79	1.05	1.4	1.87
3	0.74	1.18	1.36	1.68
4	0.82	1.06	1.15	1.75
5	0.9	1.25	1.38	1.77
6	0.86	1.11	1.39	1.57
7	0.83	1.24	1.26	1.86
8	0.81	1.12	1.24	1.68
9	0.84	1.13	1.28	1.74
10	0.89	1.2	1.16	1.73
Mean	**0.842**	**1.133**	**1.28**	**1.718**
S.D.	0.05808	0.08512	0.09786	0.10942

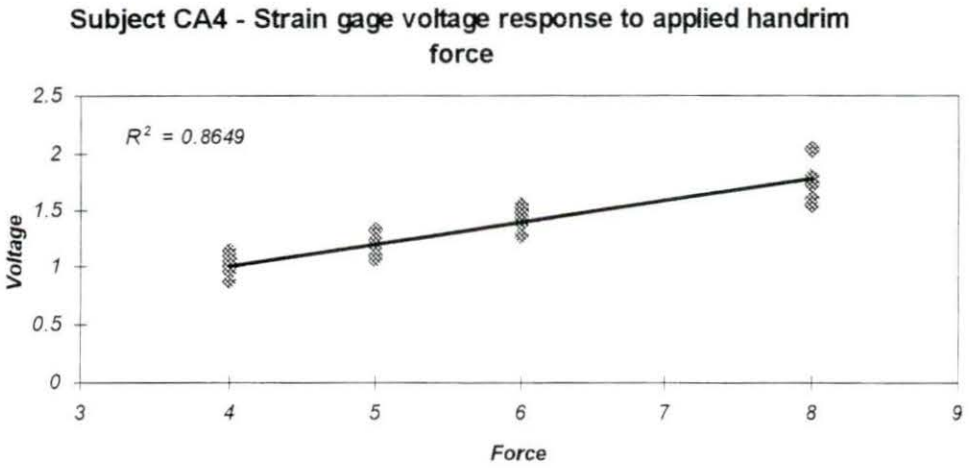

Initial calibration, subject weight - 130 lb

Trial #	4 lb	5 lb	6 lb	8 lb
1	1.07	1.33	1.27	1.74
2	1.1	1.1	1.44	1.72
3	1.03	1.1	1.4	2.02
4	1.09	1.1	1.55	1.74
5	1.04	1.11	1.41	1.8
6	1.15	1.09	1.54	1.73
7	0.96	1.17	1.28	1.6
8	0.88	1.07	1.37	2.04
9	1.01	1.24	1.51	1.53
10	1.01	1.06	1.48	1.73
Mean	**1.034**	**1.137**	**1.425**	**1.765**
S.D.	0.07647	0.0859	0.09902	0.15987

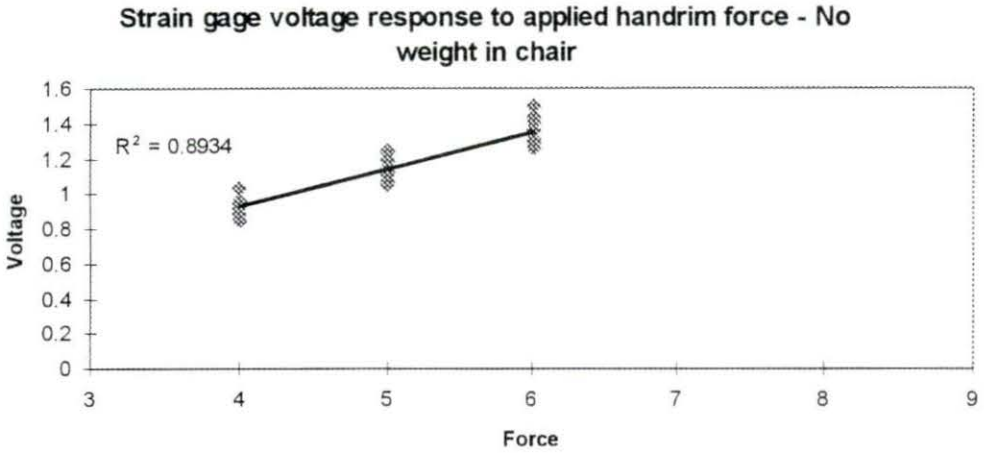

Initial calibration, no weight in wheelchair

Trial #	4 lb	5 lb	6 lb
1	0.88	1.1	1.41
2	0.96	1.19	1.36
3	1.03	1.11	1.26
4	0.95	1.14	1.5
5	0.92	1.12	1.31
6	0.94	1.05	1.36
7	0.92	1.24	1.29
8	0.85	1.12	1.43
9	0.88	1.07	1.29
10	0.94	1.2	1.3
Mean	**0.927**	**1.134**	**1.351**
S.D.	0.05056	0.05966	0.07607

Strain gage voltage response to applied handrim force, final calibration

Trial #	5 lb	6 lb	8 lb	10 lb
1	1.217	1.351	1.842	2.405
2	1.135	1.382	1.857	2.538
3	1.23	1.38	1.955	2.513
4	1.111	1.388	1.98	2.506
5	1.224	1.38	1.954	2.584
6	1.513	1.4	2.206	2.537
7	1.275	1.51	2.23	2.577
8	1.278	1.45	2.015	2.687
9	1.25	1.494	2.159	2.408
10	1.27	1.459	2.093	2.675
Mean	**1.2503**	**1.4194**	**2.0291**	**2.543**
S.D.	0.1084	0.0546	0.1378	0.0946

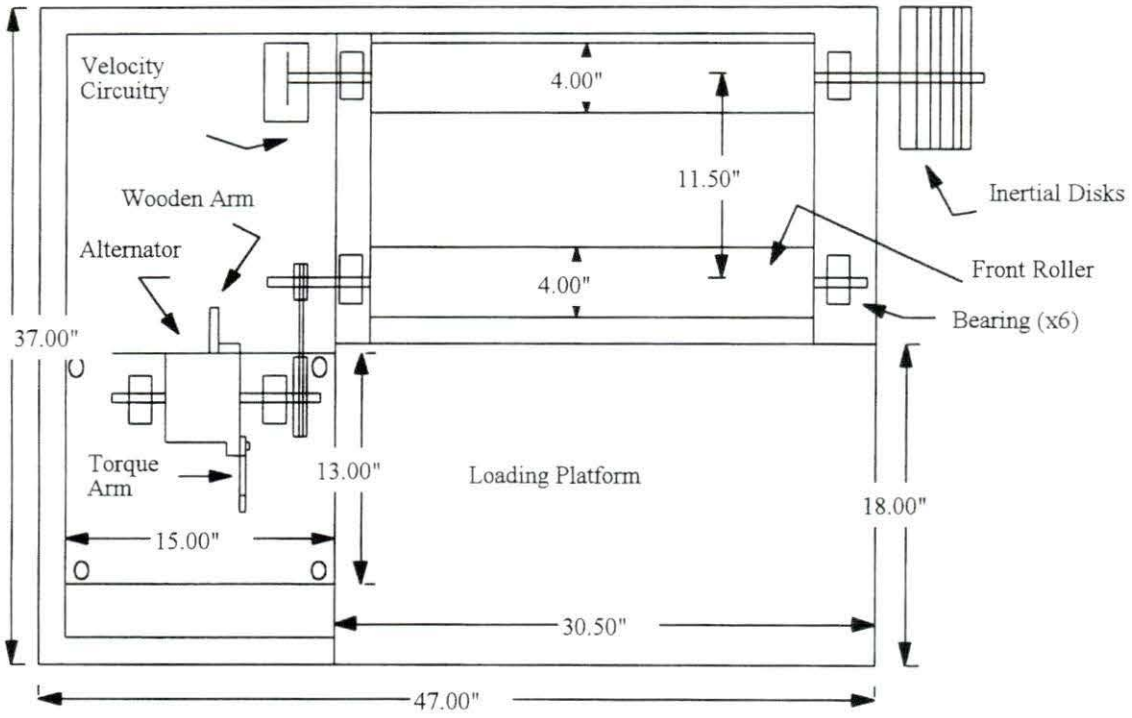

Top View

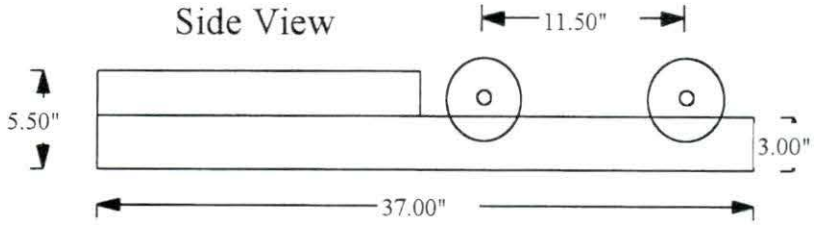

Wheelchair dynamometer top and side view dimensions

Wheelchair Dynamometer

Velocity Display Circuit Schematic

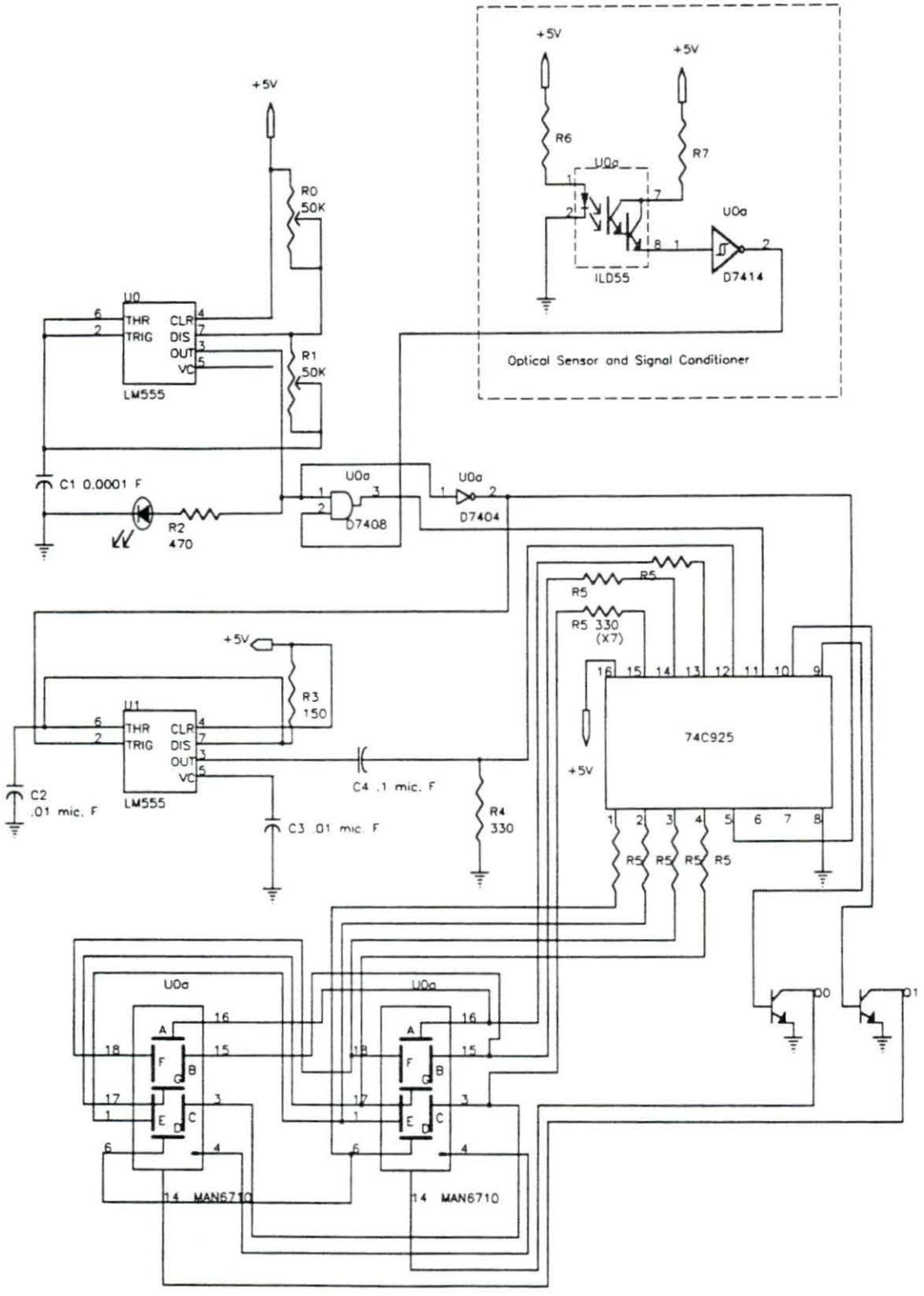

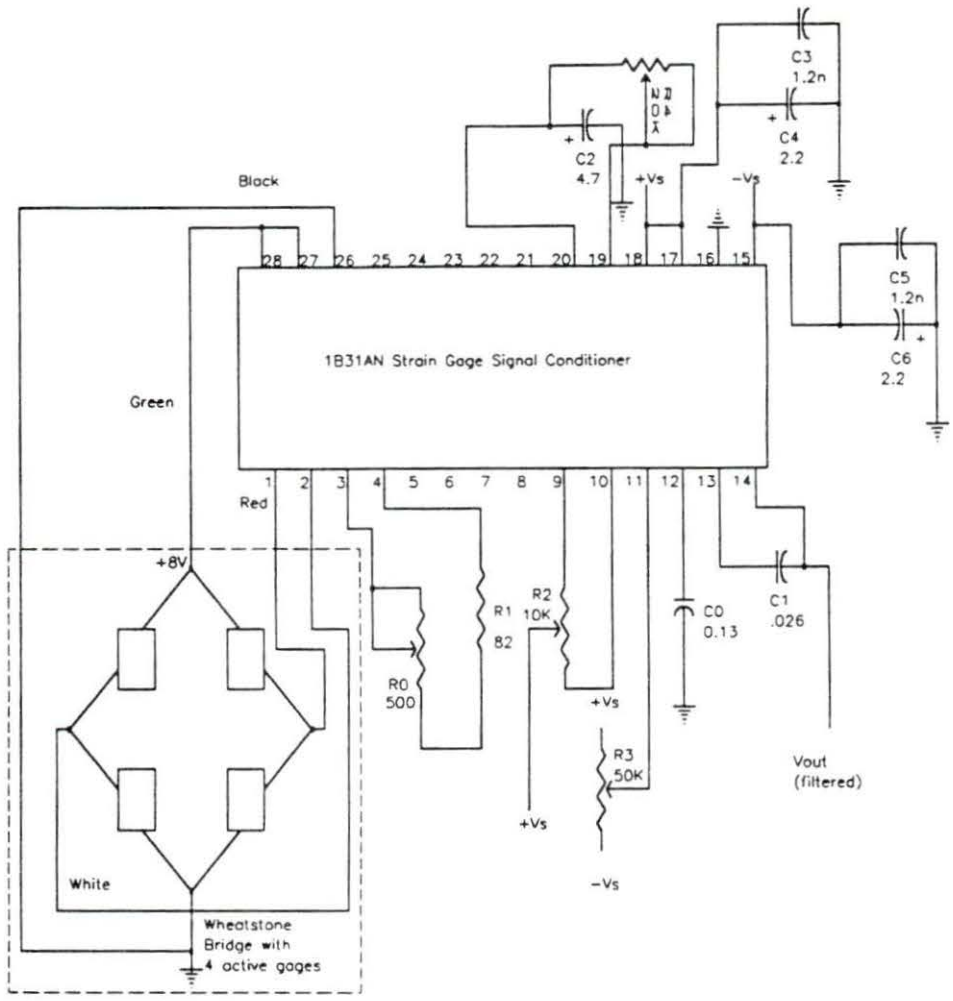

Wheelchair Dynamometer
Strain Gage Signal Conditioner Schematic

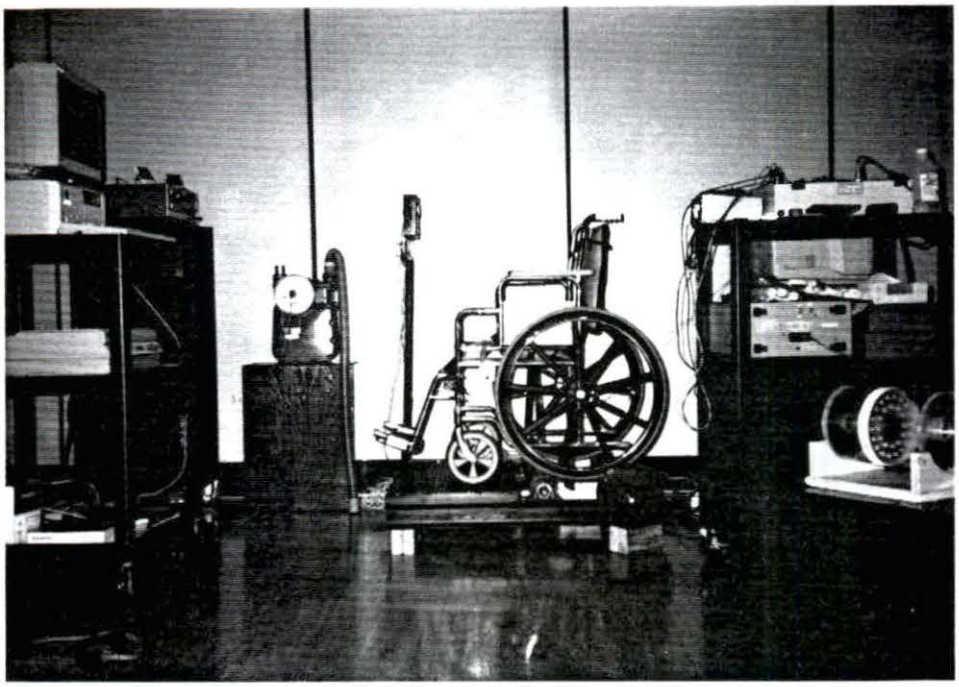

Experimental setup showing wheelchair, dynamometer, air flow meter, EMG amplifier, and oxygen monitoring equipment

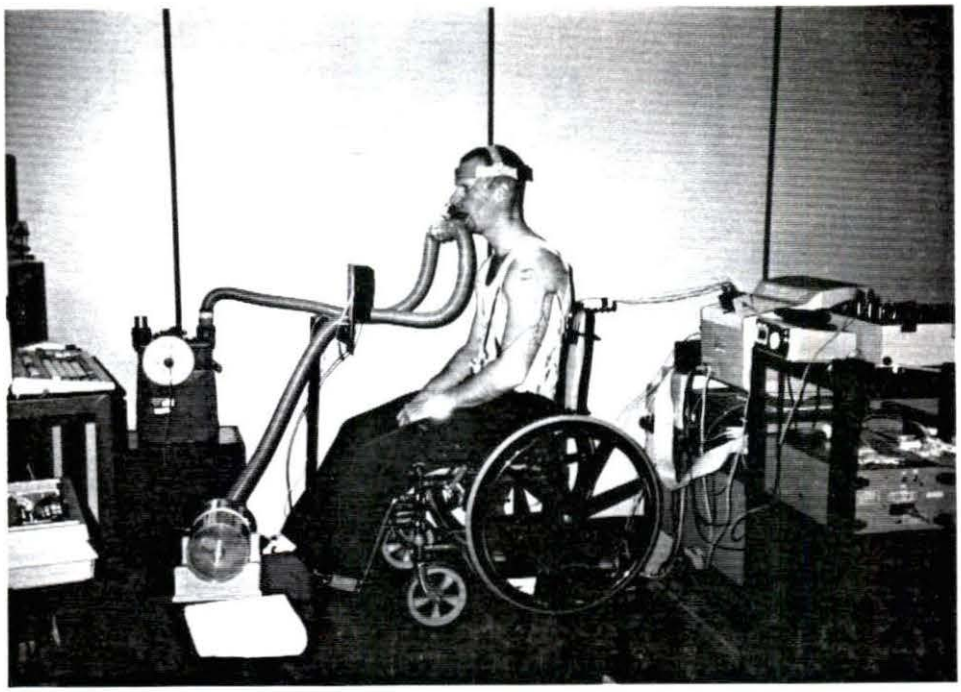

Subject oxygen uptake, EMG, and reflective marker setup

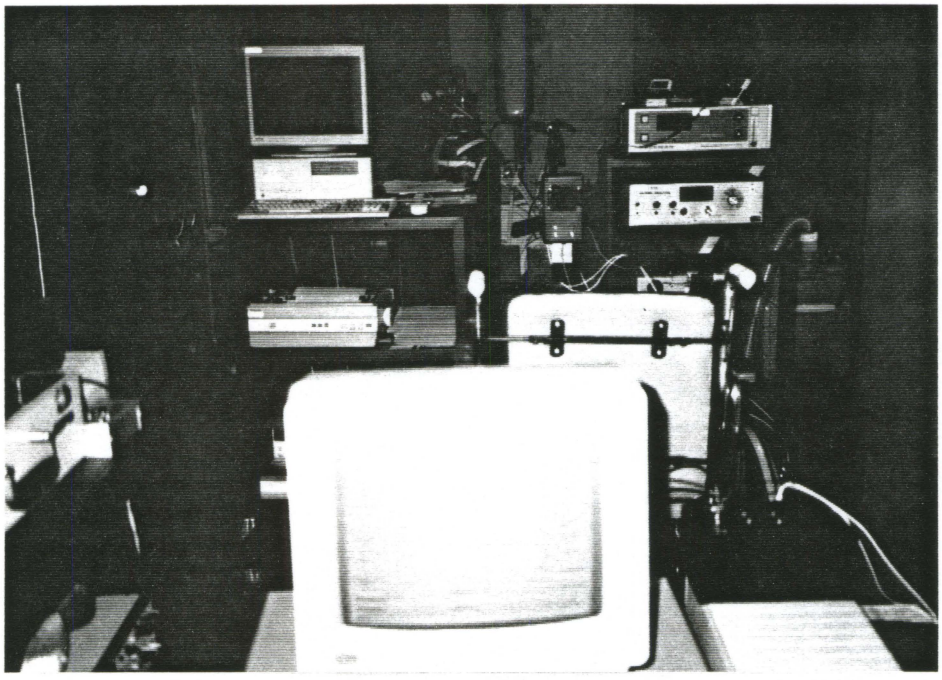

Rear of wheelchair showing computers (strain gage/EMG and oxygen uptake), velocity display, and O_2/CO_2 analyzers

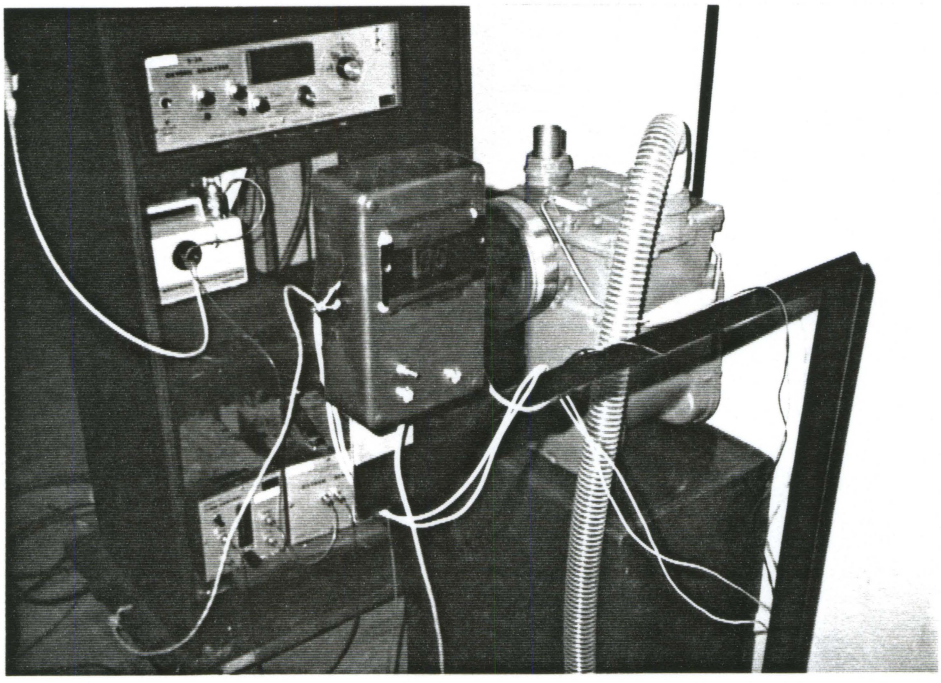

Velocity display

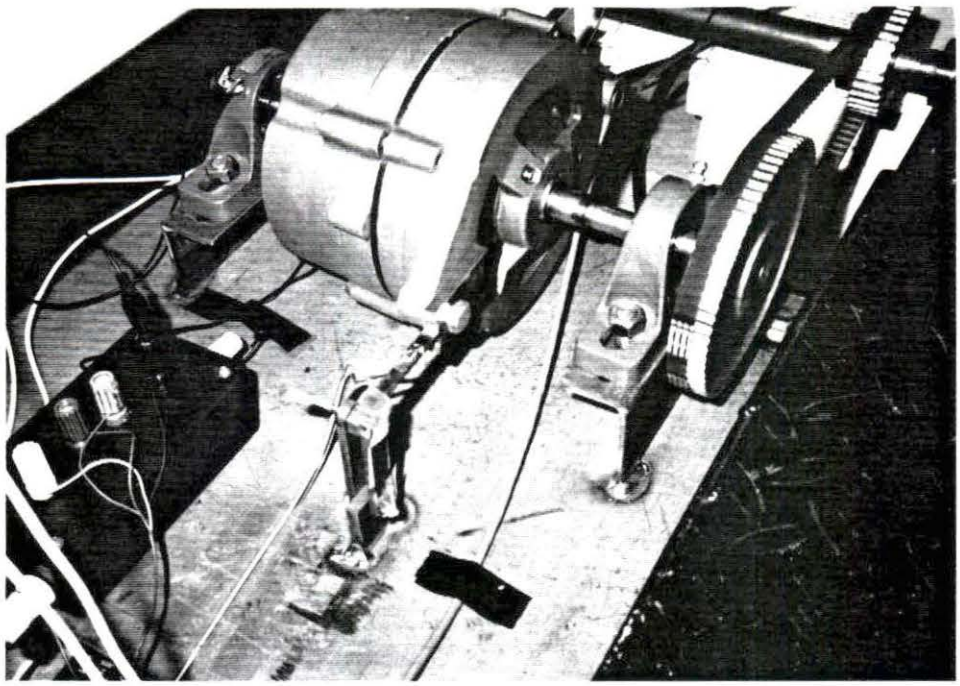

Alternator and strain gage assembly

APPENDIX C:

KINEMATIC PARAMETER DATA
KINEMATIC STATISTICAL TABLES

Kinematic parameter data - low velocity

	Prop. time msec.	Rec. time msec.	Cycle time msec.	% Prop time	% Rec time	Energy Output W	Work/stroke J
AB-1	343.67	607.33	951.00	36.12	63.86	19.64	18.68
AB-2	397.33	670.67	1068.00	37.23	62.80	19.05	20.34
AB-3	476.50	854.00	1330.50	35.85	64.19	18.36	24.43
AB-4	360.00	619.67	979.67	36.75	63.25	18.87	18.49
AB-5	458.50	948.50	1407.00	32.67	67.41	17.56	24.71
Mean	**407.20**	**740.03**	**1147.23**	**35.72**	**64.30**	**18.70**	**21.33**
St. Dev.	58.73	152.77	208.52	1.79	1.82	0.78	3.05
WD-1	266.67	343.33	610.00	43.58	56.28	19.69	12.01
WD-2	431.00	637.50	1068.50	40.35	59.66	19.03	20.33
WD-3	258.00	373.33	631.33	40.87	59.13	22.31	14.08
WD-4	416.67	621.00	1037.67	40.09	59.85	20.57	21.34
WD-5	675.00	794.00	1469.00	45.95	54.05	21.16	31.09
Mean	**409.47**	**553.83**	**963.30**	**42.17**	**57.80**	**20.55**	**19.77**
St. Dev.	169.08	191.10	356.14	2.53	2.54	1.28	7.47

Kinematic parameter data - medium velocity

	Prop. time msec.	Rec. time msec.	Cycle time msec.	% Prop time	% Rec time	Energy Output W	Work/stroke J
AB-1	294.00	526.67	820.67	35.93	64.18	34.55	28.35
AB-2	343.67	651.67	995.33	34.54	65.47	33.55	33.40
AB-3	377.67	692.67	1070.33	35.33	64.72	38.50	41.21
AB-4	327.33	520.33	847.67	38.58	61.38	33.57	28.45
AB-5	390.33	770.67	1161.00	33.65	66.38	27.61	32.05
Mean	**346.60**	**632.40**	**979.00**	**35.61**	**64.43**	**33.56**	**32.69**
St. Dev.	38.81	108.24	144.96	1.87	1.89	3.90	5.25
WD-1	306.33	461.00	767.33	39.89	60.08	31.47	24.15
WD-2	395.00	619.33	1014.33	38.94	61.06	34.14	34.63
WD-3	227.33	367.33	594.67	38.22	61.77	43.19	25.68
WD-4	367.00	546.00	913.00	40.27	59.80	35.18	32.12
WD-5	487.33	702.33	1189.67	40.99	59.04	32.31	38.43
Mean	**356.60**	**539.20**	**895.80**	**39.66**	**60.35**	**35.26**	**31.00**
St. Dev.	97.35	131.09	227.97	1.09	1.07	4.67	6.02

Kinematic parameter data - high velocity

	Prop. time msec.	Rec. time msec.	Cycle time msec.	% Prop time	% Rec time	Energy Output W	Work/stroke J
AB-1	260.67	506.00	766.67	33.98	66.00	47.30	36.26
AB-2	260.33	492.33	752.67	34.60	65.41	48.86	36.78
AB-3	242.67	543.67	786.33	30.87	69.14	51.78	40.71
AB-4	246.67	484.33	731.00	33.76	66.26	48.51	35.46
AB-5	260.67	511.00	771.67	33.68	66.22	45.21	34.89
Mean	**254.20**	**507.47**	**761.67**	**33.38**	**66.61**	**48.33**	**36.82**
St. Dev.	8.82	22.85	20.95	1.45	1.46	2.40	2.29
WD-1	324.00	490.00	814.00	39.78	60.20	44.79	36.46
WD-2	267.33	526.33	793.67	33.62	66.32	53.56	42.51
WD-3	292.67	467.00	759.67	38.52	61.47	53.33	40.51
WD-4	256.00	394.00	650.00	39.37	60.62	48.05	31.23
WD-5	381.67	643.00	1024.67	37.25	62.75	52.03	53.32
Mean	**304.33**	**504.07**	**808.40**	**37.71**	**62.27**	**50.35**	**40.81**
St. Dev.	50.52	91.49	136.46	2.48	2.46	3.81	8.22

Start angle (SA), end angle (EA), and push angle (PA) data

	Low			Medium			High		
	SA	EA	PA	SA	EA	PA	SA	EA	PA
AB-1	90	167	77	90	167	77	90	193	103
AB-2	90	167	77	64	167	103	64	167	103
AB-3	64	167	103	64	180	116	64	193	129
AB-4	90	193	103	90	193	103	90	193	103
AB-5	77	193	116	77	193	116	77	193	116
Mean	**82**	**177**	**95**	**77**	**180**	**103**	**77**	**188**	**111**
St. Dev.	12	14	17	13	13	16	13	12	12
WD-1	116	167	51	103	193	90	64	193	129
WD-2	90	193	103	64	193	129	64	193	129
WD-3	90	154	64	90	167	77	39	167	128
WD-4	90	180	90	77	193	116	64	193	129
WD-5	39	193	154	39	193	154	39	193	154
Mean	**85**	**177**	**92**	**75**	**188**	**113**	**54**	**188**	**134**
St. Dev.	28	17	40	25	12	31	14	12	11

Propulsion time - Low velocity F-test for variance		
	AB	*WD*
Mean	407.2	409.4666667
Variance	3448.963889	28589.36667
Observations	5	5
df	4	4
F	8.289262395	
P(F<=f) one-tail	0.032271235	
F Critical one-tail	0.156537894	

Propulsion time - Low velocity T-test		
	AB	*WD*
Mean	407.2	409.4666667
Variance	3448.963889	28589.36667
Observations	5	5
Hypothesized Mean Difference	0	
df	5	
t Stat	-0.028316379	
P(T<=t) one-tail	0.489252636	
t Critical one-tail	2.015049176	
P(T<=t) two-tail	0.978505273	
t Critical two-tail	2.570577635	

Propulsion time - Medium velocity F test for variance		
	AB	*WD*
Mean	346.6	356.6
Variance	1506.077778	9477.633333
Observations	5	5
df	4	4
F	6.292924226	
P(F<=f) one-tail	0.05124889	
F Critical one-tail	0.156537894	

Propulsion time - Medium velocity T-test		
	AB	*WD*
Mean	346.6	356.6
Variance	1506.077778	9477.633333
Observations	5	5
Pooled Variance	5491.855556	
Hypothesized Mean Difference	0	
df	8	
t Stat	-0.213358747	
P(T<=t) one-tail	0.418192043	
t Critical one-tail	1.85954832	
P(T<=t) two-tail	0.836384086	
t Critical two-tail	2.306005626	

Propulsion time - High velocity F-test for variance		
	AB	*WD*
Mean	254.2	304.3333333
Variance	77.75555556	2552.111111
Observations	5	5
df	4	4
F	32.82223492	
P(F<=f) one-tail	0.002570815	
F Critical one-tail	0.156537894	

Propulsion time - High velocity T-test		
	AB	*WD*
Mean	254.2	304.3333333
Variance	77.75555556	2552.111111
Observations	5	5
Hypothesized Mean Difference	0	
df	4	
t Stat	-2.185972623	
P(T<=t) one-tail	0.047057177	
t Critical one-tail	2.131846486	
P(T<=t) two-tail	0.094114354	
t Critical two-tail	2.776450856	

Recovery time - Low velocity F-test for variance		
	AB	***WD***
Mean	740.0333333	553.8333333
Variance	23338.97778	36520.5
Observations	5	5
df	4	4
F	1.564785757	
P(F<=f) one-tail	0.33751372	
F Critical one-tail	0.156537894	

Recovery time - Low velocity T-test		
	AB	***WD***
Mean	740.0333333	553.8333333
Variance	23338.97778	36520.5
Observations	5	5
Pooled Variance	29929.73889	
Hypothesized Mean Difference	0	
df	8	
t Stat	1.70175963	
P(T<=t) one-tail	0.06360679	
t Critical one-tail	1.85954832	
P(T<=t) two-tail	0.127213579	
t Critical two-tail	2.306005626	

Recovery time - Medium velocity F-test for variance		
	AB	*WD*
Mean	632.4	539.2
Variance	11714.85556	17183.36667
Observations	5	5
df	4	4
F	1.466801412	
P(F<=f) one-tail	0.359768971	
F Critical one-tail	0.156537894	

Recovery time - Medium velocity T-test		
	AB	*WD*
Mean	632.4	539.2
Variance	11714.85556	17183.36667
Observations	5	5
Pooled Variance	14449.11111	
Hypothesized Mean Difference	0	
df	8	
t Stat	1.225929092	
P(T<=t) one-tail	0.127542894	
t Critical one-tail	1.85954832	
P(T<=t) two-tail	0.255085787	
t Critical two-tail	2.306005626	

Recovery time - High velocity F-test for variance		
	AB	*WD*
Mean	507.4666667	504.0666667
Variance	522.3111111	8371.188889
Observations	5	5
df	4	4
F	16.02720813	
P(F<=f) one-tail	0.00994234	
F Critical one-tail	0.156537894	

Recovery time - High velocity T-test		
	AB	*WD*
Mean	507.4666667	504.0666667
Variance	522.3111111	8371.188889
Observations	5	5
Hypothesized Mean Difference	0	
df	4	
t Stat	0.080617173	
P(T<=t) one-tail	0.469809423	
t Critical one-tail	2.131846486	
P(T<=t) two-tail	0.939618847	
t Critical two-tail	2.776450856	

Cycle time - Low velocity F-test for variance		
	AB	*WD*
Mean	1147.233333	963.3
Variance	43482.35556	126838.1722
Observations	5	5
df	4	4
F	2.917003244	
P(F<=f) one-tail	0.162251155	
F Critical one-tail	0.156537894	

Cycle time - Low velocity T-test		
	AB	*WD*
Mean	1147.233333	963.3
Variance	43482.35556	126838.1722
Observations	5	5
Pooled Variance	85160.26389	
Hypothesized Mean Difference	0	
df	8	
t Stat	0.996579493	
P(T<=t) one-tail	0.174076619	
t Critical one-tail	1.85954832	
P(T<=t) two-tail	0.348153237	
t Critical two-tail	2.306005626	

Cycle time - Medium velocity F-test for variance		
	AB	*WD*
Mean	979	895.8
Variance	21012.61111	51972.14444
Observations	5	5
df	4	4
F	2.473378685	
P(F<=f) one-tail	0.200938291	
F Critical one-tail	0.156537894	

Cycle time - Medium velocity T-test		
	AB	*WD*
Mean	979	895.8
Variance	21012.61111	51972.14444
Observations	5	5
Pooled Variance	36492.37778	
Hypothesized Mean Difference	0	
df	8	
t Stat	0.688640007	
P(T<=t) one-tail	0.255261464	
t Critical one-tail	1.85954832	
P(T<=t) two-tail	0.510522928	
t Critical two-tail	2.306005626	

Cycle time - High velocity F-test for variance		
	AB	*WD*
Mean	761.6666667	808.4
Variance	438.7222222	18621.3
Observations	5	5
df	4	4
F	42.44439661	
P(F<=f) one-tail	0.001565084	
F Critical one-tail	0.156537894	

Cycle time - High velocity T-test		
	AB	*WD*
Mean	761.6666667	808.4
Variance	438.7222222	18621.3
Observations	5	5
Hypothesized Mean Difference	0	
df	4	
t Stat	-0.756920138	
P(T<=t) one-tail	0.245617409	
t Critical one-tail	2.131846486	
P(T<=t) two-tail	0.491234818	
t Critical two-tail	2.776450856	

% Propulsion time - Low velocity F-test for variance		
	AB	***WD***
Mean	35.72352565	42.16900062
Variance	3.209862452	6.404602575
Observations	5	5
df	4	4
F	1.995288792	
P(F<=f) one-tail	0.259958588	
F Critical one-tail	0.156537894	

% Propulsion time - Low velocity T-test		
	AB	***WD***
Mean	35.72352565	42.16900062
Variance	3.209862452	6.404602575
Observations	5	5
Pooled Variance	4.807232513	
Hypothesized Mean Difference	0	
df	8	
t Stat	-4.64812037	
P(T<=t) one-tail	0.000824352	
t Critical one-tail	1.85954832	
P(T<=t) two-tail	0.001648703	
t Critical two-tail	2.306005626	

% Propulsion time - Medium velocity F-test for variance		
	AB	*WD*
Mean	35.60806805	39.66029696
Variance	3.501640767	1.196666623
Observations	5	5
df	4	4
F	2.926162308	
P(F<=f) one-tail	0.161572301	
F Critical one-tail	6.388233942	

% Propulsion time - Med. velocity T-test		
	AB	*WD*
Mean	35.60806805	39.66029696
Variance	3.501640767	1.196666623
Observations	5	5
Pooled Variance	2.349153695	
Hypothesized Mean Difference	0	
df	8	
t Stat	-4.180307793	
P(T<=t) one-tail	0.001539161	
t Critical one-tail	1.85954832	
P(T<=t) two-tail	0.003078321	
t Critical two-tail	2.306005626	

% Propulsion time - High velocity F-test for variance		
	AB	*WD*
Mean	33.37671148	37.70744927
Variance	2.088934541	6.152072025
Observations	5	5
df	4	4
F	2.945076499	
P(F<=f) one-tail	0.16018366	
F Critical one-tail	0.156537894	

% Propulsion time - High velocity T-test		
	AB	*WD*
Mean	33.37671148	37.70744927
Variance	2.088934541	6.152072025
Observations	5	5
Pooled Variance	4.120503283	
Hypothesized Mean Difference	0	
df	8	
t Stat	-3.373313946	
P(T<=t) one-tail	0.004868818	
t Critical one-tail	1.85954832	
P(T<=t) two-tail	0.009737636	
t Critical two-tail	2.306005626	

% Recovery time - Low velocity F-test for variance		
	AB	*WD*
Mean	64.30224873	57.79550442
Variance	3.312919276	6.448405047
Observations	5	5
df	4	4
F	1.946441947	
P(F<=f) one-tail	0.26737428	
F Critical one-tail	0.156537894	

% Recovery time - Low velocity T-test		
	AB	*WD*
Mean	64.30224873	57.79550442
Variance	3.312919276	6.448405047
Observations	5	5
Pooled Variance	4.880662162	
Hypothesized Mean Difference	0	
df	8	
t Stat	4.656872757	
P(T<=t) one-tail	0.000815028	
t Critical one-tail	1.85954832	
P(T<=t) two-tail	0.001630056	
t Critical two-tail	2.306005626	

% Recovery time - Medium velocity F-test for variance		
	AB	*WD*
Mean	64.4252925	60.34933039
Variance	3.577459086	1.155265742
Observations	5	5
df	4	4
F	3.096654697	
P(F<=f) one-tail	0.149666906	
F Critical one-tail	6.388233942	

% Recovery time - Medium velocity T-test		
	AB	*WD*
Mean	64.4252925	60.34933039
Variance	3.577459086	1.155265742
Observations	5	5
Pooled Variance	2.366362414	
Hypothesized Mean Difference	0	
df	8	
t Stat	4.189474136	
P(T<=t) one-tail	0.001519973	
t Critical one-tail	1.85954832	
P(T<=t) two-tail	0.003039946	
t Critical two-tail	2.306005626	

% Recovery time - High velocity F-test for variance		
	AB	*WD*
Mean	66.60558142	62.27101277
Variance	2.120676822	6.069497781
Observations	5	5
df	4	4
F	2.862056923	
P(F<=f) one-tail	0.166413728	
F Critical one-tail	0.156537894	

% Recovery time - High velocity T-test		
	AB	*WD*
Mean	66.60558142	62.27101277
Variance	2.120676822	6.069497781
Observations	5	5
Pooled Variance	4.095087302	
Hypothesized Mean Difference	0	
df	8	
t Stat	3.386759113	
P(T<=t) one-tail	0.00477282	
t Critical one-tail	1.85954832	
P(T<=t) two-tail	0.009545639	
t Critical two-tail	2.306005626	

Work per stroke - Low velocity F-test for variance		
	AB	*WD*
Mean	21.32874908	19.77111202
Variance	9.283750956	55.86686436
Observations	5	5
df	4	4
F	6.017703903	
P(F<=f) one-tail	0.055129086	
F Critical one-tail	0.156537894	

Work per stroke - Low velocity T-test		
	AB	*WD*
Mean	21.32874908	19.77111202
Variance	9.283750956	55.86686436
Observations	5	5
Pooled Variance	32.57530766	
Hypothesized Mean Difference	0	
df	8	
t Stat	0.431511141	
P(T<=t) one-tail	0.338744857	
t Critical one-tail	1.85954832	
P(T<=t) two-tail	0.677489713	
t Critical two-tail	2.306005626	

Work per stroke - Medium velocity F-test for variance		
	AB	*WD*
Mean	32.69429895	31.00250498
Variance	27.56755398	36.23387489
Observations	5	5
df	4	4
F	1.314366698	
P(F<=f) one-tail	0.398752015	
F Critical one-tail	0.156537894	

Work per stroke - Medium velocity T-test		
	AB	*WD*
Mean	32.69429895	31.00250498
Variance	27.56755398	36.23387489
Observations	5	5
Pooled Variance	31.90071444	
Hypothesized Mean Difference	0	
df	8	
t Stat	0.473606084	
P(T<=t) one-tail	0.324217914	
t Critical one-tail	1.85954832	
P(T<=t) two-tail	0.648435828	
t Critical two-tail	2.306005626	

Work per stroke - High velocity F-test for variance		
	AB	*WD*
Mean	36.81976489	40.80530372
Variance	5.264629642	67.51129908
Observations	5	5
df	4	4
F	12.82356095	
P(F<=f) one-tail	0.01494221	
F Critical one-tail	0.156537894	

Work per stroke - High velocity T-test		
	AB	*WD*
Mean	36.81976489	40.80530372
Variance	5.264629642	67.51129908
Observations	5	5
Hypothesized Mean Difference	0	
df	5	
t Stat	-1.044667705	
P(T<=t) one-tail	0.172014144	
t Critical one-tail	2.015049176	
P(T<=t) two-tail	0.344028287	
t Critical two-tail	2.570577635	

Start Angle - Low velocity T-test		
	AB	***WD***
Mean	82.2	85
Variance	135.2	788
Observations	5	5
Pooled Variance	461.6	
Hypothesized Mean Difference	0	
df	8	
t Stat	-0.206060683	
P(T<=t) one-tail	0.42094542	
t Critical one-tail	1.85954832	
P(T<=t) two-tail	0.84189084	
t Critical two-tail	2.306005626	

Start Angle - Medium velocity T-test		
	AB	***WD***
Mean	77	74.6
Variance	169	607.3
Observations	5	5
Pooled Variance	388.15	
Hypothesized Mean Difference	0	
df	8	
t Stat	0.192611162	
P(T<=t) one-tail	0.426031622	
t Critical one-tail	1.85954832	
P(T<=t) two-tail	0.852063245	
t Critical two-tail	2.306005626	

Start Angle - High velocity T-test		
	AB	*WD*
Mean	77	54
Variance	169	187.5
Observations	5	5
Pooled Variance	178.25	
Hypothesized Mean Difference	0	
df	8	
t Stat	2.723849269	
P(T<=t) one-tail	0.013046433	
t Critical one-tail	1.85954832	
P(T<=t) two-tail	0.026092866	
t Critical two-tail	2.306005626	

End Angle - Low velocity T-test		
	AB	*WD*
Mean	177.4	177.4
Variance	202.8	287.3
Observations	5	5
Pooled Variance	245.05	
Hypothesized Mean Difference	0	
df	8	
t Stat	0	
P(T<=t) one-tail	0.5	
t Critical one-tail	1.85954832	
P(T<=t) two-tail	1	
t Critical two-tail	2.306005626	

End Angle - Medium velocity T-test		
	AB	*WD*
Mean	180	187.8
Variance	169	135.2
Observations	5	5
Pooled Variance	152.1	
Hypothesized Mean Difference	0	
df	8	
t Stat	-1	
P(T<=t) one-tail	0.173296754	
t Critical one-tail	1.85954832	
P(T<=t) two-tail	0.346593507	
t Critical two-tail	2.306005626	

End Angle - High velocity T-test		
	AB	*WD*
Mean	187.8	187.8
Variance	135.2	135.2
Observations	5	5
Pooled Variance	135.2	
Hypothesized Mean Difference	0	
df	8	
t Stat	0	
P(T<=t) one-tail	0.5	
t Critical one-tail	1.85954832	
P(T<=t) two-tail	1	
t Critical two-tail	2.306005626	

Push Angle - Low velocity T-test		
	AB	*WD*
Mean	95.2	92.4
Variance	304.2	1608.3
Observations	5	5
Pooled Variance	956.25	
Hypothesized Mean Difference	0	
df	8	
t Stat	0.143166798	
P(T<=t) one-tail	0.444849409	
t Critical one-tail	1.85954832	
P(T<=t) two-tail	0.889698818	
t Critical two-tail	2.306005626	

Push Angle - Medium velocity T-test		
	AB	*WD*
Mean	103	113.2
Variance	253.5	942.7
Observations	5	5
Pooled Variance	598.1	
Hypothesized Mean Difference	0	
df	8	
t Stat	-0.659452129	
P(T<=t) one-tail	0.264064157	
t Critical one-tail	1.85954832	
P(T<=t) two-tail	0.528128314	
t Critical two-tail	2.306005626	

Push Angle - High velocity T-test		
	AB	*WD*
Mean	110.8	133.8
Variance	135.2	127.7
Observations	5	5
Pooled Variance	131.45	
Hypothesized Mean Difference	0	
df	8	
t Stat	-3.171885818	
P(T<=t) one-tail	0.006578614	
t Critical one-tail	1.85954832	
P(T<=t) two-tail	0.013157229	
t Critical two-tail	2.306005626	

APPENDIX D:

RECTIFIED AND SMOOTHED MIDDLE DELTOID AND LATERAL TRICEPS EMG PLOTS

AB-1, low, deltoid, rect.

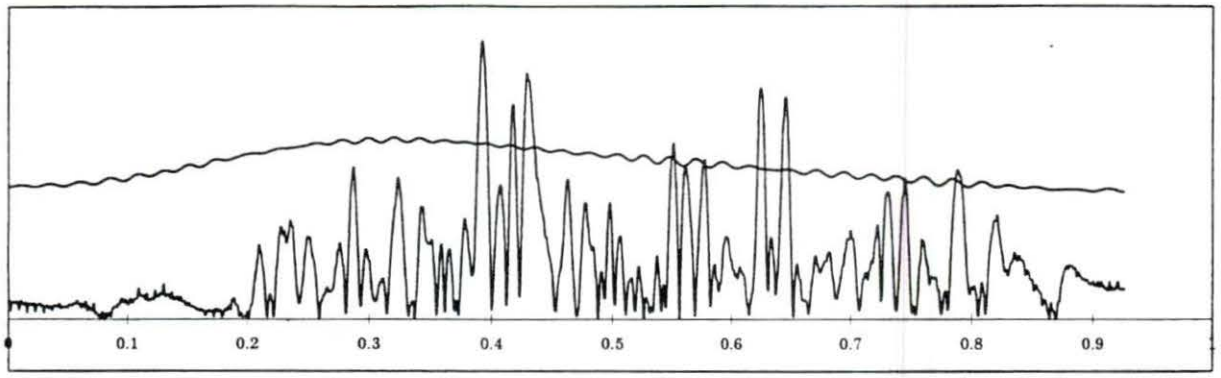

AB-1, low, deltoid, smoothed

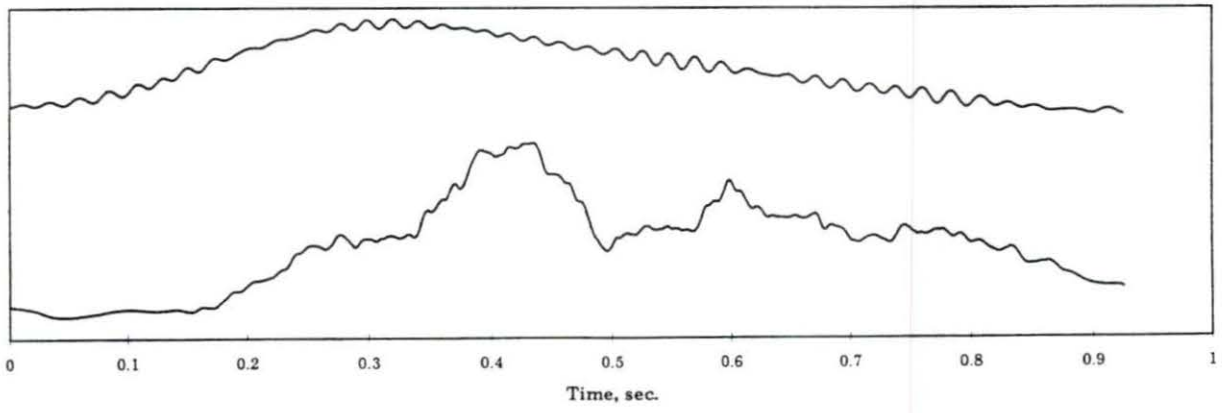

AB-1, low, tricep, rect.

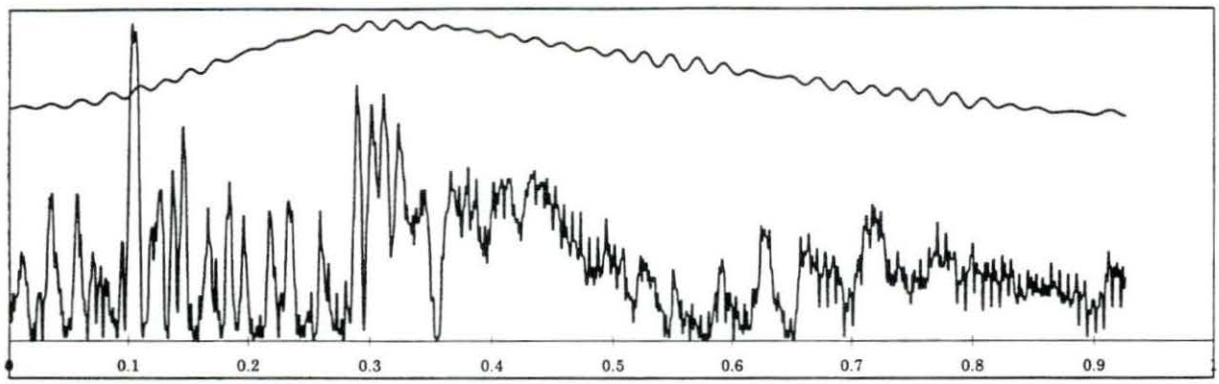

AB-1, low, tricep, smoothed

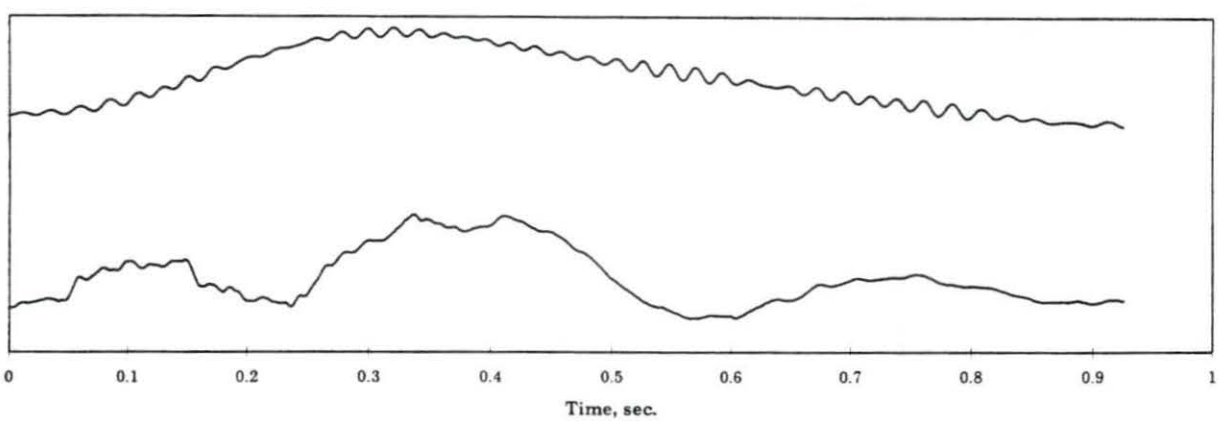

AB-1, medium, deltoid, rect.

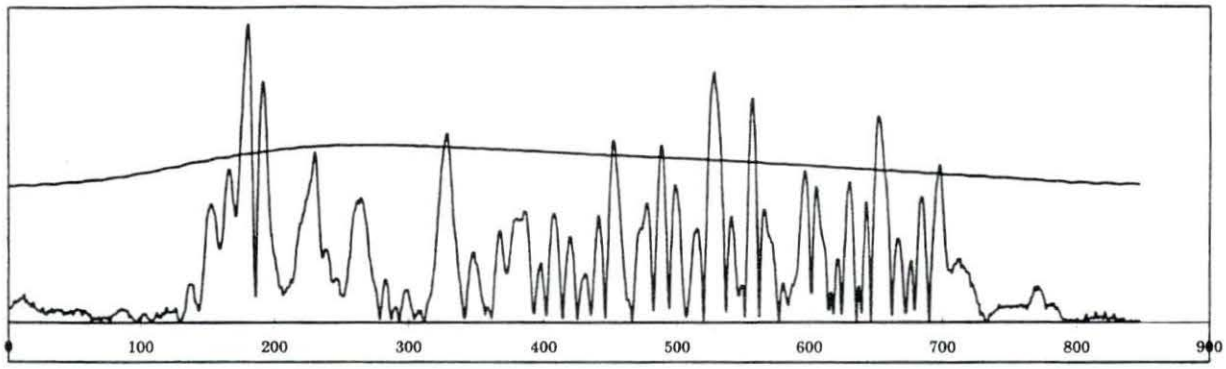

AB-1, medium, deltoid, smoothed

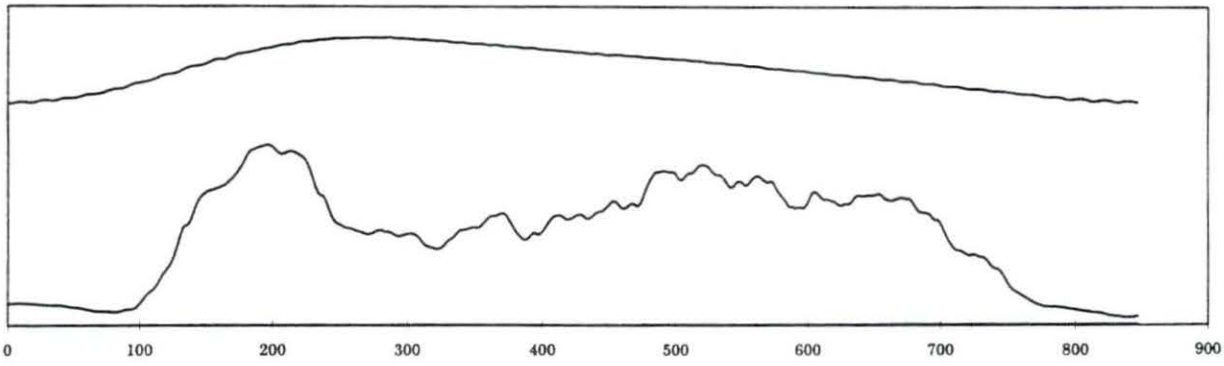

AB-1, medium, tricep, rect.

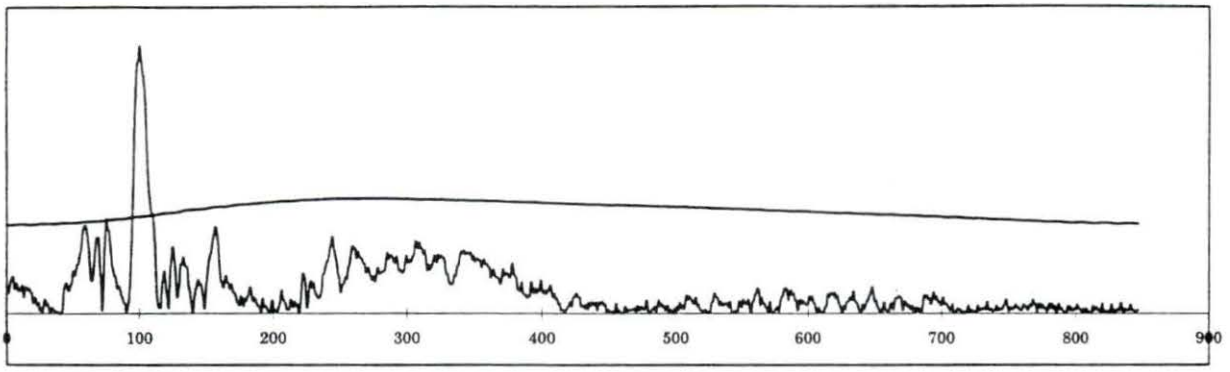

AB-1, medium, tricep, smoothed

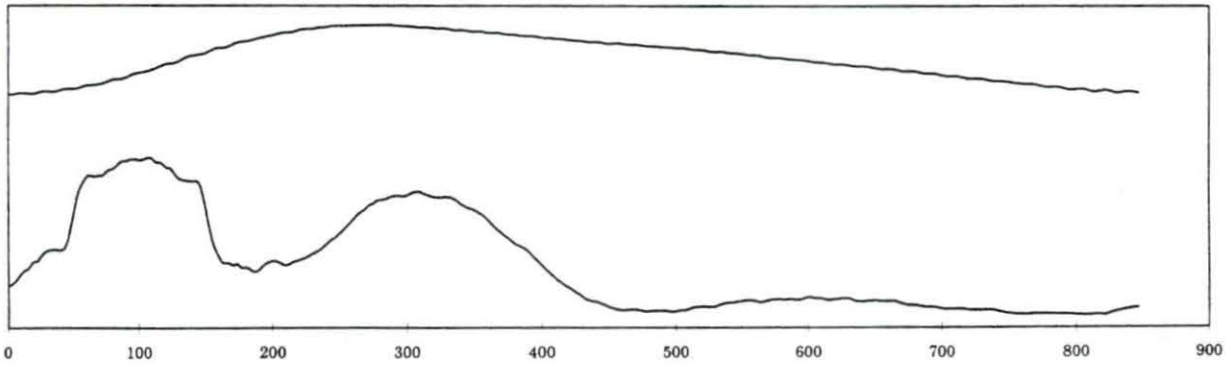

AB-1, high, deltoid, rect.

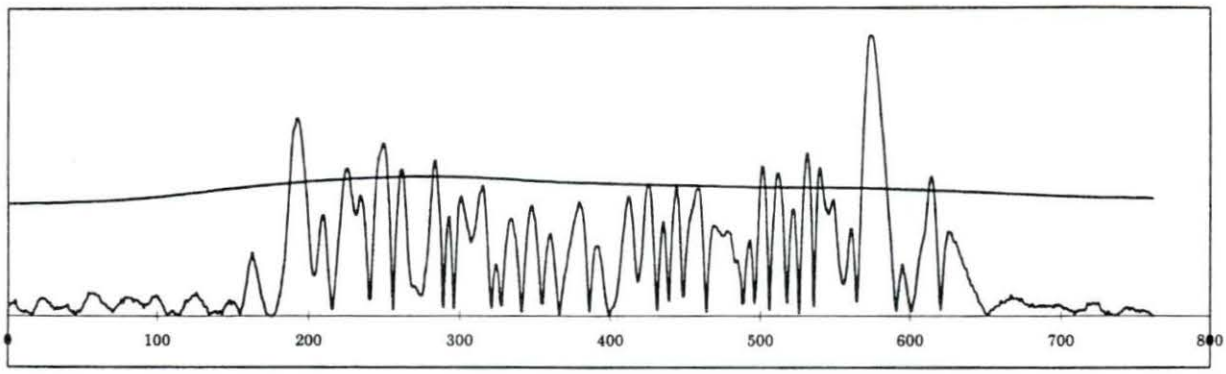

AB-1, high, deltoid, smoothed

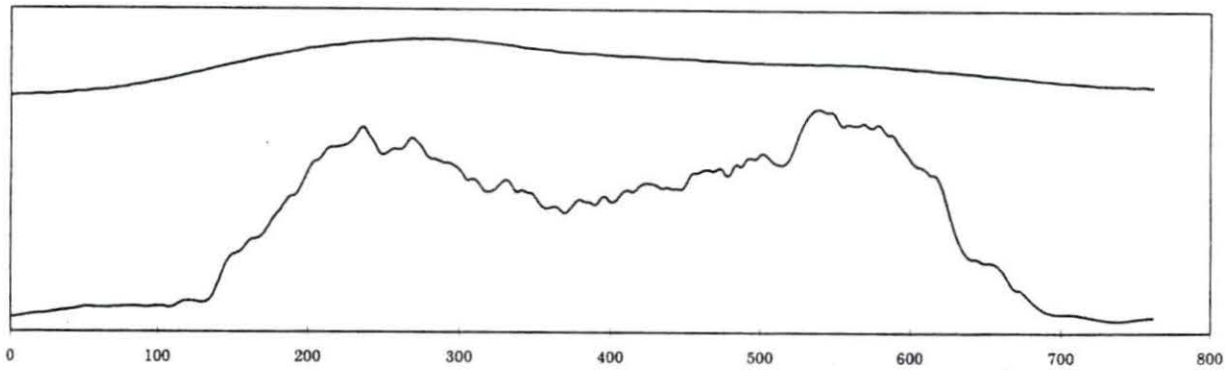

AB-1, high, tricep, rect.

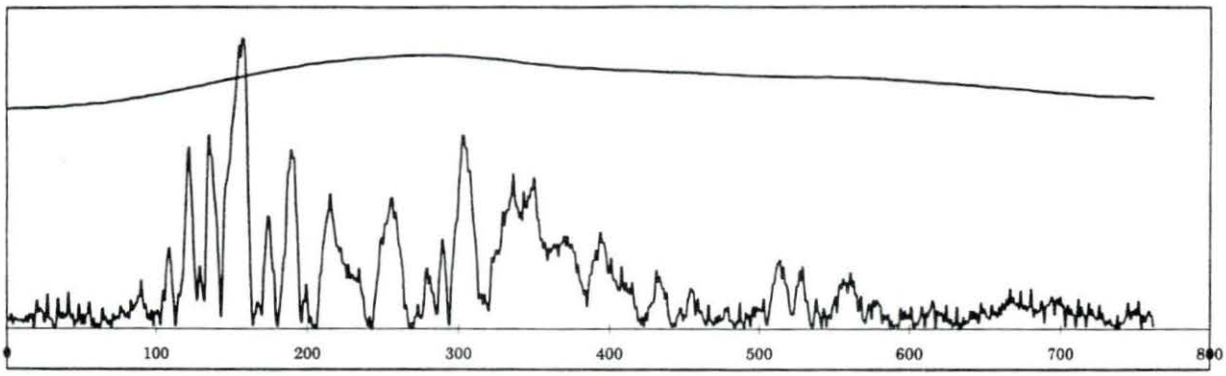

AB-1, high, tricep, smoothed

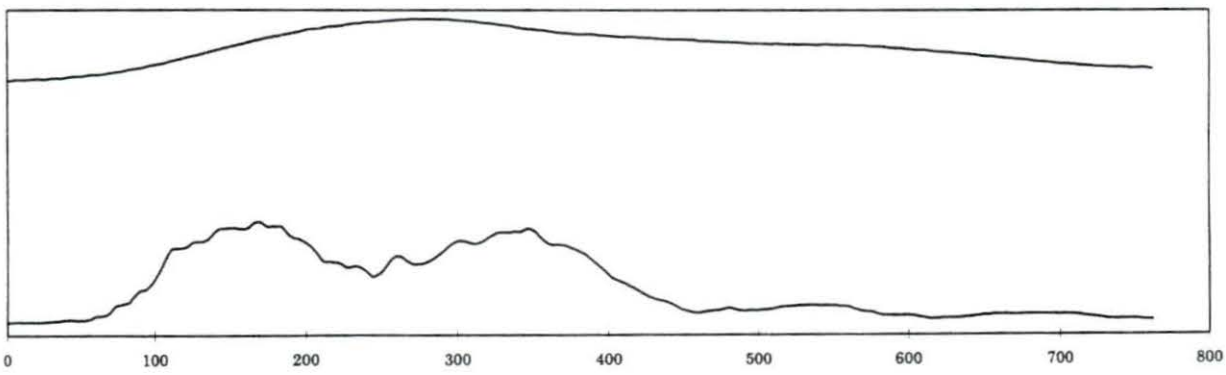

AB-2, low, deltoid, rect.

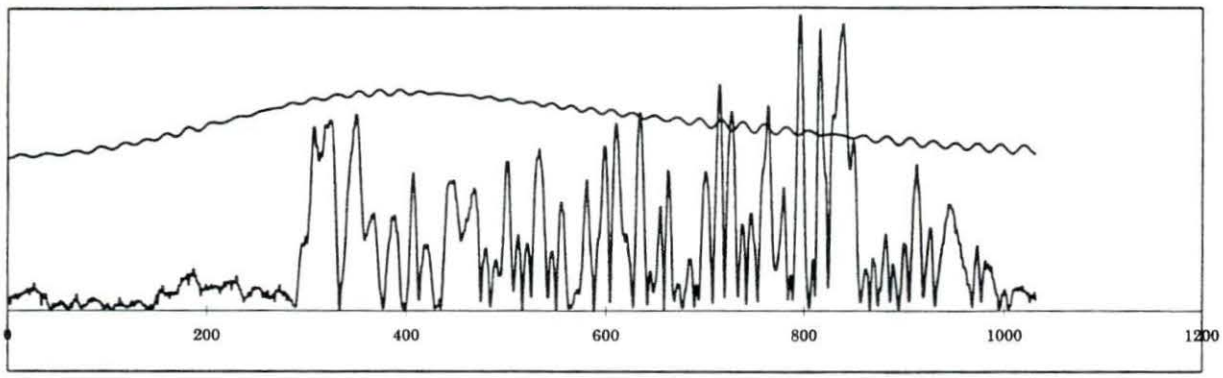

AB-2, low, deltoid, smoothed

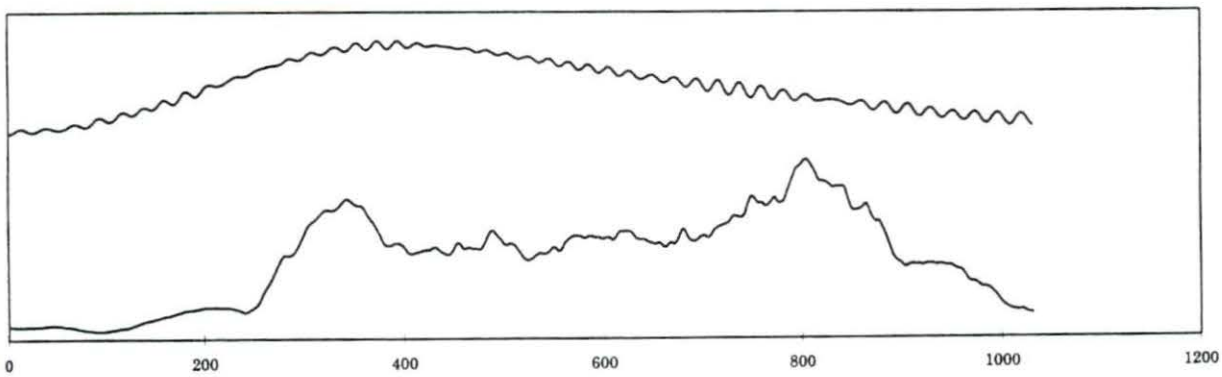

AB-2, low, tricep, rect.

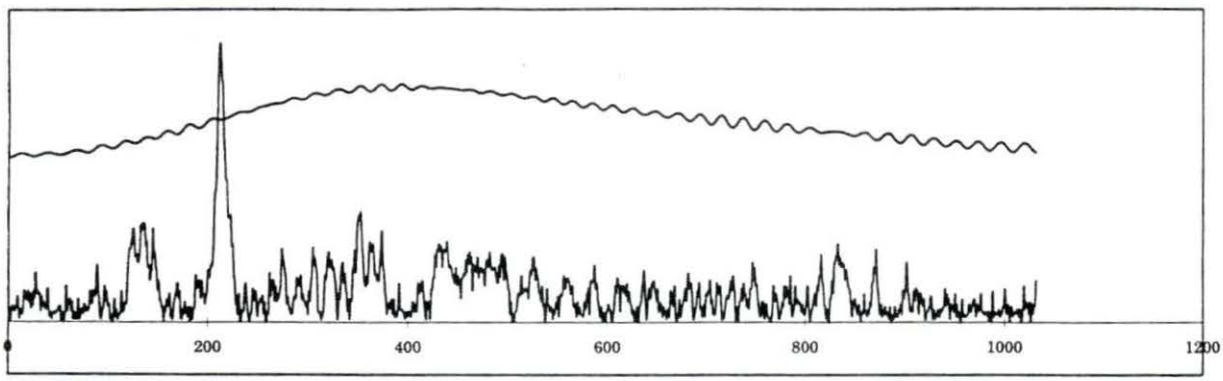

AB-2, low, tricep, smoothed

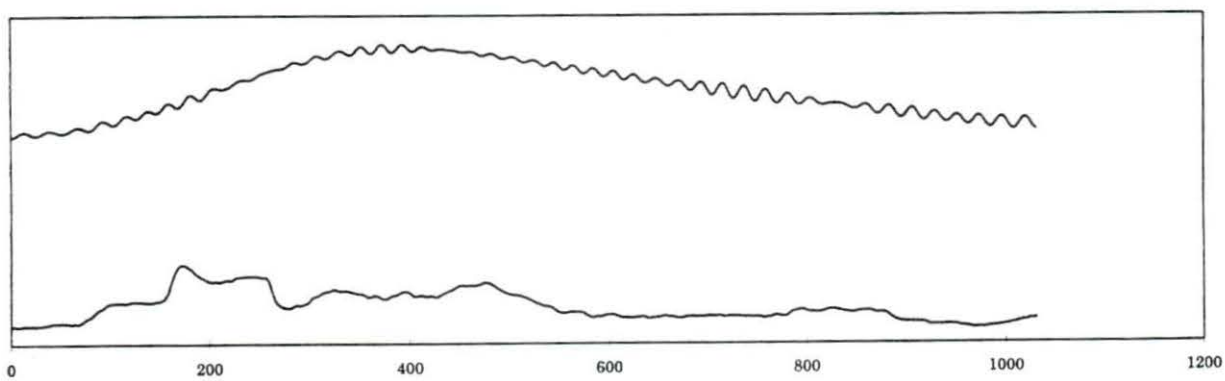

AB-2, medium, deltoid, rect.

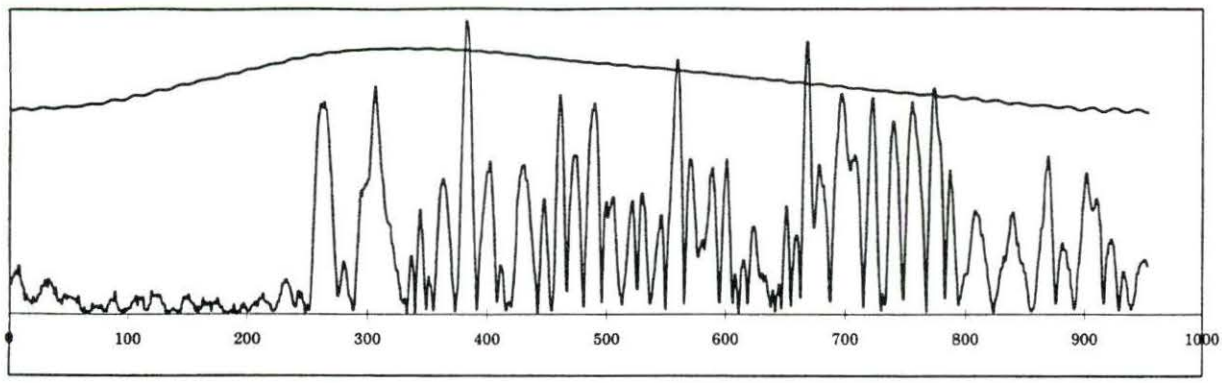

AB-2, medium, deltoid, smoothed

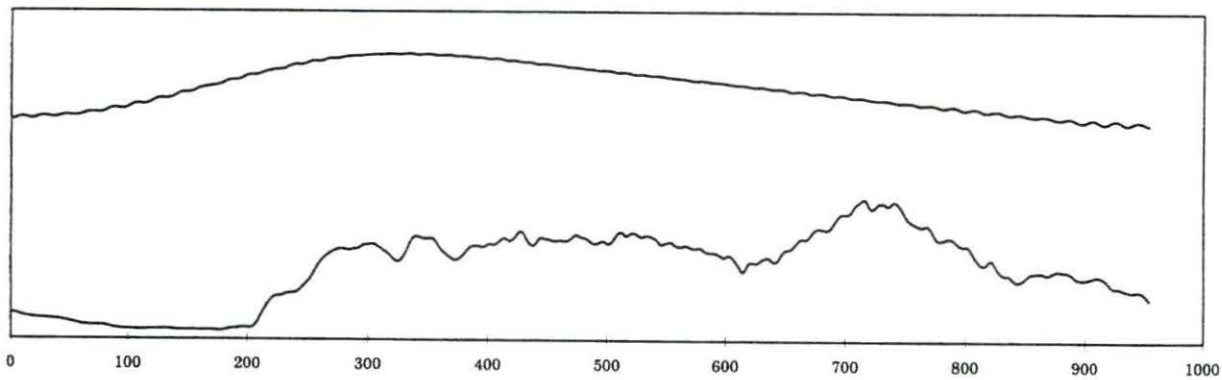

AB-2, medium, tricep, rect.

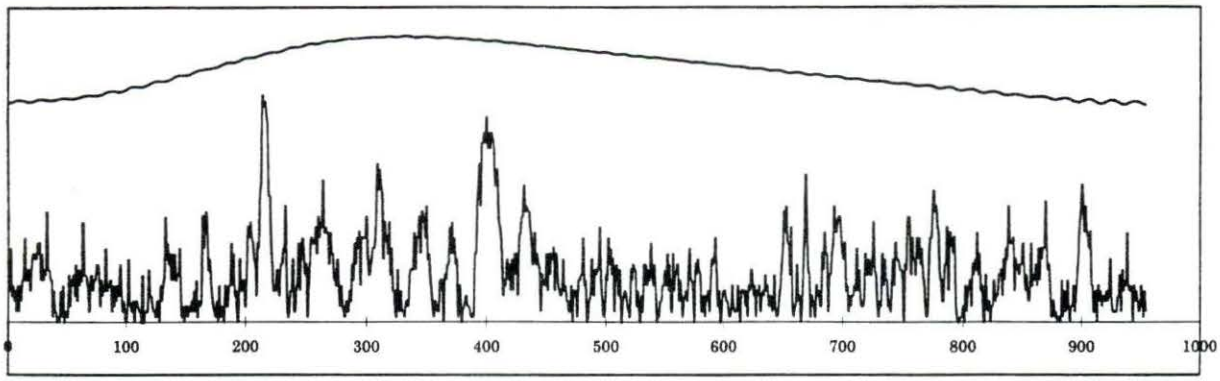

AB-2, medium, tricep, smoothed

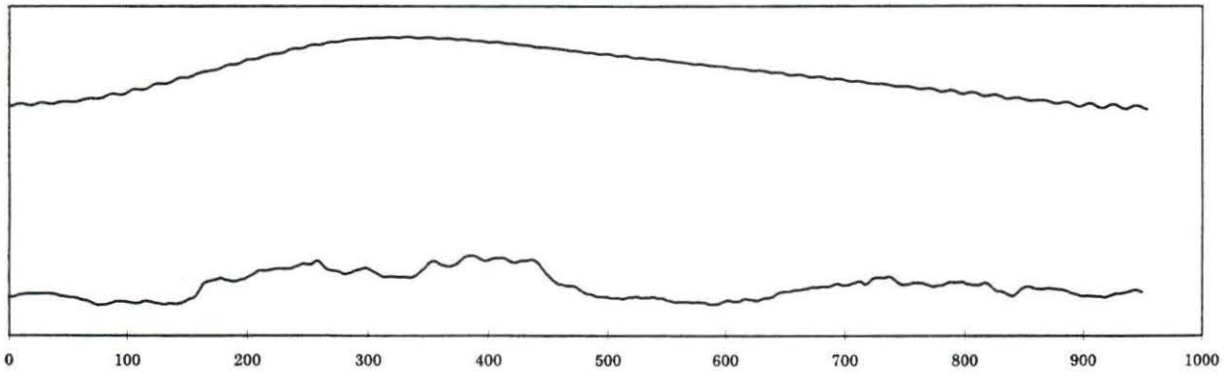

AB-2, high, deltoid, rect.

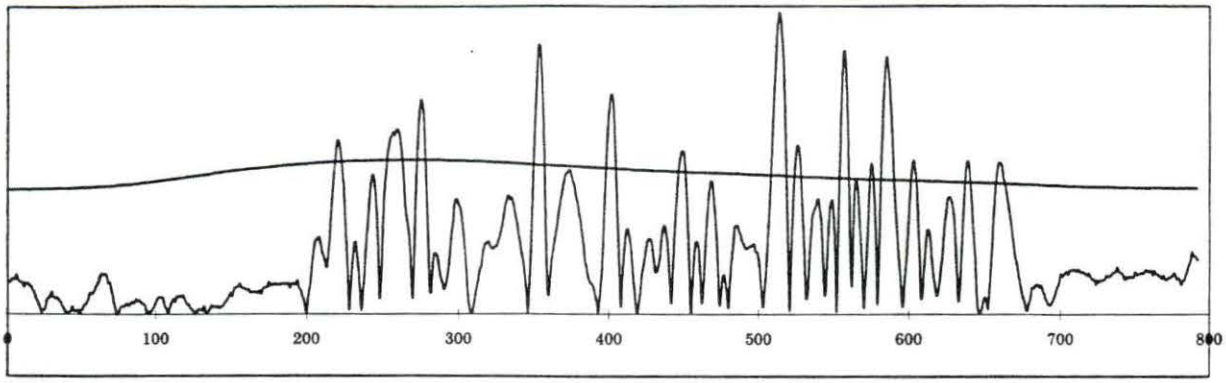

AB-2, high, deltoid, smoothed

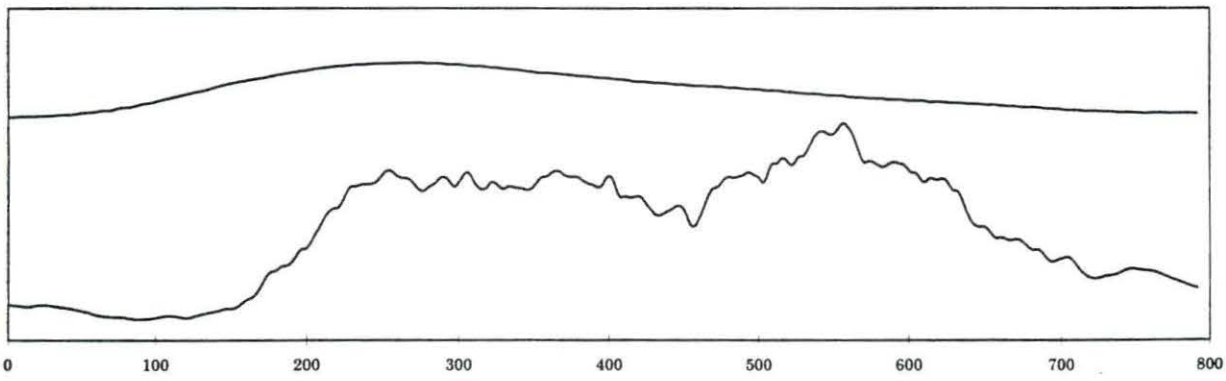

AB-2, high, tricep, rect.

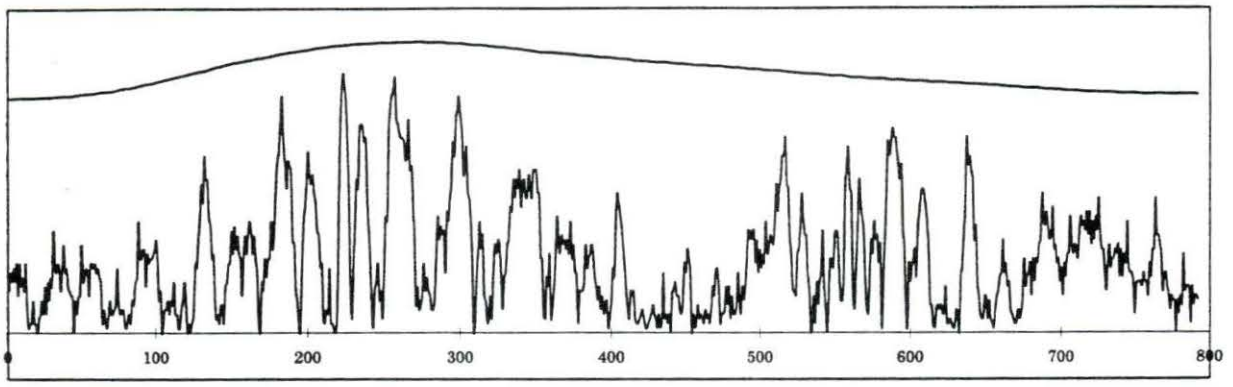

AB-2, high, tricep, smoothed

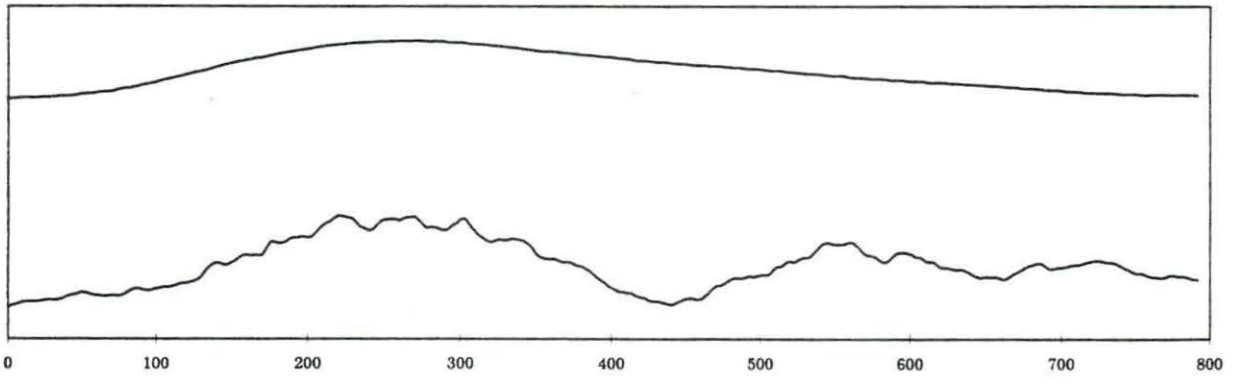

AB-3, low, deltoid, rect.

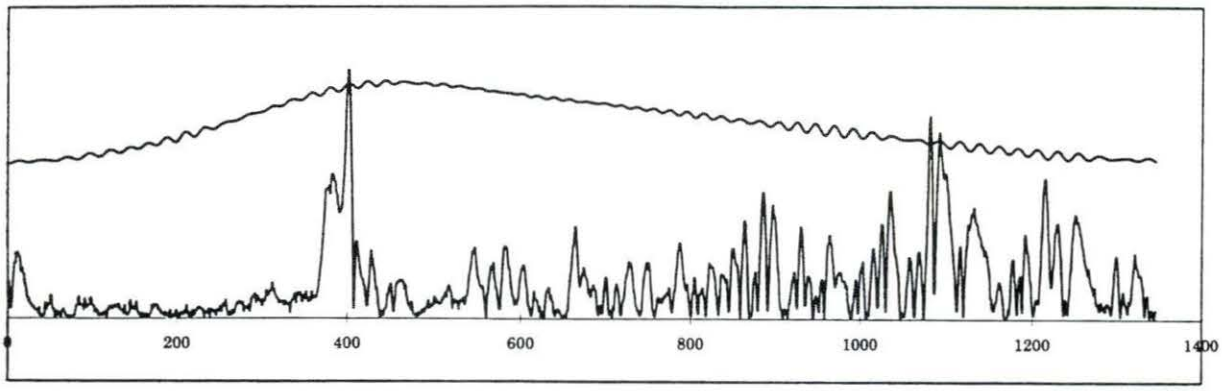

AB-3, low, deltoid, smoothed

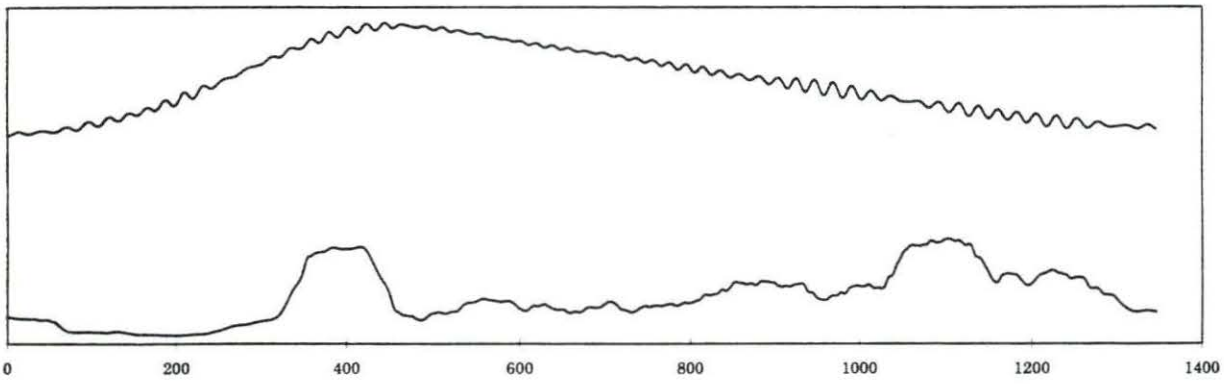

AB-3, low, tricep, rect.

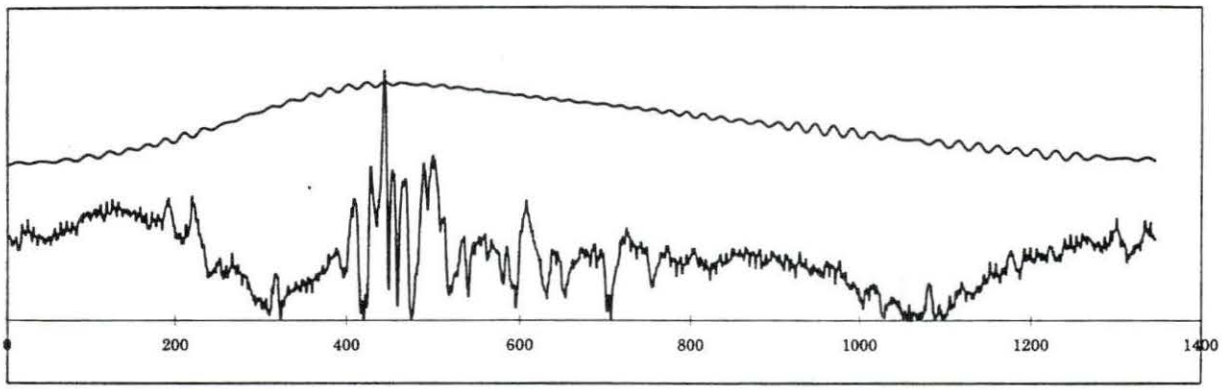

AB-3, low, tricep, smoothed

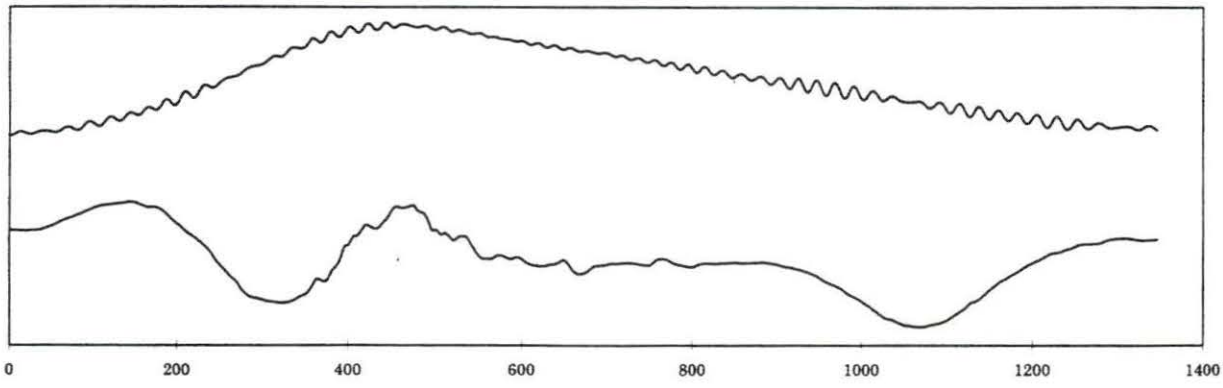

AB-3, medium, deltoid, rect.

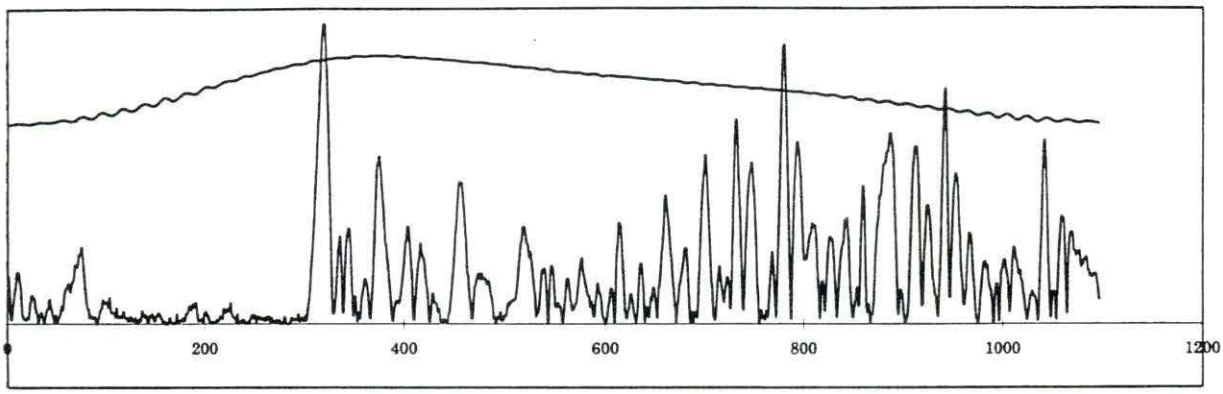

AB-3, medium, deltoid, smoothed

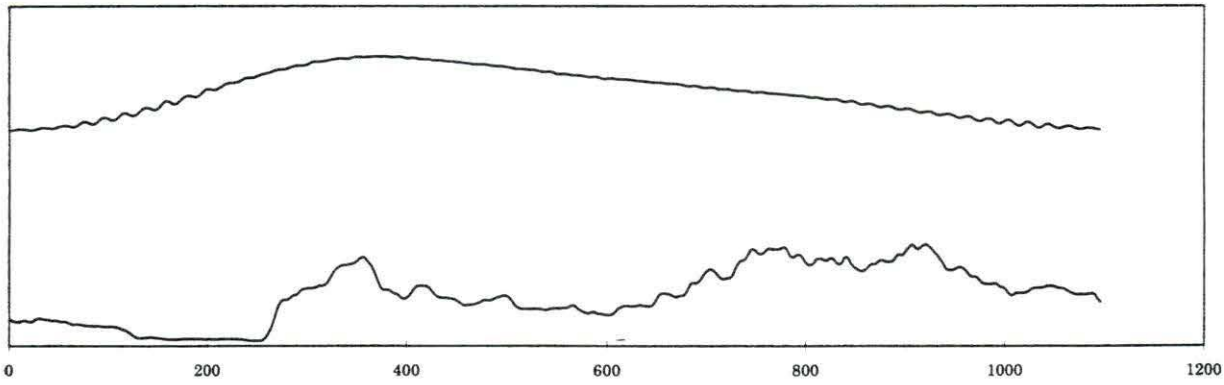

AB-3, medium, tricep, rect.

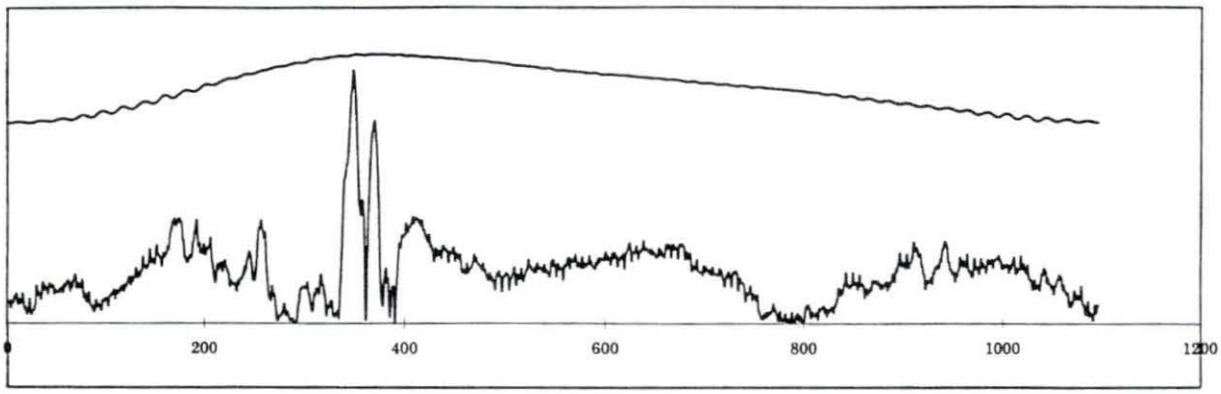

AB-3, medium, tricep, smoothed

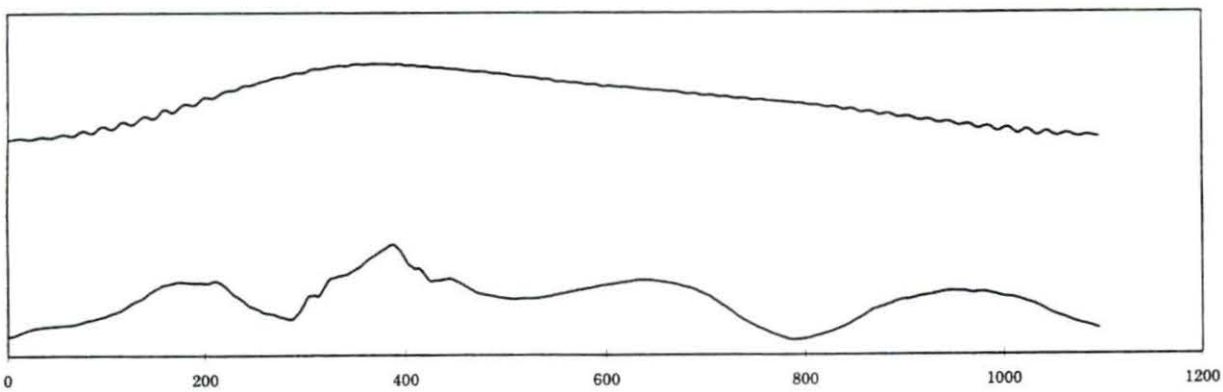

AB-3, high, deltoid, rect.

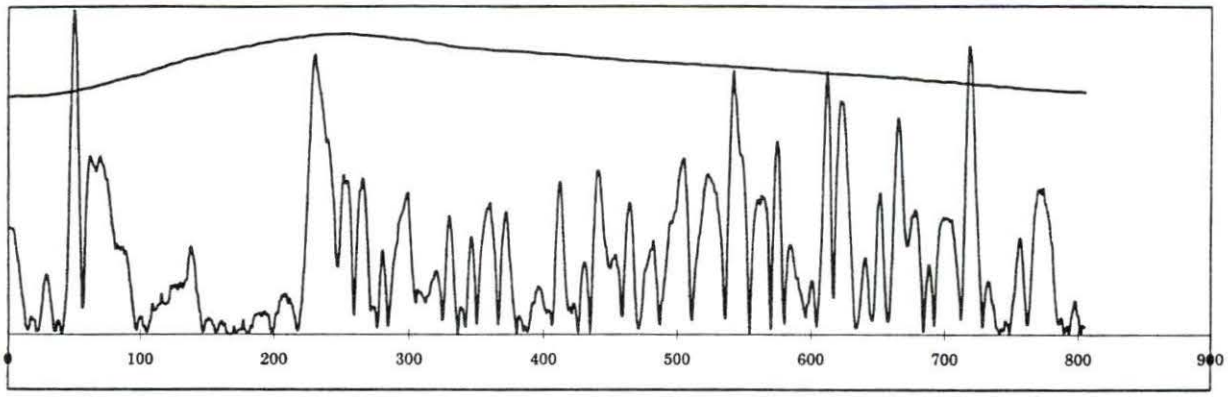

AB-3, high, deltoid, smoothed

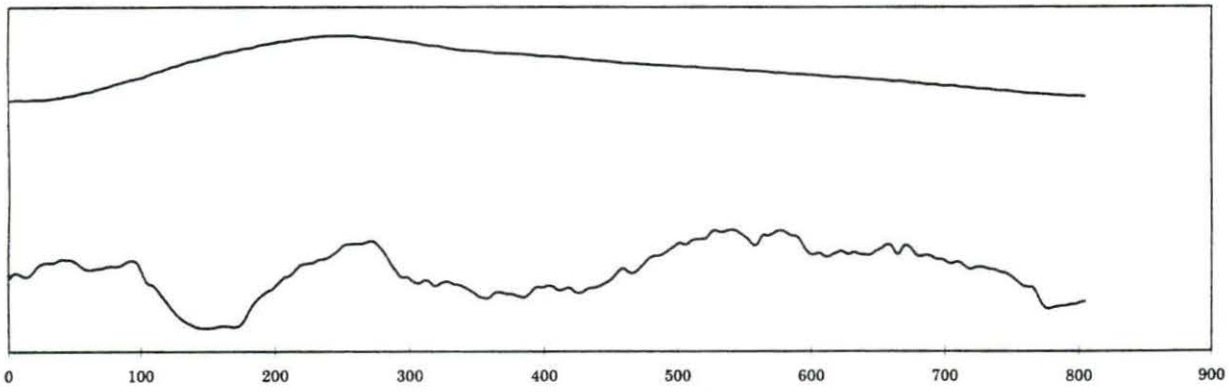

AB-3, high, tricep, rect.

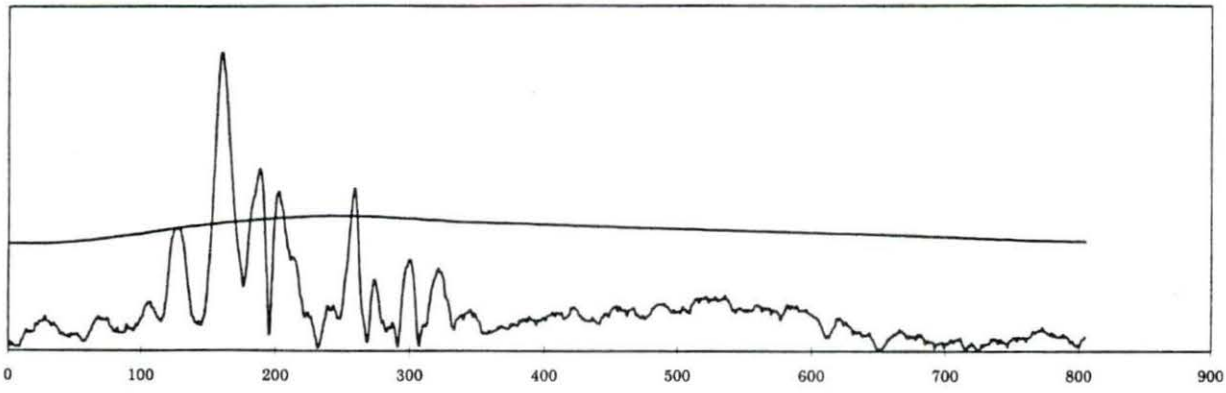

AB-3, high, tricep, smoothed

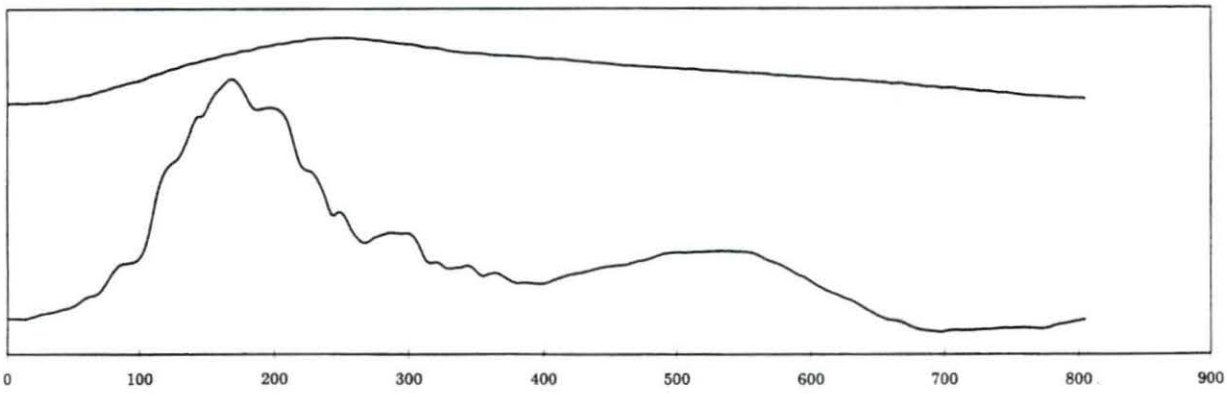

AB-4, low, deltoid, rect.

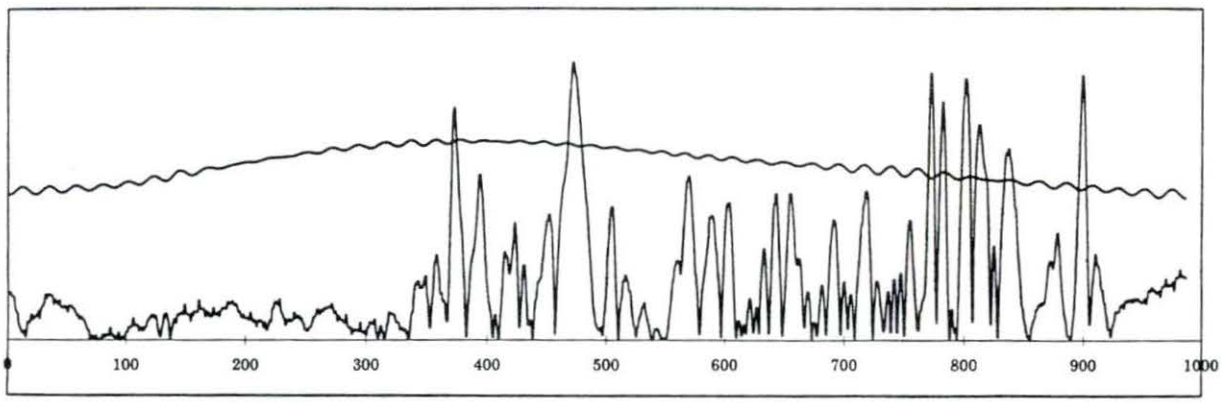

AB-4, low, deltoid, smoothed

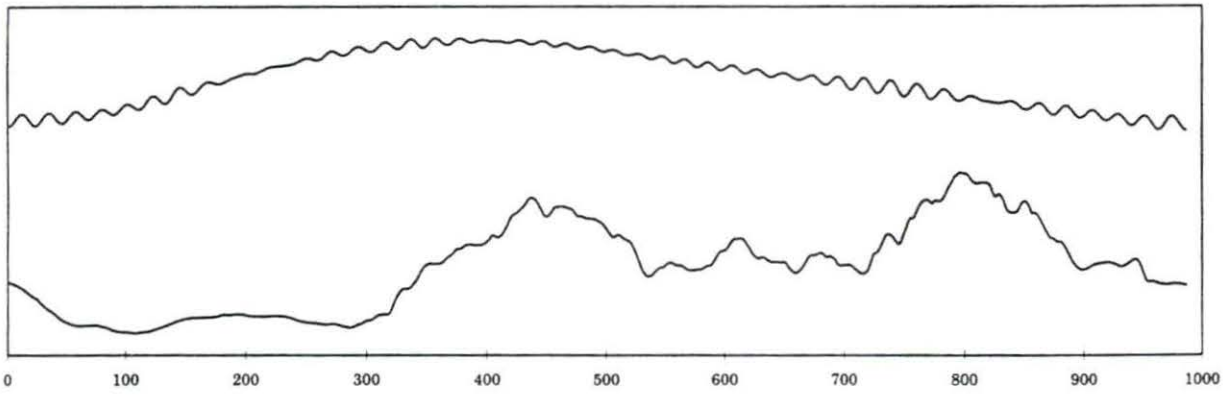

AB-4, low, tricep, rect.

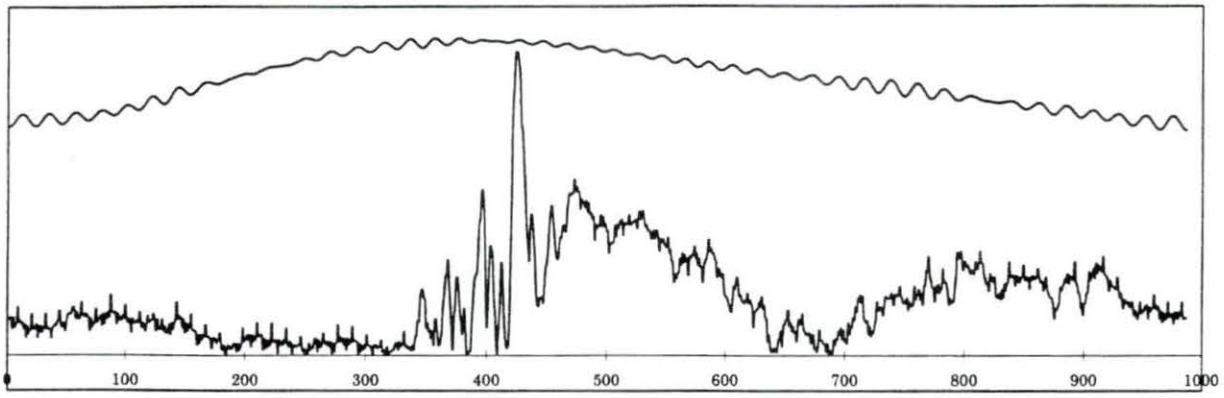

AB-4, low, tricep, smoothed

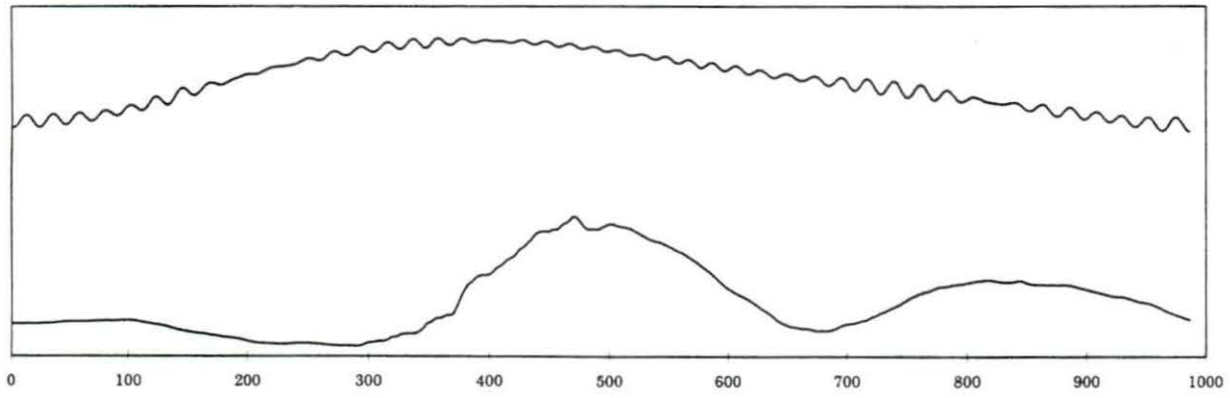

AB-4, medium, deltoid, rect.

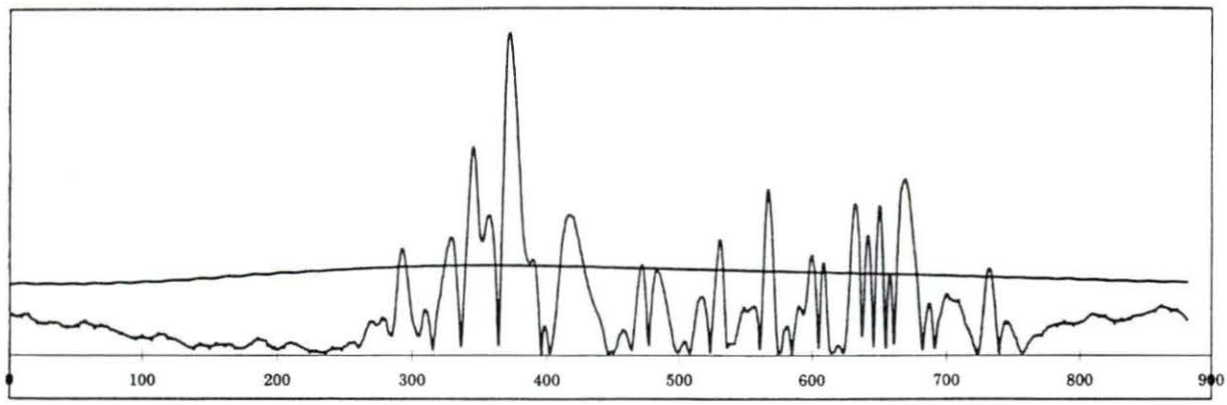

AB-4, medium, deltoid, smoothed

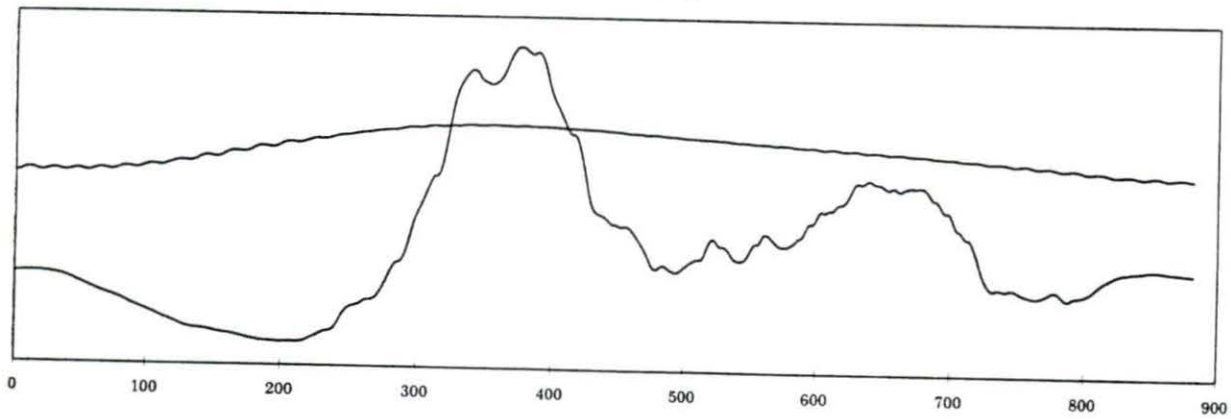

AB-4, medium, tricep, rect.

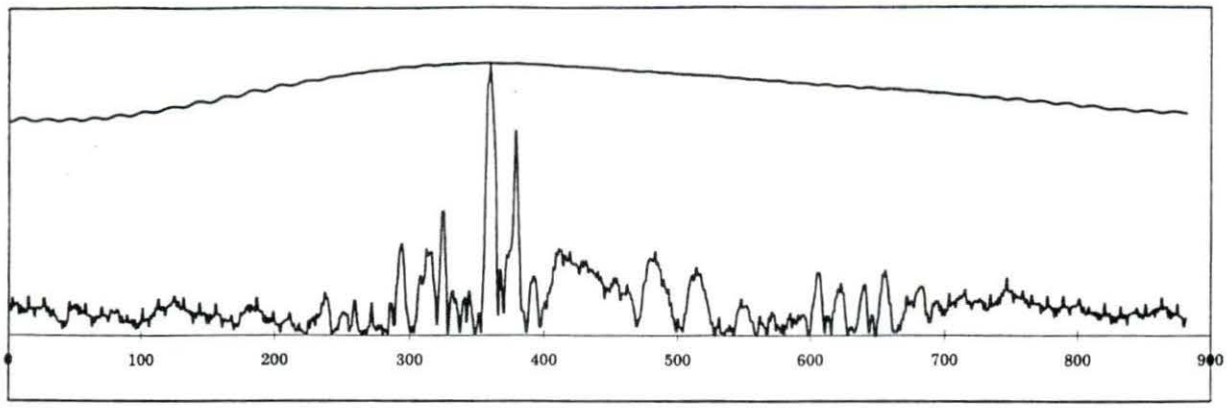

AB-4, medium, tricep, smoothed

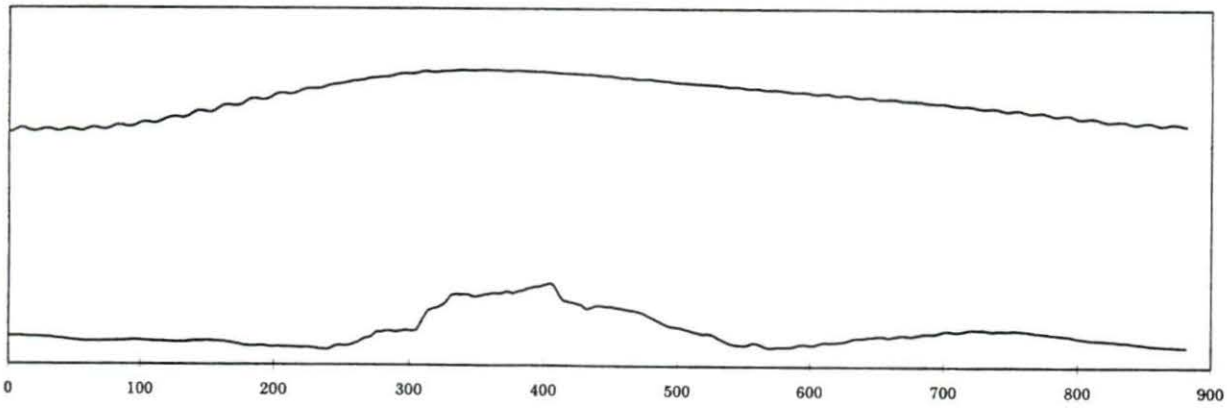

AB-4, high, deltoid, rect.

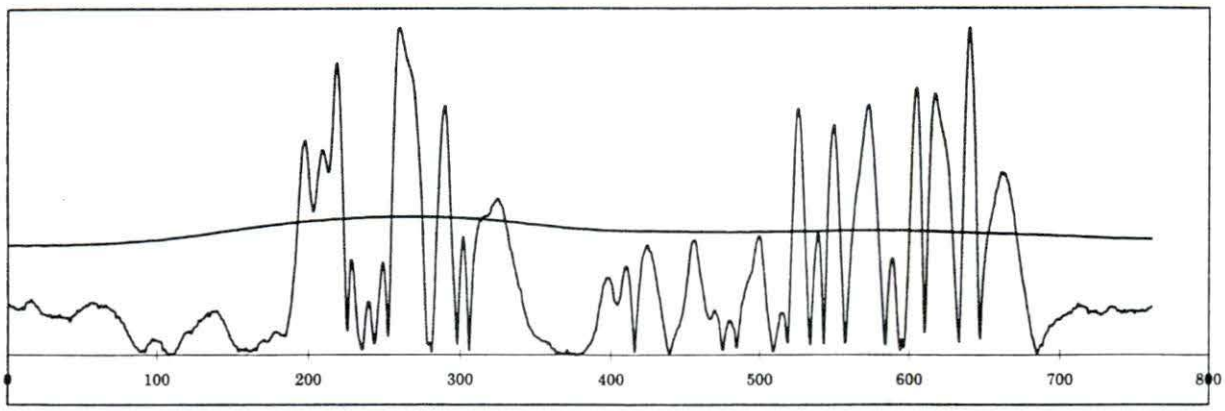

AB-4, high, deltoid, smoothed

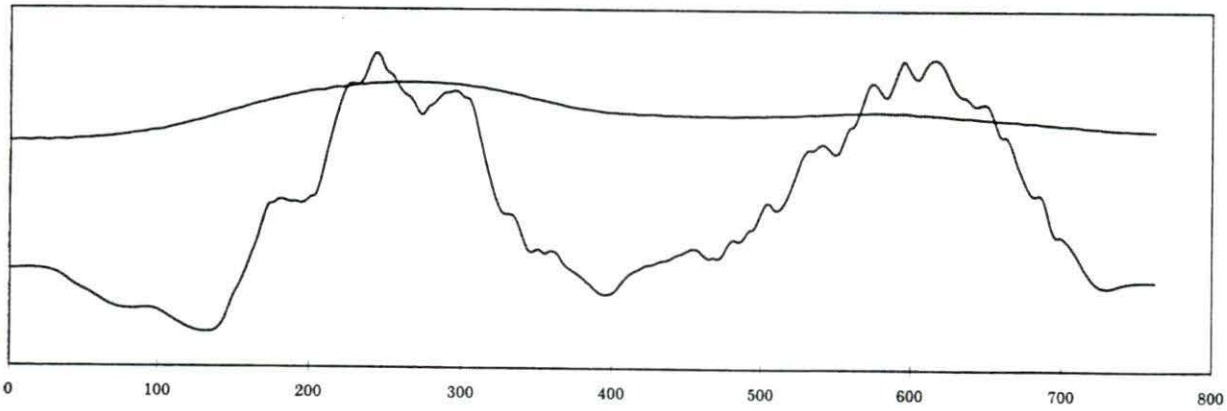

AB-4, high, tricep, rect.

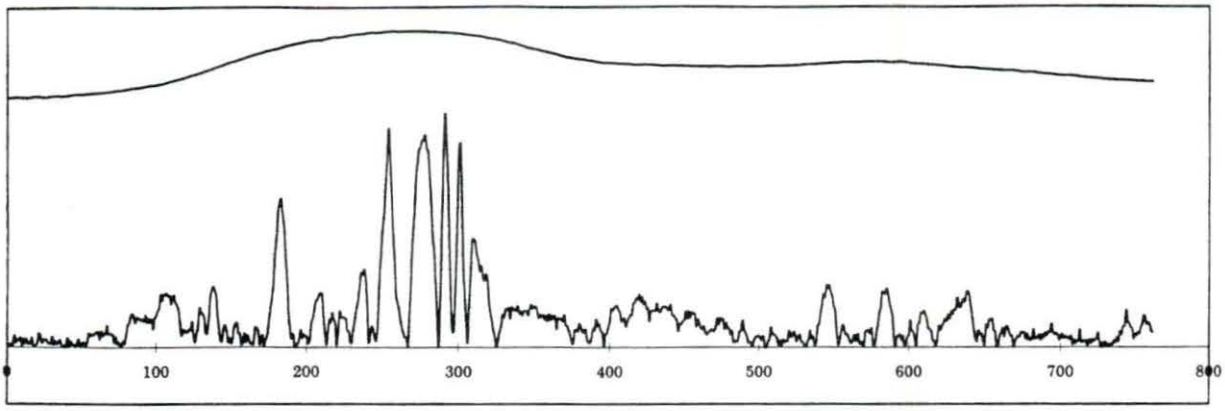

AB-4, high, tricep, smoothed

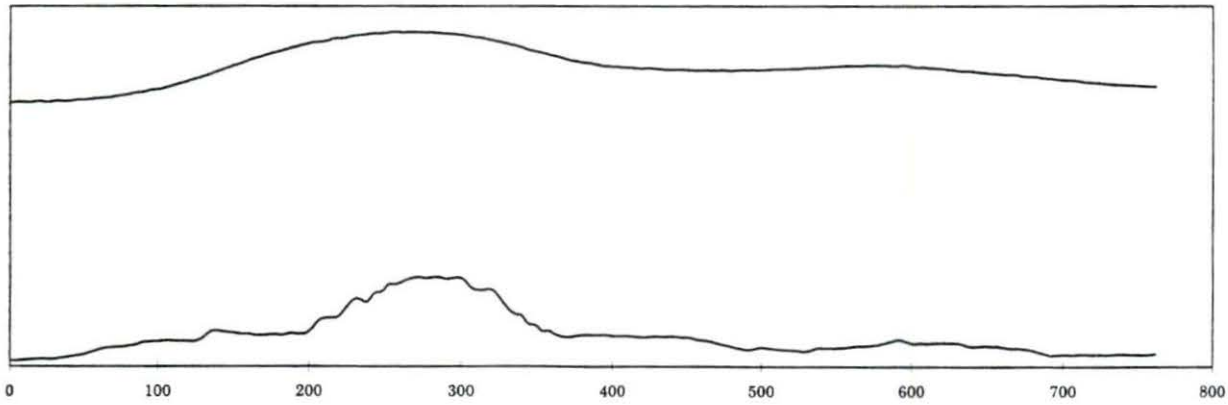

AB-5, low, deltoid, rect.

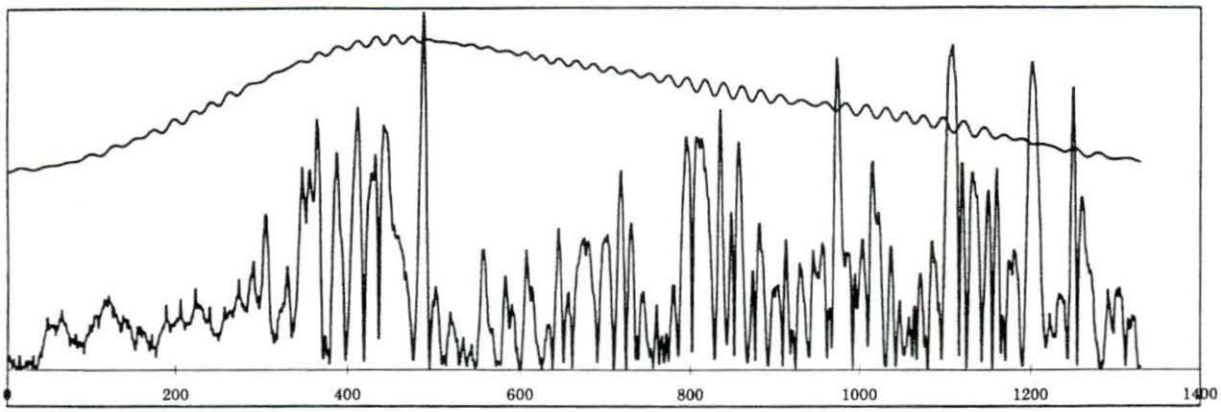

AB-5, low, deltoid, smoothed

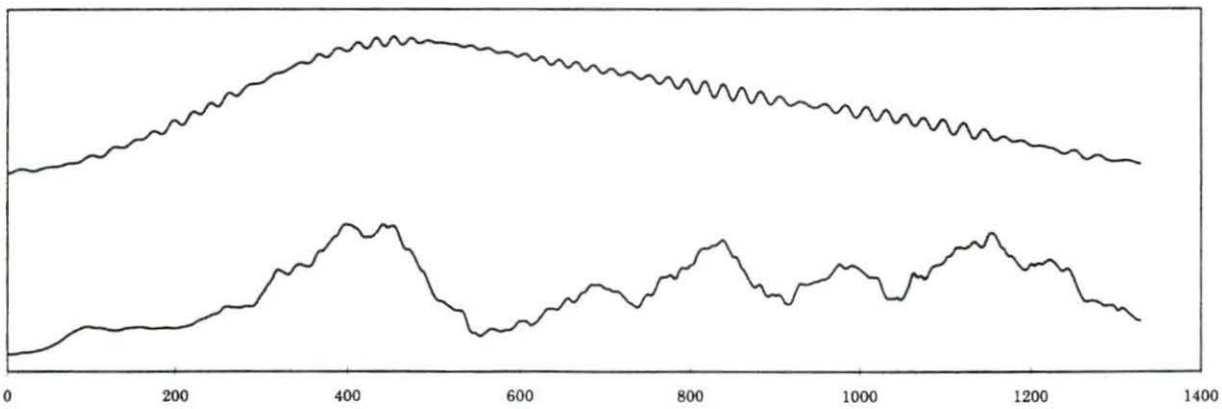

AB-5, low, tricep, rect.

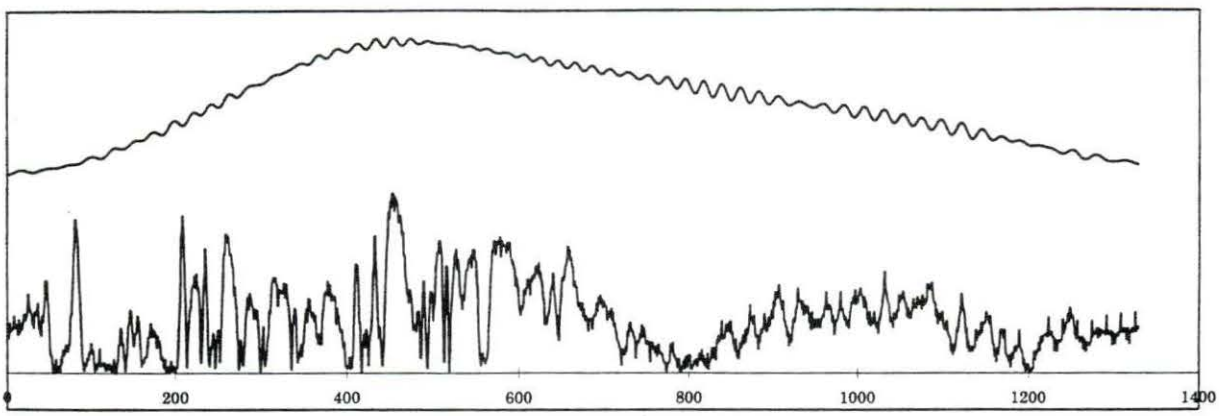

AB-5, low, tricep, smoothed

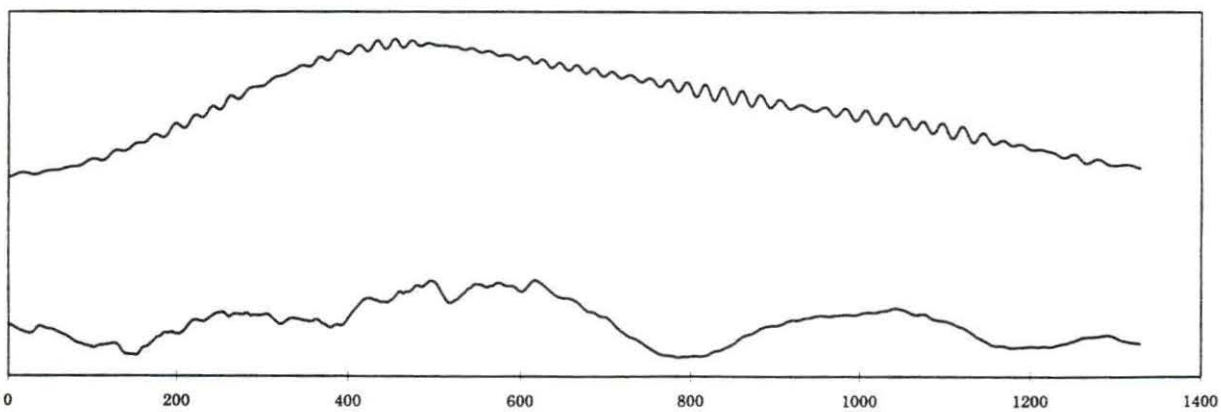

AB-5, medium, deltoid, rect.

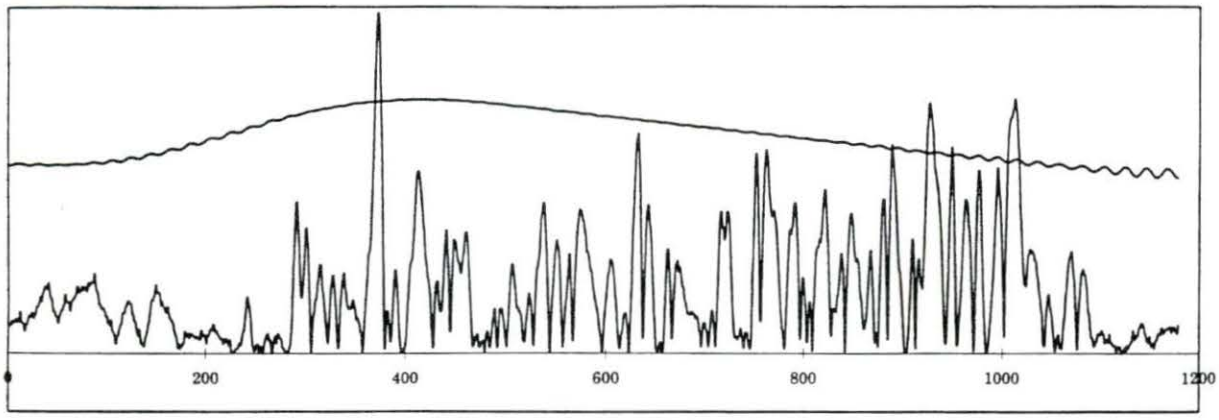

AB-5, medium, deltoid, smoothed

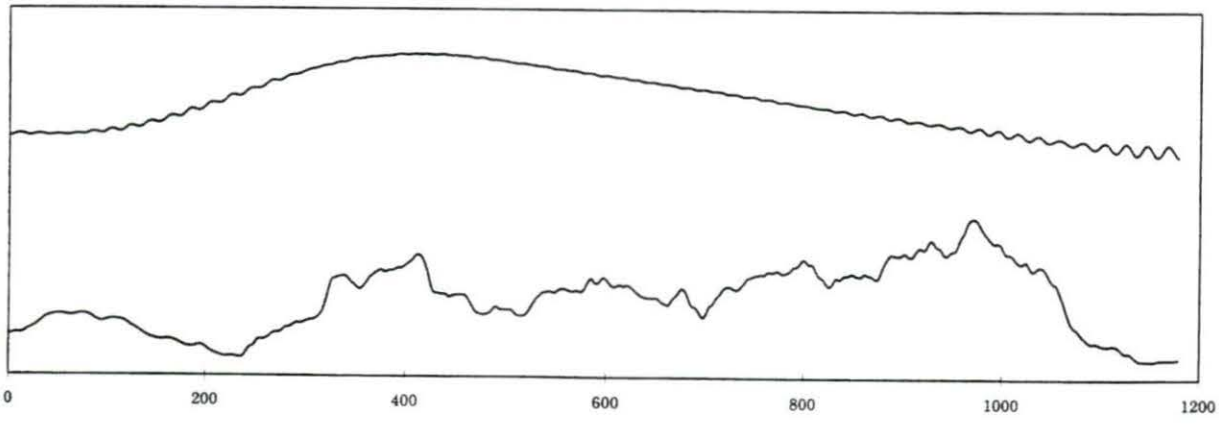

AB-5, medium, tricep, rect.

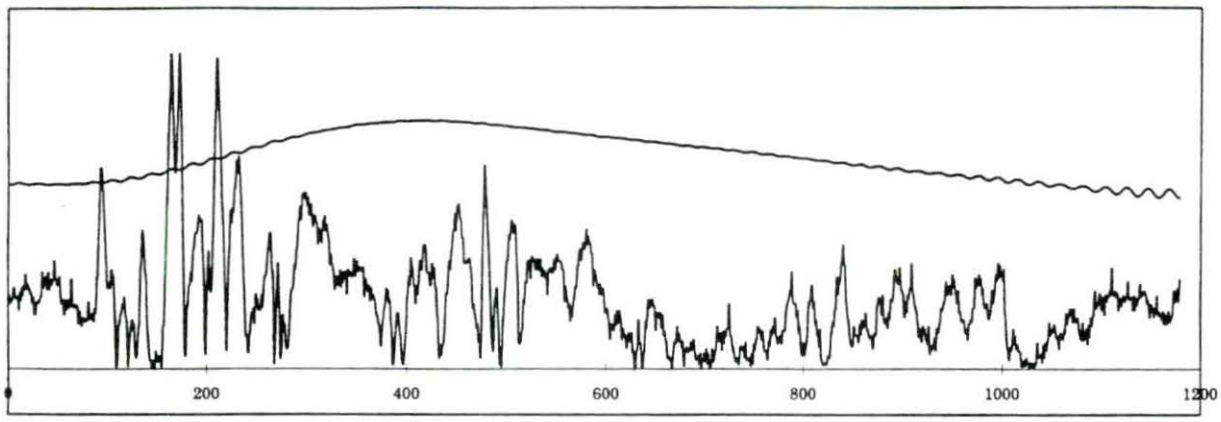

AB-5, medium, tricep, smoothed

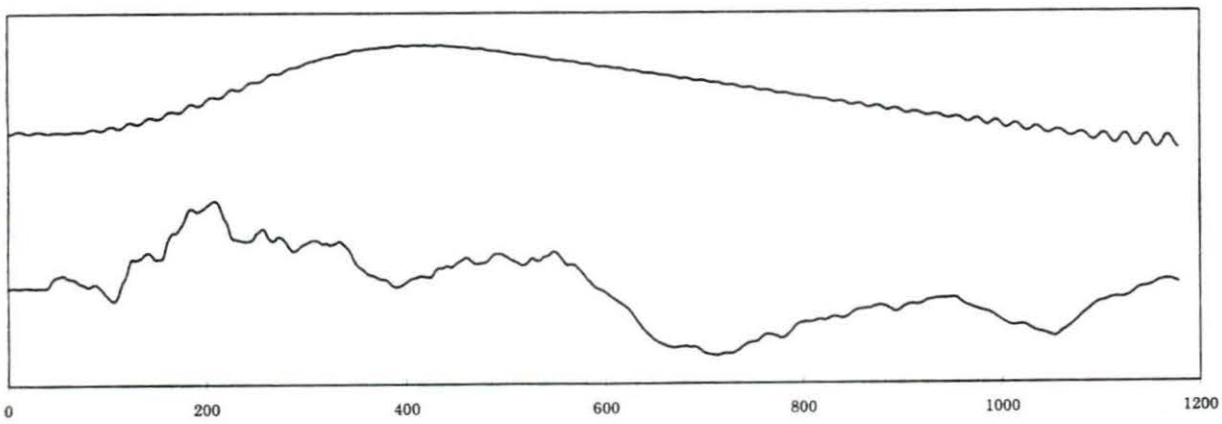

AB-5, high, deltoid, rect.

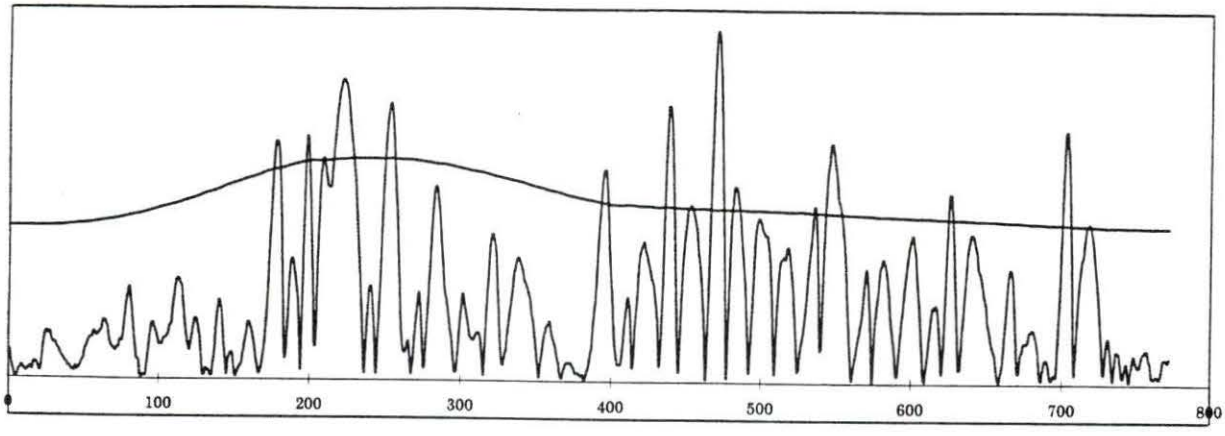

AB-5, high, deltoid, smoothed

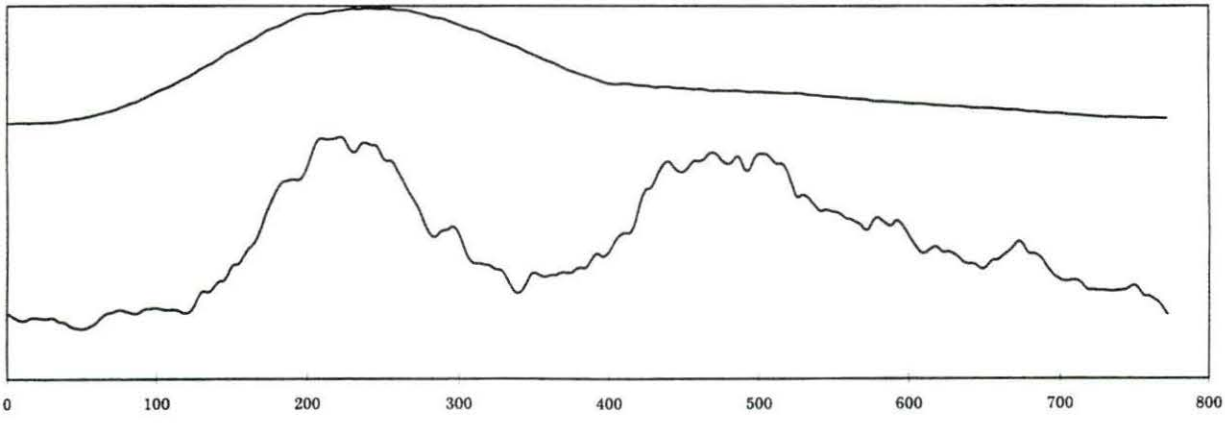

AB-5, high, tricep, rect.

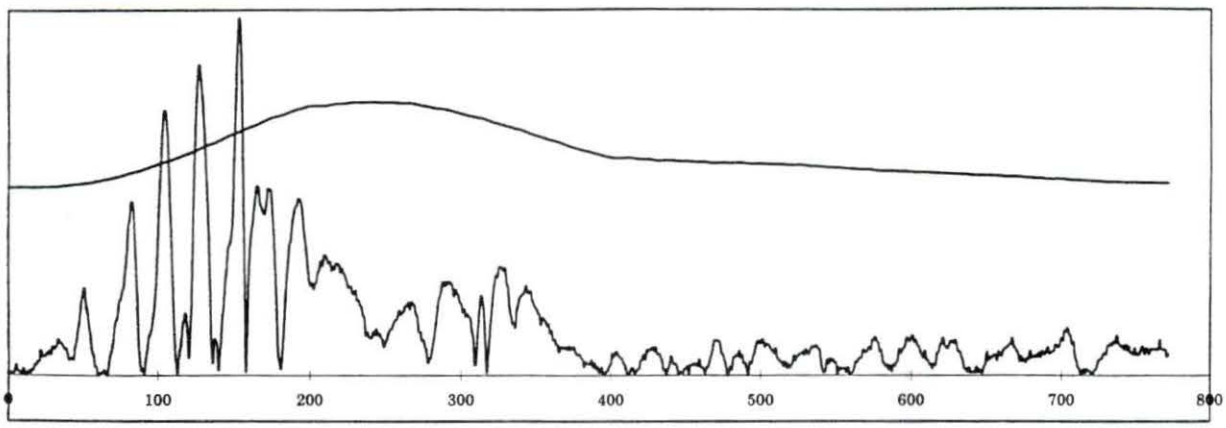

AB-5, high, tricep, smoothed

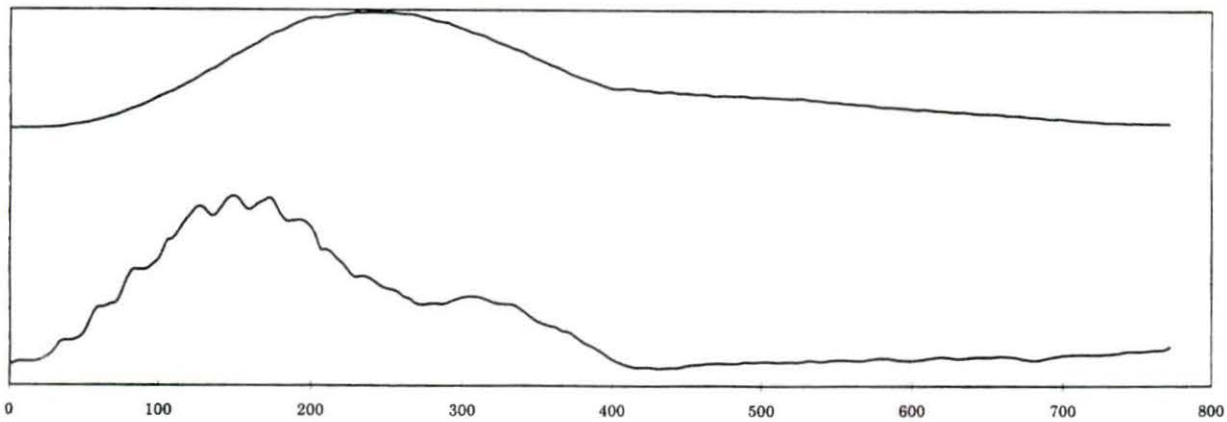

WD-1, low, deltoid, rect.

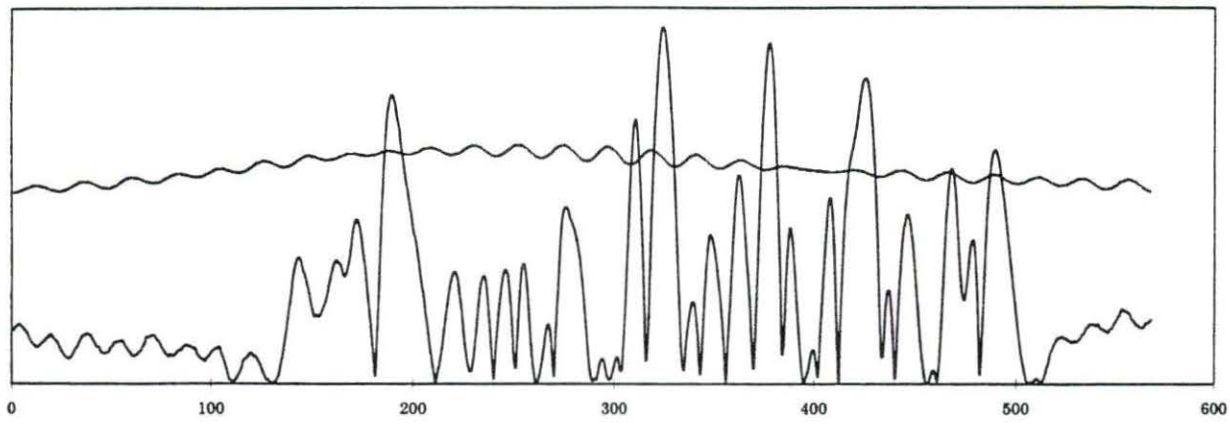

WD-1, low, deltoid, smoothed

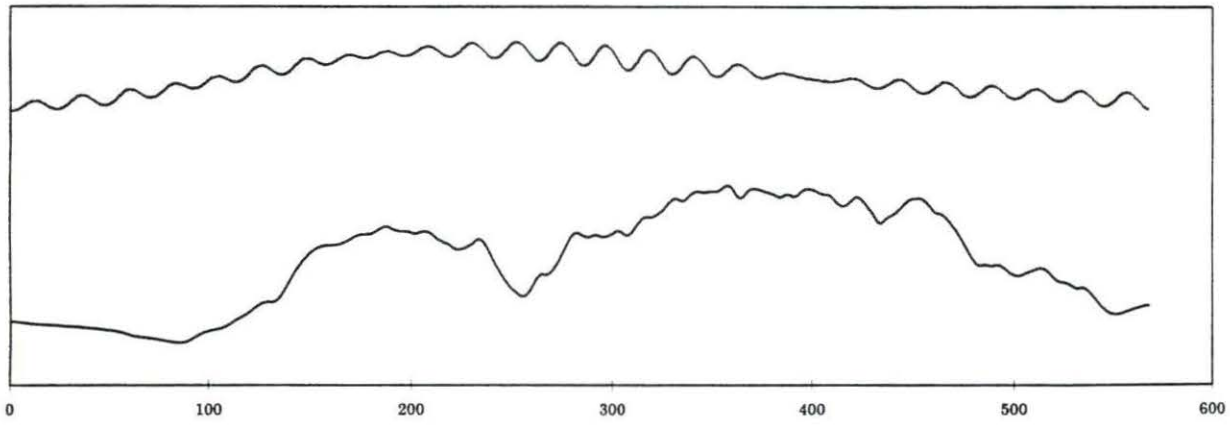

WD-1, low, tricep, rect.

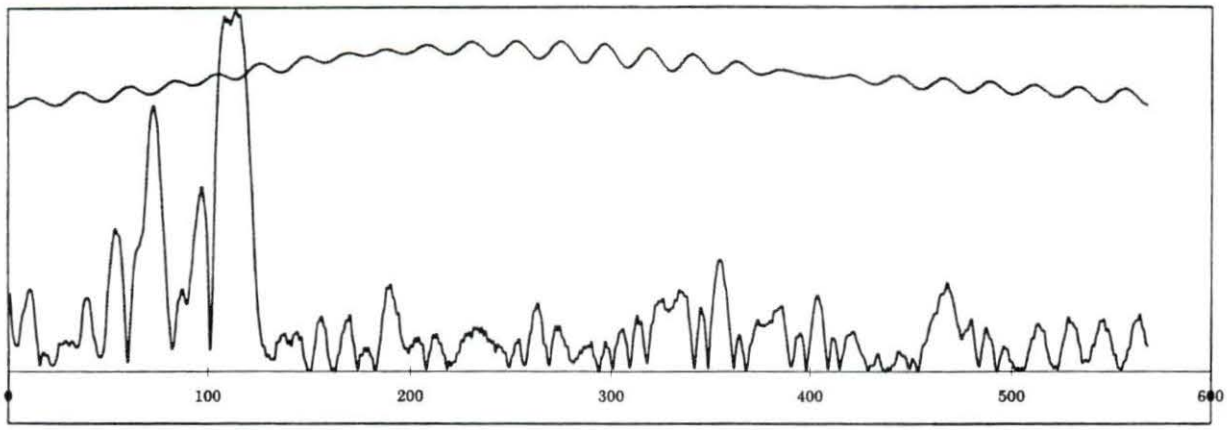

WD-1, low, tricep, smoothed

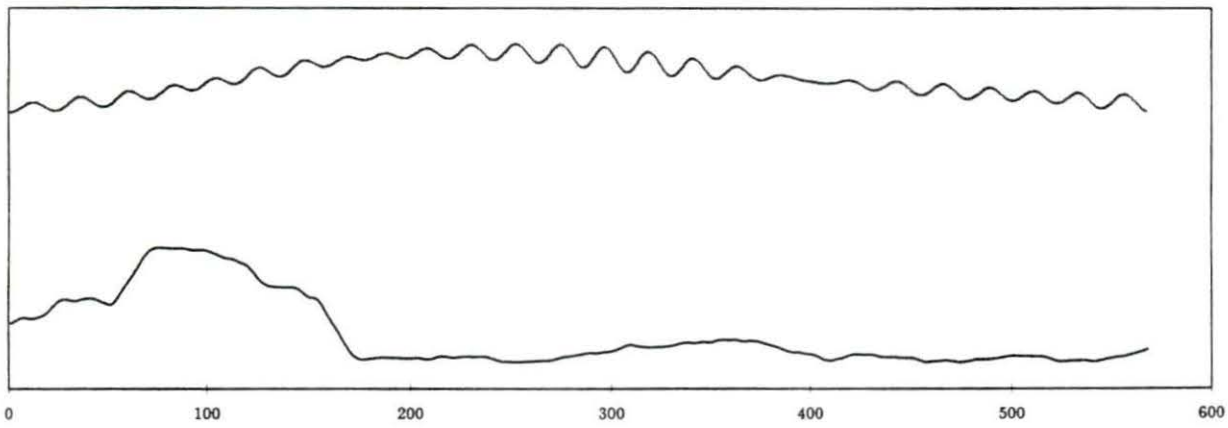

WD-1, medium, deltoid, rect.

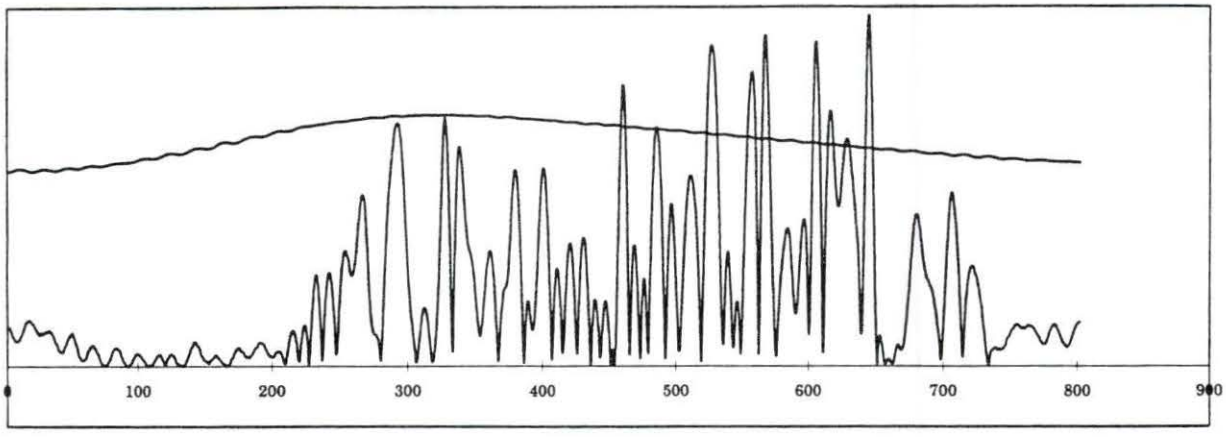

WD-1, medium, deltoid, smoothed

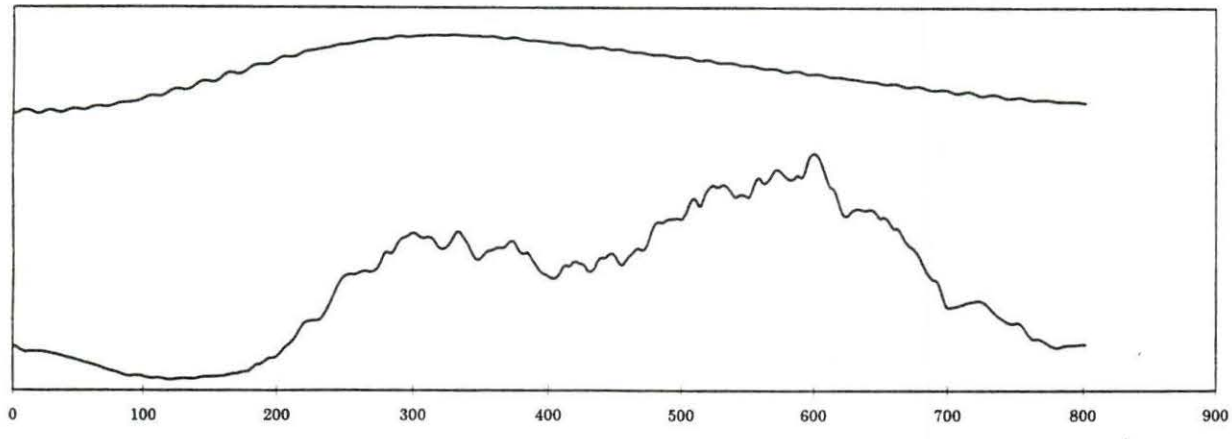

WD-1, medium, tricep, rect.

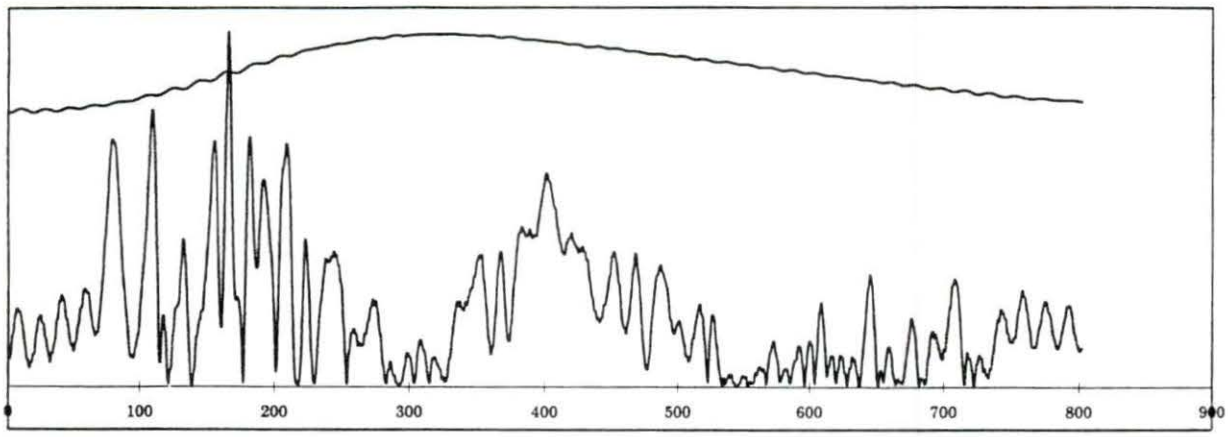

WD-1, medium, tricep, smoothed

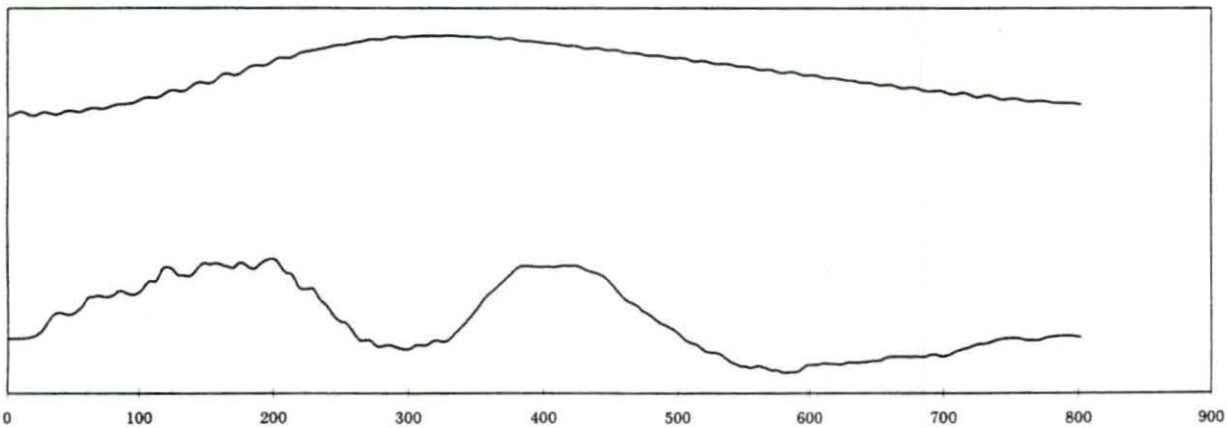

WD-1, high, deltoid, rect.

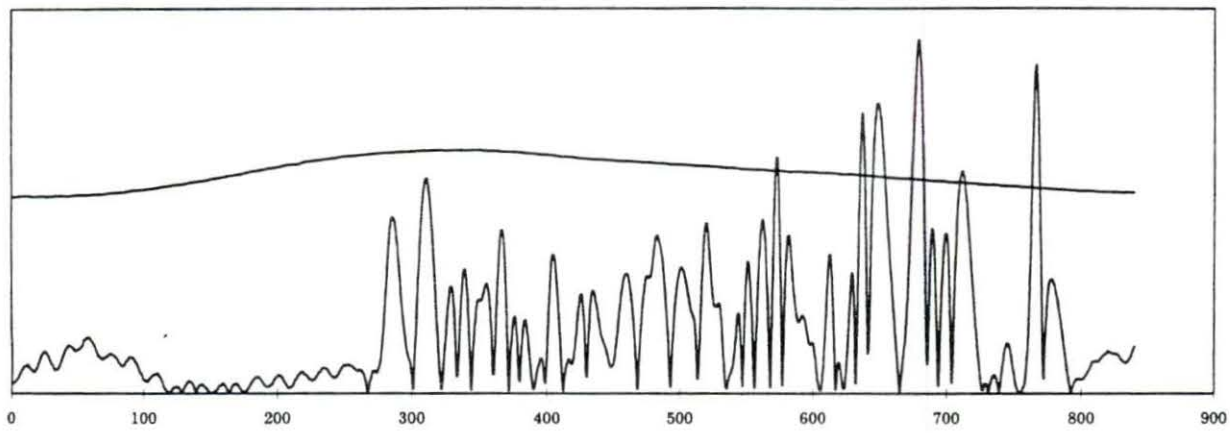

WD-1, high, deltoid, smoothed

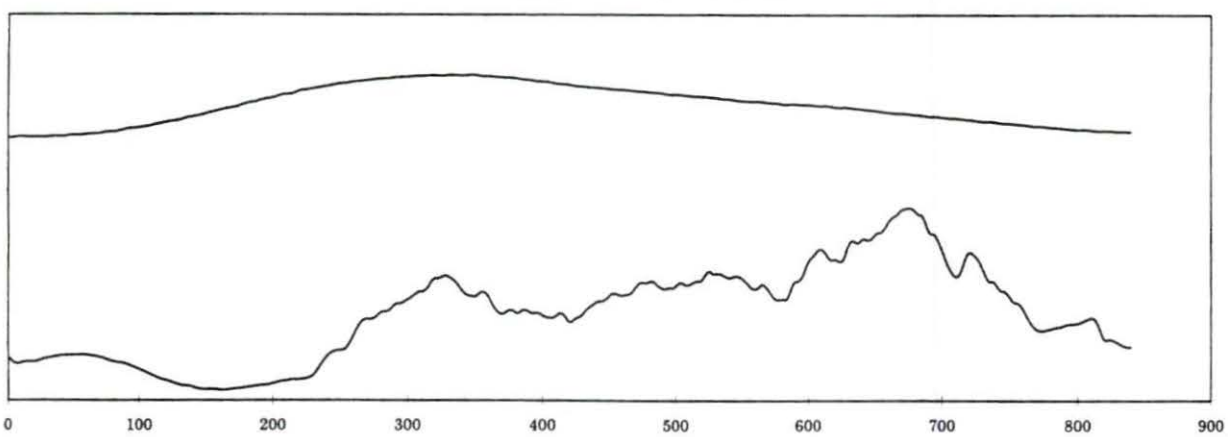

WD-1, high, tricep, rect.

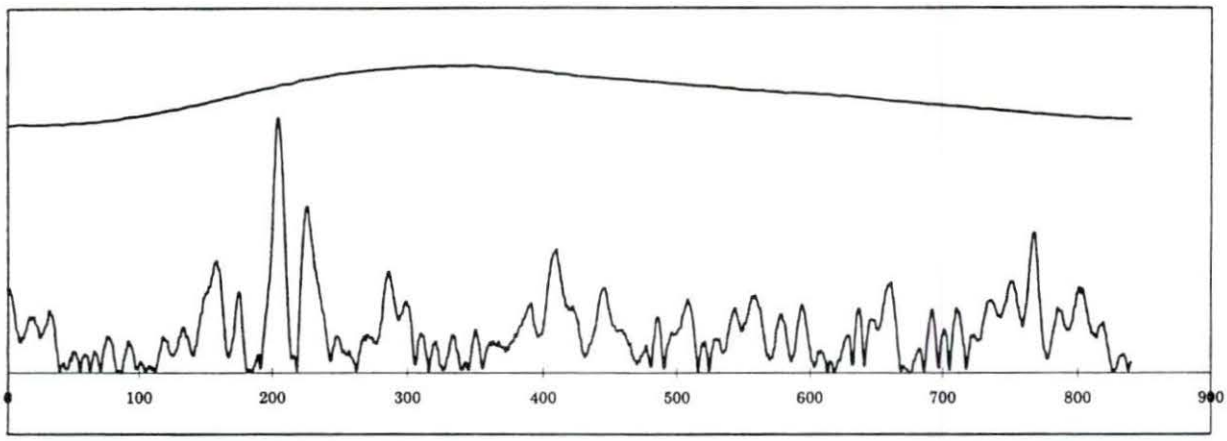

WD-1, high, tricep, smoothed

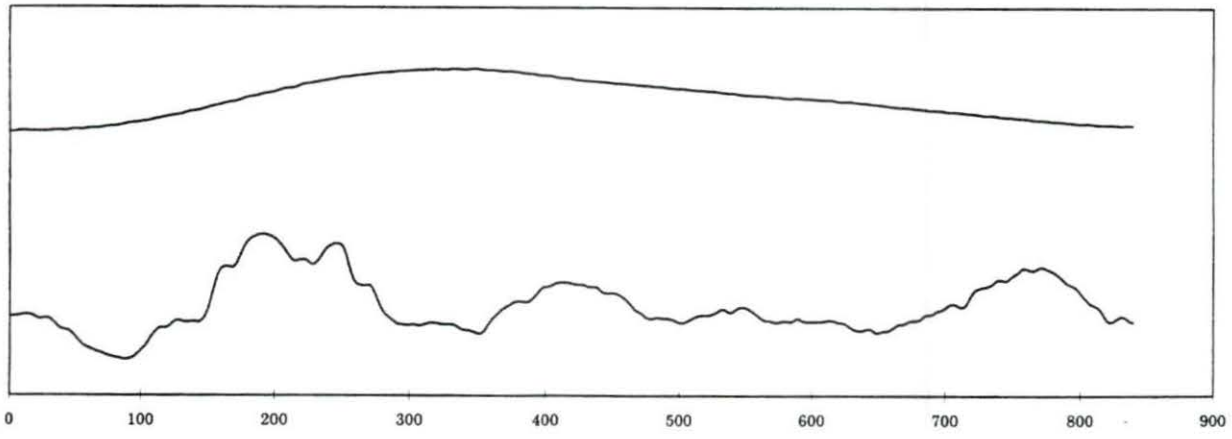

WD-2, low, deltoid, rect.

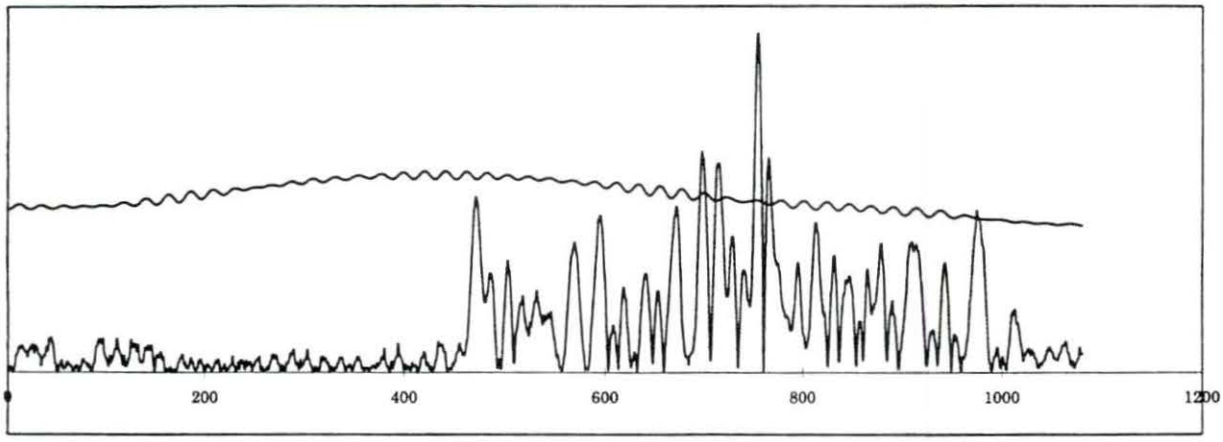

WD-2, low, deltoid, smoothed

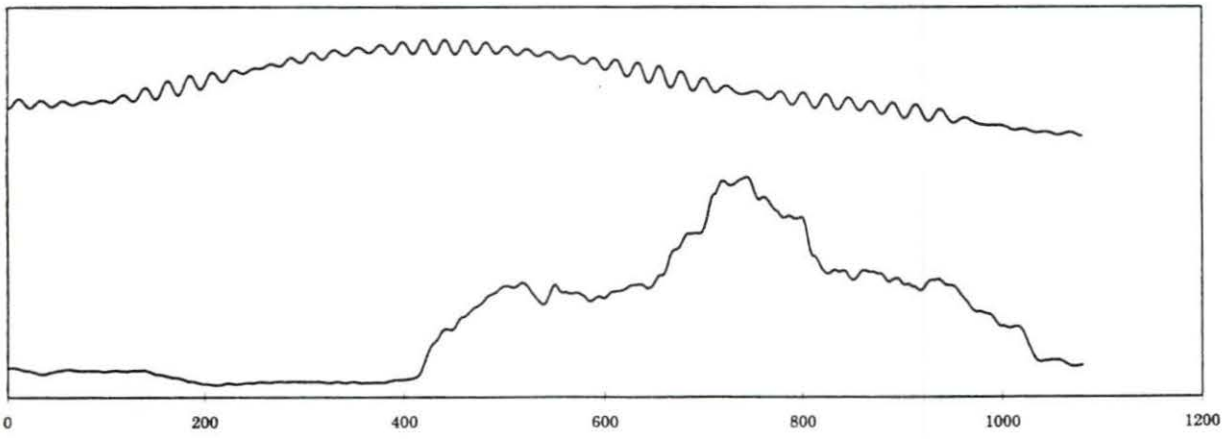

WD-2, low, tricep, rect.

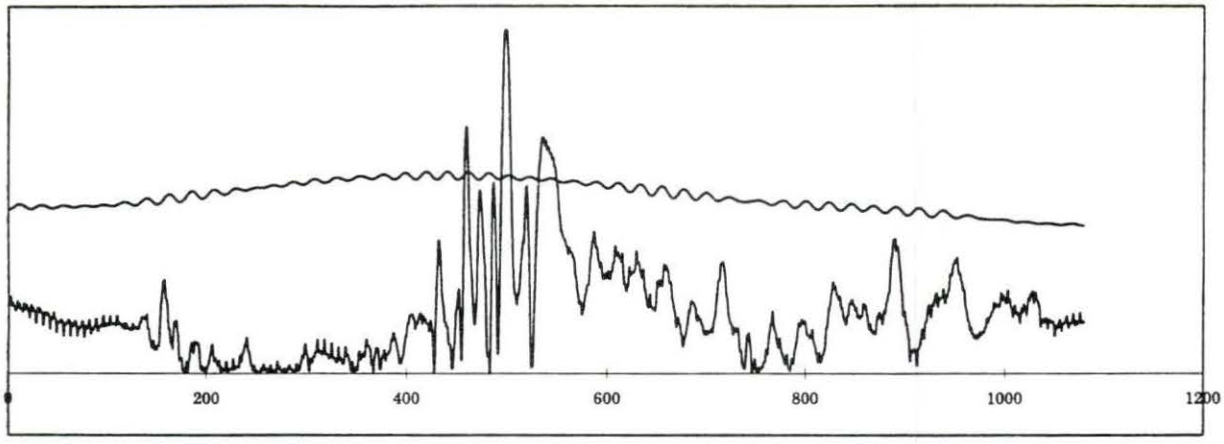

WD-2, low, tricep, smoothed

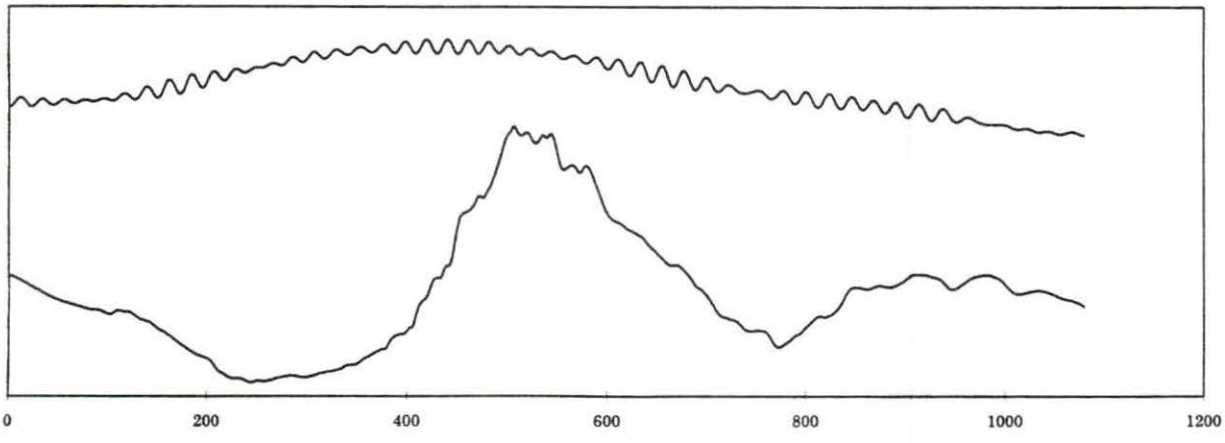

WD-2, medium, deltoid, rect.

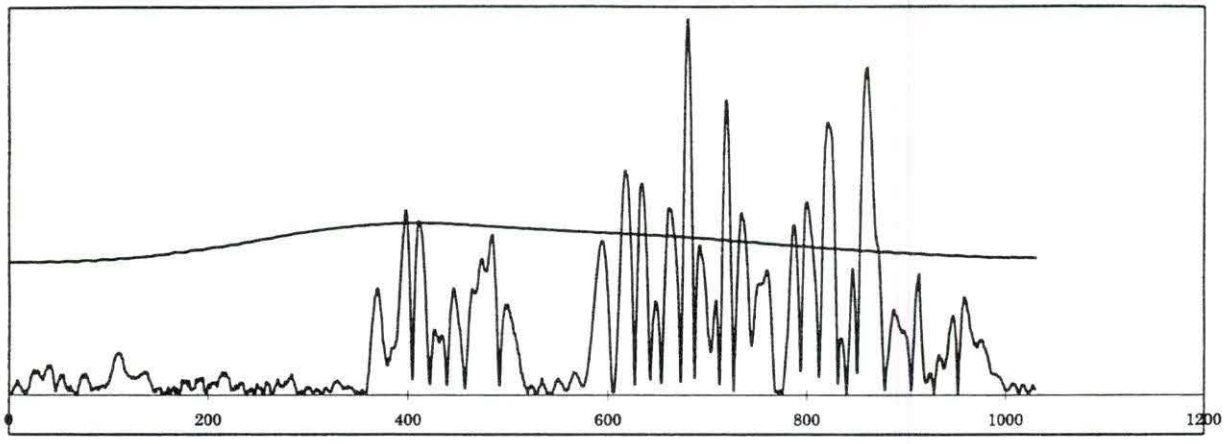

WD-2, medium, deltoid, smoothed

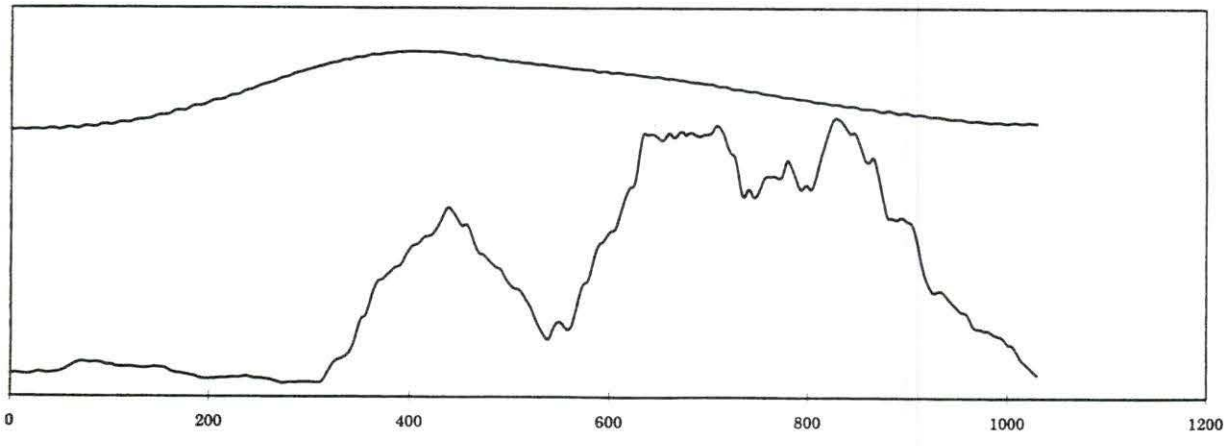

WD-2, medium, tricep, rect.

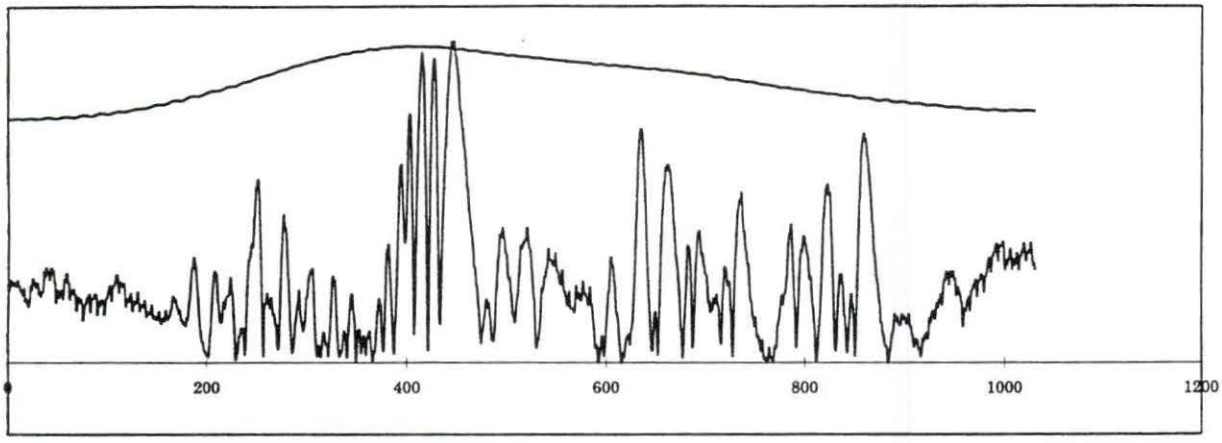

WD-2, medium, tricep, smoothed

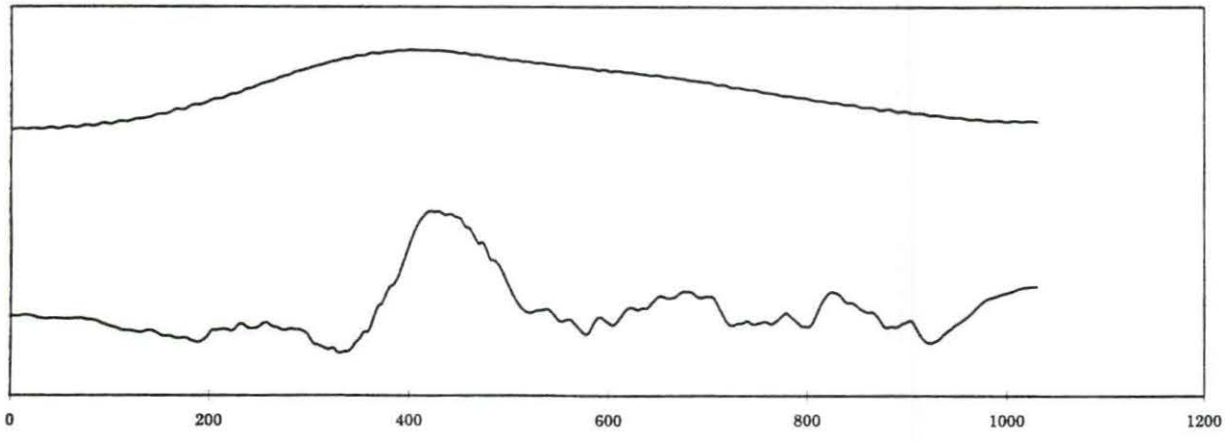

WD-2, high, deltoid, rect.

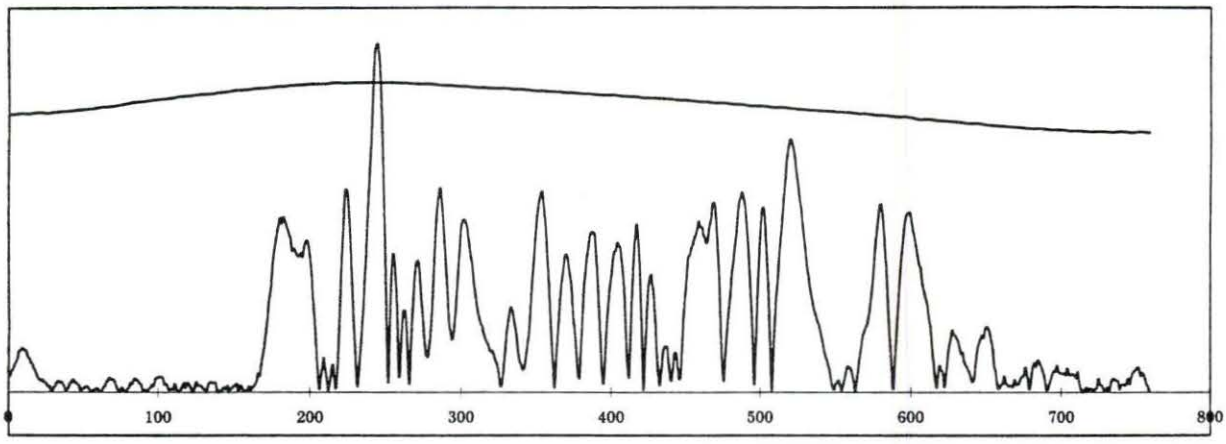

WD-2, high, deltoid, smoothed

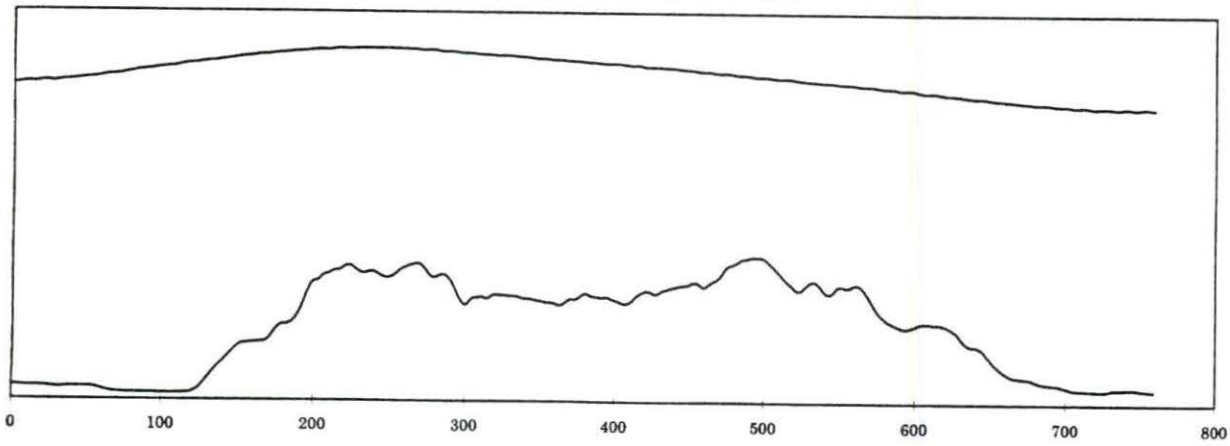

WD-2, high, tricep, rect.

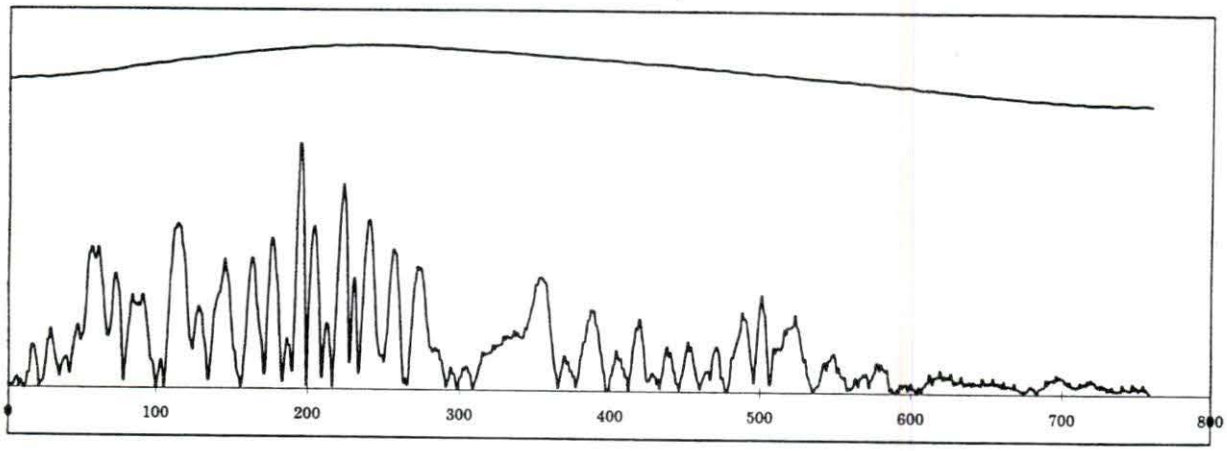

WD-2, high, tricep, smoothed

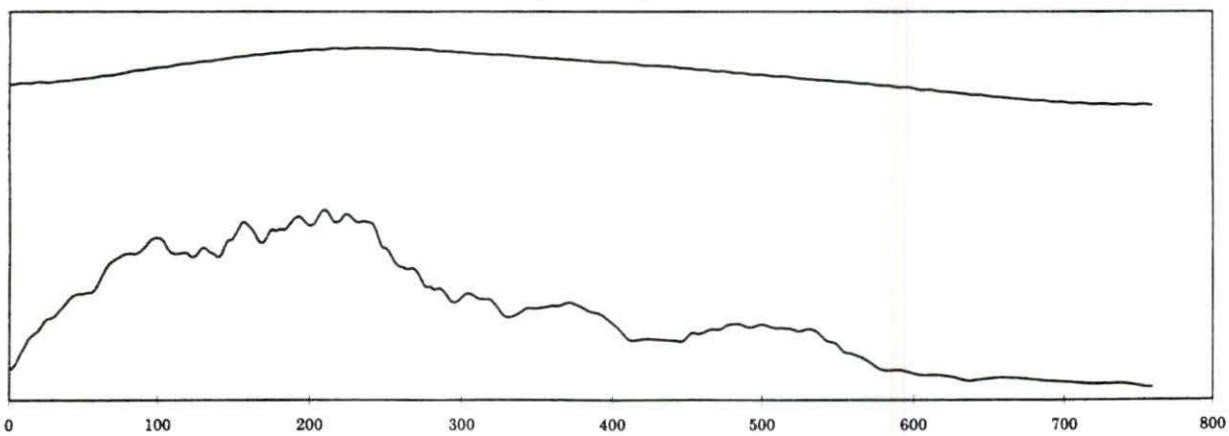

WD-3, low, deltoid, rect.

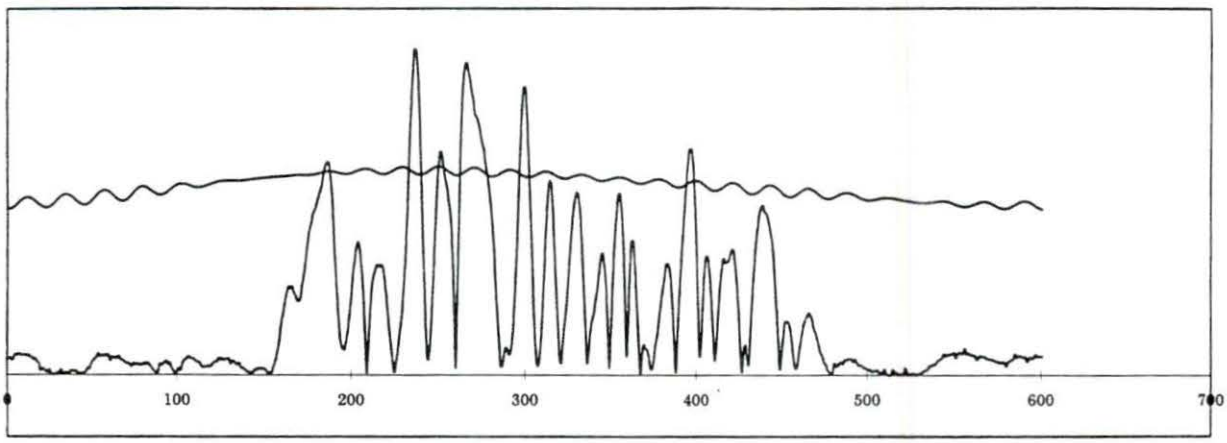

WD-3, low, deltoid, smoothed

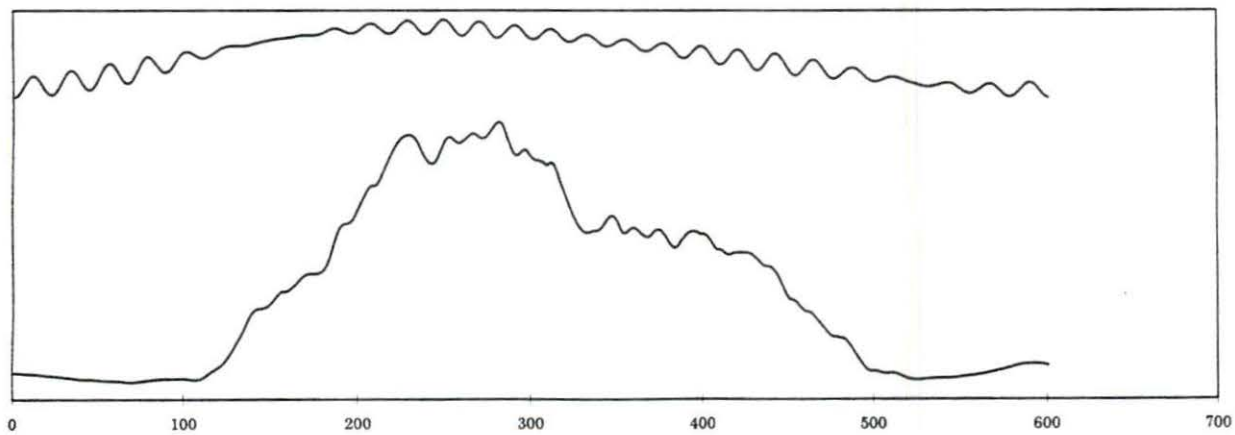

WD-3, low, tricep, rect.

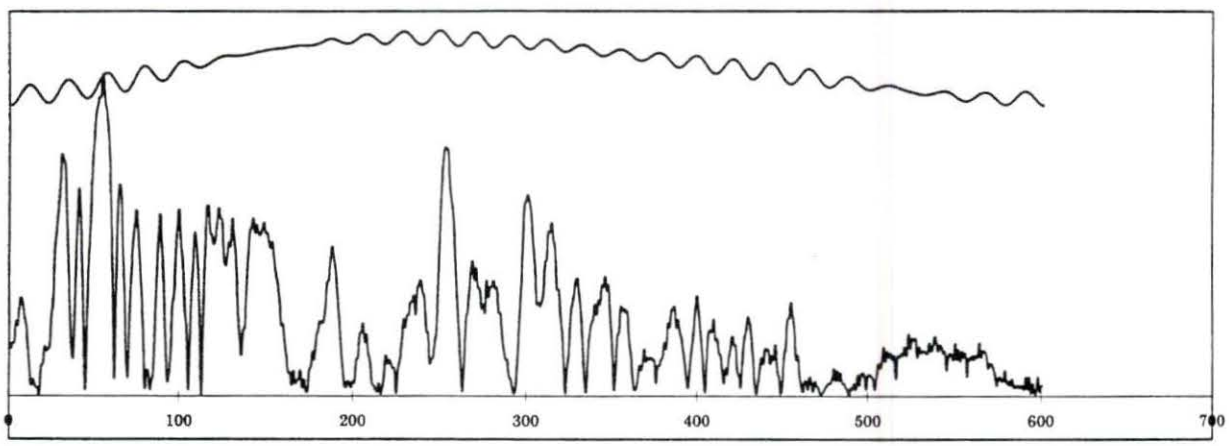

WD-3, low, tricep, smoothed

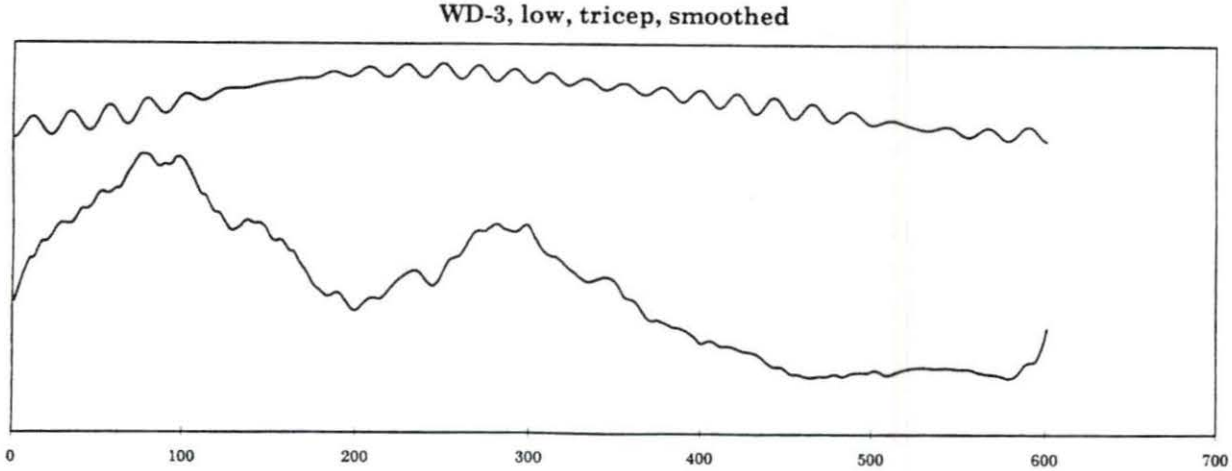

WD-3, medium, deltoid, rect.

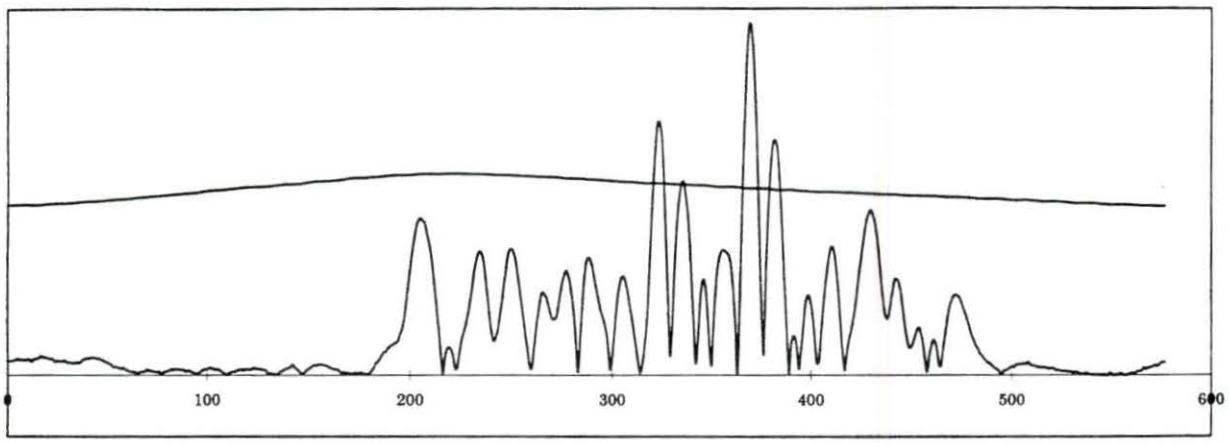

WD-3, medium, deltoid, smoothed

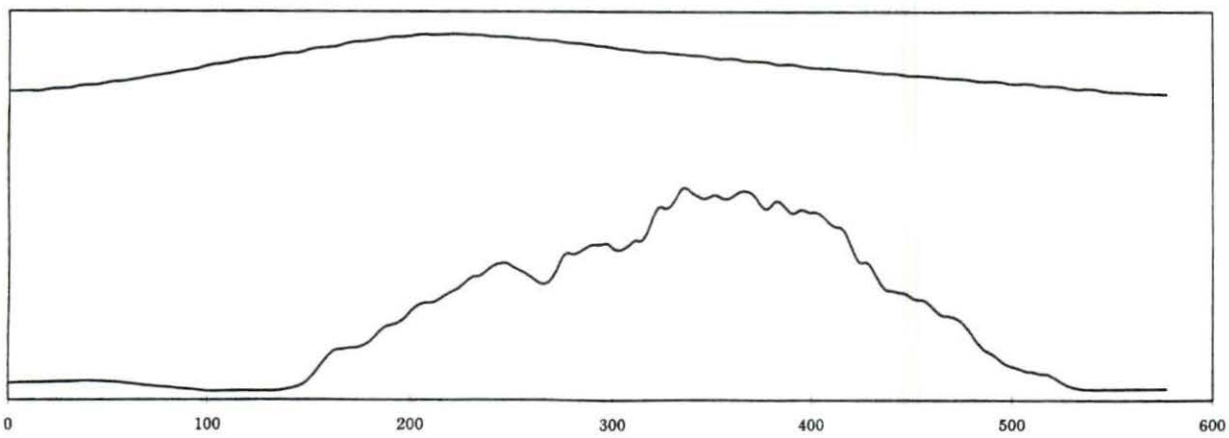

WD-3, medium, tricep, rect.

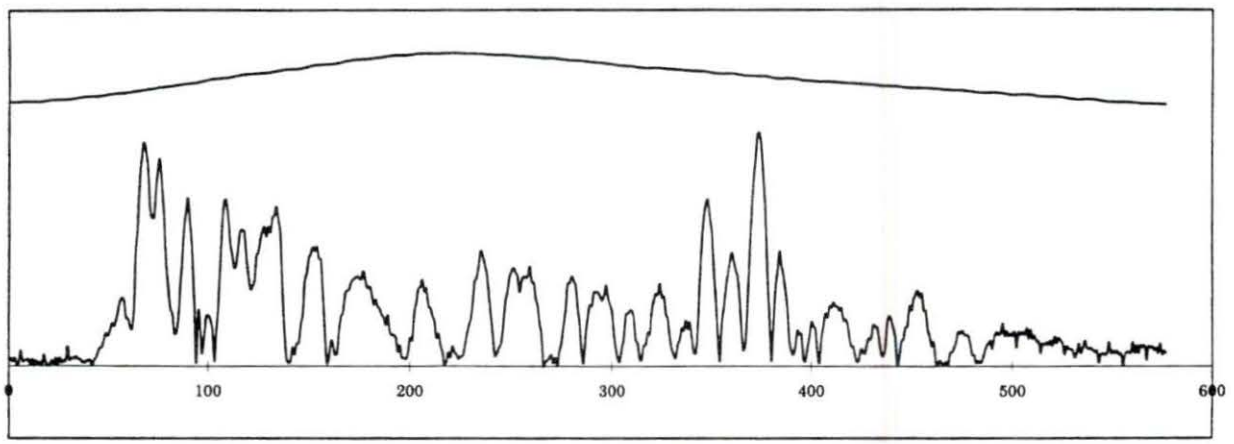

WD-3, medium, tricep, smoothed

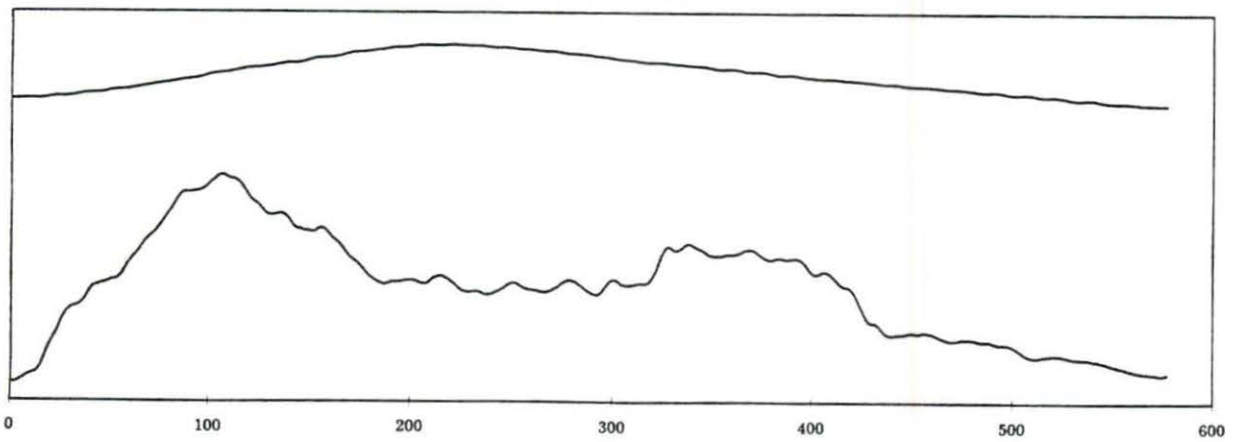

WD-3, high, deltoid, rect.

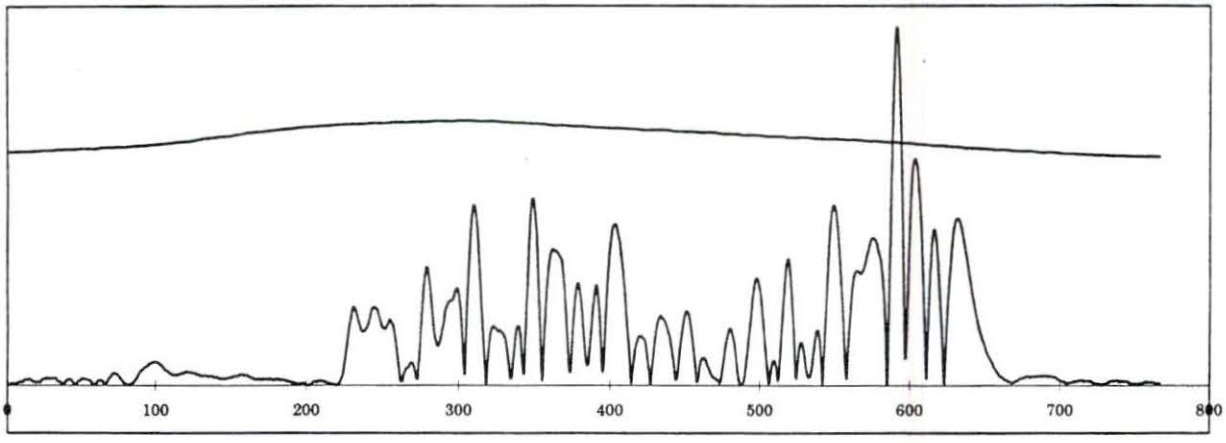

WD-3, high, deltoid, smoothed

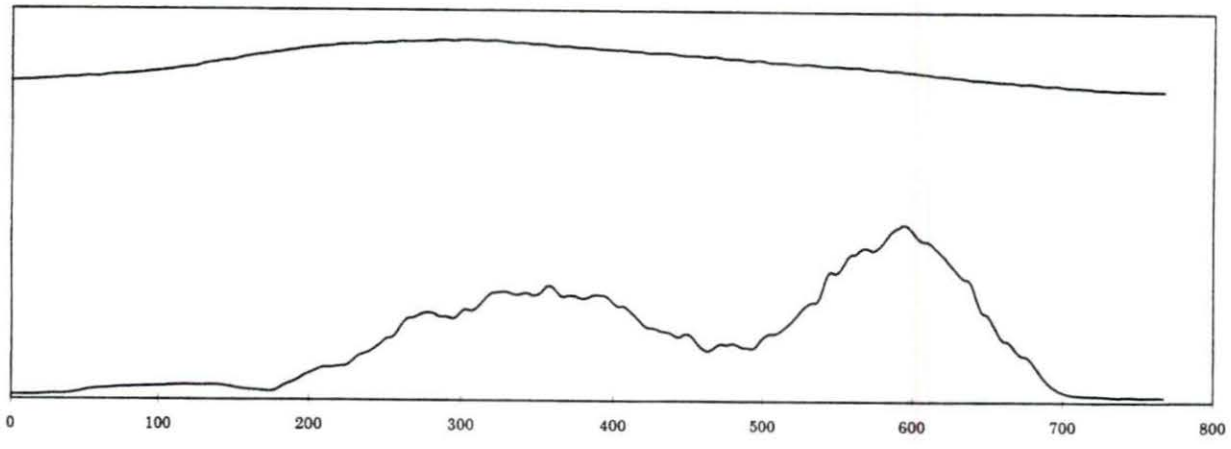

WD-3, high, tricep, rect.

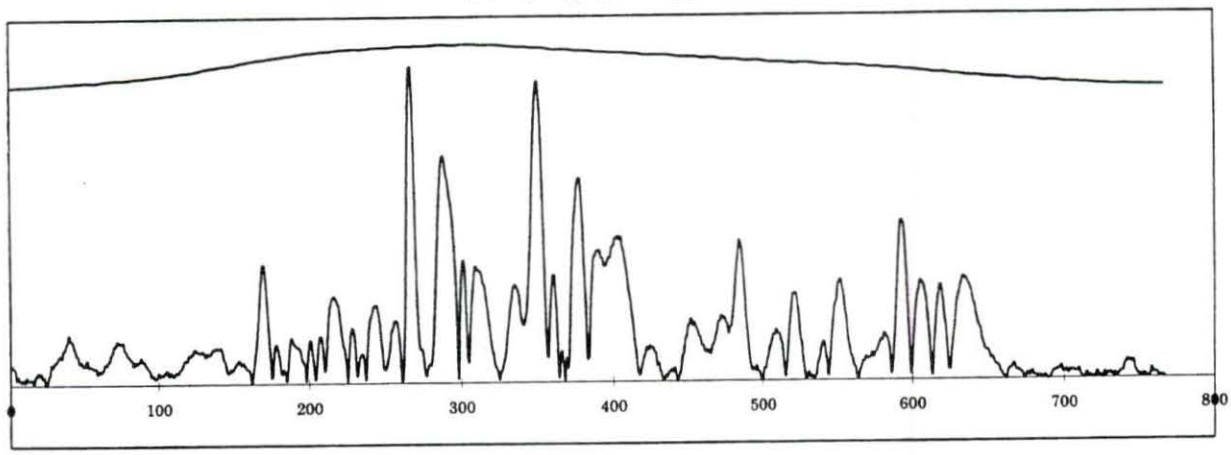

WD-3, high, tricep, smoothed

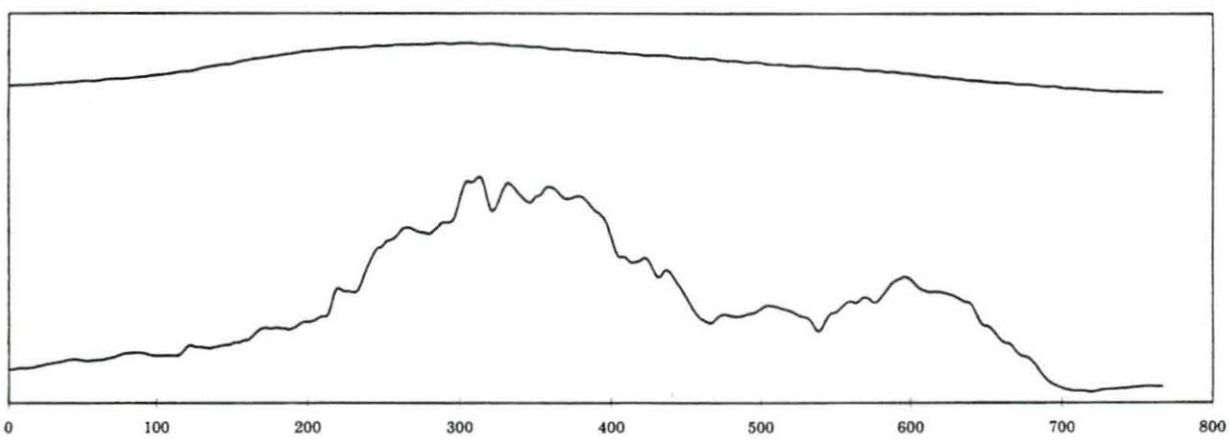

WD-4, low, deltoid, rect.

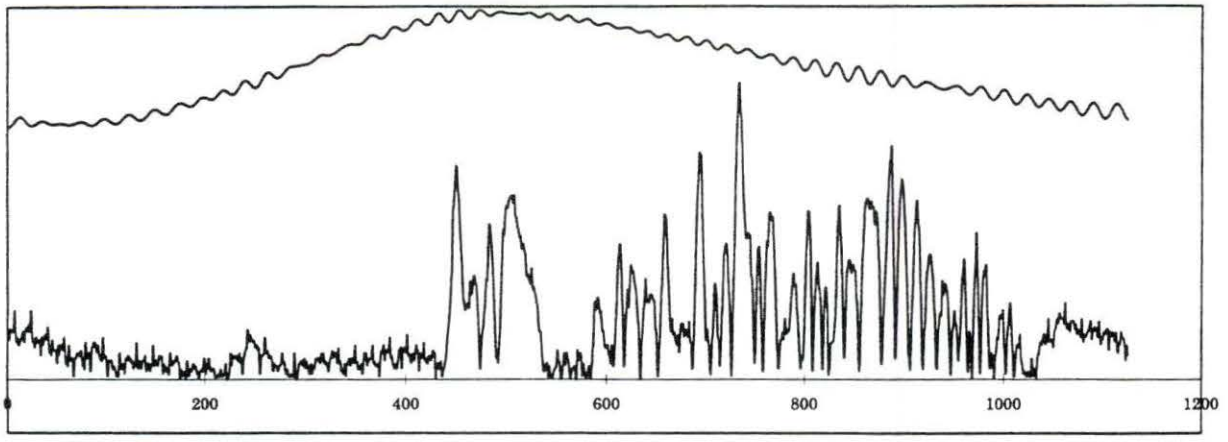

WD-4, low, deltoid, smoothed

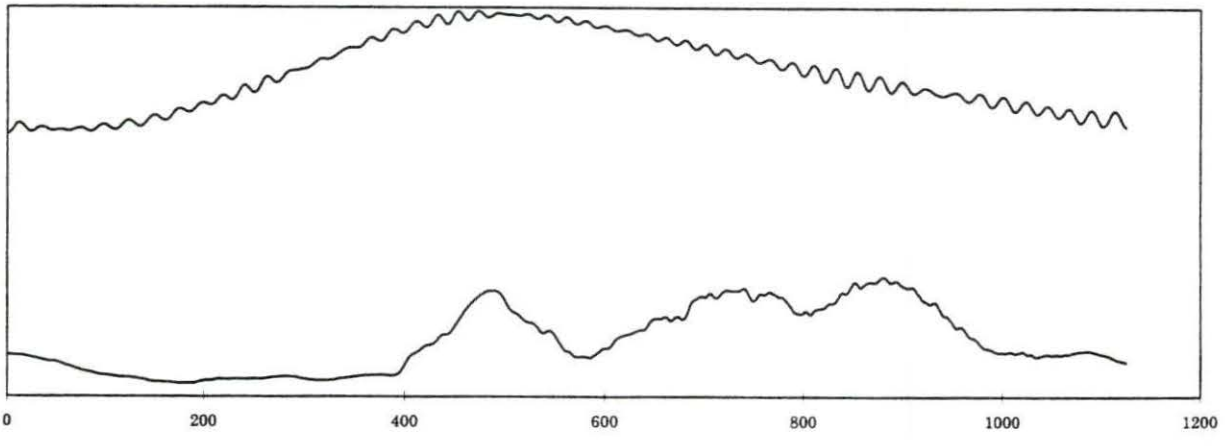

WD-4, low, tricep, rect.

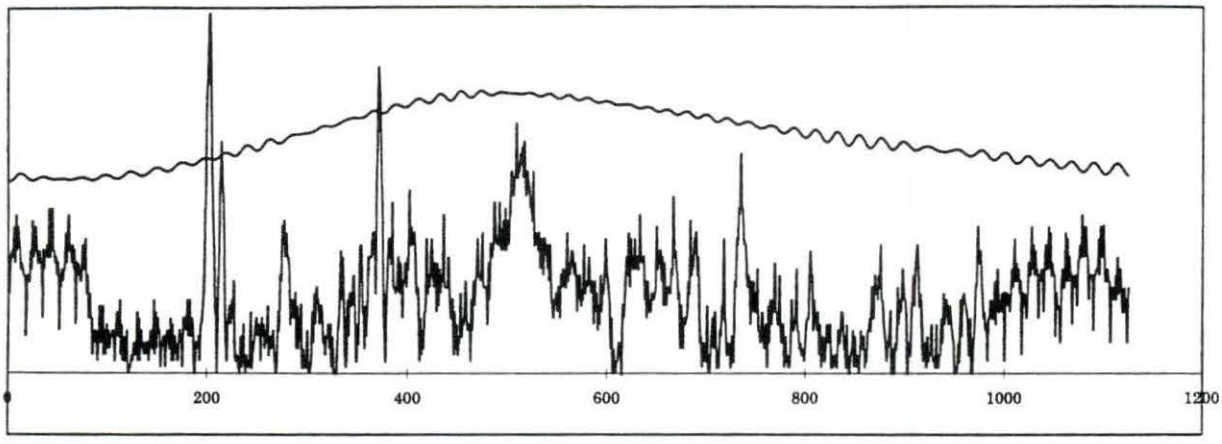

WD-4, low, tricep, smoothed

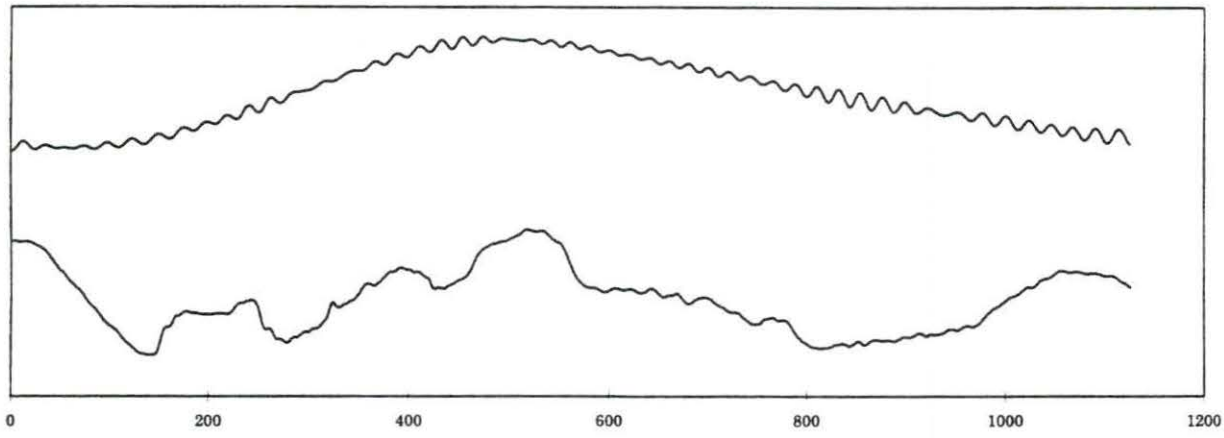

WD-4, medium, deltoid, rect.

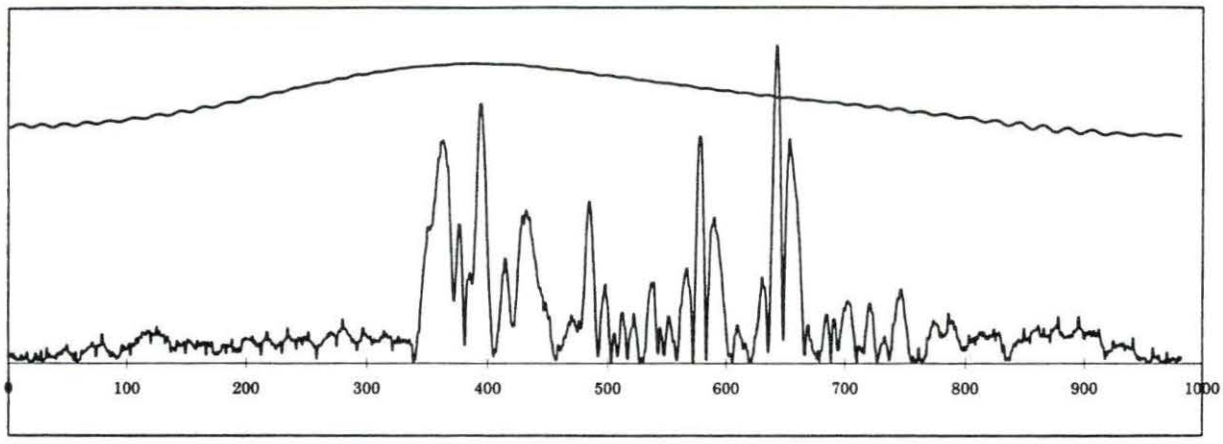

WD-4, medium, deltoid, smoothed

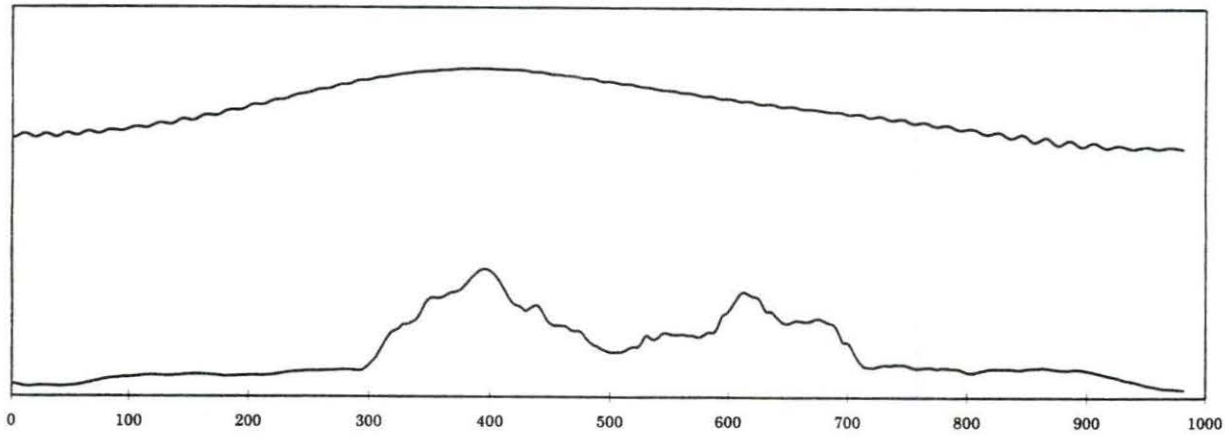

WD-4, medium, tricep, rect.

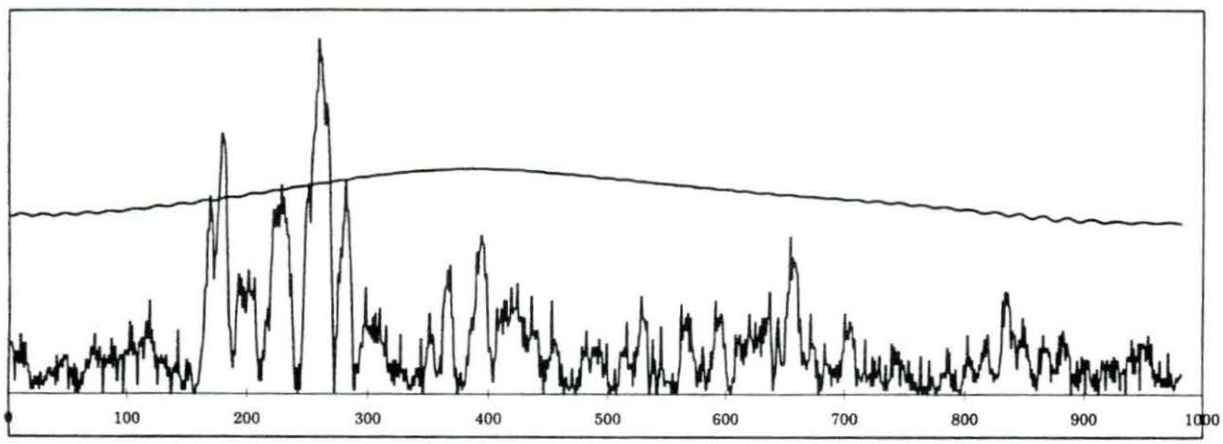

WD-4, medium, tricep, smoothed

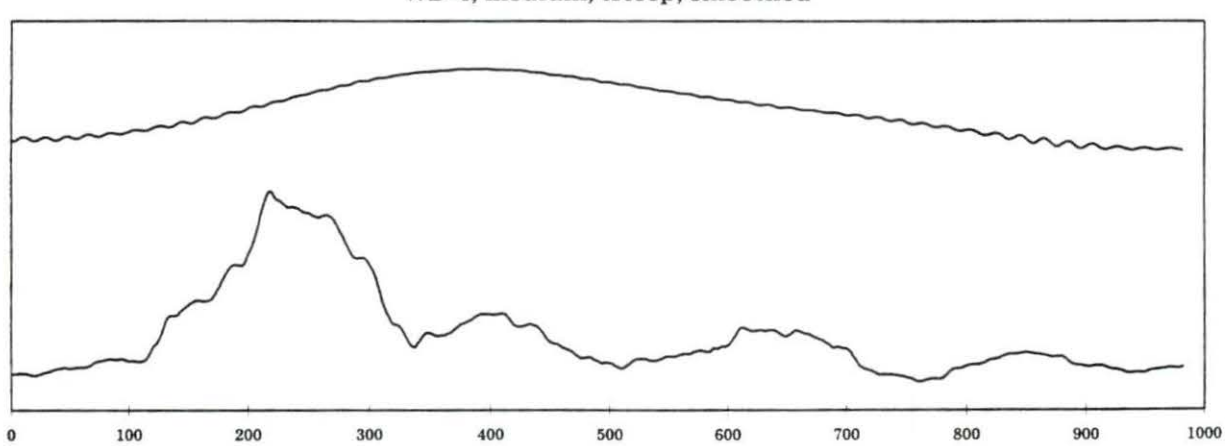

WD-4, high, deltoid, rect.

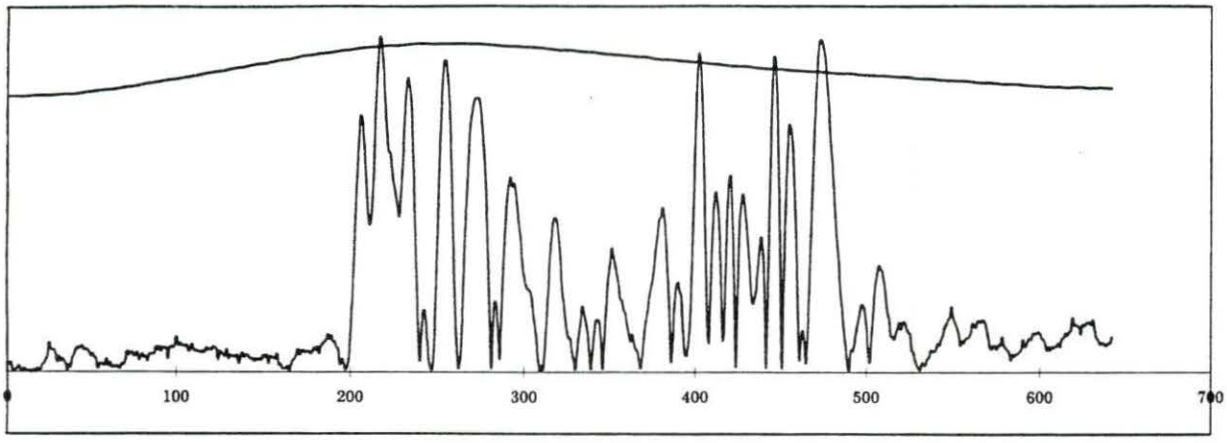

WD-4, high, deltoid, smoothed

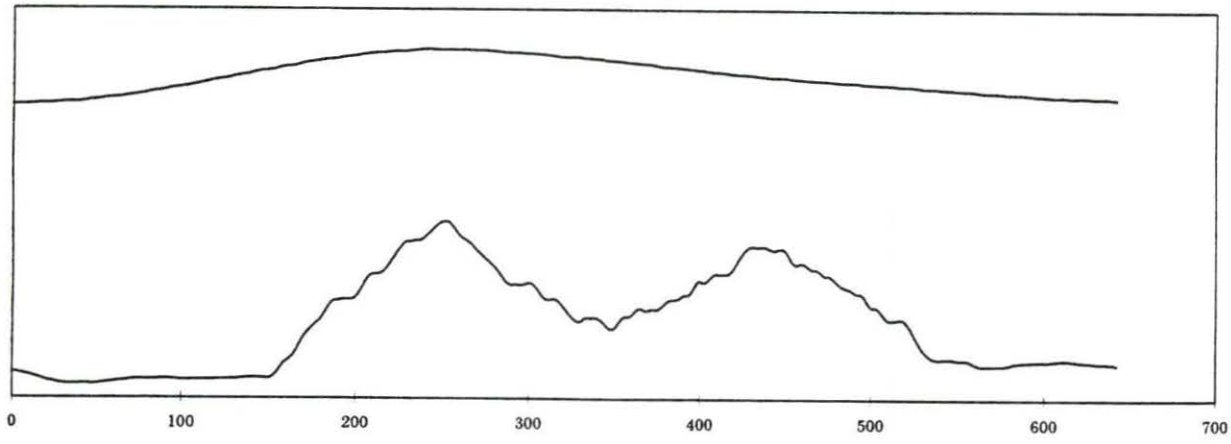

WD-4, high, tricep, rect.

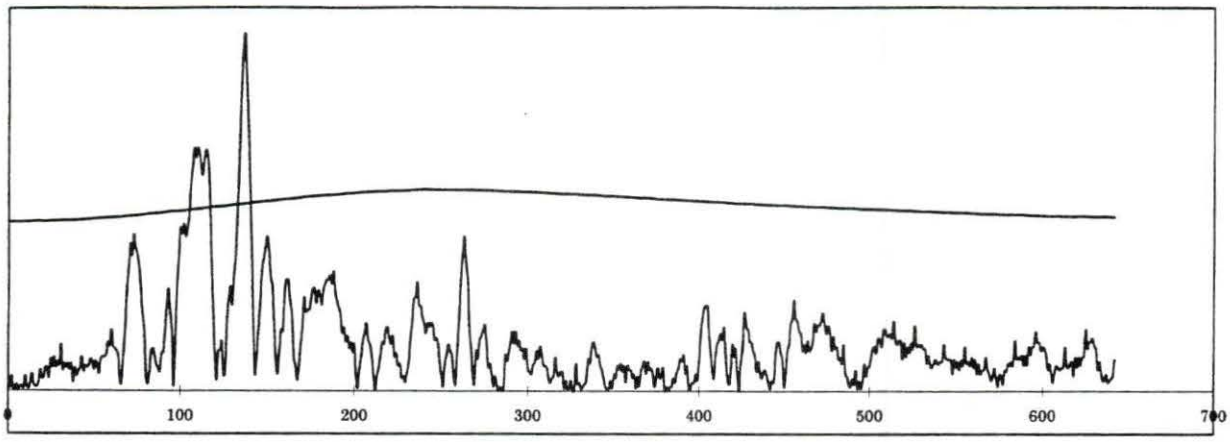

WD-4, high, tricep, smoothed

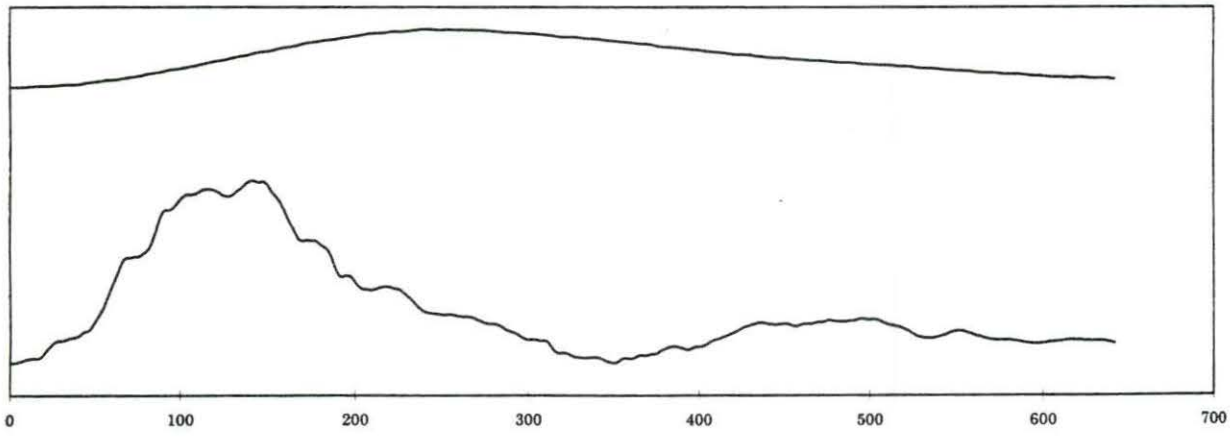

WD-5, low, deltoid, rect.

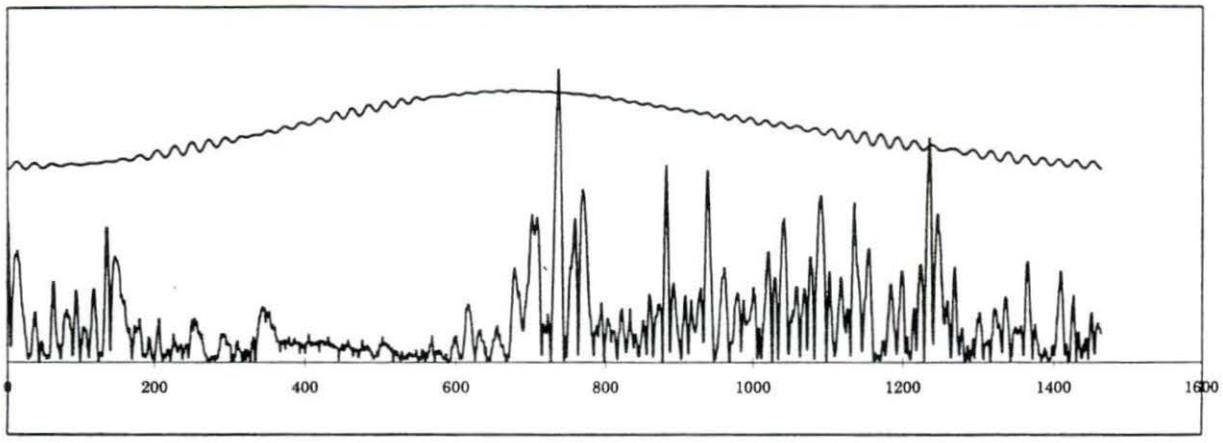

WD-5, low, deltoid, smoothed

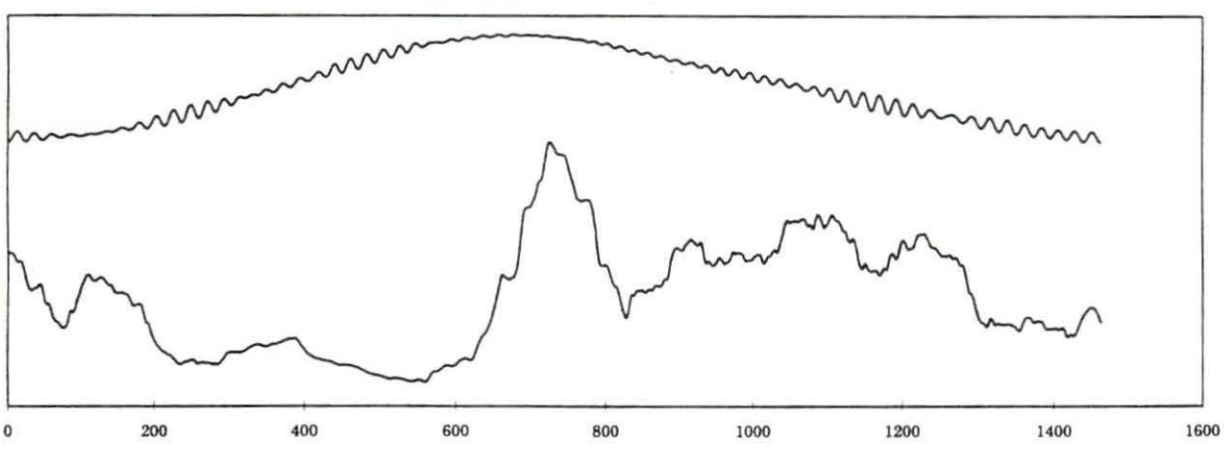

WD-5, low, tricep, rect.

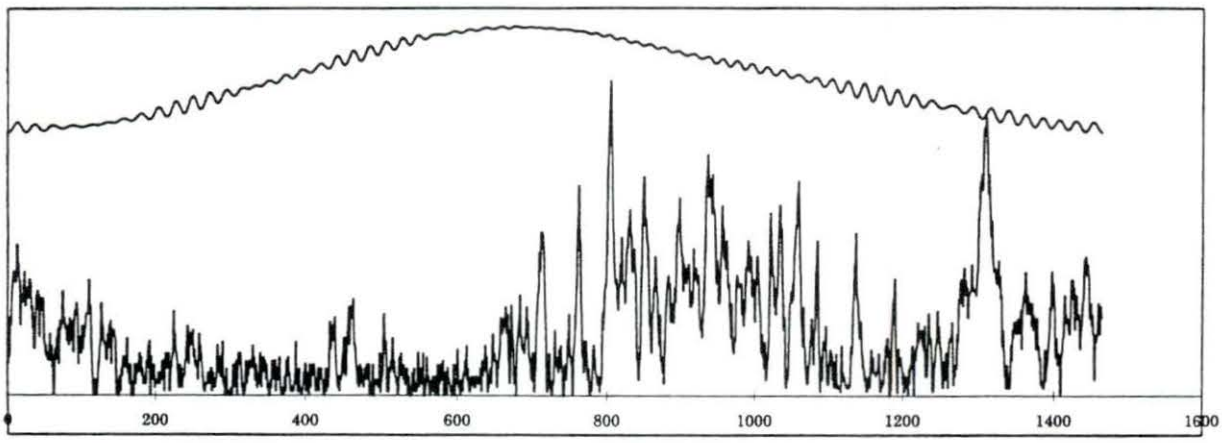

WD-5, low, tricep, smoothed

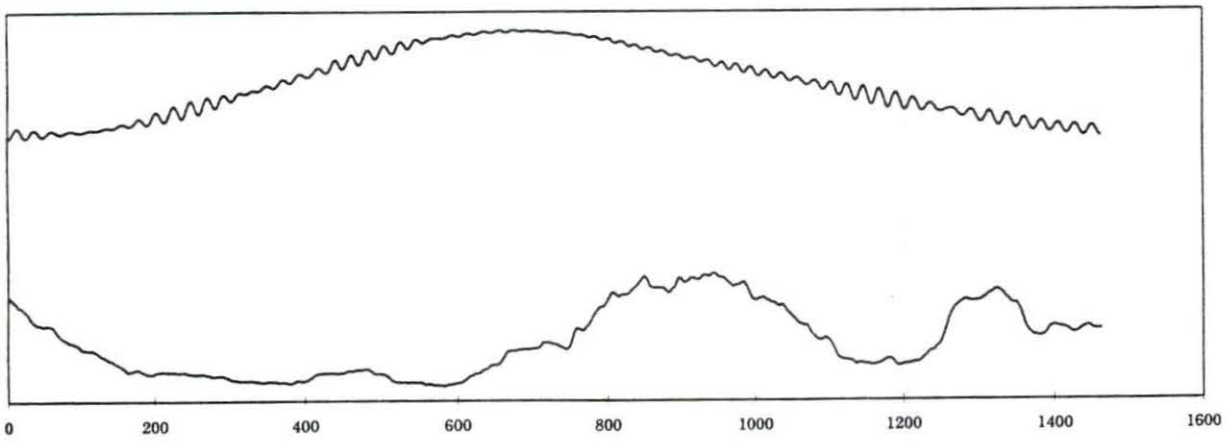

WD-5, medium, deltoid, rect.

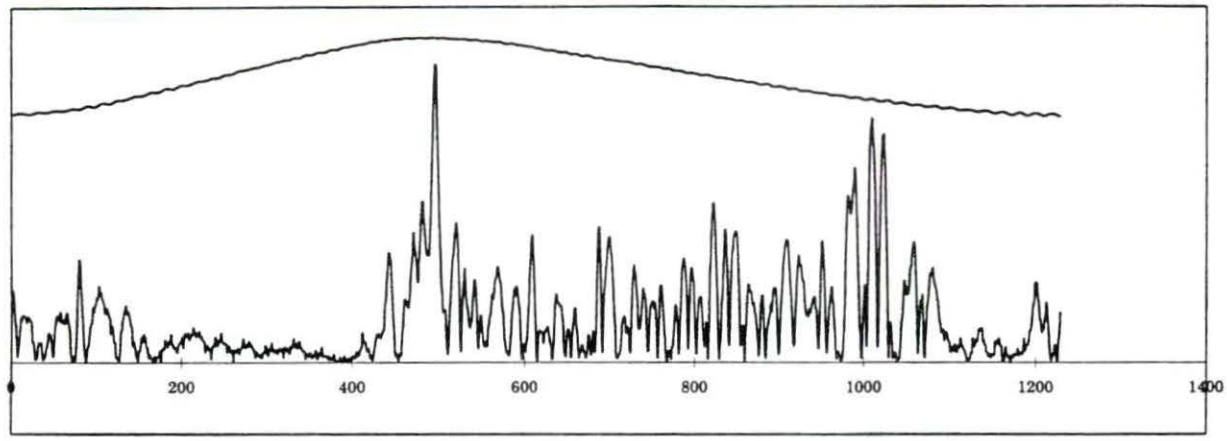

WD-5, medium, deltoid, smoothed

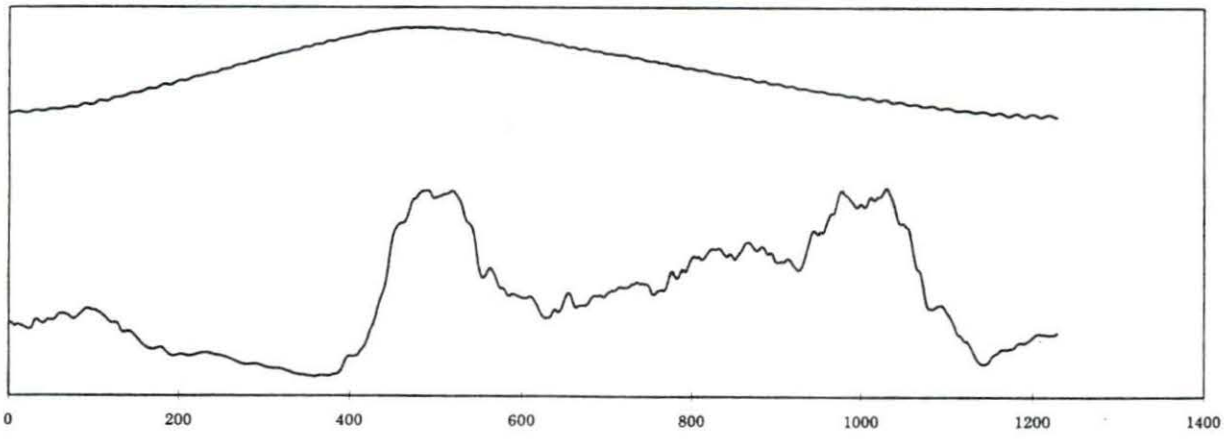

WD-5, medium, tricep, rect.

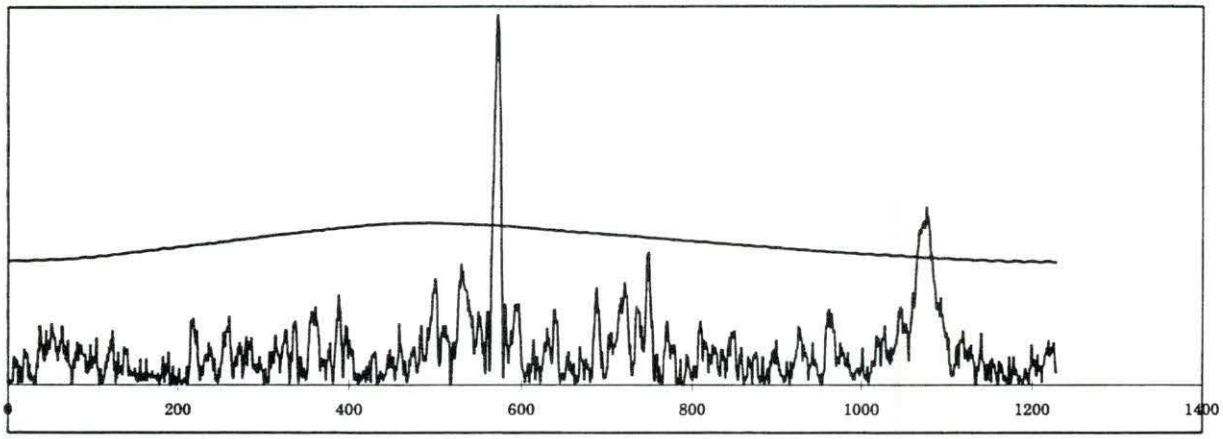

WD-5, medium, tricep, smoothed

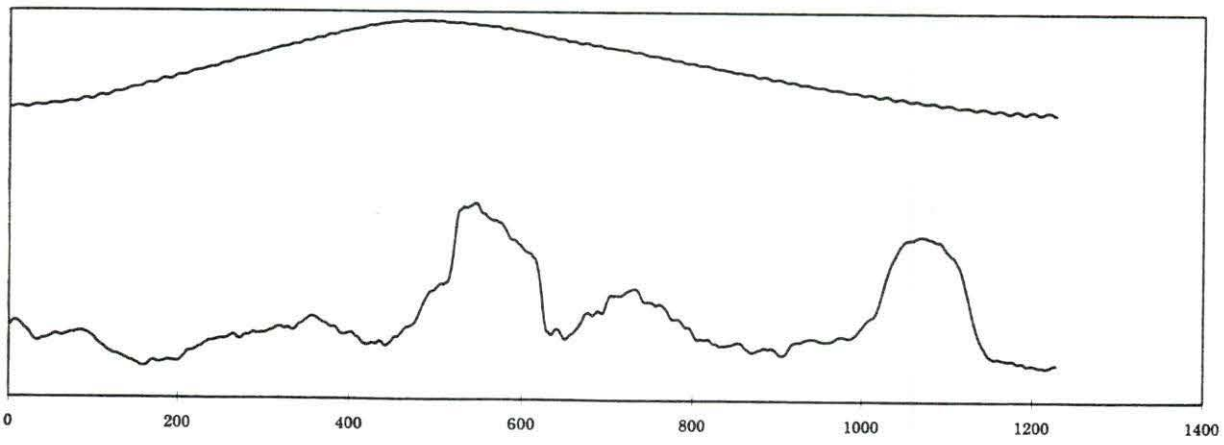

WD-5, high, deltoid, rect.

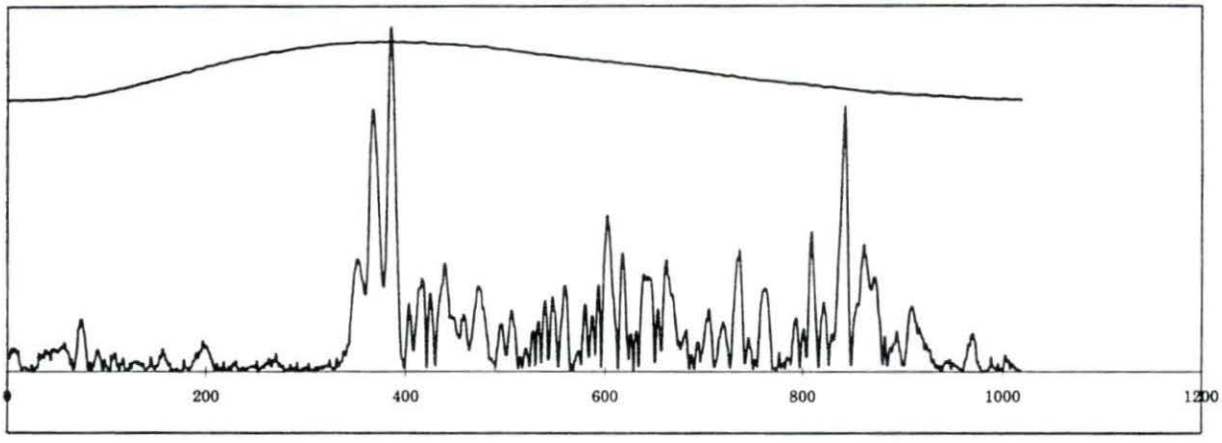

WD-5, high, deltoid, smoothed

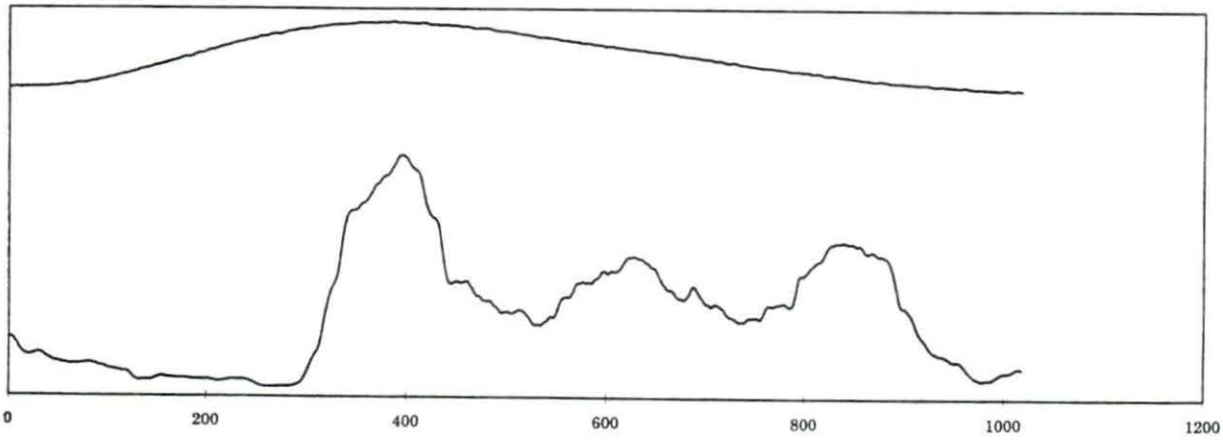

WD-5, high, tricep, rect.

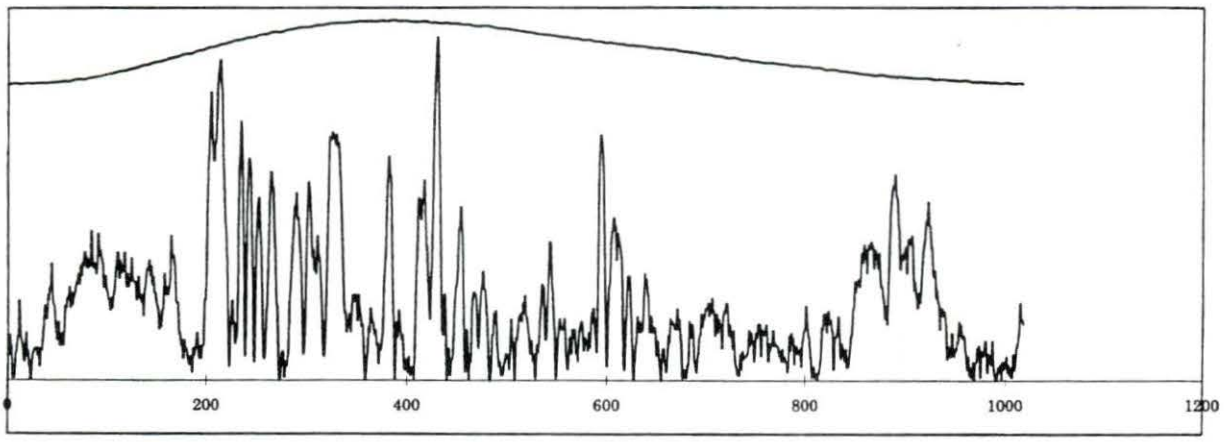

WD-5, high, tricep, smoothed

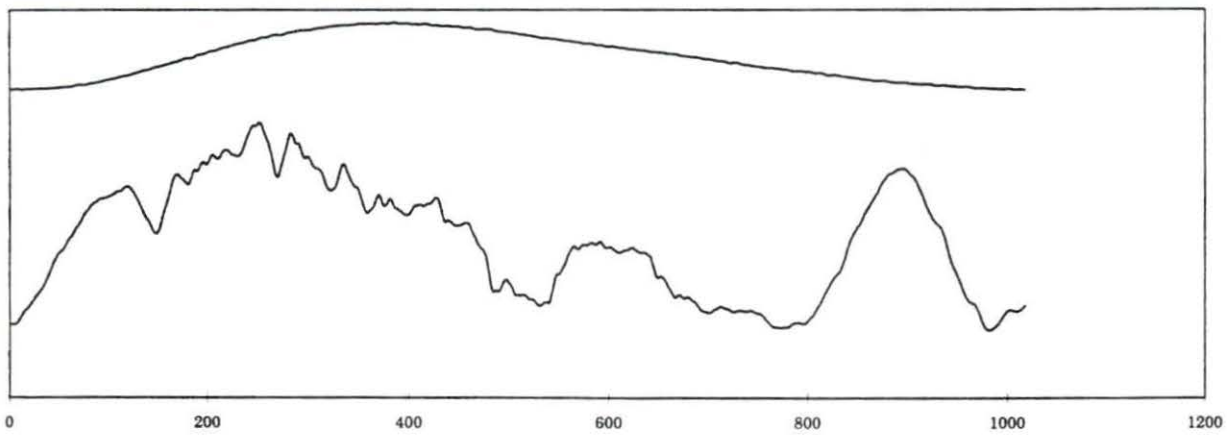

APPENDIX E:

HUMAN SUBJECT APPROVAL AND CONSENT FORM

Information for Review of Research Involving Human Subjects

Iowa State University

(Please type and use the attached instructions for completing this form)

1. Title of Project: A study comparing propulsion efficiency, electromyographic activity, and kinematic trends between able-bodied and wheelchair dependent individuals ~~while propelling a manually powered wheelchair on a wheelchair dynamometer~~

2. I agree to provide the proper surveillance of this project to insure that the rights and welfare of the human subjects are protected. I will report any adverse reactions to the committee. Additions to or changes in research procedures after the project has been approved will be submitted to the committee for review. I agree to request renewal of approval for any project continuing more than one year.

Typed Name of Principal Investigator	Date	Signature of Principal Investigator
Scott A. Draper	9/26/94	Scott A. Draper

Department	Campus Address	Campus Telephone
Biomedical Engineering	1174 Vet Med	294-6520

3. Signatures of other investigators

	Date	Relationship to Principal Investigator
P E Patterson	9/27/94	Major Professor

RECEIVED SEP 28 '94 ISU GRADUATE COLLEGE

4. Principal Investigator(s) (check all that apply)
☐ Faculty ☐ Staff ☒ Graduate Student ☐ Undergraduate Student

5. Project (check all that apply)
☐ Research ☒ Thesis or dissertation ☐ Class project ☐ Independent Study (490, 590, Honors project)

6. Number of subjects (complete all that apply)
__ # Adults, non-students __ # ISU student __ # minors under 14 __ # minors 14 - 17 __X other (explain) 20 male subjects including able-bodied and wheelchair dependent individuals who are either ISU students or adults from the surrounding Ames area

7. Brief description of proposed research involving human subjects: **(See instructions, Item 7.** Use an additional page if needed.)

Please refer to attached page A

(Please do not send research, thesis, or dissertation proposals.)

8. Informed Consent:
☒ Signed informed consent will be obtained. (Attach a copy of your form.)
☐ Modified informed consent will be obtained. (See instructions, item 8.)
☐ Not applicable to this project.

9. Confidentiality of Data: Describe below the methods to be used to ensure the confidentiality of data obtained. (See instructions, item 9.)

Please refer to attached page A

10. What risks or discomfort will be part of the study? Will subjects in the research be placed at risk or incur discomfort? Describe any risks to the subjects and precautions that will be taken to minimize them. (The concept of risk goes beyond physical risk and includes risks to subjects' dignity and self-respect as well as psychological or emotional risk. See instructions, item 10.)

Please refer to attached page A

11. **CHECK ALL** of the following that apply to your research:
- ☐ A. Medical clearance necessary before subjects can participate
- ☒ B. Samples (Blood, tissue, etc.) from subjects
- ☐ C. Administration of substances (foods, drugs, etc.) to subjects
- ☒ D. Physical exercise or conditioning for subjects
- ☐ E. Deception of subjects
- ☐ F. Subjects under 14 years of age and/or ☐ Subjects 14 - 17 years of age
- ☐ G. Subjects in institutions (nursing homes, prisons, etc.)
- ☐ H. Research must be approved by another institution or agency (Attach letters of approval)

If you checked any of the items in 11, please complete the following in the space below (include any attachments):

Items A - D Describe the procedures and note the safety precautions being taken.

Item E Describe how subjects will be deceived; justify the deception; indicate the debriefing procedure, including the timing and information to be presented to subjects.

Item F For subjects under the age of 14, indicate how informed consent from parents or legally authorized representatives as well as from subjects will be obtained.

Items G & H Specify the agency or institution that must approve the project. If subjects in any outside agency or institution are involved, approval must be obtained prior to beginning the research, and the letter of approval should be filed.

Last Name of Principal Investigator Draper

277

hecklist for **Attachments and Time Schedule**

he following are attached (please check):

2. ☒ Letter or written statement to subjects indicating clearly:
   a) purpose of the research
   b) the use of any identifier codes (names, #'s), how they will be used, and when they will be removed (see Item 17)
   c) an estimate of time needed for participation in the research and the place
   d) if applicable, location of the research activity
   e) how you will ensure confidentiality
   f) in a longitudinal study, note when and how you will contact subjects later
   g) participation is voluntary; nonparticipation will not affect evaluations of the subject

3. ☒ Consent form (if applicable)

4. ☐ Letter of approval for research from cooperating organizations or institutions (if applicable)

5. ☐ Data-gathering instruments

6. Anticipated dates for contact with subjects:

First Contact	Last Contact
11/1/94	12/30/94
Month / Day / Year	Month / Day / Year

7. If applicable: anticipated date that identifiers will be removed from completed survey instruments and/or audio or visual tapes will be erased:

6/1/95
Month / Day / Year

8. Signature of Departmental Executive Officer | Date | Department or Administrative Unit

Mary Helen Greer | 9/27/94 | Biomedical Engineering

Decision of the University Human Subjects Review Committee:

X Project Approved ___ Project Not Approved ___ No Action Required

Patricia M. Keith
Name of Committee Chairperson

9/29/94
Date

Fred Lorenz
Signature of Committee Chairperson

1/90

Attachment A

7. This project will involve the recording and evaluation of wheelchair propulsion efficiency, EMG data, and kinematic data of both able-bodied and wheelchair dependent persons while propelling a manually powered wheelchair on a specially designed wheelchair dynamometer, which simulates wheelchair propulsion but allows the subject to remain stationary for easier data collection.

To evaluate propulsion efficiency, oxygen consumption will be measured using a closed-circuit spirometer. The subject will be instructed to breathe through the spirometer tube for several minutes prior to beginning the test in order to become accustomed to it and to ease anxiety to avoid hyperventilation during the test. The subject will be instructed to maintain a certain velocity at a preset resistance on the dynamometer for approximately 3 minutes, at which time a 5 second period of data collection will occur. A cool-down period of 1-2 minutes will then follow as well as a resting period of 10-15 minutes prior to beginning the next test. The velocity and/or resistance will then be changed and the protocol repeated 3-4 more times. No attempt to elicit a VO_2 max. response will be made. All tests will be run submaximally. The subject's heartrate will also be monitored and the test immediately ceased if a predetermined maximum heartrate is exceeded.

To evaluate EMG activity, surface electrodes will be adhered to the muscles of interest (arm, shoulder, back, and chest muscles) using an adhesive disk and an electrolyte conductive gel. A grounding electrode will also be adhered to the wrist or leg. The EMG signal will be amplified and sent to a computer-based data acquisition system for data storage and analysis. EMG data will be collected for each combination of velocity and propulsion resistance described above.

To evaluate kinematics, infrared sensitive markers will be placed on the wrist, elbow, and shoulder of the subject. The subject will be videotaped from the side during the propulsion cycle and the motion of the markers digitized for analysis.

The subject should complete all tests within a 2-3 hour period. If the subject feels excessively fatigued or cannot continue for any reason, the subject may return at a later time to conclude the tests. The subjects will range in age from 18 to 45 years.

9. Each subject will be assigned a code, such as ab-1 or wd-3 to be used throughout the experiment and in the write-up of the thesis. Subject identity will be kept on a floppy disk stored in a locked laboratory and will not be available to anyone other than the principle investigator and the major professor supervising the experiment.

10. The attachment of the EMG electrodes and kinematic markers should present no discomfort to the subject. It is expected that the subject will experience the normal effects of exercise including lactic acid buildup in the muscles causing a mild burning sensation as well as an increased heartrate and respiratory rate. The subject will be instructed to report any dizziness, severe or sharp pain, nausea, or other abnormal discomforts, at which time the test will immediately cease. The heartrate will also be monitored and the test will cease if it exceeds a clinically accepted maximum value for the subject's age. It is

foreseeable that the subject could experience muscle cramping or soreness following the tests. However, no permanent effects are expected.

11D. As stated above, the testing procedure requires that the subject experience moderate exercise for a period of approximately 5 minutes followed by a 10-15 minute rest period between tests. The normal effects of exercise are expected and the test will cease if any abnormalities occur as described above. In the case of a muscle cramp, research staff will be present to assist in relaxing the muscle. The subject will be in complete control during the entire experiment and will not be physically bound to the wheelchair in any way which would prevent the cessation of the experiment by the subject.

Signed Informed Consent Form for Study of Manual Wheelchair Propulsion Parameters

1. The intent of this study is to analyze the differences in propulsion efficiency (work done divided by work expended), electromyographic trends (electrical signals generated when a muscle contracts), and kinematic trends (patterns of movement) between a group of able-bodied subjects and a group of wheelchair bound subjects. We are interested in these differences both for further insight into wheelchair propulsion in general, as well as to provide information to aid further researchers in conducting studies involving manual wheelchair propulsion.

   The tests will consist of two exercise bouts involving propelling a wheelchair on a stationary apparatus called a dynamometer which has the capability of recording both propulsion velocity and applied handrim force information. You will be instructed to attempt to maintain a specified velocity (50 on the display) for a period of two minutes, after which time the velocity will be increased to 70 and 90 with two minutes of propulsion at each velocity level. You will then be given a 15 minute rest and the test will be repeated, starting with 90 and ending with 50. Data will be collected at each velocity level.

   During the tests, you will be breathing into a tube which is connected to an apparatus called a spirometer. This device records the amount of oxygen that you are consuming per minute and is an indication of the amount of work that your body is generating to perform the task. This tube may seem awkward and uncomfortable at first. However, you should get used to it and you will be instructed to practice breathing into the tube for a couple of minutes prior to the beginning of testing.

   To record muscle activity, electrodes will be placed over the deltoid and triceps muscles. The area where the electrode will be placed will be shaved, cleansed with rubbing alcohol, and gently abraded to remove dead skin in order to achieve good electrical contact. A conductive electrode gel will also be used between your skin and the electrode. This procedure should produce no discomfort to you, although it is possible that you could experience some slight irritation due to the electrode gel (stinging, redness, etc.). This irritation should discontinue shortly after the gel is removed. In addition, you may have small reddish marks for several days where the electrodes were placed. To record kinematic data, reflective markers will be placed on your wrist, elbow, and shoulder joints. You will be videotaped while propelling the wheelchair in order to determine timing parameters such as cycle frequency and the start and stop of each propulsion cycle.

The motion of the reflective markers may also be digitized in order to compare the patterns of motion of the joints. You should experience no discomfort due to these procedures. All electrical equipment is for recording purposes only and safety precautions have been taken to ensure that you are in no danger electrically.

2. You will be in complete control of all motion during the testing period and should immediately stop the test if you experience severe pain or serious discomfort such as dizziness, nausea, muscle cramping, etc. However, you should experience the effects of exercise including mild muscle burning and an increased heartrate and respiratory rate, as well as an increased difficulty in breathing. These effects should be moderate however and you should stop the test if you feel any abnormalities.
3. You should feel free to ask any questions about the equipment, testing procedure, or research in general at any time.
4. You will not be bound in any way to complete the testing and may withdraw consent at any time.
5. All data and personal information will be kept confidential. You name will not appear in any publications or thesis work.
6. The time required of you will be approximately 2 hours. It is expected that all of the tests will be run in one setting. However, if you feel that you cannot continue due to fatigue, etc. you are free to return at a later time to redo the testing.
7. Emergency treatment of any injury that may occur as a direct result of participation in the research will be treated by the Iowa State University Student Health Services, Student Services Building, and/or referred to Mary Greeley Hospital or another physician. Compensation for treatment of any injuries that may occur as a result of participation in the research may or may not be paid by Iowa State University depending on the Iowa Tort Claims Act. Claims for compensation will be handled by the Iowa State University Vice President for Business and Finance.

By signing below you state that you have read this consent form, understand it, have had your questions pertaining to it satisfactorily answered, and voluntarily agree to participate in the study accepting the risks entailed by it. You also understand that you may discontinue participation at any time and for any reason without objection by the researchers or anyone involved with the study.

Volunteer Subject:_____ Date:_____

Researcher/Witness:_____

APPENDIX F:

LAB WINDOWS DATA ACQUISITION AND ANALYSIS PROGRAMS

```
/* Wheelchair data acquisition and storage program */
/* Written in C by Scott A. Draper */
/* Biomedical Engineering Department */
/* Iowa State University */
/* Ames, Iowa  1994 */

#include "wheelchr.h"

#define numchans       3
#define rate          3000.0
#define numpoints      15000
#define labpc_brd_code  9
#define lpm16_brd_code  13

main()
{
 char fi[45];
 char buff[10];
 char conf[50];
 int status,panel_hdl,handle,quit,i,ctrl, choice;
 int chans[numchans],board,boardtype,gains[numchans];
 long numTimeOutTicks, size;
 int data[numpoints], file;
 int pane1,pane2,pop;
 int t[numpoints/numchans], e1[numpoints/numchans];
 int e2[numpoints/numchans];
 int gain0, gain1, gain2;
 int subj, torq, veloc, total, overflow, velocity;
 double meantorq, meane1, meane2, factor, freq, meantorque, bal, mt;
 double meanemg1, meanemg2;
 double scaled_t[numpoints/numchans], scaled_e1[numpoints/numchans];
 double scaled_e2[numpoints/numchans], tf[numpoints/numchans];
 double cutoff, st[numpoints/numchans];

   /* Open and Display Panels */
 status = OpenInterfaceManager();
 /*MessagePopup("Wheelchair Propulsion User Interface");
 MessagePopup("Written by Scott A. Draper");
 MessagePopup("Biomedical Engineering Dept., Iowa State Univ.");*/
 panel_hdl=LoadPanel("wheelchr.uir",wc);
 pane1 = LoadPanel("wheelchr.uir", emg1);
 pane2 = LoadPanel("wheelchr.uir", emg2);
```

```
status = DisplayPanel(panel_hdl);
ConfigurePrinter ("LPT1", 1, 8.0, 10.0, 1);

/* Initialize data array to zero */
/*for (i=0;i<numpoints;i++)
  {data[i] = 0;}*/


quit = 0;
board = 1;
boardtype = 0;

/* Fill the channel array for MIO boards */
for (i=0;i<numchans;i++)
{
  chans[i] = i;
}
/* Get board type */
status = Init_DA_Brds(board, &boardtype);
SetCtrlVal(panel_hdl, wc_error, status);

/* Calculate and set a timeout limit */
numTimeOutTicks=(numpoints/rate)*20;
if(numTimeOutTicks<20L) numTimeOutTicks=20L;
status=Timeout_Config (board,numTimeOutTicks);

GetCtrlVal(panel_hdl, wc_gain1, &gain0);
GetCtrlVal(panel_hdl, wc_gain2, &gain1);
GetCtrlVal(panel_hdl, wc_gain3, &gain2);
gains[0] = gain0;
gains[1] = gain1;
gains[2] = gain2;

/* Heart of Program */
while (!quit)
{
  GetCtrlVal(panel_hdl, wc_gain1, &gain0);
  GetCtrlVal(panel_hdl, wc_gain2, &gain1);
  GetCtrlVal(panel_hdl, wc_gain3, &gain2);
  gains[0] = gain0;
  gains[1] = gain1;
  gains[2] = gain2;
```

```
status = GetUserEvent(0, &handle, &ctrl);
switch(ctrl)
{
   case wc_quit:
   /* User presses the quit button */
   quit = 1;
   break;

   case wc_adstart:
   /* User starts data acquisition */
   DeletePlots(panel_hdl, wc_torqu);
   DeletePlots(pane1, emg1_emg1);
   DeletePlots(pane2, emg2_emg2);
   SetCtrlVal(panel_hdl, wc_error, 0);
   DIG_Prt_Config(1, 1, 0, 1);
   SetCtrlVal(panel_hdl, wc_led, 1);
   DIG_Out_Port(1, 1, 1111);
   status = SCAN_Op (1, numchans, chans, gains, data, numpoints, rate,
            0.0);
   DIG_Out_Port(1, 1, 0);
   SetCtrlVal(panel_hdl, wc_led, 0);

   /* Get demuxed data and put into individual arrays */
   for (i=0; i < numpoints-2; i++)
      {if (i%numchans == 0)
         {t[i/numchans] = data[i];
         e1[i/numchans] = data[i+1];
         e2[i/numchans] = data[i+2];}}


   GetCtrlVal(panel_hdl, wc_bal, &bal);
   status = DAQ_VScale (1, chans[0], gains[0], 1.0, 0.0,
            numpoints/numchans, t, scaled_t);
   status = DAQ_VScale (1, chans[1], gains[1], 1.0, 0.0,
            numpoints/numchans, e1, scaled_e1);
   status = DAQ_VScale (1, chans[2], gains[2], 1.0, 0.0,
            numpoints/numchans, e2, scaled_e2);

   /* Adjust Data for initial Voltage Offset */
   for (i=0;i<numpoints/numchans;i++)
   {
```

```
   st[i] = scaled_t[i] - bal;
}
GetCtrlVal(panel_hdl, wc_cutoff, &cutoff);
Bw_LPF (st, numpoints/numchans, rate/numchans, cutoff, 5, tf);

/* Calculate Mean Values of arrays and display */

Mean(tf, numpoints/numchans, &meantorq);
Mean(scaled_e1, numpoints/numchans, &meane1);
Mean(scaled_e2, numpoints/numchans, &meane2);

SetCtrlVal(panel_hdl, wc_mt, meantorq);
SetCtrlVal(panel_hdl, wc_me1, meane1);
SetCtrlVal(panel_hdl, wc_me2, meane2);
SetCtrlVal(panel_hdl, wc_error, 99);

PlotY (panel_hdl, wc_torqu, tf, numpoints/numchans, 4, 0, 0, 1, 15);

break;

case wc_print:
OutputGraph (0, "", 0, panel_hdl, wc_torqu);
break;

case wc_prtscn:
OutputScreen (0, "");
break;

case wc_lpf:
DeletePlots(panel_hdl, wc_torqu);
GetCtrlVal(panel_hdl, wc_cutoff, &cutoff);
GetCtrlVal(panel_hdl, wc_bal, &bal);
for (i=0;i<numpoints/numchans;i++)
{
   st[i] = scaled_t[i] - bal;
}

Bw_LPF (st, numpoints/numchans, rate/numchans, cutoff, 5, tf);
Mean(tf, numpoints/numchans, &meantorq);
SetCtrlVal(panel_hdl, wc_mt, meantorq);
PlotY (panel_hdl, wc_torqu, tf, numpoints/numchans, 4, 0, 0, 1, 15);
break;
```

```
case wc_emg1:
status = InstallPopup(pane1);
PlotStripChart(pane1,emg1_emg1,scaled_e1,100,0,0,4);
GetPopupEvent(1,&pop);
if (pop == 1)
   {RemovePopup(0);}
break;

case wc_emg2:
status = InstallPopup(pane2);
PlotStripChart(pane2,emg2_emg2,scaled_e2,100,0,0,4);
GetPopupEvent(1,&pop);
if (pop == 1)
   {RemovePopup(0);}
break;

case wc_tor:
DeletePlots (panel_hdl, wc_torqu);
PlotY (panel_hdl, wc_torqu, st, numpoints/numchans, 4, 0, 0, 1, 15);
break;

case wc_save:
/* User wishes to save data to disk */
GetCtrlVal(panel_hdl, wc_subj, &subj);
GetCtrlVal(panel_hdl, wc_velset, &veloc);
GetCtrlVal(panel_hdl, wc_torset, &torq);
GetCtrlVal(panel_hdl, wc_velocity, &velocity);
Fmt(fi, "%s<c:\\school\\wheelchr.dat\\subj%i\\s%iv%it%i.dat",
   subj, subj, veloc, torq);
status = GetFileInfo (fi, &size);
if (status == 1)
   {Fmt(conf, "%s<You are appending data to an existing file.");
   choice = MessagePopup(conf);}
SetCtrlVal(panel_hdl, wc_savebox, fi);
file = OpenFile(fi, 2, 1, 1);
SetCtrlVal(panel_hdl, wc_savled, 1);
FmtFile(file, "\n\n\n");
for (i=0;i<numpoints-2;i+=3)
   {
   FmtFile(file, "%s<%i[w5]\t", data[i]);
   FmtFile(file, "%s<%i[w5]\t", data[i+1]);
```

```
   FmtFile(file, "%s<%i[w5]\n", data[i+2]);
   }
FmtFile(file, "%s<%i[w5]", velocity);
SetCtrlVal(panel_hdl, wc_savled, 0);
SetCtrlVal(panel_hdl, wc_error, 99);
CloseFile(file);
DeletePlots(pane1, emg1_emg1);
DeletePlots(pane2, emg2_emg2);
break;

case wc_disp:
/* User wishes to re-plot previously saved file */
GetCtrlVal(panel_hdl, wc_subj, &subj);
GetCtrlVal(panel_hdl, wc_velset, &veloc);
GetCtrlVal(panel_hdl, wc_torset, &torq);
Fmt(fi, "%s<c:\\school\\wheelchr.dat\\subj%i\\s%iv%it%i.dat",
     subj, subj, veloc, torq);
SetCtrlVal(panel_hdl, wc_dataread, fi);
file = OpenFile(fi, 1, 2, 1);
SetCtrlVal(panel_hdl, wc_getled, 1);
for (i=0;i<numpoints-2;i+=3)
   {
   ScanFile(file, "%s>%i\t", &data[i]);
   ScanFile(file, "%s>%i\t", &data[i+1]);
   ScanFile(file, "%s>%i\n", &data[i+2]);
   }
SetCtrlVal(panel_hdl, wc_getled, 0);
CloseFile(file);

GetCtrlVal(panel_hdl, wc_bal, &bal);
DeletePlots(panel_hdl, wc_torqu);
DeletePlots(pane1, emg1_emg1);
DeletePlots(pane2, emg2_emg2);
for (i=0; i < numpoints-2; i++)
   {if (i%numchans == 0)
      {t[i/numchans] = data[i];
      e1[i/numchans] = data[i+1];
      e2[i/numchans] = data[i+2];}}

status = DAQ_VScale (1, chans[0], gains[0], 1.0, 0.0,
          numpoints/numchans, t, scaled_t);
```

```
        status = DAQ_VScale (1, chans[1], gains[1], 1.0, 0.0,
                numpoints/numchans, e1, scaled_e1);
        status = DAQ_VScale (1, chans[2], gains[2], 1.0, 0.0,
                numpoints/numchans, e2, scaled_e2);
        for (i=0;i<numpoints/numchans;i++)
        {
           st[i] = scaled_t[i] - bal;
        }
        GetCtrlVal(panel_hdl, wc_cutoff, &cutoff);
        Bw_LPF (st, numpoints/numchans, rate/numchans, cutoff, 5, tf);

        /* Calculate Mean Values of arrays and display */
        Mean(tf, numpoints/numchans, &meantorq);
        Mean(scaled_e1, numpoints/numchans, &meane1);
        Mean(scaled_e2, numpoints/numchans, &meane2);

        SetCtrlVal(panel_hdl, wc_mt, meantorq);
        SetCtrlVal(panel_hdl, wc_me1, meane1);
        SetCtrlVal(panel_hdl, wc_me2, meane2);
        SetCtrlVal(panel_hdl, wc_led, 0);
        SetCtrlVal(panel_hdl, wc_error, 99);

        PlotY (panel_hdl, wc_torqu, tf, numpoints/numchans, 4, 0, 0, 1, 15);

        break;
     }
  }

  /* End of program */
  status = Init_DA_Brds(board, &boardtype);
  status = CloseInterfaceManager();

  return;
}
```

```
/* Wheelchair data analysis program */
/* Written in C by Scott A. Draper */
/* Biomedical Engineering Department */
/* Iowa State University */
/* Ames, Iowa 1994-95 */

#define numpoints 15000
#define rate 3000
#define TRUE 1
#define FALSE 0
#define numchans 3
#include "awc_data.h"
void main(void)
{  int status, ctrl, handle, quit, panel, subj, velset, trial, i, vd;
   int peak1, track1, st1, track2, stp1, track3, st2, track4, stp2, track5;
   int st3, track6, stp3, track7, st4, track8, diff, add, numcy, stp5, track9;
   int e1strt, e1stp, e2strt, e2stp, st5, track10;
   int file, data[numpoints+1], cutoff, emgpan, go, run, ehandle, ectrl;
   int t[numpoints/numchans], e1[numpoints/numchans];
   int e2[numpoints/numchans];
   double scaled_t[numpoints/numchans], scaled_e1[numpoints/numchans];
   double scaled_e2[numpoints/numchans], bal, st[numpoints/numchans];
   double vms;
   double farray[1000], lpfout[numpoints/numchans + 1000], max1, max2;
   double e1mvc[numpoints/numchans], e2mvc[numpoints/numchans], mfilt;
   double thrcycle[8000], thrmean, meanpow, msg, coefff[100];
   double e1dbl[numpoints/numchans], e2dbl[numpoints/numchans];
   double recte1[numpoints/numchans], recte2[numpoints/numchans];
   double e1high, e1lpf[numpoints/numchans+100];
   double lpfout1[numpoints/numchans+600];
   double e2high, e2lpf[numpoints/numchans+100], mrecte1;
   double mae1[numpoints/numchans];
   double mae2[numpoints/numchans], mrecte2;
   double smooth[numpoints/numchans];
   double hpf1[numpoints/numchans], hpf2[numpoints/numchans];
   char fi[45], buff[10];

   status = OpenInterfaceManager();
   panel = LoadPanel("awc_data.uir", wda1);
   emgpan = LoadPanel("awc_data.uir", emg);
   status = DisplayPanel(panel);
   go = TRUE;
```

```
while (go)
{
   status = GetUserEvent(0, &handle, &ctrl);
   switch(ctrl)
{
   case wda1_quit:
   go = FALSE;
   break;

   case wda1_loadfile:
   /* User wishes to load previously acquired data file*/
   DeletePlots (panel, wda1_plot1);
   track1=0;
   track2=0;
   track3=0;
   track4=0;
   track5=0;
   track6=0;
   track7=0;
   track8=0;
   track9=0;
   track10=0;
   GetCtrlVal(panel, wda1_subj, &subj);
   GetCtrlVal(panel, wda1_velset, &velset);
   GetCtrlVal(panel, wda1_trial, &trial);
   Fmt(fi, "%s<c:\\school\\wheelchr.dat\\subj%i\\s%iv%it%i.dat",
        subj, subj, velset, trial);
   SetCtrlVal(panel, wda1_dataread, fi);
   file = OpenFile(fi, 1, 2, 1);
   SetCtrlVal(panel, wda1_getled, 1);
   for (i=0;i<numpoints-2;i+=3)
      {
      ScanFile(file, "%s>%i\t", &data[i]);
      ScanFile(file, "%s>%i\t", &data[i+1]);
      ScanFile(file, "%s>%i\n", &data[i+2]);
      }
   ScanFile(file, "%s>%i", &data[numpoints]);
   SetCtrlVal(panel, wda1_getled, 0);
   CloseFile(file);

   vd = data[numpoints];
   SetCtrlVal (panel, wda1_velocity, vd);
```

```
/* Data array separated into three arrays (t, e1, e2) */
for (i=0; i<numpoints-2; i++)
   {if (i%numchans == 0)
   {t[i/numchans] = data[i];
   e1[i/numchans] = data[i+1];
   e2[i/numchans] = data[i+2];}}

/* Strain gage array scaled to units of voltage */
for (i=0; i<numpoints/numchans; i++)
   {
   scaled_t[i] = t[i]/204.8;
   }

/* Adjust strain gage data to compensate for initial */
/* starting bridge balance if desired */
GetCtrlVal(panel, wda1_bal, &bal);
for (i=0;i<numpoints/numchans;i++)
{
   st[i] = scaled_t[i] - bal;
}

GetCtrlVal(panel, wda1_cutoff, &cutoff);
Bw_LPF (st, numpoints/numchans, rate/numchans, cutoff, 5, lpfout1);
for (i=0;i<numpoints/numchans;i++)
{
   lpfout[i] = lpfout1[i+600];
}

/* Strain gage data smoothing algorithm */
for (i=100;i<numpoints/numchans-100;i++)
{
   smooth[i] = (st[i-100]+st[i-95]+st[i-90]+st[i-85]+st[i-80]+
            st[i-75]+st[i-70]+st[i-65]+st[i-60]+st[i-55]+
            st[i-50]+st[i-45]+st[i-40]+st[i-35]+st[i-30]+
            st[i-25]+st[i-20]+st[i-15]+st[i-10]+st[i-5]+st[i]+
            st[i+5]+st[i+10]+st[i+15]+st[i+20]+st[i+25]+
            st[i+30]+st[i+35]+st[i+40]+st[i+45]+st[i+50]+
            st[i+55]+st[i+60]+st[i+65]+st[i+70]+st[i+75]+
            st[i+80]+st[i+85]+st[i+90]+st[i+95]+st[i+100]+
            st[i-97]+st[i-92]+st[i-87]+st[i-82]+st[i-77]+
            st[i-72]+st[i-67]+st[i-62]+st[i-57]+st[i-52]+
```

```
            st[i-47]+st[i-42]+st[i-37]+st[i-32]+st[i-27]+
            st[i-22]+st[i-17]+st[i-12]+st[i-7]+st[i-2]+
            st[i+97]+st[i+92]+st[i+87]+st[i+82]+st[i+77]+
            st[i+72]+st[i+67]+st[i+62]+st[i+57]+st[i+52]+
            st[i+47]+st[i+42]+st[i+37]+st[i+32]+st[i+27]+
            st[i+22]+st[i+17]+st[i+12]+st[i+7]+st[i+2])/81;
}
PlotY (panel, wda1_plot1, smooth, numpoints/numchans, 4, 0, 0, 1, 15);
Mean (lpfout1, numpoints/numchans, &msg);
SetCtrlVal(panel, wda1_meansg, msg);

/* Algorithm to isolate 1-4 complete propulsion cycles */
for (i=1;i<numpoints/numchans-1;i++)
{
if ((lpfout[i]>lpfout[i-1]) && (lpfout[i]>lpfout[i+1]) && (track1==0))
{peak1=i+1;
track1=1;}
if ((track1==1)&&(lpfout[i]<lpfout[i-
  1])&&(lpfout[i]<lpfout[i+1])&&(track2==0))
{st1=i+1;
track2=1;}
if ((track1==1)&&(track2==1)&&(lpfout[i]>lpfout[i-
  1])&&(lpfout[i]>lpfout[i+1])
  &&(track3==0))
{stp1=i+1;
track3=1;}
if ((track1==1)&&(track2==1)&&(lpfout[i]<lpfout[i-
  1])&&(lpfout[i]<lpfout[i+1])
  &&(track3==1)&&(track4==0))
{st2=i+1;
track4=1;}
if ((track1==1)&&(track2==1)&&(lpfout[i]>lpfout[i-
  1])&&(lpfout[i]>lpfout[i+1])
  &&(track3==1)&&(track4==1)&&(track5==0))
{stp2=i+1;
track5=1;}
if ((track1==1)&&(track2==1)&&(lpfout[i]<lpfout[i-
  1])&&(lpfout[i]<lpfout[i+1])
  &&(track3==1)&&(track4==1)&&(track5==1)&&(track6==0))
{st3=i+1;
track6=1;}
```

```
      if ((track1==1)&&(track2==1)&&(lpfout[i]>lpfout[i-
        1])&&(lpfout[i]>lpfout[i+1])

&&(track3==1)&&(track4==1)&&(track5==1)&&(track6==1)&&(track7==0))
      {stp3=i+1;
      track7=1;}
      if ((track1==1)&&(track2==1)&&(lpfout[i]<lpfout[i-
        1])&&(lpfout[i]<lpfout[i+1])

&&(track3==1)&&(track4==1)&&(track5==1)&&(track6==1)&&(track7==1)
        &&(track8==0))
      {st4=i+1;
      track8=1;}
      if ((track1==1)&&(track2==1)&&(lpfout[i]>lpfout[i-
        1])&&(lpfout[i]>lpfout[i+1])

&&(track3==1)&&(track4==1)&&(track5==1)&&(track6==1)&&(track7==1)
         &&(track8==1)&&(track9==0))
      {stp5=i+1;
      track9=1;}
      if ((track1==1)&&(track2==1)&&(lpfout[i]<lpfout[i-
        1])&&(lpfout[i]<lpfout[i+1])

&&(track3==1)&&(track4==1)&&(track5==1)&&(track6==1)&&(track7==1)
         &&(track8==1)&&(track9==1)&&(track10==0))
      {st5=i+1;
      track10=1;}
      }
      SetCtrlVal (panel, wda1_start1, st1);
      SetCtrlVal (panel, wda1_stop1, stp1);
      SetCtrlVal (panel, wda1_start2, st2);
      SetCtrlVal (panel, wda1_stop2, stp2);
      SetCtrlVal (panel, wda1_start3, st3);
      SetCtrlVal (panel, wda1_stop3, stp3);
      SetCtrlVal (panel, wda1_start4, st4);

      break;

      case wda1_tcp:
      /* User wishes to plot previously isolated propulsion cycles */
      DeletePlots (panel, wda1_plot1);
      GetCtrlVal (panel, wda1_numcy, &numcy);
```

```
if (numcy == 1)
{diff = st2 - st1;}
if (numcy == 2)
{diff = st3 - st1;}
if (numcy == 3)
{diff = st4 - st1;}
if (numcy == 4)
{diff = st5 - st1;}
add = st1;
for (i=0;i<diff+1;i++)
{
   thrcycle[i] = lpfout[i+add-1];
}
PlotY (panel, wda1_plot1, thrcycle, diff, 4, 0, 0, 1, 15);
Mean (thrcycle, diff+1, &thrmean);

/* Scale the mean voltage to units of force (N) */
thrmean = thrmean / 0.0599 + 2.005;

/* Scale the velocity display to units of velocity (m/s) */
vms = vd * 0.0129;
SetCtrlVal (panel, wda1_meanfor, thrmean);
SetCtrlVal (panel, wda1_meanvel, vms);

/* Calculate mean power output */
meanpow = thrmean*vms;
SetCtrlVal (panel, wda1_meanpow, meanpow);

break;

case wda1_lpf:
DeletePlots (panel, wda1_plot1);
GetCtrlVal(panel, wda1_cutoff, &cutoff);
Bw_LPF (st, numpoints/numchans, rate/numchans, cutoff, 5, lpfout1);
for (i=0;i<numpoints/numchans;i++)
{
   lpfout[i] = lpfout1[i+600];
}
PlotY (panel, wda1_plot1, lpfout, numpoints/numchans-600, 4, 0, 0, 1,
        15);
break;
```

```
case wda1_emganal:
HidePanel (panel);
DisplayPanel (emgpan);
DeletePlots (emgpan, emg_emg1);
DeletePlots (emgpan, emg_emg2);
for (i=0;i<numpoints/numchans;i++)
   {
      e1dbl[i] = e1[i];
      e2dbl[i] = e2[i];
   }
PlotY (emgpan, emg_emg1, e1, numpoints/numchans, 1, 0, 0, 1, 15);
PlotY (emgpan, emg_emg2, e2, numpoints/numchans, 1, 0, 0, 1, 15);
run = TRUE;
while (run)
{
   status = GetUserEvent(0, &ehandle, &ectrl);
   switch(ectrl)
   {
      case emg_main:
      HidePanel (emgpan);
      DisplayPanel (panel);
      run = FALSE;
      break;

      case emg_rectify1:
      /* Rectify EMG-1 data array */
      DeletePlots (emgpan, emg_emg1);
      Abs1D (e1dbl, numpoints/numchans, recte1);
      PlotY (emgpan, emg_emg1, recte1, numpoints/numchans, 4, 0, 0, 1,
            15);
      Mean (recte1, numpoints/numchans, &mrecte1);
      SetCtrlVal(emgpan, emg_mean1, mrecte1);
      break;

      case emg_rectify2:
      /* Rectify EMG-2 data array */
      DeletePlots (emgpan, emg_emg2);
      Abs1D (e2dbl, numpoints/numchans, recte2);
      PlotY (emgpan, emg_emg2, recte2, numpoints/numchans, 4, 0, 0, 1,
            15);
      Mean (recte2, numpoints/numchans, &mrecte2);
      SetCtrlVal(emgpan, emg_mean2, mrecte2);
```

```
break;

case emg_lpf1:
/* EMG-1 smoothing algorithm */
DeletePlots (emgpan, emg_emg1);
for (i=50;i<numpoints/numchans-50;i++)
{
   mae1[i] = (recte1[i-50]+recte1[i-49]+
         recte1[i-48]+recte1[i-47]+
         recte1[i-46]+recte1[i-45]+recte1[i-44]+
         recte1[i-43]+recte1[i-42]+recte1[i-41]+
         recte1[i-40]+recte1[i-39]+
         recte1[i-38]+recte1[i-37]+
         recte1[i-36]+recte1[i-35]+recte1[i-34]+
         recte1[i-33]+recte1[i-32]+recte1[i-31]+
         recte1[i-30]+recte1[i-29]+
         recte1[i-28]+recte1[i-27]+
         recte1[i-26]+recte1[i-25]+recte1[i-24]+
         recte1[i-23]+recte1[i-22]+recte1[i-21]+
         recte1[i-20]+recte1[i-19]+
         recte1[i-18]+recte1[i-17]+
         recte1[i-16]+recte1[i-15]+recte1[i-14]+
         recte1[i-13]+recte1[i-12]+recte1[i-11]+
         recte1[i-10]+recte1[i-9]+
         recte1[i-8]+recte1[i-7]+
         recte1[i-6]+recte1[i-5]+recte1[i-4]+
         recte1[i-3]+recte1[i-2]+recte1[i-1]+
         recte1[i]+
         recte1[i+50]+recte1[i+49]+
         recte1[i+48]+recte1[i+47]+
         recte1[i+46]+recte1[i+45]+recte1[i+44]+
         recte1[i+43]+recte1[i+42]+recte1[i+41]+
         recte1[i+40]+recte1[i+39]+
         recte1[i+38]+recte1[i+37]+
         recte1[i+36]+recte1[i+35]+recte1[i+34]+
         recte1[i+33]+recte1[i+32]+recte1[i+31]+
         recte1[i+30]+recte1[i+29]+
         recte1[i+28]+recte1[i+27]+
         recte1[i+26]+recte1[i+25]+recte1[i+24]+
         recte1[i+23]+recte1[i+22]+recte1[i+21]+
         recte1[i+20]+recte1[i+19]+
         recte1[i+18]+recte1[i+17]+
```

```
            recte1[i+16]+recte1[i+15]+recte1[i+14]+
            recte1[i+13]+recte1[i+12]+recte1[i+11]+
            recte1[i+10]+recte1[i+9]+
            recte1[i+8]+recte1[i+7]+
            recte1[i+6]+recte1[i+5]+recte1[i+4]+
            recte1[i+3]+recte1[i+2]+recte1[i+1])/101;

}
Mean (mae1, numpoints/numchans, &mfilt);
SetCtrlVal(emgpan, emg_mean1, mfilt);
PlotY (emgpan, emg_emg1, mae1, numpoints/numchans, 4, 0, 0, 1,
       15);
break;

case emg_lpf2:
/* EMG-2 smoothing algorithm */
DeletePlots (emgpan, emg_emg2);
for (i=50;i<numpoints/numchans-50;i++)
{
   mae2[i] = (recte2[i-50]+recte2[i-49]+
            recte2[i-48]+recte2[i-47]+
            recte2[i-46]+recte2[i-45]+recte2[i-44]+
            recte2[i-43]+recte2[i-42]+recte2[i-41]+
            recte2[i-40]+recte2[i-39]+
            recte2[i-38]+recte2[i-37]+
            recte2[i-36]+recte2[i-35]+recte2[i-34]+
            recte2[i-33]+recte2[i-32]+recte2[i-31]+
            recte2[i-30]+recte2[i-29]+
            recte2[i-28]+recte2[i-27]+
            recte2[i-26]+recte2[i-25]+recte2[i-24]+
            recte2[i-23]+recte2[i-22]+recte2[i-21]+
            recte2[i-20]+recte2[i-19]+
            recte2[i-18]+recte2[i-17]+
            recte2[i-16]+recte2[i-15]+recte2[i-14]+
            recte2[i-13]+recte2[i-12]+recte2[i-11]+
            recte2[i-10]+recte2[i-9]+
            recte2[i-8]+recte2[i-7]+
            recte2[i-6]+recte2[i-5]+recte2[i-4]+
            recte2[i-3]+recte2[i-2]+recte2[i-1]+
            recte2[i]+
            recte2[i+50]+recte2[i+49]+
            recte2[i+48]+recte2[i+47]+
```

```
            recte2[i+46]+recte2[i+45]+recte2[i+44]+
            recte2[i+43]+recte2[i+42]+recte2[i+41]+
            recte2[i+40]+recte2[i+39]+
            recte2[i+38]+recte2[i+37]+
            recte2[i+36]+recte2[i+35]+recte2[i+34]+
            recte2[i+33]+recte2[i+32]+recte2[i+31]+
            recte2[i+30]+recte2[i+29]+
            recte2[i+28]+recte2[i+27]+
            recte2[i+26]+recte2[i+25]+recte2[i+24]+
            recte2[i+23]+recte2[i+22]+recte2[i+21]+
            recte2[i+20]+recte2[i+19]+
            recte2[i+18]+recte2[i+17]+
            recte2[i+16]+recte2[i+15]+recte2[i+14]+
            recte2[i+13]+recte2[i+12]+recte2[i+11]+
            recte2[i+10]+recte2[i+9]+
            recte2[i+8]+recte2[i+7]+
            recte2[i+6]+recte2[i+5]+recte2[i+4]+
            recte2[i+3]+recte2[i+2]+recte2[i+1])/101;

}
Mean (mae2, numpoints/numchans, &mfilt);
SetCtrlVal(emgpan, emg_mean2, mfilt);
PlotY (emgpan, emg_emg2, mae2, numpoints/numchans, 4, 0, 0, 1,
        15);
Breakpoint ();

break;

case emg_hpf1:
/* EMG-1 high pass filter (not used) */
DeletePlots (emgpan, emg_emg1);
for (i=1;i<numpoints/numchans-1;i++)
{
   hpf1[i] = (2*recte1[i]-recte1[i+1]-recte1[i-1])/4;
}
Abs1D (hpf1, numpoints/numchans, hpf1);
PlotY (emgpan, emg_emg1, hpf1, numpoints/numchans, 4, 0, 0, 1,
        15);
break;

case emg_hpf2:
/* EMG-2 high pass filter (not used) */
```

```
            DeletePlots (emgpan, emg_emg2);
            for (i=1;i<numpoints/numchans-1;i++)
            {
               hpf2[i] = (2*recte2[i]-recte2[i+1]-recte2[i-1])/4;
            }
            Abs1D (hpf2, numpoints/numchans, hpf2);
            PlotY (emgpan, emg_emg2, hpf2, numpoints/numchans, 4, 0, 0, 1,
                  15);
            break;

         }
      }
      break;

   }
   }
return;
}
```